

ENDOTHELIAL RESPONSES TO ACUTE INFLAMMATION

**Thesis submitted for the degree of
Ph.D at the University of Leicester**

by

Mr Chris Stephen Milner MBChB, BSc, MRCS(Eng)

Department of Cardiovascular Sciences

University of Leicester

March 2008

UMI Number: U594488

All rights reserved

INFORMATION TO ALL USERS

The quality of this reproduction is dependent upon the quality of the copy submitted.

In the unlikely event that the author did not send a complete manuscript and there are missing pages, these will be noted. Also, if material had to be removed, a note will indicate the deletion.



UMI U594488

Published by ProQuest LLC 2013. Copyright in the Dissertation held by the Author.
Microform Edition © ProQuest LLC.

All rights reserved. This work is protected against
unauthorized copying under Title 17, United States Code.



ProQuest LLC
789 East Eisenhower Parkway
P.O. Box 1346
Ann Arbor, MI 48106-1346

ABSTRACT

Studies into Angiopoietin-1 and Tie Receptor Signalling During Endothelial Responses to Acute Inflammation by Chris Milner

Endothelial dysfunction is a major component of the systemic inflammatory response syndrome (SIRS) triggered by major tissue injury including burns. Such dysfunction leads to excessive vascular permeability and endothelial-leucocyte interactions resulting in endothelial cell death and organ damage. Angiopoietin-1, a key regulator of angiogenesis, has recently been identified as a potent anti-permeability and anti-inflammatory agent targeting the endothelium, and operates through two different receptors, Tie1 and Tie2. Identifying specific roles of each receptor in mediating the protective effects of Ang1 is essential for designing drug therapy for pathological inflammatory responses, and this therefore formed the objective of this research project. Specifically, *in vitro* models of endothelial permeability, survival and adhesion molecule expression have been established to study the effects of Ang-1 on Tie receptor deficient HUVEC generated by SiRNA techniques. Tie receptor knock-down was highly effective in HUVEC, and subsequent experiments using these cells proved the hypothesis that Tie2 is the principal receptor mediating Ang-1 induced endothelial survival and reduced endothelial permeability. In addition, absent Tie1 was found to increase baseline endothelial permeability and apoptosis in HUVEC, whilst the full anti-apoptotic effect of VEGF was shown to require both Tie1 and Tie2, adding to other data indicating a novel form of heterodimeric transactivation between the two receptors. Using the developed cell adhesion molecule (CAM) assay, experiments using naive HUVEC quantitated the anti-inflammatory effects of Ang-1 following stimulation by key pro-inflammatory cytokines such as Il-1. Moreover, preliminary experiments using plasma from patients with SIRS demonstrated the usefulness of the inflammatory CAM assay as a model for studying endothelial inflammatory responses in humans. Finally, experiments combining SIRS plasma with Ang-1 demonstrated a possible role for Ang-1 in the inhibition of SIRS plasma induced CAM expression.

ACKNOWLEDGEMENTS

I am very grateful to my supervisor Dr Nicholas Brindle for giving me the opportunity to undertake this research, particularly at the outset when there were very limited funding opportunities. He was always available for support and provided great reassurance during the times of frustration associated with any original research project. I am very pleased to have been the fourth student Nick has supervised to have progressed into higher surgical training in Plastic Surgery, and I wish him all the best of luck with similar students of the future.

I would like to sincerely thank the Healing Foundation and The Royal College of Surgeons of England for providing financial support for this work. I am especially grateful for the opportunities given to me by Mr Brendan Eley of the Healing Foundation and Mr Martyn Coomer of The Royal College of Surgeons, not least because they both introduced me to some truly inspiring individuals involved with both the raising and dispersal of research funds.

My thanks go to Jo Jeory and Nisha Patel who along with the other technical staff of the Vascular Surgery Group provided continuous assistance with experiments and lab husbandry.

Finally, I owe a great debt of gratitude to everyone at the Department of Plastic Surgery at Leicester Royal Infirmary, for providing me with the opportunity to continue my training in the speciality whilst undertaking my research. Whilst undoubtedly benefiting my progression into higher surgical training, it served as a constant reminder of the sick patient that all of this research has been dedicated towards.

DEDICATION

To Gill, who makes everything possible and brings happiness beyond any I had imagined.
May the discoveries of science mirror the wonderful discovery of the soul mate.

ABBREVIATIONS

Ang	Angiopoietin
APS	Ammonium Persulphate
bFGF	Basic Fibroblast Growth Factor
bp's	Base Pairs
BSA	Bovine Serum Albumin
CAM	Cell Adhesion Molecule
cDNA	Complementary Deoxyribonucleic Acid
ddH ₂ O	Double distilled Water
DABCO	1,4-diazabicyclo[2.2.2]octane
DEPC	Diethyl Pyrocarbonate
DMSO	Dimethyl Sulfoxide
DNA	Deoxyribonucleic Acid
dsDNA	Double Stranded Deoxyribonucleic Acid
DTT	Dithiothreitol
EC	Endothelial Cell
ECGS	Endothelial Cell Growth Factor
ECGM	Endothelial Cell Growth Medium
ECL	Enhanced Chemiluminescence
EDTA	Ethylenediaminetetraacetic Acid
EGF	Epidermal Growth Factor
FCS	Foetal Calf Serum
FITC	Fluorescein Isothiocyanate Conjugated
HRP	Horse Radish Peroxidase
HUVEC	Human Umbilical Vein Endothelial Cell
ID	Intracellular Domain
IEJ	Inter Endothelial Junction
IP	Immunoprecipitation
kDa	Kilo Daltons
MAPK	Mitogen Activated Protein Kinase
MLC	Myosin Light Chain

MLCK	Myosin Light Chain Kinase
MODS	Multiple Organ Dysfunction Syndrome
MOF	Multiple Organ Failure
mRNA	Messenger Ribonucleic Acid
NF κ B	Nuclear Factor kappa B
NO	Nitric Oxide
PAGE	Polyacrylamide Gel Electrophoresis
PAF	Platelet Activating Factor
PAR-1	Protease Activated Receptor-1
PBS	Phosphate Buffered Saline
PCR	Polymerase Chain Reaction
PDGF	Platelet Derived Growth Factor
PI3K	Phosphoinositide 3-Kinase
PKC	Protein Kinase C
PMA	Phorbol Myristate Acetate
PBD	Phosphate Binding Domain
PBS	Phosphate Buffered Saline
RNA	Ribonucleic Acid
RTK	Receptor Tyrosine Kinase
RT-PCR	Reverse Transcriptase PCR
SDS	Sodium Dodecyl Sulphate
SIRS	Systemic Inflammatory Response Syndrome
SH2	Src Homology-2
TAE	Tris Acetate
TBS	Tris Buffered Saline
TEMED	N,N,N',N'-Tetramethylethylenediamene
TF	Tissue Factor
Tie	Tyrosine Kinase with Immunoglobulin and EGF Homology Domains
TNF	Tumour Necrosis Factor
TR	Transmembrane Region
TEM	Trans Endothelial Migration
WCC	White Cell Count
WCL	Whole Cell Lysate

VEGF

Vascular Endothelial Growth Factor

GENERAL CONTENTS

Abstract.....	I
Acknowledgements.....	II
Dedication.....	III
Abbreviations.....	IV
General Contents.....	VII
CHAPTER ONE	
Introduction.....	1
CHAPTER TWO	
Materials and Methods.....	27
CHAPTER THREE	
Generation of Tie Deficient HUVEC and Studies of Endothelial Permeability.....	46
CHAPTER FOUR	
Tie Receptors and Endothelial Survival.....	70
CHAPTER FIVE	
Effects of Ang-1 on Endothelial Cell Adhesion Molecule Expression and the Role of Tie1 and Tie2.....	92
CHAPTER SIX	
Ang-1 Stimulation and Intracellular Signalling Events in Tie Deficient HUVEC.....	117
CHAPTER SEVEN	
Effects of Human SIRS Plasma on Endothelial Inflammatory Responses.....	129
CHAPTER EIGHT	
General Discussion.....	142
Appendices.....	153
Bibliography.....	155

CHAPTER ONE: INTRODUCTION

1.1: Acute Inflammation and Systemic Pathophysiology:	1
1.1.1: The Systemic Inflammatory Response Syndrome:	3
1.1.2: SIRS Therapy and the Vascular Endothelium:	4
1.2: Tie Receptors and the Angiopoietin Family of Growth Factors:	6
1.2.1: Angiopoietin / Tie Signalling in the Regulation of Endothelial Permeability:	9
1.2.1.1: Mechanisms of Inter-Endothelial Permeability Control:	10
1.2.1.2: Induction of Permeability:	13
1.2.1.3: Angiopoietin Regulation of Endothelial Permeability:	15
1.2.2: Angiopoietin / Tie Signalling in Endothelial Survival:	17
1.2.2.1: Mechanism of Endothelial Apoptosis:	18
1.2.2.2: Angiopoietin-1 Mediated Survival in Endothelial Cells:	20
1.2.3: Angiopoietin / Tie Signalling and Inflammatory Activation of the Endothelium:	22
1.3: Summary:	25
1.4: Aims & Objectives:	25

FIGURES:

Figure 1.1 Simplified schematic illustration of events involved in acute inflammation..... 2

Figure 1.2 Schematic illustration of events following endothelial activation during the acute inflammatory response..... 5

Figure 1.3 Schematic illustration of the Tie1 and Tie2 receptor tyrosine kinases..... 7

Figure 1.4 Schematic illustration of inter-endothelial adhesion mediated by VE-Cadherin at an adherens junction..... 12

Figure 1.5 Schematic illustration of key events involved with endothelial barrier reduction by thrombin..... 14

Figure 1.6 Schematic illustration of the known effects of Ang-1 on endothelial monolayer barrier functions..... 16

Figure 1.7 Schematic illustration of the caspase system and cell death by apoptosis..... 19

Figure 1.8 Schematic illustration of Ang-1 mediated survival signalling in endothelial cells..... 21

Figure 1.9 Schematic illustration of the three stages involved in leucocyte transendothelial migration (TEM)..... 23

TABLES:

Table 1.1 SIRS criteria..... 3

CHAPTER TWO: MATERIALS AND METHODS

2.1: General Chemicals:	27
2.2: General Solutions:	27
2.3: Commercial Kits:	28
2.4: Antibodies:	29
2.5: Growth Factors and Cytokines:	29
2.6: SiRNA Sequences:	30
2.7: Culture of HUVEC:	30
2.8: Culture of HMEC 98:	31
2.9: Culture of EA.hy 926:	32
2.10: Calculation of Cell Number:	32
2.11: Transfection Protocol:	32
2.12: Protein Separation by Sodium Dodecyl Sulphate PolyAcrylamide Gel Electrophoresis (SDS-PAGE):	33
2.13: Western Blotting:	36
2.14: Immunoblotting:	36
2.15: Measurement of Immunoblot Band Intensity:	38
2.16: Endothelial Monolayer Permeability:	38
2.16.1: FITC-Dextran Method (1):	40
2.16.2: HRP Method (2):	40
2.17: Apoptosis Detection by Cleaved Caspase-3/7 Assay:	41
2.18: Endothelial Cell Adhesion Molecule (CAM) Assay:	43
2.19: Preparation and Processing of Human Plasma Samples:	44
2.20: Statistical Analyses:	45

FIGURES:

Figure 2.1	Phase contrast image of cultured HUVEC superimposed with fluorescence image of same cells following transfection with Rhodamine-labelled control SiRNA.....	35
Figure 2.2	Schematic illustration of in vitro endothelial cell permeability model.....	39
Figure 2.3	Photomicrograph of permeability insert membrane both without (A), and with an endothelial cell monolayer present (H&E stained).....	39
Figure 2.4	Schematic illustration of the chemical interactions involved in the CaspaseGlo 3/7™ caspase detection assay.....	42

TABLES:

Table 2.1	Gel formulations used for SDS-PAGE.....	34
Table 2.2	Summary of antibodies used and their diluted conditions.....	37
Table 2.3	Primary fluorescent and secondary HRP-linked antibody dilutions for the detection of ICAM-1, VCAM-1 and E-Selectin expressed on the endothelial cell surface.....	44

**CHAPTER THREE: GENERATION OF TIE DEFICIENT HUVEC AND STUDIES
OF ENDOTHELIAL PERMEABILITY**

3.1.1: Creation of Tie Deficient HUVEC:.....46

3.1.2: SiRNA Generation of Tie1 and Tie2 Deficient HUVEC:.....48

3.2.1: Regulation of Endothelial Permeability: The Role of Tie Receptor Signalling:.....52

3.2.2: Establishment of an Endothelial Permeability Assay:.....52

3.2.3: Endothelial Permeability and Angiopoietin-1:56

3.2.4: Modifications to the Permeability Assay:.....56

3.2.5: Angiopoietin-1 Mediated Inhibition of Permeability in HUVEC:.....58

3.2.6: Endothelial Permeability in Tie1 Deficient HUVEC:61

3.2.7: Endothelial Permeability in Tie2 Deficient HUVEC:64

3.3: Discussion:.....67

FIGURES:

Figure 3.1	Schematic illustration of events involved in RNA interference.....	47
Figure 3.2	Western blot image of SiRNA silenced Tie1 expression.....	49
Figure 3.3	Time-course experiment for Tie receptor knock-down following SiRNA treatment in HUVEC.....	51
Figure 3.4	HMEC-98 endothelial cell permeability and the effects of Thrombin at Different Concentrations.....	54
Figure 3.5	Colour Photomicrograph of HMEC-98 Monolayer Under Resting Conditions (A), and Following Stimulation with 2U / ml Thrombin....	55
Figure 3.6	Colour photomicrograph of HMEC-98 actin cytoskeleton following Phalloidin staining, with and without thrombin stimulation.....	55
Figure 3.7	HMEC-98 permeability following stimulation with Ang-1 & Thrombin.....	57
Figure 3.8	HUVEC monolayer permeability under baseline and Ang-1 stimulated conditions.....	59
Figure 3.9	HUVEC monolayer permeability following stimulation with Ang-1 and COMP-Ang1.....	60

Figure 3.10	Endothelial permeability assay comparing Tie1 deficient HUVEC with random SiRNA transfected control HUVEC.....	62
Figure 3.11	Summative data on endothelial permeability in Tie1 deficient HUVEC.....	63
Figure 3.12	Endothelial permeability assay comparing Tie2 deficient HUVEC with random SiRNA transfected control HUVEC.....	65
Figure 3.13	Summative data on endothelial permeability in Tie2 deficient HUVEC.....	66

CHAPTER FOUR: TIE RECEPTORS AND ENDOTHELIAL SURVIVAL

4.1: Tie Receptors and the Regulation of Endothelial Cell Apoptosis:	70
4.2: Establishment of Apoptosis in Serum-Starved HUVEC:	71
4.3: Inhibition of Apoptosis by Angiopoietin-1 in Serum-Starved HUVEC:	71
4.4: Establishment of Tie Receptor Involvement in Angiopoietin-1 Protected Serum Starved HUVEC:	74
4.4.1: Apoptosis in Tie1 Deficient HUVEC:	74
4.4.2: Apoptosis in Tie2 Deficient HUVEC:	78
4.4.3: Caspase Sensitivity to Low-Dose Angiopoietin-1:	81
4.5: An Investigation into VEGF Inhibited Apoptosis in Tie Receptor Deficient HUVEC:	85
4.6: Discussion:	89

FIGURES:

Figure 4.1	Caspase production in serum-starved HUVEC over time.....	72
Figure 4.2	Anti-apoptotic effect of Ang-1 on serum-starved HUVEC.....	73
Figure 4.3	Representative HUVEC Western Blot 48 hours after transfection with Tie1 SiRNA or Random SiRNA.....	76
Figure 4.4	Combined normalised results from three individual caspase experiments with Tie1 deficient and control HUVEC.....	77
Figure 4.5	Representative HUVEC Western Blot 48 hours after Transfection with either Tie2 SiRNA or random SiRNA.....	79
Figure 4.6	Combined normalised results from three individual caspase experiments with Tie2 deficient and random control HUVEC.....	80
Figure 4.7	Graph demonstrating the magnitude of Ang-1 inhibition of caspase production in control, Tie1 and Tie2 deficient HUVEC.....	82
Figure 4.8	Differential Caspase production in Tie1 deficient and control HUVEC following stimulation with low-dose Ang-1.....	83
Figure 4.9	Caspase Production in Tie1 Deficient and Control HUVEC Following Stimulation with Low Dose Ang-1: The Comparative Magnitude of Ang-1 Response.....	84
Figure 4.10	Apoptosis in Tie1 deficient HUVEC with or without VEGF₁₆₅.....	86

Figure 4.11	Apoptosis in Tie2 deficient HUVEC with or without VEGF₁₆₅.....	87
Figure 4.12	Reduction in anti-apoptotic efficiency in VEGF treated Tie1 and Tie2 deficient HUVEC	88

**CHAPTER FIVE: EFFECTS OF ANG-1 ON ENDOTHELIAL CELL ADHESION
MOLECULE EXPRESSION AND THE ROLE OF TIE1 AND TIE2**

5.1: Cell Adhesion Molecule Expression in Endothelial Cells and Their Regulation by Angiopoietin / Tie Signalling:92

5.2: Induction of CAM Expression in Endothelial Cells:.....93

5.3: CAM Quantitation Assay:93

5.4: CAM Expression and Ang-1 Stimulation:102

5.5: CAM Expression Studies in Tie deficient Endothelial Cells:109

5.6: Discussion:.....114

FIGURES:

Figure 5.1	VCAM-1 expression in HMEC-98 (A) and HUVEC (B) visualised by immunohistochemistry.....	94
Figure 5.2	Quantitative measurement of ICAM-1, VCAM-1 and E-Selectin expression in HMEC-98, by cell-ELISA.....	96
Figure 5.3	Quantitation of VCAM-1 expression in HMEC-98 following Il-1 or TNFα stimulation.....	98
Figure 5.4	Quantitative measurement of ICAM-1, VCAM-1 and E-Selectin expression in IL-1 stimulated HUVEC.....	99
Figure 5.5 (a)	Expression of VCAM-1, ICAM-1 and E-Selectin expression in HUVEC exposed to increasing concentrations of TNFα.....	100
Figure 5.5 (b)	Expression of VCAM-1, ICAM-1 and E-Selectin expression in HUVEC exposed to increasing concentrations of Il-1	101
Figure 5.6	HUVEC CAM expression in response to VEGF₁₆₅ stimulation with and without Ang-1.....	103
Figure 5.7	HUVEC CAM expression in response to variable Il-1 concentrations, with and without Ang-1.....	104
Figure 5.8 (a)	Percentage VCAM-1 inhibition in HUVEC stimulated with increasing concentrations of Il-1 in the presence of Ang-1	105

Figure 5.8	Percentage ICAM-1 inhibition in HUVEC stimulated with increasing concentrations of Il-1 in the presence of Ang-1	105
(b)		
Figure 5.8	Percentage E-Selectin inhibition in HUVEC stimulated with increasing concentrations of Il-1 in the presence of Ang-1	106
(c)		
Figure 5.9	Quantitated CAM expression in Il-1 stimulated HUVEC with increasing concentrations of Ang-1.....	108
Figure 5.10	Percentage inhibition of VCAM-1 expression in Il-1 stimulated HUVEC exposed to increasing concentrations of Ang-1.....	111
(a)		
Figure 5.10	Percentage inhibition of ICAM-1 expression in Il-1 stimulated HUVEC exposed to increasing concentrations of Ang-1.....	111
(b)		
Figure 5.10	Percentage inhibition of E-Selectin expression in Il-1 stimulated HUVEC exposed to increasing concentrations of Ang-1.....	112
(c)		
Figure 5.11	VCAM-1 expression in Il-1 stimulated Tie1 deficient, Tie2 deficient and control HUVEC exposed to increasing concentrations of Ang-1...	113

**CHAPTER SIX: ANG-1 STIMULATION AND INTRACELLULAR SIGNALLING
 EVENTS IN TIE DEFICIENT HUVEC**

6.1: Intracellular Signalling in Tie deficient HUVEC:.....117

6.2: Discussion:.....127

FIGURES:

Figure 6.1	Quantitative measurement of Tie receptor expression in Tie1 deficient, Tie2 deficient and control HUVEC.....	118
Figure 6.2	Ang-1 stimulated Akt phosphorylation in Tie1 deficient, Tie2 deficient and control HUVEC.....	119
Figure 6.3	Ang-1 stimulated p42 MAPK phosphorylation in Tie1 deficient, Tie2 deficient and control HUVEC	121
Figure 6.4	Quantitative measurement of Tie receptor expression in Tie1 deficient, Tie2 deficient, Tie1&2 deficient and control HUVEC.....	123
Figure 6.5	Ang-1 stimulated Akt phosphorylation in Tie1 deficient, Tie2 deficient, Tie1&2 deficient and control HUVEC.....	124
Figure 6.6	Ang-1 stimulated p42 MAPK phosphorylation in Tie1 deficient, Tie2 deficient, Tie1&2 deficient and control HUVEC.....	126

**CHAPTER SEVEN: EFFECTS OF HUMAN SIRS PLASMA ON ENDOTHELIAL
INFLAMMATORY RESPONSES**

7.1: Effects of Plasma From SIRS Patients on Endothelial Inflammatory Responses: .129

7.2: SIRS plasma and CAM expression:.....129

7.3: SIRS plasma and Endothelial Permeability:134

7.4: SIRS plasma and Endothelial Survival:138

7.5: Discussion:.....140

FIGURES:

Figure 7.1	CAM expression profile for HUVEC exposed to increasing proportions of plasma from a healthy control.....	130
Figure 7.2	CAM expression profile for HUVEC exposed to increasing proportions of plasma from patient number 2.....	132
Figure 7.3	CAM expression profile in HUVEC exposed to 20% plasma from patient number 2 together with increasing concentrations of Ang-1....	133
Figure 7.4	HUVEC permeability assay with variable proportions of plasma from patient number 2.....	136
Figure 7.5	HUVEC permeability assay with low-density monolayer and plasma from patient number 2 and control plasma.....	137
Figure 7.6	Caspase activity in serum-starved HUVEC exposed to increasing proportions of control plasma or plasma from patient number 2.....	139

CHAPTER EIGHT: GENERAL DISCUSSION

8. General Discussion and Future Work:142

8.1 Endothelial Permeability:144

8.2 Endothelial Survival:147

8.3 Endothelial CAM Expression & Current Sepsis Strategies:151

FIGURES:

Figure 8.1	Schematic Illustration of some Effects of Ang-1 on Endothelial Cells.....	143
Figure 8.2	Schematic Illustration of Ang-1 roles in Endothelial Cell Permeability Control.....	146
Figure 8.3	Schematic Illustration Depicting Ang-1 Role in the Control of Endothelial Cell Apoptosis.....	149

APPENDICES

Meeting Presentations - Scientific:.....153
Meeting Presentations – Academic & Fundraising:.....154
Papers:.....154
Ethics Approval

BIBLIOGRAPHY

References:.....155

1.1: Acute Inflammation and Systemic Pathophysiology:

Acute inflammation is a highly adaptable, sensitive and specific defence system, capable of dealing with a vast array of invading micro-organisms, as well as co-ordinating the repair of damaged tissue, with minimal disruption to overall function (1). Acting in close concert with the coagulation system, acute inflammation is a multi-step process involving interactions between signalling mediators, pre-formed protein cascades, leucocytes and the vascular endothelium (Figure 1.1). By virtue of its major reliance on positive-feedback pro-inflammatory cascades, complementary control measures exist that are essential in restricting the magnitude of the inflammatory response to a level best suited to deal with the initiating stimulus (2, 3). However, major tissue damage or overwhelming infection can exceed this local auto-regulation, allowing pro-inflammatory processes to prevail and ultimately spill over into the systemic circulation as the initiating event of the Systemic Inflammatory Response Syndrome (SIRS). Released pro-inflammatory mediators then circulate in the blood and are free to bind specific receptors expressed by vascular endothelial cells and circulating leucocytes in areas remote to the zone of tissue injury. This activates leucocytes and endothelial cells, transforming both into an inflammatory phenotype and thus enabling the inflammatory cycle to progressively spread through *de novo* territory, ever more remote from the initiating stimulus. From a pathological perspective, the presence of acute inflammation in healthy tissue can disrupt normal tissue function, precipitating organ dysfunction and ultimately failure. Whilst the interplay between cells, mediators and cascades in acute inflammation is extremely complex, specific areas of it will be discussed in turn, especially in the context of three key areas of SIRS-related endothelial pathology, emphasising the current limitations and potential future options for SIRS therapy.

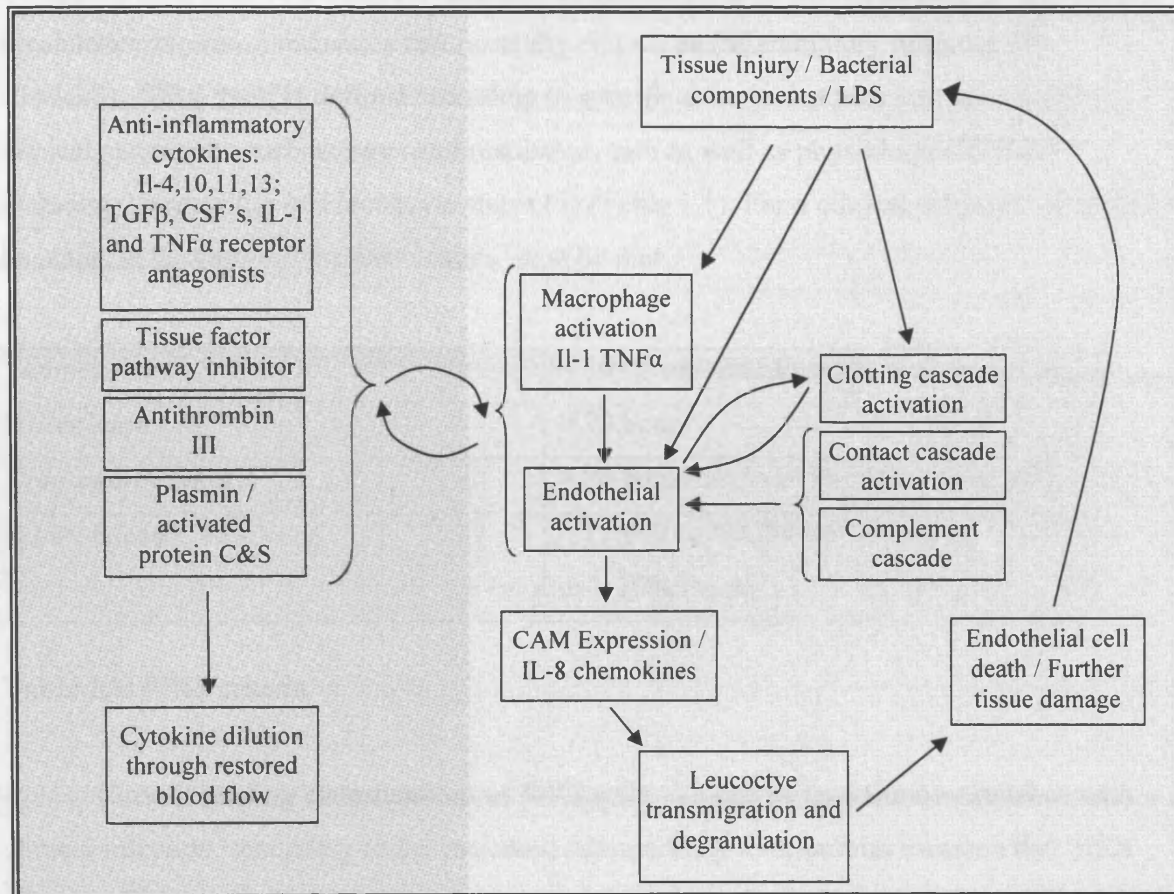


Figure 1.1: Simplified schematic illustration of events involved in acute inflammation. Pro-inflammatory and clotting events shown on the right (pink box); compensatory anti-inflammatory measures shown in blue to the left. Both systems are activated concurrently following initiating stimuli, with anti-inflammatory component activation acting to limit the numerous forward-feedback pro-inflammatory cascades to that necessary for dealing with the initiating stimulus. Predomination of either system leads to pathological sequelae known as the compensatory anti-inflammatory response syndrome (CARS) or systemic inflammatory response syndrome (SIRS).

1.1.1: The Systemic Inflammatory Response Syndrome:

The systemic inflammatory response syndrome is not a fixed entity but rather a qualifying term used to describe a spectrum of pathological severity that follows the breakdown of control measures that normally delimit an inflammatory response (4). Clinically, SIRS itself is defined according to specific criteria that take into account both clinical parameters such as heart and respiratory rate as well as physiological indices including temperature and leucocyte status (5) (Table 1.1). For a clinical diagnosis of SIRS to be made, at least two of the four criteria must be met.

Temperature	< 36° C or > 38° C
Heart Rate	> 90 bpm
Respiratory Rate	> 20 breaths/min or PaCO ₂ < 32 mmHg
White Blood Cell Count	> 12,000 or < 4,000 cells/mm ³ or > 10% bands

Table 1.1: SIRS criteria.

Current grading classifications of SIRS acknowledge its frequent co-existence with clinical infection, secondary to the increased susceptibility to microbial invasion that SIRS associated leucocyte dysfunction and coagulopathy brings (4, 6). Therefore, once SIRS has been identified in the presence of infection, it is termed sepsis, progressing through severe sepsis (if associated with organ dysfunction), septic shock, multi-organ dysfunction syndrome (MODS) and finally organ failure and death. Although there is a considerable armamentarium of anti-microbial drugs available to limit SIRS associated infection, the generalised inflammatory response has remained the principal determinant of outcome because of its direct pathological impact on the patient. This finding follows several clinical studies that demonstrate high mortality rates despite early anti-microbial therapy, plus similar mortality rates in both culture positive and culture negative patient groups (5, 7, 8). Furthermore, as each organ system progressively fails, mortality rates rise steeply, regardless of treatment with anti-endotoxin antibodies (9). So although mortality from SIRS frequently follows and coexists with infection, major tissue injury alone is sufficient to trigger an uncontrolled inflammatory response, without the need for associated clinical infection (8, 10). This is particularly important for SIRS associated with major tissue damage associated with burn

injury, polytrauma or major surgery, where overwhelming inflammation follows widespread activation of tissue macrophages and the alternative complement pathway (11-13). This situation underlines the need for a better understanding of those factors that actually drive the systemic inflammatory response, irrespective of co-infection or what the initiating stimulus actually was (14). Moreover, it appears that genetic factors play a significant part in determining the voracity and host susceptibility to SIRS, meaning that no two patients are likely to react in the same way to a given initiating event (15).

1.1.2: SIRS Therapy and the Vascular Endothelium:

Current anti-SIRS therapies have attempted to break the inflammatory cycle at relatively specific points within the overall inflammatory mechanism, including mediator targets, components of the clotting system, cell-cell interactions and cell signalling targets to name but a few (6, 16). Unfortunately, only activated protein C has as yet, been shown to significantly reduce the mortality of patients with severe sepsis (17). The failure of other approaches undoubtedly relates to the tremendous complexity of the inflammatory mechanism, complete with multiple parallel pathways that interlink separate components of the process together by multiple routes. This may explain why specific inhibition of single cytokines has generally failed to halt the pathological progression of systemic inflammation, typified by the poor outcomes in clinical trials with both Il-1 and TNF α antagonists (18, 19). These and other results highlight the need to break the inflammatory cycle at a more fundamental level; a point where different parallel pathways have already converged to produce a net functional outcome. One such possible target is the endothelium, which performs a core role in both co-ordinating and contributing to much of the inflammatory response, following its early activation by inflammatory signals (16). Endothelial activation describes a change in endothelial behaviour manifest through specific mediator production, altered permeability, interaction with circulating leucocytes (with associated endothelial apoptosis) and activation of the coagulation cascade (20) (Figure 1.2).

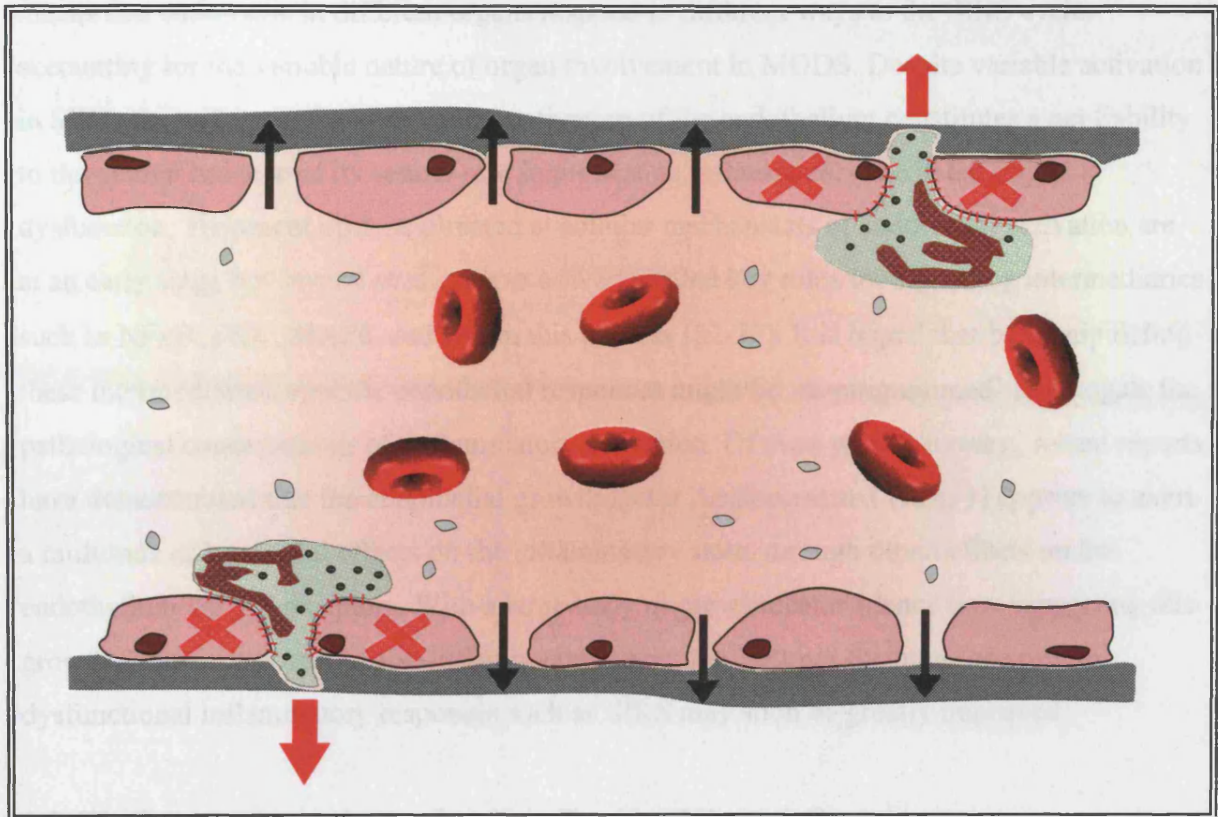


Figure 1.2: Schematic illustration of events following endothelial activation during the acute inflammatory response. Figure presents a cut-away view of a small blood vessel containing erythrocytes, platelets and leucocytes. Blood bourn cytokines activate both circulating leucocytes and the endothelium, leading to complementary cell adhesion molecule expression and leucocyte diapedesis between individual endothelial cells (red arrows). Leucocyte – endothelial interaction also results in endothelial apoptosis (red crosses), exposing basement membrane components and propagating coagulation. Finally, endothelial cell cytoskeletal changes produce large gaps between individual endothelial cells through which large quantities of protein-rich fluid can leak out into the interstitium (black arrows).

Endothelial activation per se is not an all-or-nothing response however, and reflects the endothelium's inherent flexibility as it functions to integrate the specific needs of local tissues and systemic events in a manner that varies both temporally and spatially (21). This means that endothelia in different organs respond in different ways to the SIRS cycle, accounting for the variable nature of organ involvement in MODS. Despite variable activation in SIRS, the widespread and sustained activation of the endothelium constitutes a net liability to the patient because of its central role in promoting inflammatory mediated organ dysfunction. Treatment options directed at cellular mechanisms of endothelial activation are at an early stage but several studies have now identified key roles for signalling intermediaries such as NF κ B, PKC, MAPK and NO in this process (22-27). It is hoped that by manipulating these intermediaries, specific endothelial responses might be 're-programmed' to abrogate the pathological consequences of inflammatory activation. Of even greater interest, recent reports have demonstrated that the endothelial growth factor Angiopoietin-1 (Ang-1) appears to exert a multitude of beneficial effects on the inflammatory state, through direct effects on the endothelium via Tie receptors. With a large body of pre-clinical evidence now supporting this growth factor as a potential anti-inflammatory agent, the fortunes for future therapy in dysfunctional inflammatory responses such as SIRS may soon be greatly improved.

1.2: Tie Receptors and the Angiopoietin Family of Growth Factors:

Tie1 and Tie2 (short for tyrosine kinase with immunoglobulin-like and EGF-like domains) were discovered in the early 1990's during experiments designed to identify novel receptor tyrosine kinases (RTK's) involved in development of the cardiovascular system (28-30). Subsequent work to isolate a ligand for these receptors led to the discovery of the Angiopoietin family of growth factors, of which Ang-1 and 2 are the best understood, recognised for their agonist and antagonist properties respectively (31-33). Both Tie1 and Tie2 are expressed on the surface of endothelial cells and share considerable sequence homology, containing extracellular, transmembrane and intracellular domains (Figure 1.3). The extracellular portion begins with two immunoglobulin loops, followed by three EGF-like domains, then a second immunoglobulin loop, finally ending with three fibronectin type-III domains adjacent to the plasma membrane. Intracellularly lies a tyrosine kinase domain split by a kinase insert sequence, finally ending with the carboxy terminal tail (28, 34, 35) (36).

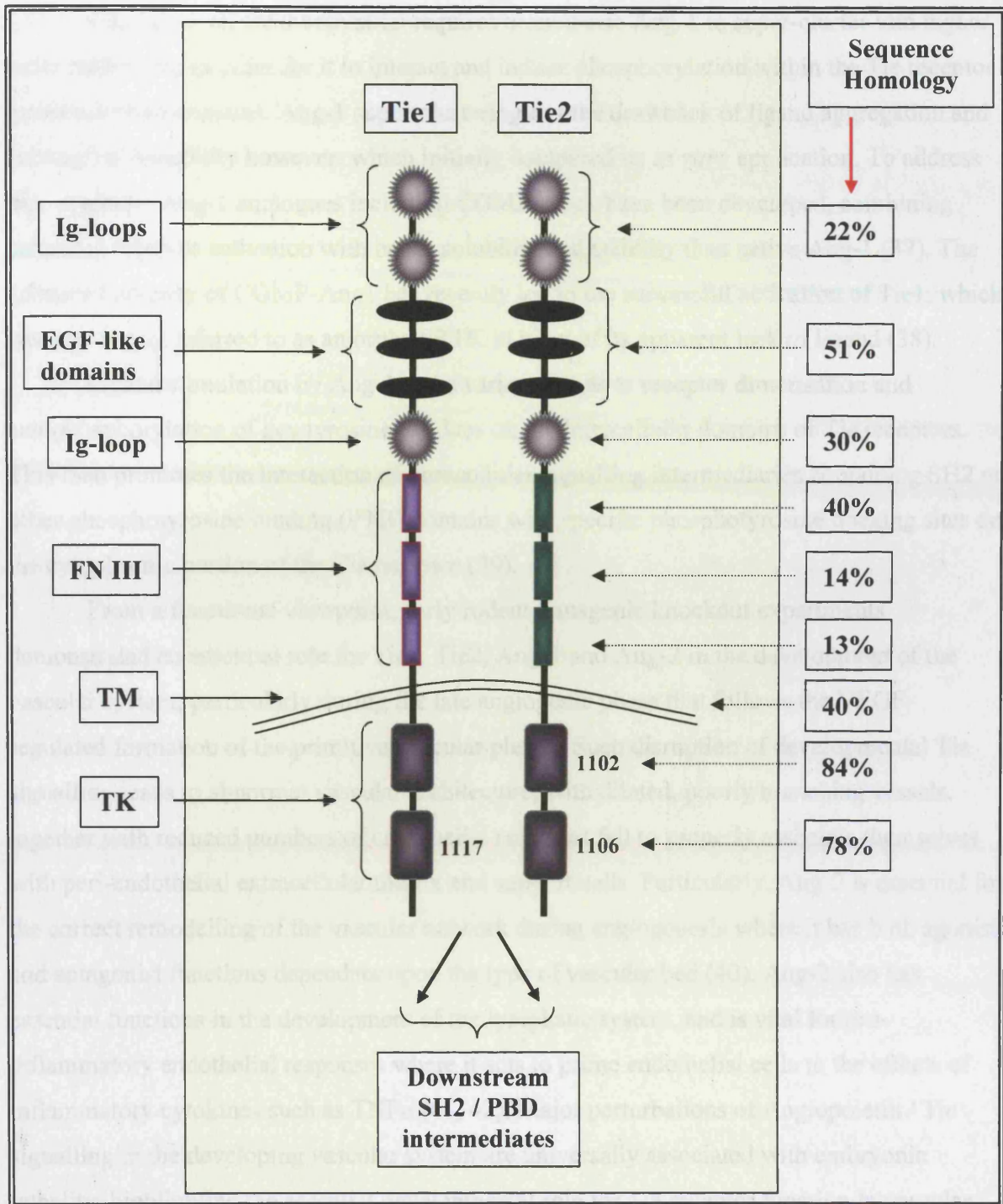


Figure 1.3: Schematic illustration of the Tie1 and Tie2 receptor tyrosine kinases. The molecular domain structure is highlighted on the left, whilst the sequence homology between key portions of each receptor are displayed on the right (FN III – Fibronectin type III repeat, TM – transmembrane region, TK – tyrosine kinase region, SH2 – Src homology 2 intermediates, PBD – phosphate binding domains).

Successful receptor activation requires monomeric Ang-1 to super-cluster into higher order multimers, in order for it to interact and induce phosphorylation within the Tie receptor tyrosine kinase domains. Ang-1 super-clustering has the drawback of ligand aggregation and subsequent instability however, which initially hampered its *in vitro* application. To address this, synthetic Ang-1 analogues including COMP-Ang1 have been developed, combining enhanced receptor activation with better solubility and stability than native Ang-1 (37). The enhanced potency of COMP-Ang1 has recently led to the successful activation of Tie1, which was previously referred to as an orphan RTK in view of its apparent lack of ligand (38).

Ligand stimulation by Ang-1 or its variants leads to receptor dimerisation and autophosphorylation of key tyrosine residues on the intracellular domains of Tie receptors. This then promotes the interaction of intracellular signalling intermediaries containing SH2 or other phosphotyrosine binding (PTB) domains with specific phosphotyrosine docking sites on the cytoplasmic portion of the Tie receptor (39).

From a functional viewpoint, early rodent transgenic knockout experiments demonstrated an essential role for Tie1, Tie2, Ang-1 and Ang-2 in the development of the vascular system, particularly during the late angiogenic phase that follows the VEGF-regulated formation of the primitive vascular plexus. Such disruption of developmental Tie signalling leads to abnormal vascular architecture, with dilated, poorly branching vessels, together with reduced numbers of endothelial cells that fail to properly associate themselves with peri-endothelial extracellular matrix and support cells. Particularly, Ang-2 is essential for the correct remodelling of the vascular network during angiogenesis where it has both agonist and antagonist functions dependant upon the type of vascular bed (40). Ang-2 also has essential functions in the development of the lymphatic system, and is vital for pro-inflammatory endothelial responses where it acts to prime endothelial cells to the effects of inflammatory cytokines such as TNF α (41, 42). Major perturbations of Angiopoietin / Tie signalling in the developing vascular system are universally associated with embryonic lethality, highlighting the essential developmental role for Tie receptor function in vascular maturation (33, 35, 42-44). Beyond neonatal angiogenesis, Tie receptor signalling retains an essential role in mature vessels, with Ang-1 promoting vascular quiescence, and Ang-2 destabilising the vasculature to allow vessel growth or regression as necessary for local tissue requirements (45, 46). Further *in vitro* and *in vivo* studies with both native and synthetic Ang-1 variants have now provided specific detail for its vascular stabilising actions, including roles involved in promoting endothelial survival (47), maintenance of endothelial barrier function (48), and the minimisation of cell adhesion molecule (CAM) expression necessary for

endothelial-leucocyte interactions (47). As will be described in the next section, all three of these endothelial roles form core components of acute inflammation, and the impact upon them from Ang-1 signalling undoubtedly feature in the ligands beneficial impact in animal models of sepsis (46).

In contrast to Ang-1 / Tie signalling, VEGF is active at the very earliest stages of vasculogenesis, where perturbations of either its timing or level of expression are universally fatal (49, 50). VEGF has an essential mitogenic effect on endothelial cells, and directs their migration, maturation and indeed specification into arteries or veins. After development, VEGF retains an important role in vascular homeostasis, acting as a pro-survival factor, particularly in fenestrated vascular beds. During inflammatory responses, VEGF participates by inducing endothelial permeability as well as CAM expression (51-54). As will be discussed, Ang-1 acts in part to counteract these pro-inflammatory effects of VEGF.

Finally, in comparing the mitogenic effects of Ang-1 with VEGF, the majority of *in vitro* experiments with Ang-1 report migration of endothelial cells and capillary tubule formation but no increase in overall cell number (46, 55, 56), except work by Kanda et al., which did find a proliferative effect under similar conditions (57). Sustained, systemic administration of Ang-1 in rodent models has been shown to induce vascular proliferation however, resulting in larger, more numerous and increasingly branched vessels (33, 37). Whilst an angiogenic role for Ang-1 signalling has less of a direct part to play in acute inflammation, its administration as the synthetic analogue COMP-Ang1 has been shown to be remarkably effective at accelerating wound healing in a diabetic model of microvascular dysfunction (58). Where wound healing represents the biological end point for any acute inflammatory response, this can only be of benefit in situations where SIRS follows major tissue injury such as after a major burn.

1.2.1: Angiopoietin / Tie Signalling in the Regulation of Endothelial Permeability:

One of the most important roles for the endothelium during the acute inflammatory response concerns the regulated passage of blood components and inflammatory cells between the blood stream and the interstitium (59). In the resting state, endothelial permeability occurs either across endothelial cells themselves (transcellular route) or between them (paracellular route). Transcellular permeability involves the receptor-mediated transport of macromolecules and is critical for the establishment of correct osmotic forces across the endothelium. Paracellular permeability on the other hand has the potential to allow the

passage of all blood components across the endothelium, contingent upon the degree of separation between individual endothelial cells at inter-endothelial cell junctions (IEJs). Inter-endothelial permeability is normally maintained at a low level, allowing only the free passage of water and molecules of up to 3 nm in diameter by simple diffusion. During inflammatory responses however, certain vessels (especially post-capillary venules) greatly increase their permeability, mainly as a result of inter-endothelial gap formation through which all blood components can freely pass (60-63). This is an essential property of inflammation, allowing blood-borne immunoglobulins, cytokines and effector inflammatory cells to swiftly deploy from the circulation into sites of infection or tissue injury. However, where regulatory mechanisms restricting inflammation become overwhelmed as part of the SIRS process, the beneficial properties of enhanced permeability are offset by the unwanted leakage that occurs in vascular beds remote from the original source of the inflammatory stimulus (16). The lack of permeability control to large MW molecules distorts trans-vascular osmotic balance, with leaked protein persisting in the sub-endothelial space potentiating oedema further. This exacerbates tissue hypoxia, and is accompanied by inappropriate extravasation of phagocytes that interact with and pass across the activated endothelium (64). Unfortunately, leucocyte extravasation in this context merely propagates the inflammatory process, thereby accounting for a significant part of the organ dysfunction associated with severe SIRS. To date, despite great interest in the endothelium as a target for breaking the inflammatory cycle, no agent is as yet available that effectively inhibits excessive permeability associated with systemic inflammatory disease states, or at least not without an unacceptable cost from side effects (65). However, recent work with Ang-1 has identified a potent anti-permeability effect on both quiescent and *in vitro* models of endothelial activation. Whether this property will be of clinical benefit *in vivo* will depend to what extent Ang-1 controls the overall endothelial response to pro-permeability signalling. To this end, much work has been done to both define the mechanisms underlying endothelial permeability regulation as well as the specific actions upon this brought about by Angiopoietin signalling.

1.2.1.1: Mechanisms of Inter-Endothelial Permeability Control:

The vast majority of inflammatory-stimulated vascular leakage occurs by the paracellular route, through the IEJ. Under resting conditions, the generation of an effective inter-endothelial barrier is achieved through adhesive protein complexes known as tight junctions (TJs) and adherens junctions (AJs). Whilst TJs are particularly abundant in relatively

impermeable vessels such as those found at the blood brain barrier, adherens junctions predominate in the comparatively loose IEJ's found in post-capillary venules (66, 67). Given the latter vessels highly responsive role in inflammation, the adherens junction is recognised as a prime regulator of IEJ permeability, and is based around the transmembrane glycoprotein VE-Cadherin. Figure 1.4 presents a simplified illustration of the interaction between two endothelial cells at an adherens junction.

Adherens junction adhesion is mediated through homophilic calcium-dependent bonding between the extracellular portions of VE-Cadherin. Through intermediary catenin molecules, the cytoplasmic tail of VE-Cadherin then associates with the actin cytoskeleton, maintaining its peripheral distribution and forming a bridge through which cytoskeletons of adjacent cells are indirectly coupled (68). This association is critical for IEJ adhesion, serving to counterbalance the cytoskeletal traction that otherwise acts to produce intercellular separation, especially when re-distributed to form centralised stress fibers (69-71). Indeed, the coupling of inter-cellular VE-Cadherin is inherently important in the maintenance of the peripherally orientated actin cytoskeleton. During IEJ establishment and subsequent inflammatory disruption, AJ mediated cell-cell adhesion is largely governed by the phosphorylation state of cadherin-catenin components, and specific kinases and phosphatases exist for this purpose (59, 72, 73).

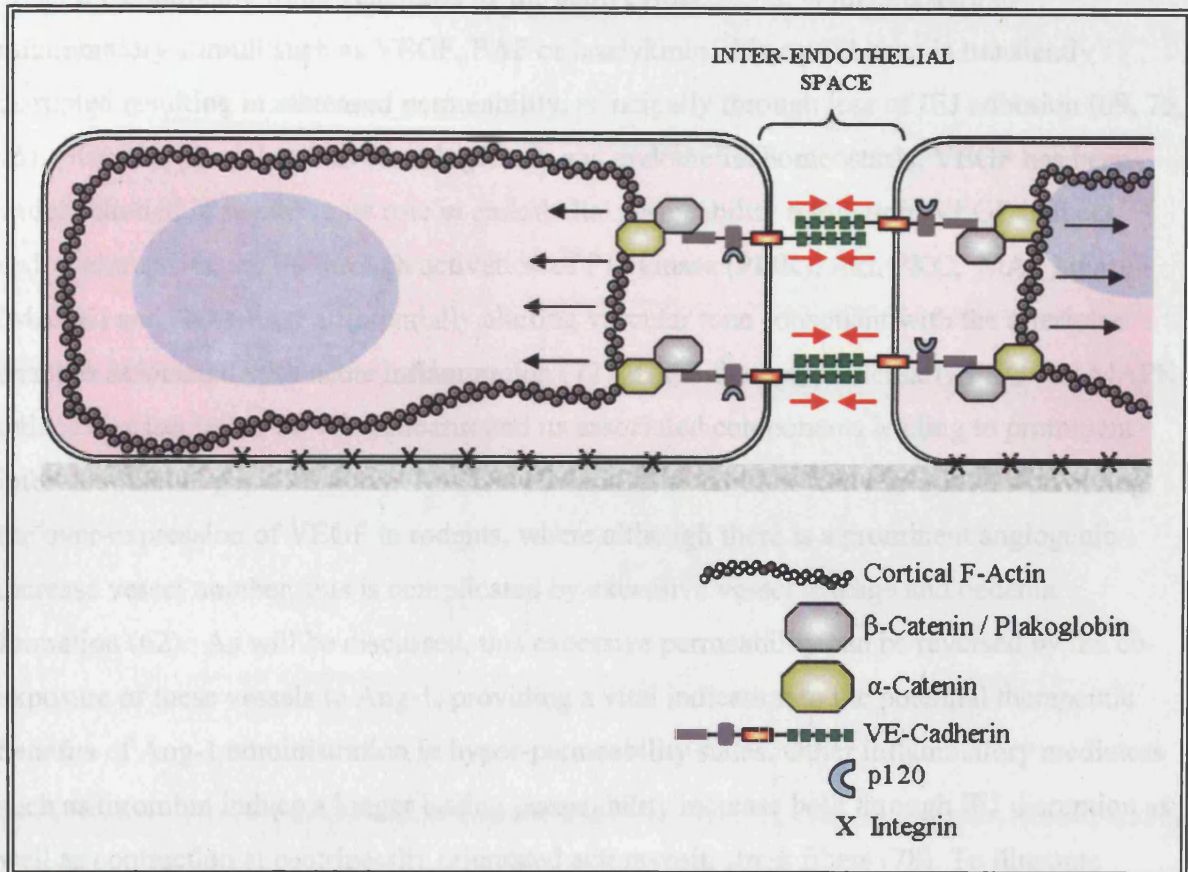


Figure 1.4: Schematic illustration of inter-endothelial adhesion mediated by VE-Cadherin at an adherens junction. Inter-endothelial adhesion results from calcium dependent homophilic binding of VE-Cadherin extracellular domains. The cytoplasmic tail of VE-Cadherin associates with β -catenin, which in turn binds to the actin cytoskeleton via α -catenin. A third catenin, p120 is an essential regulatory component of adherens junctions, and binds to the juxtamembrane region of VE-Cadherin (74). Intercellular adhesion at adherens junctions (red arrows) serves to counterbalance the centripetally orientated force generated by the cortical cytoskeleton (black arrows) to maintain tight barrier control (see main text for details).

1.2.1.2: Induction of Permeability:

Under resting conditions, strong cell-cell and cell-matrix cohesion is sufficient to offset the contractile force generated by the actin cytoskeleton. With exposure to inflammatory stimuli such as VEGF, PAF or bradykinin, this equilibrium is transiently disrupted resulting in increased permeability, principally through loss of IEJ adhesion (69, 75, 76). Given its pivotal role in vasculogenesis and endothelial homeostasis, VEGF has been widely studied in regard to its role in endothelial permeability regulation. VEGF induces endothelial permeability through activation of PI3 kinase (PI3K), Akt, PKC, MAP kinase (MAPK) and NO whilst differentially altering vascular tone consonant with the arteriolar changes associated with acute inflammation (77). These factors, particularly PKC and MAPK induce disassociation of VE-Cadherin and its associated components leading to prominent inter-endothelial gap formation. This is well demonstrated in *in vivo* experiments involving the over-expression of VEGF in rodents, where although there is a prominent angiogenic increase vessel number, this is complicated by excessive vessel leakage and oedema formation (62). As will be discussed, this excessive permeability can be reversed by the co-exposure of these vessels to Ang-1, providing a vital indication to the potential therapeutic benefits of Ang-1 administration in hyper-permeability states. Other inflammatory mediators such as thrombin induce a longer lasting permeability increase both through IEJ disruption as well as contraction at centripetally orientated actomyosin stress fibers (78). To illustrate enhanced permeability by actomyosin contraction and IEJ disruption, Figure 1.5 presents a summary of the signalling events involved in endothelial leakage induced by thrombin. Weakened IEJ adhesion follows PKC mediated phosphorylation of VE-Cadherin-catenin components (54, 79-81). Phosphorylated AJ components then lead to the dissociation of the AJ complex, and in the case of VEGF, VE-Cadherin has been shown to be internalised away from the cell membrane in a MAPK / Src dependent manner (52, 53, 82). This allows separation to occur between IEJ cell membranes, the extent of which depends upon the contractile state of the actin cytoskeleton. Inter-endothelial gap formation follows actomyosin contraction secondary to myosin light chain kinase phosphorylation of myosin light chain (MLC) (83). This process is perpetuated by RhoA / Rho kinase inhibition of myosin light chain phosphatase through the prevention of MLC de-phosphorylation (84). RhoA is also involved in the re-organisation of cortical F-actin to centrally located actin stress fibers (85, 86), producing maximal centripetal force generation and the creation of large inter-endothelial gaps. In a similar manner to thrombin, neutrophils induce inter-endothelial gaps both through

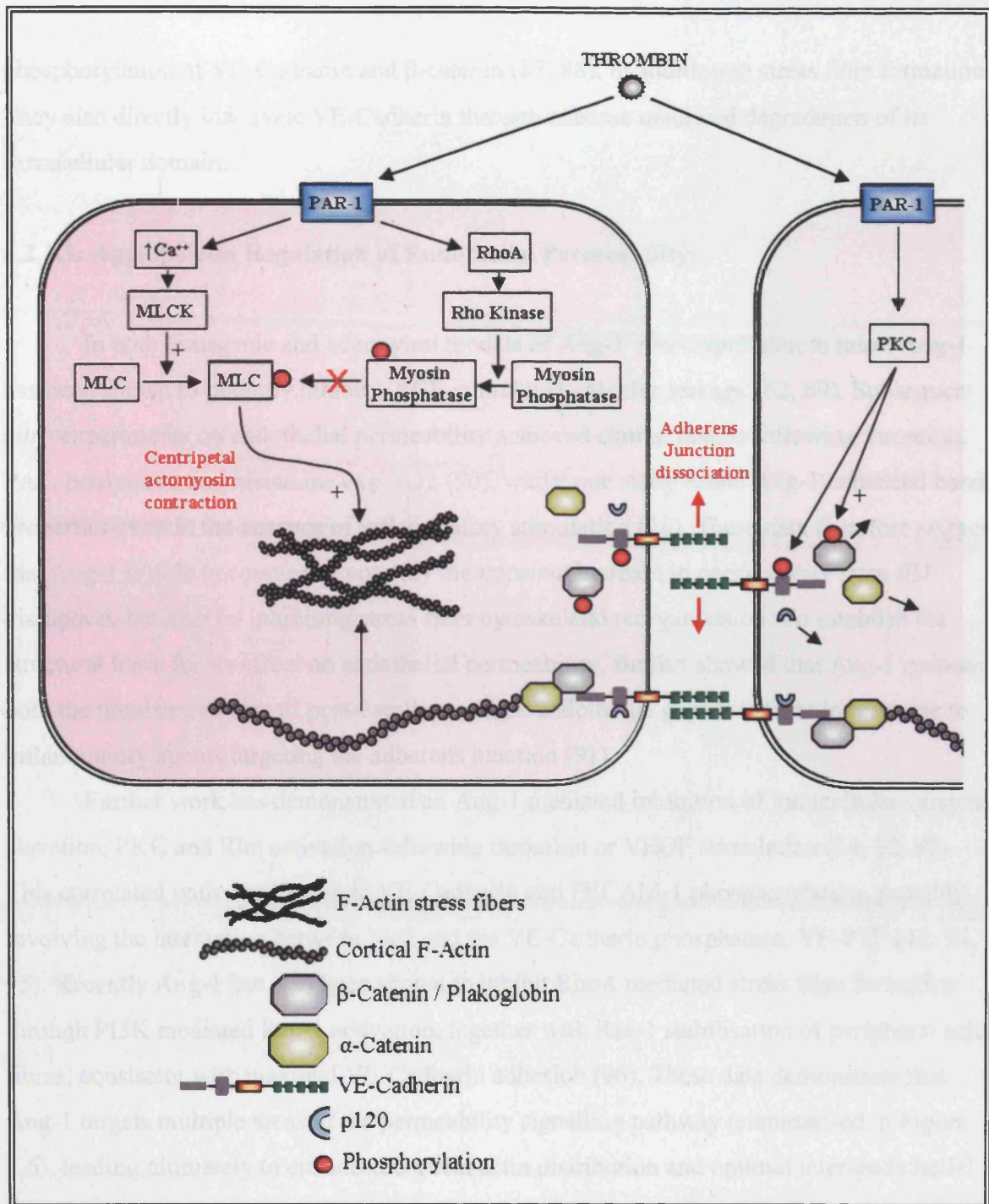


Figure 1.5: Schematic illustration of key events involved with endothelial barrier reduction by thrombin. Increased endothelial permeability results from both the dissociation of VE-Cadherin-catenin complexes and activation of centripetally-orientated actomyosin contraction. Shown are the calcium dependent activation of myosin light chain kinase and its phosphorylation of myosin II light chain following thrombin stimulation of the receptor PAR-1. This step allows actomyosin coupling and is augmented by RhoA mediated inhibition of myosin phosphatase and stimulation of centralised stress fiber formation. Certain isoforms of PKC directly phosphorylate VE-Cadherin components leading to loss of interendothelial linkage and dissociation of associated p120 and β -catenin.

phosphorylation of VE-Cadherin and β -catenin (87, 88), in addition to stress fibre formation. They also directly inactivate VE-Cadherin through elastase mediated degradation of its extracellular domain.

1.2.1.3: Angiopoietin Regulation of Endothelial Permeability:

In both transgenic and adenoviral models of Ang-1 over-expression in mice, Ang-1 has been shown to potently inhibit VEGF-stimulated vascular leakage (62, 89). Subsequent *in vitro* experiments on endothelial permeability achieved similar results following thrombin, PAF, bradykinin and histamine exposure (90), whilst one study found Ang-1 enhanced barrier properties even in the absence of inflammatory stimulation (48). These data therefore suggest that Ang-1 is able to counteract not only the transient increase in permeability from IEJ disruption, but also by inhibiting stress fiber cytoskeletal reorganisation. To establish the structural basis for its effect on endothelial permeability, Baffert showed that Ang-1 reduces both the number and size of post-capillary venule endothelial gaps that form in response to inflammatory agents targeting the adherens junction (91).

Further work has demonstrated an Ang-1 mediated inhibition of intracellular calcium elevation, PKC and Rho activation following thrombin or VEGF stimulation (54, 92, 93). This correlated with a reduction in VE-Cadherin and PECAM-1 phosphorylation, possibly involving the interaction between Tie2 and the VE-Cadherin phosphatase, VE-PTP (48, 94, 95). Recently Ang-1 has also been shown to inhibit RhoA mediated stress fibre formation through PI3K mediated Rac-1 activation, together with Rac-1 stabilisation of peripheral actin fibres, consistent with maximal VE-Cadherin adhesion (96). These data demonstrate that Ang-1 targets multiple areas of the permeability signalling pathway (summarised in Figure 1.6), leading ultimately to enhanced cortical actin distribution and optimal inter-endothelial AJ cohesion.

In contrast to Ang-1, Ang-2 can exert an antagonistic effect at Tie 2 receptors, and recent work suggests that this plays a significant role in systemic inflammatory states. In two recent studies, patients with sepsis have been found to have elevated levels of circulating Ang-2, correlating most closely with the severity of illness and serum TNF α level (97, 98). Murine and *in vitro* studies using Ang-2 have demonstrated an increase in both endothelial monolayer permeability and apoptosis (98-101).

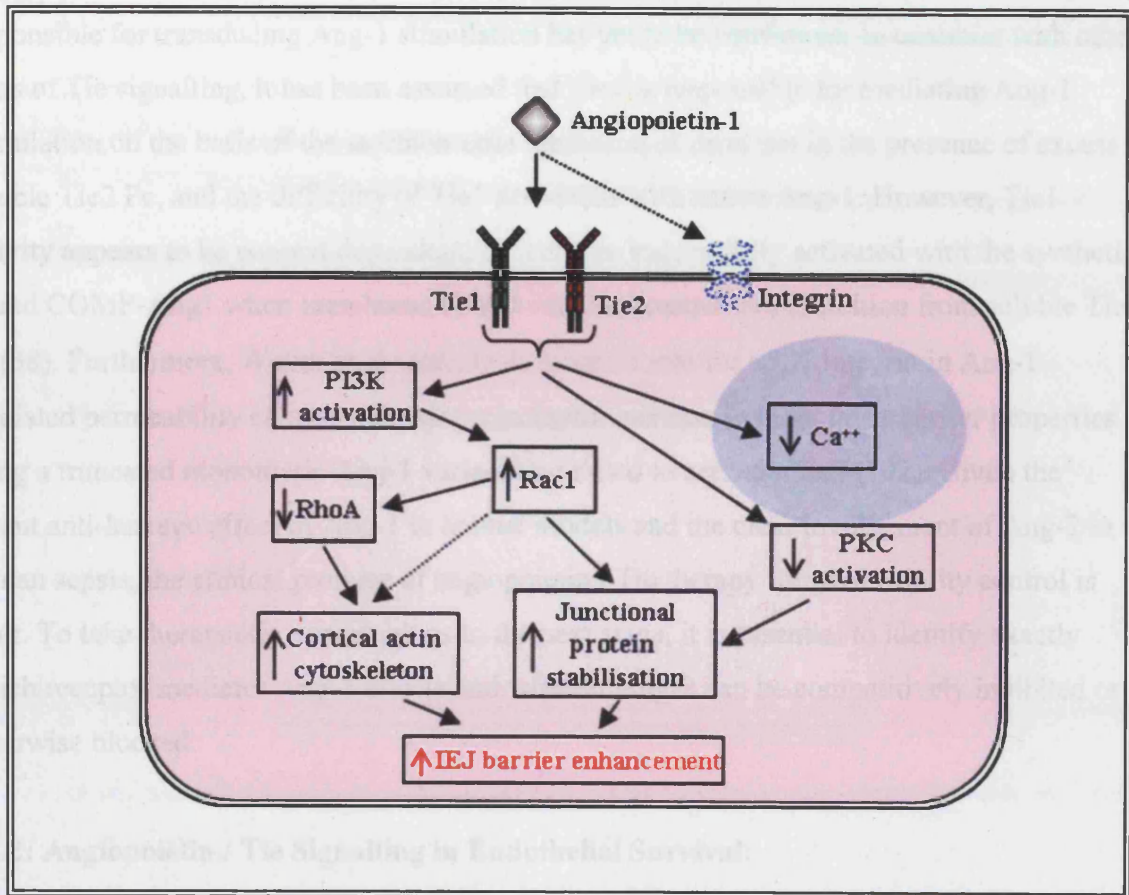


Figure 1.6: Schematic illustration of the known effects of Ang-1 on endothelial monolayer barrier functions. Operating through either Tie1, Tie2 or integrin receptors, Ang-1 reduces baseline monolayer permeability through inhibition of junctional protein phosphorylation, including VE-Cadherin. In addition, Ang-1 inhibits Ca⁺⁺ elevation and Rho kinase / PKC activation that follows endothelial activation with thrombin.

As Ang-2 inhibits Tie2 phosphorylation (32), these data suggest that endothelial barrier integrity and survival both depend on some level of constitutive Tie2 activity. Consistent with this, in one study gene silencing of Tie2 led to RhoA dependent myosin light chain phosphorylation and cytoskeletal changes associated with enhanced endothelial leakage, in the same manner as that seen following stimulation with Ang-2 (98).

Despite consensus agreement on permeability signalling, which cell surface receptor is responsible for transducing Ang-1 stimulation has yet to be confirmed. In common with other areas of Tie signalling, it has been assumed that Tie2 is responsible for mediating Ang-1 stimulation on the basis of the stoichiometric inhibition of its effect in the presence of excess soluble Tie2 Fc, and the difficulty of Tie1 activation with native Ang-1. However, Tie1 activity appears to be context dependent, as it can be successfully activated with the synthetic ligand COMP-Ang1 when membrane bound with no competitive inhibition from soluble Tie1 Fc (38). Furthermore, Weber et al recently proposed a role for $\alpha 5\beta 1$ integrin in Ang-1 mediated permeability control following successful increase in monolayer barrier properties using a truncated monomeric Ang-1 variant that failed to activate Tie2 (102). Given the potent anti-leakage effect of Ang-1 in animal models and the clear involvement of Ang-2 in human sepsis, the clinical promise of angiopoietin / Tie therapy for permeability control is clear. To take therapeutic opportunities to the next stage, it is essential to identify exactly which receptor mediates Ang-1 effects and whether Ang-2 can be competitively inhibited or otherwise blocked.

1.2.2: Angiopoietin / Tie Signalling in Endothelial Survival:

The formation of a functional vascular system through vasculogenesis and subsequent angiogenesis necessitates a delicate balance of both endothelial cell growth and regression (49). This endothelial turnover is co-ordinated by cues derived from components of the extracellular matrix, soluble signalling factors and interactions with surrounding cells. Indeed, during early vasculogenesis, VEGF and bFGF play critical anti-apoptotic roles in endothelial cells, and represent the major stimuli for the formation of the primitive vascular network. Further remodelling and vessel stratification then occurs during the subsequent process of angiogenesis, with stable interactions being formed between endothelial cells and pericytes embedded in the basement membrane (103). Of key importance in this regard is the effects of pericyte derived Ang-1 (33), and under competition with the antagonist actions of Ang-2,

acting to de-stabilise endothelial-pericyte interactions. Removal of certain growth stimuli (such as VEGF) can lead to endothelial apoptosis and vessel regression in certain mature vascular beds (104), whilst signalling factors such as Endostatin, Angiostatin and Thrombospondin actively induce endothelial cell apoptosis and vessel regression (105). In a similar manner, reduced adhesion to structural extracellular elements is also pro-apoptotic to endothelial cells (106), resulting in the apoptotic process known as anoikis.

Beyond vessel growth and development, endothelial cell apoptosis is now recognised to play a key role in several pathological disease processes including inflammation (107). Maintaining integrity of the endothelium is essential if widespread microvascular coagulation is to be counteracted, as evidenced by the endothelial cell apoptosis acknowledged to be a vital step in the pathogenesis of acute thrombosis around atherosclerotic plaques (108). Furthermore, inflammatory microvascular damage is centrally involved in bacterial invasion, where gram negative LPS is a potent stimulant for endothelial apoptosis (109), that will once again reveal sub-endothelial collagen and promote thrombosis. Endothelial apoptosis is also likely to play a significant part in the progressive tissue necrosis seen in the zone of stasis within cutaneous burns, a topic of great scientific interest given the burn induced endothelial dysfunction and its ability to recover with rapid and appropriate first aid treatment.

1.2.2.1: Mechanism of Endothelial Apoptosis:

At the heart of the apoptotic process is the caspase family of cysteine proteases. These enzymes form the machinery that effect the dissolution of a cell and its constituents following cleavage of their target proteins after an aspartate residue (110). At the outset of apoptosis (Figure 1.7), initiator caspases undergo auto-activation, going on to catalytically cleave and activate effector pro-caspases. Effector caspase activation marks the point of no return towards irreversible cell death, and involves the degradation of numerous cellular targets including nuclear proteins, proteins involved in signal transduction pathways and cytoskeletal targets (107). Extrinsic caspase activation is an essential route for removal of unwanted endothelial cells during development and is mediated by activation of trans-membrane receptors of the tumour necrosis factor superfamily, including TNFR and Fas (111).

Intrinsic apoptosis involves the release of cytochrome c from mitochondria from various stimuli to form the so-called Apoptosome, which then leads into the activation of initiator caspase 9 and subsequently effector caspase 3. This form of apoptosis involves irreversibly damaged cells (eg. those damaged by ionising radiation), or those devoid of growth factor signalling (T12) amongst others.

12.12: Angiopoietin-1 Mediated Survival of Endothelial Cells

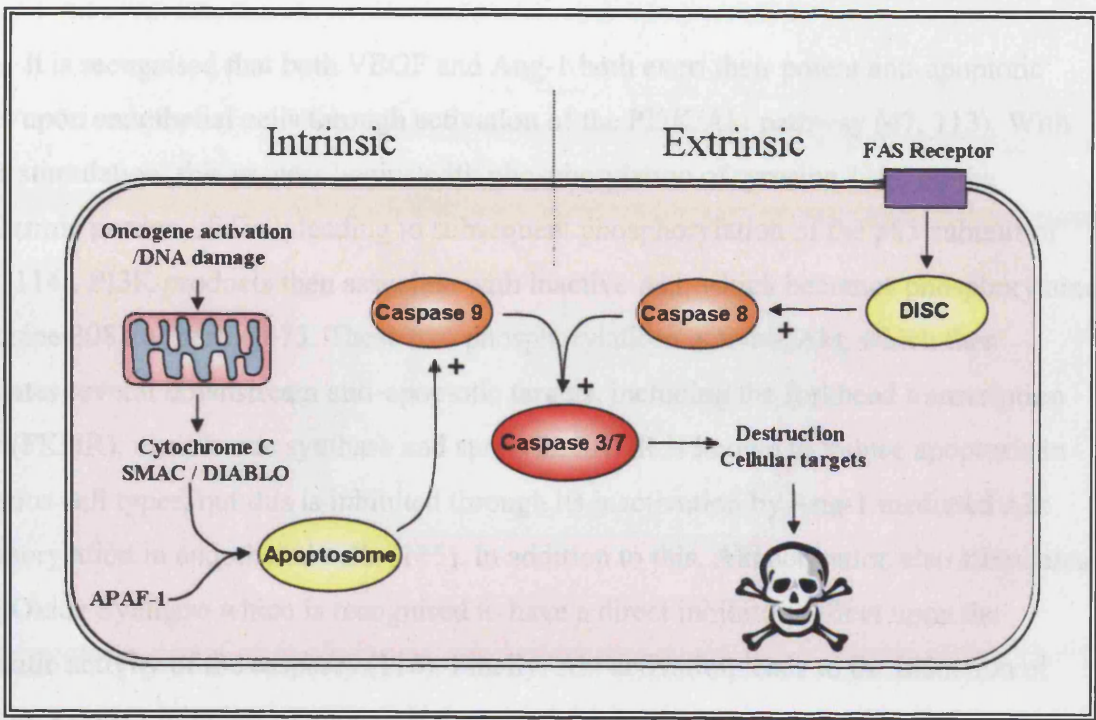


Figure 1.7: Schematic illustration of the Caspase system and cell death by apoptosis. Initiator caspases are activated by either intrinsic or extrinsic mechanisms (see text) which in turn lead to irreversible demolition of cell constituents by the effector caspases 3 and 7.

Intrinsic caspase activation involves the release of cytochrome c and other intermediates from mitochondria to form the so-called Apoptosome, which then feeds into the activation of initiator caspase 9 and subsequently effector caspase 3. This form of apoptosis removes irrevocably damaged cells (e.g. those damaged by ionising radiation), or those devoid of growth factor signalling (112) amongst others.

1.2.2.2: Angiopoietin-1 Mediated Survival in Endothelial Cells:

It is recognised that both VEGF and Ang-1 both exert their potent anti-apoptotic effects upon endothelial cells through activation of the PI3K/Akt pathway (47, 113). With Ang-1 stimulation, this process begins with phosphorylation of tyrosine 1102 on the cytoplasmic portion of Tie2, leading to subsequent phosphorylation of the p85 subunit of PI3K (114). PI3K products then associate with inactive Akt, which becomes phosphorylated at tyrosine 308 and serine 473. These two phosphorylations activate Akt, which then modulates several downstream anti-apoptotic targets, including the forkhead transcription factor (FKHR), nitric oxide synthase and survivin. FKHR is known to induce apoptosis in numerous cell types, but this is inhibited through its inactivation by Ang-1 mediated Akt phosphorylation in endothelial cells (115). In addition to this, Akt activation also stimulates Nitric Oxide Synthase which is recognised to have a direct inhibitory effect upon the enzymatic activity of the caspases (116). Finally, Akt activation leads to the induction of survivin, a potent inhibitor of apoptosis that also inhibits the Caspase system (117, 118). These events are summarised in Figure 1.8.

Whilst much is known about the role of Tie2 in Ang-1 mediated survival, the part played by Tie1 in this process has only recently been proposed due to its relative insensitivity to known Tie receptor ligands. However, data from both *in vivo* and *in vitro* work have now implicated Tie1 in endothelial cell survival (43, 119). By identifying the possibility of a significant role for Tie1 in mediating endothelial survival there is the possibility that this may form a target for future therapeutic intervention.

Under normal conditions, the endothelium presents a relatively non-adherent surface to circulating leucocytes that come into contact with the vessel wall. Furthermore, the cellular component of circulating blood is predominantly kept away from the vessel wall and away from the luminal surface of the endothelium. However, inflammatory changes

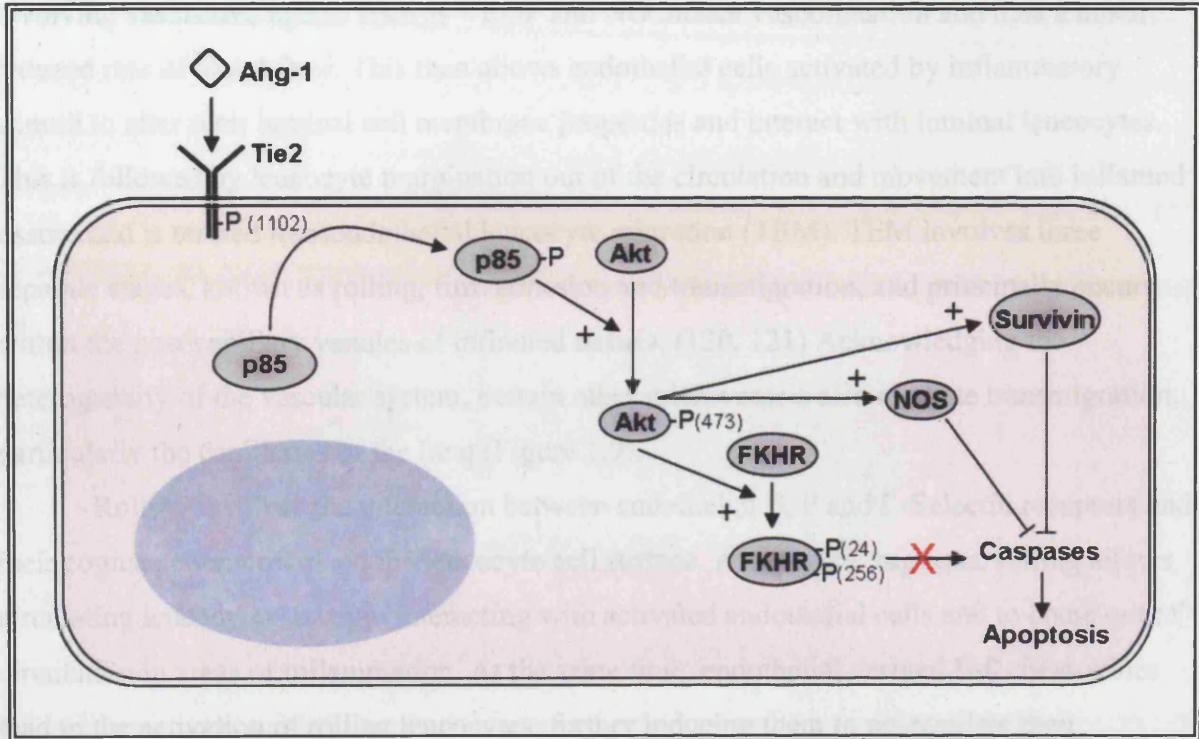


Figure 1.8: Schematic illustration of Ang-1 mediated survival signalling in endothelial cells. Ang-1 activates Tie2 and subsequently Akt through the PI3K pathway. Activated Akt then inhibits FKHR, whilst stimulating NO and Survivin production. This in turn leads to reduced apoptosis through inhibition of Caspase activity.

1.2.3: Angiopoietin / Tie Signalling and Inflammatory Activation of the Endothelium:

Under normal conditions, the endothelium presents a relatively non-adherent surface to circulating leucocytes that come into chance contact with the vessel wall. Furthermore, the cellular component of circulating blood is predominantly kept towards the centre of the vessel and away from the luminal surface of the endothelium. However, inflammatory changes involving vasoactive agents such as VEGF and NO induce vasodilatation and thus a much reduced rate of blood flow. This then allows endothelial cells activated by inflammatory stimuli to alter their luminal cell membrane properties and interact with luminal leucocytes. This is followed by leucocyte margination out of the circulation and movement into inflamed tissues and is termed transendothelial leucocyte migration (TEM). TEM involves three separate stages, known as rolling, firm adhesion and transmigration, and principally occurs within the post capillary venules of inflamed tissues. (120, 121) Acknowledging the heterogeneity of the vascular system, certain other microvessels also mediate transmigration, particularly the capillaries of the lung (Figure 1.9).

Rolling involves the interaction between endothelial E, P and L-Selectin receptors and their cognate counterparts on the leucocyte cell surface. As its name suggests, rolling allows circulating leucocytes to begin interacting with activated endothelial cells and to come out of circulation in areas of inflammation. At the same time, endothelial derived Il-8 chemokines lead to the activation of rolling leucocytes, further inducing them to up-regulate their production of endothelial specific adhesion molecules (122). Rolling is followed by firm adhesion, mediated by binding between leucocyte integrins and the immunoglobulin superfamily ligands, intercellular adhesion molecule-1 (ICAM-1) and vascular cell adhesion molecule-1 (VCAM-1) expressed on the endothelial cell surface. Although there are several leucocyte integrins, CD11a/LFA-1 and CD11b/MAC-1 (both β_2 integrins) together with VLA-4 (a β_1 integrin) represent those most important for leucocyte binding, each binding to endothelial ICAM-1 and VCAM-1 respectively (120). Firm adhesion is the most important component of the transmigration process, underlined by the lethal consequences of its absence in the clinical syndrome leucocyte adhesion deficiency (LAD), which as its name suggests, is characterised by a failure of ICAM-1 binding. Finally, leucocyte diapedesis across the endothelium is dependent upon binding between PECAM-1 expressed on both leucocyte and endothelial cells, where this is particularly well concentrated at inter-endothelial junctions. Disruption of PECAM-1 binding has been shown to prevent effective leucocyte

transmigration in both *in vitro* and *in vivo* models of inflammation (123). The physical process of transmigration requires the disruption of VE-Cadherin-mediated inter-endothelial coupling, together with Rho-GTPase controlled actin stress fibre formation. Both of which result in inter-endothelial gap formation that permits leucocyte passage between individual endothelial cells (124, 125).

These morphological alterations to endothelial cell shape highlight the communication role that endothelial CAMs serve over and above their intercellular adhesive capacities. Indeed, signals arising between endothelial cells and leucocytes produces clustering of adhesion

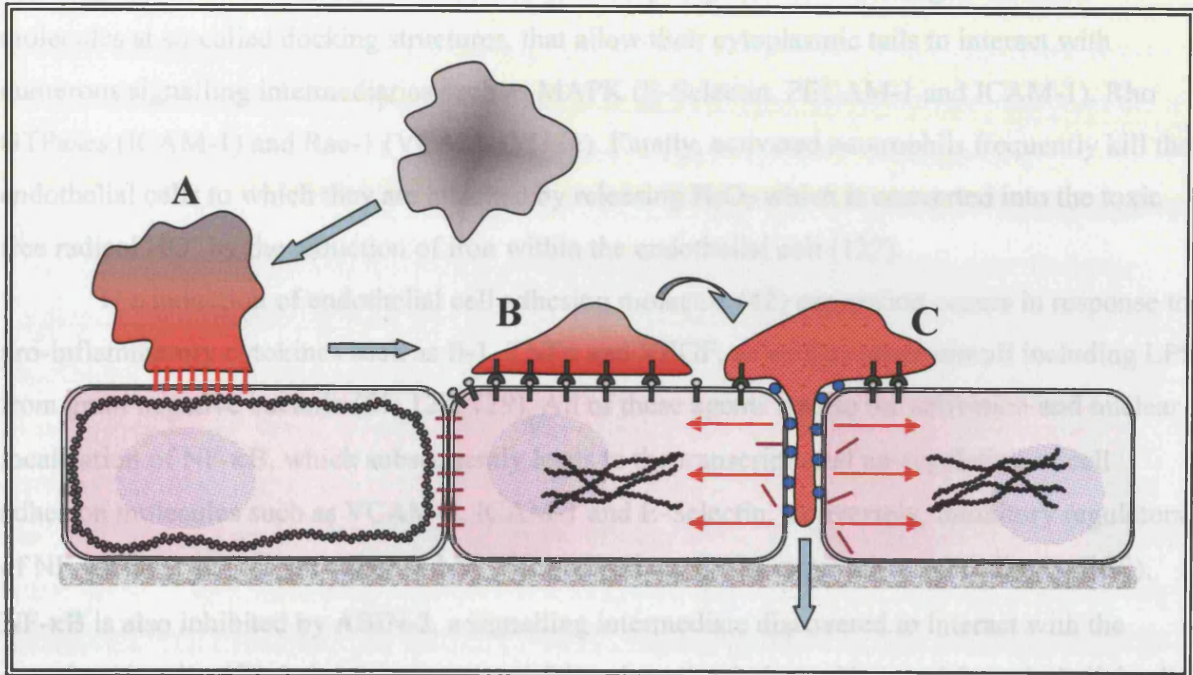


Figure 1.9: Schematic illustration of the three stages involved in leucocyte transendothelial migration (TEM). Circulating leucocytes contact selectins expressed on the luminal surface of activated endothelial cells in the process of rolling (A). This progresses to firm adhesion (B) through leucocyte β_2 and β_1 integrin binding to ICAM-1 and VCAM-1 expressed on the endothelial surface respectively. Finally, transendothelial migration follows interaction between endothelium and leucocyte PECAM-1, associated with the formation of inter-endothelial gaps. Gap formation involves the internalisation of VE-Cadherin (Shown) together with actin re-organisation to form stress fibers as described in the text (C). The progressive activation of adherent leucocytes is denoted by the progressive change from grey to red in response to Il-8 family chemokines released by the activated endothelium.

transmigration in both *in vitro* and *in vivo* models of inflammation (123). The physical process of transmigration requires the disruption of VE-Cadherin mediated inter-endothelial coupling, together with Rho GTPase controlled actin stress fibre formation, both of which result in inter-endothelial gap formation that permits leucocyte passage between individual endothelial cells (124, 125).

These morphological alterations to endothelial cell shape highlight the communication role that endothelial CAM's serve over and above their intercellular adhesive capacities. Indeed, areas of contact between endothelial cells and leucocytes produces clustering of adhesion molecules at so-called docking structures, that allow their cytoplasmic tails to interact with numerous signalling intermediaries such as MAPK (E-Selectin, PECAM-1 and ICAM-1), Rho GTPases (ICAM-1) and Rac-1 (VCAM-1) (126). Finally, activated neutrophils frequently kill the endothelial cells to which they are attached by releasing H₂O₂ which is converted into the toxic free radical HO[•] by the reduction of iron within the endothelial cell (127).

The induction of endothelial cell adhesion molecule (42) expression occurs in response to pro-inflammatory cytokines such as Il-1, TNF α and VEGF, as well as other stimuli including LPS from gram negative bacteria (51, 128, 129). All of these agents lead to the activation and nuclear localisation of NF- κ B, which subsequently leads to the transcriptional up-regulation of cell adhesion molecules such as VCAM-1, ICAM-1 and E-Selectin. Conversely, inhibitory regulators of NF- κ B such as I κ B are enhanced by NO and reduce CAM expression accordingly (130). NF- κ B is also inhibited by ABIN-2, a signalling intermediate discovered to interact with the cytoplasmic tail of Tie2 that is up-regulated following stimulation with Ang-1 in endothelial cells. Paradoxically, Ang-1 has been reported to transiently enhance the inflammatory activation of both endothelial cells and leucocytes by increasing membrane P-selectin translocation and β_2 integrin expression on each cell type respectively (131). However, the majority of evidence at present argues for Ang-1 acting in an anti-inflammatory manner where, for example, it is able to counteract VEGF CAM up-regulation as well as other pro-inflammatory mediators up-regulated by VEGF such as tissue factor (132, 133). Moreover, Ang-1 has also been shown to inhibit TNF α induced leucocyte trans-endothelial migration, by localising and maintaining the de-phosphorylated state of PECAM-1 at interendothelial junctions, as well as inhibiting Il-8 chemokine production (48, 90). Finally, *in vivo* work by Fiedler et al. identified a vital pro-inflammatory role for the Tie receptor antagonist Ang-2, which is stored and rapidly released from Weibel-Pallade bodies following inflammatory stimulation (41). They showed that Ang-2 null mice could support leucocyte rolling in response to TNF α stimulation, but that firm adhesion between leucocytes and the endothelium was only possible in control animals. This

work suggests a context-dependent role for Ang-2 in the modulation of endothelial responsiveness to inflammatory stimulants such as TNF α , through its inhibition of Tie receptor activation. Although the NF- κ B inhibitor ABIN-2 was found to interact with Tie2 only, little else is known of the impact of Tie1, if any, in Ang-1 mediated anti-inflammatory responses in endothelial cells.

1.3: Summary:

Acute inflammation is an essential component of host defence and repair mechanisms, but paradoxically becomes harmful when anti-inflammatory control measures decompensate following certain types of infection or tissue injury as part of SIRS. Although the inflammatory process is highly complex, the vascular endothelium reprises a fundamental role in inflammatory regulation, and it is now clear that the endothelial-specific growth factor Angiopoietin-1 has a significant part to play in the orchestration of numerous aspects of the endothelial inflammatory response. Although there is limited scientific data in the literature directly evaluating Ang-1 benefits in models of SIRS and sepsis, this remains a highly attractive concept, given the specific anti-inflammatory properties recently discovered plus the disappointing results from existing anti-SIRS therapies. To this end, whilst much has been learnt about Ang-1 signalling through Tie-2, only recently has it been possible to effectively activate the Tie-1 receptor. As Tie-1 is indispensable for proper vascular development, it is not surprising that emerging data now indicates a place for the receptor in the control of mature endothelial events such as apoptosis. With this established, what other roles might Tie1 mediate? In addition, there remain questions about the potential role played by integrins following its discovery in the transduction of angiopoietin signals in endothelial cells. If integrins mediate some aspect or other of Ang-1 signalling for example, then this will be an essential consideration when attempting to develop drug therapies.

1.4: Aims and Objectives:

In general terms, current treatment modalities for patients with SIRS / sepsis remain supportive only, relying on mechanical and pharmacological assistance for malfunctioning organ systems. Despite the very poor track record of novel immuno-modulatory therapies directed against SIRS processes, this remains a key goal for improving the survival of critically ill patients. It is now clear that steering the course of the inflammatory response is

going to require intervention at a fundamental level, and the work in this thesis was begun when Ang-1 had recently been shown to have great potential by counteracting numerous aspects of dysregulated inflammation. Ideally, Ang-1 therapy will offer similar benefits to patients as it has in animal models of sepsis, through reduced endothelial inflammatory responses and improved organ function. This would contribute greatly to the ability of medical and surgical treatments to deal with the underlying disease processes that are presently hampered by SIRS sequelae. If this proves to be the case, Ang-1 will hopefully take its place as one of the very few drugs available to improve patient survival, benefiting further from the added advantage that it already exists as a component of the vascular system when it comes to considering potential drug interactions. Therefore, the aims of this research are firstly to define specific roles of each Tie receptor in mediating the anti-inflammatory effects of Ang-1, and secondly to investigate the value and potential effects of Ang-1 in *in vitro* models of SIRS / sepsis using plasma from patients with these disorders.

With these aims in mind, this study seeks to test the following hypotheses:

1. That Tie1 and Tie2 have distinct roles in mediating the anti-apoptotic, anti-inflammatory and anti-permeability effects of Ang-1.
2. That Tie1 and Tie2 have distinct roles in mediating the intracellular signalling events initiated by Ang-1.
3. That Ang1 inhibits the pro-inflammatory effects of plasma from patients with SIRS.

To address these questions, gene silencing techniques have been employed to create endothelial cells deficient in Tie1 or Tie2 or both, permitting observations on the relative contribution of each receptor sub-type in endothelial inflammatory responses. To partner these observations, key downstream signalling events associated with Ang-1 stimulation have been evaluated in Tie deficient endothelial cells. The final chapter presents provisional data for the impact of Ang-1 on endothelial cells exposed to human SIRS plasma in the context of the aforementioned models of permeability, survival and CAM expression.

2.1: General Chemicals:

Bovine Gelatin (Sigma, USA)

Haematoxylin and Eosin (Sigma, USA)

Horseradish Peroxidase (Sigma, USA).

Fluorescein isothiocyanate Conjugated Bovine Albumin (Sigma, USA)

Fluorescein isothiocyanate Conjugated Dextran, MW 10,1000 (Sigma, USA)

Fluorescein isothiocyanate labelled Phalloidin (Sigma, USA)

Marvel original dried skimmed milk, (Premier International Foods, UK)

PVA mounting solution with DABCO (Sigma, USA)

Trypan Blue Solution (Sigma, USA)

Trypsin solution (Lonza, Belgium)

Trypsin Neutralising Solution (Lonza, Belgium)

Bio-Rad Protein Assay Solution (Bio-Rad GmbH, USA)

2.2: General Solutions:

PBS: 10x stock solution (Cambrex, UK) diluted with water 1:10 to give: KH_2PO_4 144mg/l, NaCl 9000mg/l, Na_2HPO_4 795 mg/l. Mg^{++} and Ca^{++} free, pH 7.4.

TBS: 25mM Tris and 144mM NaCl, pH 7.4.

Western Blot Transfer Buffer: 25mM Tris, 190 mM glycine and 20% methanol.

SDS-PAGE Running Buffer: 25mM Tris, 190mM glycine and 0.1% Sodium Dodecyl Sulphate (SDS).

Lysis Buffer: 50mM Tris pH 7.4, 50mM NaCl, 1mM NaF, 1mM EGTA, 1mM Na Orthovanadate (added at time of use), 1 Protease inhibitor Cocktail tablet (Roche, Germany) per 10 ml, 50µl 20%TX-100 per ml.

TBS TX-100 Solution: 50 ml 10X TBS stock, 450 ml water, 2.5 ml 20% TX-100.

Blocking Buffer – *Milk*: 1g Marvel powdered milk, 20ml TBS TX-100.

Blocking Buffer – *BSA*: 1g powdered BSA, 20ml TBS TX-100.

Ammonium Persulfate (APS): 1g APS, 1ml water.

3x Sample Buffer (SB): 1M Tris pH 6.8, 20% SDS, 100% Glycerol, 100mM EDTA pH 6.8, 0.2% Bromophenol Blue.

2x Sample loading Buffer DTT: 30mg DTT, 600µl 3x SB, 300µl water.

Paraformaldehyde solution: 4g Paraformaldehyde, 100ml 1x PBS, 200µl 1M NaOH

Solution A: 90mM p-Coumaric Acid in DMSO

Solution B: 250mM Luminol in DMSO

2.3: Commercial Kits:

Falcon[®] Cell Culture Inserts (3µm) with companion 24 well tissue culture plates (Becton Dickinson, USA)

Transwell[®] Permeable Supports (Corning, USA): 6.5 mm Diameter, 3.0µm pore, polyester membrane inserts in 24 well polystyrene plates.

Re-Blot Plus Mild Antibody Stripping kit (Chemicon, USA).

Caspase-Glo[®] 3/7 Assay (Promega, USA).

Lipofectamine[™] 2000 transfection reagent (Invitrogen, USA)

Sigmafast[™] OPD HRP detection kit (Sigma, USA)

All tissue culture plastics obtained from NUNC (Denmark) unless otherwise stated.

2.4: Antibodies:

Monoclonal Anti-human VCAM-1-Fluorecein (CD106), Monoclonal Anti-human ICAM-1-Fluorecein (CD54) Monoclonal Anti-human E-Selectin-Fluorecein (CD62E) (R&D Systems, USA).

ECL Anti-Rabbit IgG Horseradish Peroxidase linked F(ab) fragment and ECL Anti-mouse IgG HRP linked whole antibody (Amersham Biosciences, UK).

HRP linked anti-Goat Immunoglobulin (DAKO, Denmark).

Anti-hTie-2 neutralising antibody (Goat) and anti-hTie-1 detection antibody (Goat) (R&D Systems, USA).

Anti-Phospho-Akt (Ser 473), anti-phospho-p44/42 MAP Kinase, Anti-Akt and Anti-p44/42 MAP Kinase (Cell Signalling, USA).

Anti-Tie1 (C18) and Anti- Tie2 (C20) (Santa Cruz Biotechnology, USA).

2.5: Growth Factors and Cytokines:

Recombinant human Angiopoietin-1 and Angiopoietin-2 (R&D Systems, USA).

Recombinant Human Interleukin1 β (IL1 β) (BD Biosciences, USA).

Recombinant Human Tumour Necrosis Factor α (TNF α) and Vascular Endothelial Growth Factor (VEGF) 165 (Peprotech, London).

Human Thrombin (Sigma, USA).

COMP-Ang-1 (Alexis, Switzerland).

Human plasma samples (Harvested as part of project-specific trial at Leicester Royal Infirmary)

Fetal Calf Serum / FCS (Biosera, UK)

2.6: SiRNA Sequences:

Bespoke purified annealed double stranded short interfering RNA sequences were produced by MWG Biotech (Germany) with the following sequences:

Random: 5' AGU CCA UAA UGA GAA UCA ACC GAU UAU 3'

Tie1: 5'AGG AGA AGC AGA CAG ACG UGA UCU GGA 3'

Tie2: 5' CGA ACC AUG AAG AUG CGU CAA CAA GCU 3'

2.7: Culture of HUVEC:

HUVEC were commercially sourced from PromoCell (Heidelberg) as a pooled cell population. All experiments utilised HUVEC between passage 3 and 10. Routine culture took place in un-coated 80cm² flasks with passage 1:3 when 90% confluency was exceeded. Excess cells at low passage number were stored in liquid nitrogen. For passage, HUVEC were gently washed with PBS, followed by trypsinisation with room temperature 2x trypsin followed by the addition of an equal volume of Trypsin Neutralising Solution after complete

cell dispersal. The cell suspension was then pelleted by centrifugation at 220g for 4 minutes before being thoroughly re-suspended in complete media.

PromoCell HUVEC were cultured in PromoCell ECGM. This consisted of a basal formulation accompanied by a separate serum supplement mix. The addition of the supplement mix produced complete ECGM (Total serum 2%), and contained:

10 ml FCS

2 ml ECGS /H

0.1 ng/ml EGF

1.0 ng/ml bFGF

1.0 µg/ml Hydrocortisone

For experiments conducted under serum-free conditions, aliquots of basal medium without addition of the supplement mix were used. It is acknowledged that culture media constituents affect the properties of cells, and that their phenotypic behaviour is likely to be dependent upon this. This is of particular relevance in the experiments using human plasma samples, where endothelial behaviour is compared to that observed from culture in the manufacturers basal or complete media preparations. PromoCell do not offer a detailed breakdown of the individual levels of growth stimulants used in the supplement mix.

2.8: Culture of HMEC 98:

The HMEC 98 cell line was a generous gift from Dr Roy Bicknell at Oxford University. They were cultured in MCDB 131 media (supplemented with L-glutamine and 20% FCS) and passaged 1:3 when 95% confluent. Cells were harvested after a PBS wash with 2x trypsin before centrifugation in complete media at 660g for 7 minutes. Re-suspended cells were then seeded on 1% gelatine coated plastic-ware and cultured at 37°C and 5%CO₂. HMEC 98 were cultured in MCDB 131 medium containing L-glutamine and 20% FCS (Gibco). Serum-free conditions were established by the omission of FCS.

2.9: Culture of EA.hy 926:

The EA.hy 926 cell line was generously provided by C J Edgell of the University of North Carolina. This immortalised cell line was maintained in D-MEM (supplemented with 4500mg/l glucose, L-glutamine, pyruvate and 10% FCS) on uncoated plastic-ware. After PBS washing, cells were passaged at 95% confluency with 2x trypsin, before being resuspended in complete EA.hy 926 media. Cells were then directly seeded as necessary without undergoing centrifugation and pellet re-suspension. EA.hy 926 endothelial cells were cultured in D-MEM supplemented with 4500mg/l glucose, L-glutamine, pyruvate and 10% FCS. Serum-free conditions were established with the omission of FCS.

2.10: Calculation of Cell Number:

Twenty microlitres of re-suspended cells were mixed with an equal volume of Trypan blue (0.4%) and viable cells only were counted in at least five separate fields under 100x magnification using a haemocytometer. The following equation was used to calculate the total number of viable cells in the overall cell suspension:

Total volume of cell suspension (ml) x 2 x [average number of viable cells per counted field ÷ 2] x 10⁴

2.11: Transfection Protocol:

PromoCell HUVEC between passage number 3 and 7 were transfected as directed in PromoCell guidelines. Specifically, HUVEC were plated at a maximum of 1.9x10⁵ cells per well of a 6-well plate. Seeded cells were allowed to settle and proliferate over the next 48 hours until a target confluency of 90 – 100% was achieved. Lipofectamine 2000 (Invitrogen) was used for all transfection. SiRNA sequences were used for all transfection experiments following resuspension in the accompanying 1x SiMAX buffer to produce a 100nmol/ml solution. 100pmol of SiRNA in 250µl Optimem media was mixed with 5µl Lipofectamine solution in 250µl Optimem at room temperature. The combined DNA-Lipofectamine mixture was then incubated for a further 20 minutes at room temperature to allow formation of DNA:Lipofectamine complexes. Prior to transfection, each cell culture well was washed once

with PromoCell low serum media and re-filled with 1 ml of the same. 500µl of the transfection mixture was then added to relevant wells followed by a 5 hour incubation period at 37° C / 5% CO₂. Following incubation, each reaction mixture was removed and replaced with 2 mls of complete HUVEC media and the cells were allowed to recover overnight. Subsequent handling of transfected cells for further experiments was exactly as described above for routine culture. Transfection efficiency was initially optimised by adjusting the quantity and ratio of individual reagents; assessing protein knock-down by Western Blotting of whole cell lysates, whilst transfection efficacy was assessed by the extent of fluorescent control DNA uptake (Figure 2.1).

2.12: Protein Separation by Sodium Dodecyl Sulphate PolyAcrylamide Gel Electrophoresis (SDS-PAGE):

Adherent cells were harvested by physical dissolution in lysis buffer and manipulated on ice during this and all subsequent stages. Lysates were centrifuged at 13,000rpm for 5 minutes at 4°C to pellet cell debris and the protein containing supernatant removed to a fresh microfuge tube. All samples were then routinely analysed for total protein concentration using Bio-Rad's Protein Assay (Bradford Assay) to allow equal gel loading. Whilst no account was made for possible lysis buffer detergent effects upon the Bradford Assay reaction, any possible effect was assumed to impact all samples in a similar manner and thus not adversely alter protein concentration from lane to lane. Approximately 40µg of protein per lane was routinely combined with 2x sample loading buffer for gel separation. The sample and loading buffer were combined, mixed thoroughly and heat-denatured at 95°C for 6 minutes, before being centrifuged ready for loading onto the gel. SDS-PAGE was performed using the BioRad mini PROTEAN® 3 electrophoresis system, with resolving gel formulations appropriate to the molecular size of the protein of interest as listed in the table below (Table 2.1)

Reagent:	Resolving Gel:			Stacking Gel:
	12%	10%	7.5%	
30% Acryl/Bis	8.0 ml	6.7 ml	5.0 ml	3.3 ml
2M Tris pH 8.8	3.7 ml	3.7 ml	3.7 ml	-
1M Tris pH 6.8	-	-	-	2.5 ml
DH ₂ O	7.9 ml	9.6 ml	10.9 ml	13.7 ml
10% SDS	200 µl	200 µl	200 µl	200 µl
10% APS	134 µl	134 µl	134 µl	200 µl
TEMED	14 µl	14 µl	14 µl	20 µl

Table 2.1: Gel formulations used for SDS-PAGE.

Figure 2.1: Phase contrast image of cultured HUVEC superimposed with fluorescence image of same cells following transfection with Rhodamine labelled control siRNA. Efficiency of transfection assessed from proportion of cells containing label compared to total number of cells.

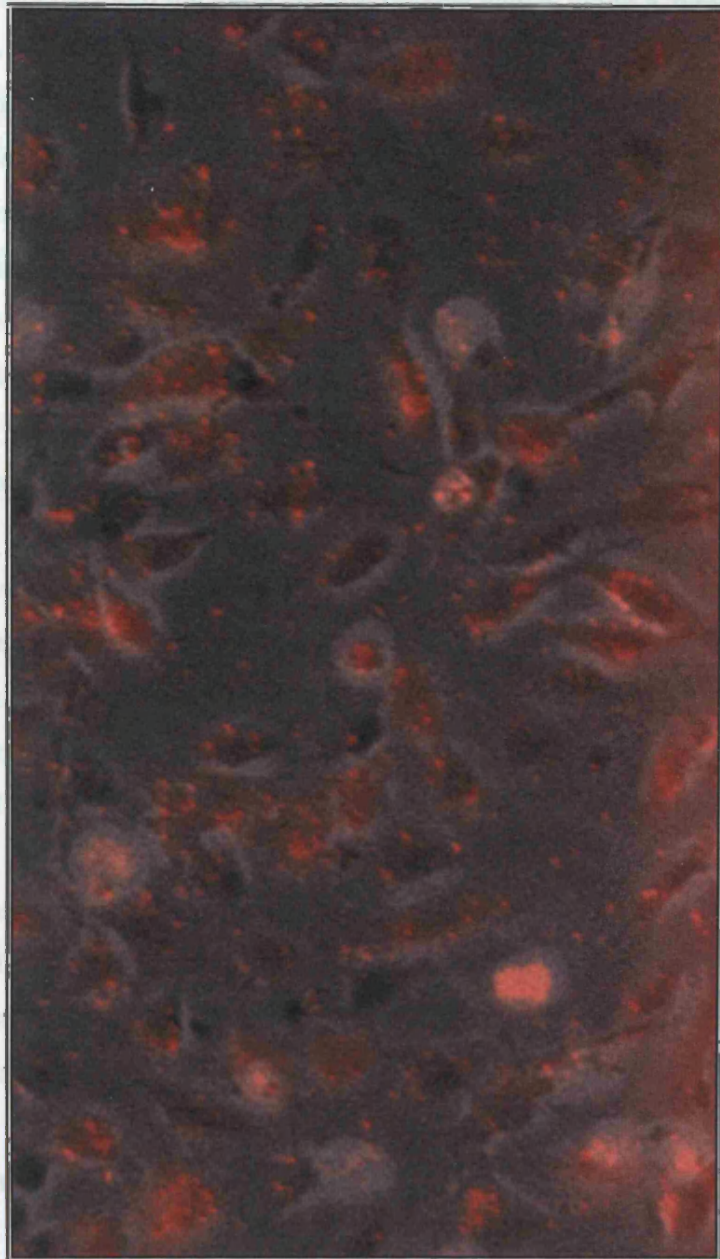


Figure 2.1: Phase contrast image of cultured HUVEC superimposed with fluorescence image of same cells following transfection with Rhodamine labelled control siRNA. Efficiency of transfection assessed from proportion of cells containing label compared to total number of cells.

The resolving gel solution was thoroughly mixed before being allowed to polymerise in the 1 mm gap between the glass electrophoresis plates, under a water-seal. Once polymerised, the stacking gel was added to the top of the resolving gel under a lane-forming comb following removal of the water seal. A total sample volume of 35 μ l was routinely loaded into each lane of the stacking gel using a Hamilton Syringe, with the left-most lane being reserved for 5 μ l of Bio-Rad Precision plus protein™ Kaleidoscope™ molecular mass standards. Once loaded the samples were electrophoresed at a constant 150 volts in running buffer (25mM Tris, 190mM glycine and 0.1% SDS) until the proteins of interest had been adequately separated as indicated by the marker standards.

2.13: Western Blotting:

Following electrophoresis, the separated proteins were electro-blotted onto a nitrocellulose membrane, using a Bio-Rad Mini TRANS BLOT cell. This was achieved by creating a transfer sandwich, comprising foam, filter paper (3mm Whatman), gel, nitrocellulose membrane, filter paper and finally foam. To ensure perfect bubble-free apposition of each part of the layer, this sandwich was created in a reservoir of transfer buffer (25mM Tris, 190 mM glycine and 20% methanol) before being locked shut in a Bio-Rad transfer cassette. Protein transfer occurred at a constant amperage of 0.15A (requiring roughly 50 volts) and was left for 2 hours to complete. Following transfer (verified by successful marker presence on the membrane) the membrane was kept immersed in TBS Triton TX-100 for downstream applications or wrapped in plastic film and stored at 4°C until required.

2.14: Immunoblotting:

Non-specific membrane binding sites were blocked with 5% Milk or 5% BSA dissolved in TBS-T for 30 minutes. This was followed by primary antibody binding using the conditions as listed in Table 2.2. Antibody binding took place inside an agitated heat-sealed plastic envelope for at least 1 hour at room temperature. Unbound primary antibody was then removed by four 15 minute washes in TBS-T. Species specific, HRP-linked secondary antibody was then added for a further hour in another heat-sealed envelope. Unbound secondary was removed with four 15 minute TBS-T washes, before protein detection using a chemiluminescence based development reaction.

Primary Antibodies:	Antibody Diluent:	Dilution Concentration:
Anti-Tie1 (C-18, Santa Cruz)	5% Milk in 1xTBS-T	1:1000
Anti-Tie2 (C-20, Santa Cruz)	5% Milk in 1xTBS-T	1:1000
Anti-Tie1 (R&D)	2.5% Milk in 1xTBS-T	1:1000
Anti-Tie2 (R&D)	2.5% Milk in 1xTBS-T	1:1000
Anti-phospho-Akt (serine 473)	5% BSA in 1xTBS-T	1:1000
Anti- Phospho -P42/44 -MAPK	5% BSA in 1xTBS-T	1:1000
Anti-Akt	5% BSA in 1xTBS-T	1:1000
Anti-p42/44-MAPK	5% BSA in 1xTBS-T	1:1000
Secondary Antibodies:	Antibody Diluent:	Dilution Concentration:
Anti-Rabbit HRP	1:1000	2:1000
Anti-Goat HRP		
Anti-Mouse HRP		

Table 2.2: Summary of antibodies used and their dilution conditions.

For chemiluminescence, the following solution was created:

1ml TRIS pH 8.5

9ml H₂O

22µl Solution A

50µl Solution B

3µl H₂O₂

The nitrocellulose membrane was immersed in this solution for 1 minute before being removed and sealed in plastic film, in turn being taped into position within a light tight cassette. Luminescent protein bands were captured on Kodak X-ray film by exposure to the membrane for variable lengths of time depending on the protein of interest. Re-probing of membranes for secondary proteins was achieved by first stripping attached antibodies in a 1x solution of Re-Blot Plus mild (Chemicon), before repeating protein detection from the membrane blocking stage.

2.15: Measurement of Immunoblot Band Intensity:

To measure the differential intensity of immunoblot bands, individual films were scanned into an IBM compatible PC using a Sharp JX-330 scanner. Quantitation of band intensity was established through the analysis of band optical density (OD value) using the ImageMaster 1D application (Pharmacia Biotech, 1995, version 1.20). OD measurement followed scanner calibration against linear manufacturer standards, encompassing the spectrum of band intensities present on the scanned immunoblots. The background film OD was then subtracted from all visible bands, which were then individually measured and recorded for subsequent graphical representation.

2.16: Endothelial Monolayer Permeability:

Measurement of endothelial cell monolayer permeability was achieved using two similar 2-chamber diffusion assay systems. In this technique, endothelial cells were grown across the semi-permeable membrane of purpose-made cell culture inserts, which, in turn, were suspended within the wells of a 24 well plate (Figure 2.2). By measuring the rate of tracer molecule diffusion across the cell-monolayer, calculations of permeability could be made. Before seeding the insert chamber with cells, the perforated membrane was coated with 1% Gelatin for HMEC-98 or 50 µg/ml Fibronectin for HUVEC for 30 minutes. Ea.Hy926 cells were seeded directly to the plastic membrane surface. Cells were then trypsinised and counted as previously described before being added at the correct density to the insert chamber for at least a 24 hour monolayer formation period. Prior to use in permeability assays, monolayer confluency was always assessed by phase contrast light microscopy (Figure 2.3). Inserts with intact monolayers then had all media changed to ensure that no net hydrostatic force was exerted across the monolayer. The cells were left for at least 2 hours to equilibrate following this media change. Cell stimulation or other treatments were only ever administered to media in the insert chamber (representing the luminal aspect of the endothelial cells) either before, with or after the addition of tracer agent. Measurement of monolayer permeability was then achieved by the addition and sampling of either FITC-labelled Dextran or HRP. This assumption of luminal vs. ab-luminal endothelial polarisation is assumed, based upon the attachment of the cells to the basement membrane derived fibronectin coating applied to the culture inserts.

FITC-Dextran Method (134):

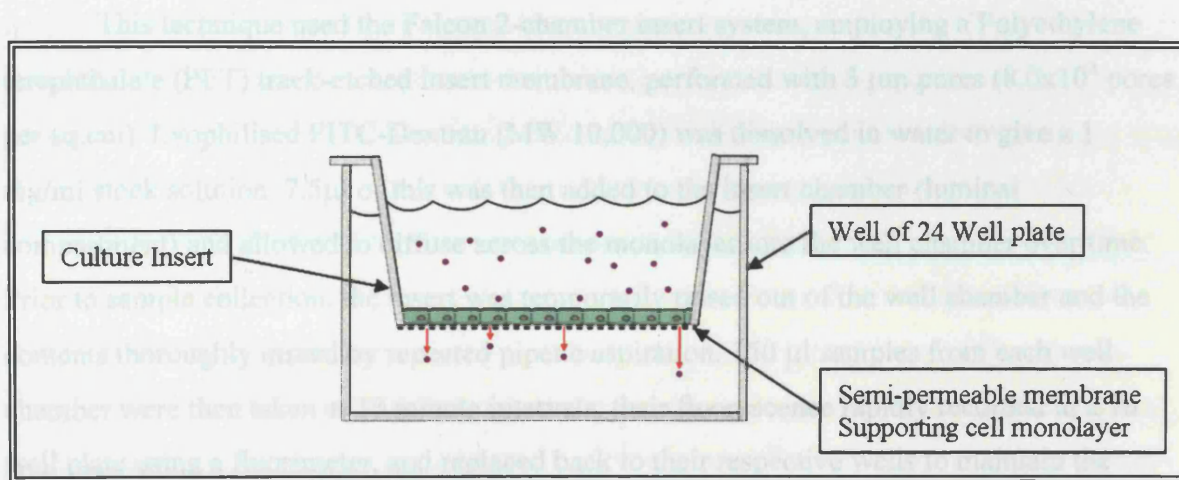


Figure 2.2: Endothelial cells were grown as a monolayer across the semi-permeable membrane of purpose-made culture inserts. Rate of tracer movement from insert to well across the monolayer allowed quantitation of permeability.

$$\text{FITC-Dextran Clearance (\%)} = \frac{\text{Lower well reading} \times 100}{\text{Total fluorescence added to upper well}}$$

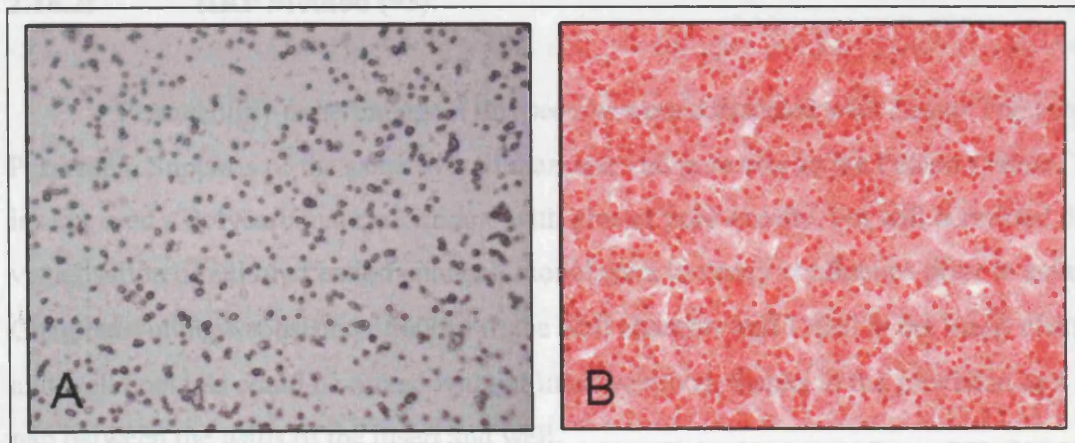


Figure 2.3: Photomicrograph A shows the perforated membrane of a permeability culture insert prior to seeding with cells. Photomicrograph B demonstrates a confluent monolayer of HMEC-98 growing on the membrane (H&E stained).

2.16.1: FITC-Dextran Method (134):

This technique used the Falcon 2-chamber insert system, employing a Polyethylene terephthalate (PET) track-etched insert membrane, perforated with 3 µm pores (8.0×10^5 pores per sq.cm). Lyophilised FITC-Dextran (MW 10,000) was dissolved in water to give a 1 mg/ml stock solution. 7.5µl of this was then added to the insert chamber (luminal compartment) and allowed to diffuse across the monolayer into the well chamber over time. Prior to sample collection, the insert was temporarily raised out of the well chamber and the contents thoroughly mixed by repeated pipette aspiration. 150 µl samples from each well chamber were then taken at 10 minute intervals, their fluorescence rapidly recorded in a 96 well plate using a fluorimeter, and replaced back to their respective wells to maintain the overall volume. At the end of the assay period, the fluorescence produced by 7.5 µl FITC-Dextran in 150µl complete media (representing insert contents at the beginning of the assay), plus the background signal produced by 150µl of complete media was also recorded. FITC-Dextran clearance could then be calculated as follows:

$$\text{FITC-Dextran Clearance (\%)} = \frac{\text{Lower well reading} \times 5}{\text{Total Fluorescence added to upper well}} \times 100$$

2.16.2: HRP Method (93):

Permeability experiments in this section were conducted with Costar Transwell® Permeable Supports of the same overall diameter and pore size as the Falcon system. These inserts used a Polycarbonate membrane with greater pore density, but still permitted direct visualisation of cultured endothelial cell monolayers to verify confluence prior to assay. Chamber volumes consisted of 600µl in the well chamber and 150µl in the insert chamber, and well contents could be mixed without insert removal, thanks to the provision of a large gap between the walls of the insert and well.

Lyophilised HRP Type VI-A (MW 44 kDa) was dissolved in water to produce a 750µg/ml solution. This was diluted 1 in 20 with endothelial cell basal medium and added to each insert chamber (0.75µg HRP total per insert). After thorough mixing as before, 5µl samples of well chamber media were collected every 10 minutes and added to 45µl sterile PBS in individual wells of a 96 well plate. The volumetric impact of removing 5µl at each

time point was felt to have negligible impact on the overall well chamber volume and therefore, no sample volume replacement was performed. At the end of the assay, the HRP present in each 5µl sample catalysed the colourimetric reaction provided by 200µl of OPD solution, made up immediately prior to use according to manufacturer guidelines (One o-phenylenediamine dihydrochloride tablet plus one urea hydrogen peroxide/buffer tablet dissolved in 20ml of water). The reaction was allowed to progress for 60 minutes exactly before all samples were read in a 96 well plate spectrophotometer at 450nm. To correct for baseline OD values, the absorption of a control well containing 5µl of culture medium in 45 µl PBS was recorded 60 minutes after the addition of 200µl OPD substrate. This value was removed from all assay values prior to graphical representation or calculation of permeability.

Early experiments were subjected to definitive verification of monolayer confluence by microscopic examination of the membrane following its removal from the insert. To enhance cell outline visualisation, monolayers were first stained with Haematoxylin and Eosin, prior to mounting on a microscope slide (Figure 2.3).

2.17: Apoptosis Detection by Cleaved Caspase-3/7 Assay:

Apoptosis in cultured HUVEC was measured indirectly through the quantitative measurement of Caspase 3 and 7 using the commercial Caspase-Glo 3/7[®] assay produced by Promega. In this system, a reagent buffer solution containing the luminogenic substrate DEVD-aminoluciferin and a recombinant luciferase enzyme is added directly to the cell culture medium in an add, mix and measure assay. With gentle agitation of the plate, the buffer solution lyses cells to liberate intracellular caspases. Released caspases 3 and 7 then cleave the substrate DEVD-aminoluciferin to form an active luminogenic substrate for the luciferase enzyme (Figure 2.4). This produces a luminescent signal proportional to the quantity of caspase enzyme present in the lysed cell population, which is recorded in a plate-reading luminometer, once both enzymatic steps reach a steady state after a one-hour incubation period. All experiments were conducted on HUVEC cultured in flat bottomed 96 well plates. HUVEC were seeded at a density of 1×10^4 cells per well 24 hours prior to assay in 100µl of complete media. Just prior to assay, each well was examined by light microscopy to ensure an even degree of overall cell confluency. Apoptosis was stimulated with media exchange for a serum-free formulation. To this, specific growth factors were added as

...volume of the reaction, thereby altering the overall well volume. Caspase production was then measured in accordance with guidelines published by Promega for use with their Caspase-Glo 3/7 assay kit. (Specifically, 50µl of the reconstituted reagent was added to each well (see total volume to the culture medium) followed by a 30 second period of agitation to assist with break-up and caspase release. In order to avoid inter-well interference in the luminometer, the reaction was allowed to develop for one hour in-situ, prior to the transfer of each well's contents to the flat-bottomed wells of a white multi-well plate.)

2.18: Endothelial Cell Apoptosis Molecule (CAM) Assay

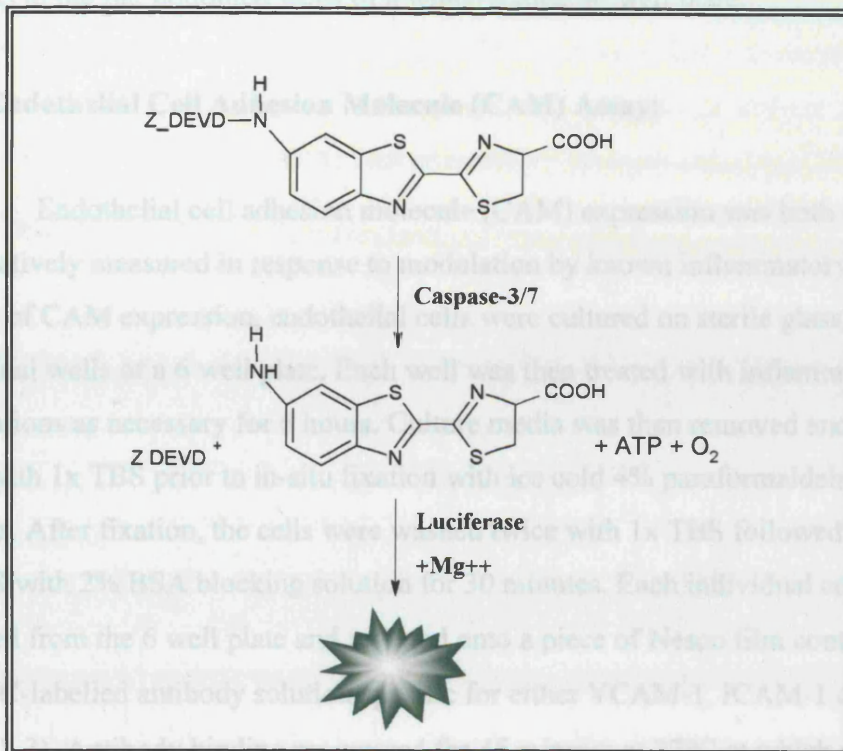
Endothelial cell adhesion molecule (CAM) expression was both qualitatively and quantitatively measured in response to stimulation by known inflammatory mediators. For images of CAM expression, endothelial cells were cultured on sterile glass coverslips within individual wells of a 6 well plate. Each well was then treated with inflammatory cytokine preparations as necessary for the assay. Cells were then removed from the cells, washed twice with 1x TBS prior to in-situ fixation with ice cold 4% paraformaldehyde solution for 30 minutes. After fixation, the cells were washed with 1x TBS followed by immersion in 1x TBS with 2% BSA blocking solution for 1 hour. Each individual coverslip was then removed from the 6 well plate and mounted onto a piece of Nucleo-Gem containing a 20µl drop of FITC-labeled antibody solution for either VCAM-1, ICAM-1 or E-Selectin (Table 2.18.1).

Figure 2.4: Endothelial cell apoptosis is measured indirectly through a quantitative caspase 3/7 assay. Caspase 3 or 7 cleaves DEVD-aminoluciferin to release a luminogenic substrate for the included luciferase enzyme. The luminescence generated by the luciferase is proportional to the quantity of caspase in the cell population.

Kronos-Scan image capture software.

To quantify CAM expression, endothelial cells were seeded at 2×10^4 in 100µl into individual wells of a 96 well plate. After 24 hours, cytokines were added to each well as necessary followed by incubation at 37°C for periods of time between 1 and 24 hours.

Experiments were stopped with two washes of 1x TBS followed by 30 minutes exposure to



necessary without significantly altering the overall well volume. Caspase production was then measured in accordance with guidelines published by Promega for use with their Caspase-Glo 3/7 assay kit. Specifically, 50µl of the reconstituted reagent was added to each well (an equal volume to the culture medium) followed by a 30 second period of agitation to assist cell break-up and caspase release. In order to avoid inter-well interference in the luminometer, the reaction was allowed to develop for one hour in-situ, prior to the transfer of each wells contents to the flat bottomed wells of a white-walled 96 well plate.

2.18: Endothelial Cell Adhesion Molecule (CAM) Assay:

Endothelial cell adhesion molecule (CAM) expression was both qualitatively and quantitatively measured in response to modulation by known inflammatory mediators. For images of CAM expression, endothelial cells were cultured on sterile glass coverslips within individual wells of a 6 well plate. Each well was then treated with inflammatory cytokine preparations as necessary for 6 hours. Culture media was then removed and the cells washed twice with 1x TBS prior to in-situ fixation with ice cold 4% paraformaldehyde solution for 30 minutes. After fixation, the cells were washed twice with 1x TBS followed by immersion in 1x TBS with 2% BSA blocking solution for 30 minutes. Each individual coverslip was then removed from the 6 well plate and inverted onto a piece of Nesco film containing a 20µl drop of FITC-labelled antibody solution specific for either VCAM-1, ICAM-1 or E-Selectin (Table 2.3). Antibody binding progressed for 45 minutes at 37°C at which point the coverslips were replaced cell-side-up into the original 6 well plate. Un-bound antibody was washed off with 1x TBS twice prior to a final wash in water to remove residual salt traces. The coverslips were then removed from the 6 well plate and mounted cell-side-down onto glass slides with a drop of PVA mounting solution containing the anti-fade compound DABCO. Finally, each coverslip was secured in place with translucent nail varnish. HUVEC immunofluorescence was visualised using an Olympus microscope with a 465 – 495nm filter. Images were captured through an attached monochrome CCD camera and stored on an IBM PC running Kroma-Scan image capture software.

To quantitate CAM expression, endothelial cells were seeded at 2×10^4 in 100µl into individual wells of a 96 well plate. After 24 hours, cytokines were added to each well as necessary followed by incubation at 37°C for periods of time between 1 and 24 hours. Experiments were stopped with two washes of 1x TBS followed by 30 minutes exposure to

4% Paraformaldehyde solution. After a further 2 washes with 1x TBS, non-specific binding sites were blocked with 2%BSA solution as described above. For primary antibody binding, FITC labelled anti-CAM antibody was diluted in 1x TBS with 2% BSA to provide 50µl volume per well. Primary antibody binding was allowed to proceed for 45 minutes at 37°C before unbound antibody removal with 4 washes with 1x TBS. To quantitate bound primary antibody, 50µl of HRP labelled anti-mouse antibody was added to each well once diluted 1:1000 in 1x TBS. Secondary antibody binding continued for 30 minutes at room temperature with gentle agitation on a rocking platform. Unbound secondary was removed with 4 further washes of 1x TBS. 200µl of fresh OPD solution was added to all wells and the colourimetric reaction allowed to progress in the dark at room temperature for around 30 minutes (varied as necessary to ensure optimal contrast between individual wells). Individual well values were then measured in a spectrophotometric plate reader at 450nm.

Primary Antibody:	Antibody Diluent:	Dilution Concentration:
Anti-VCAM-1	2% BSA in 1x TBS	1:80
Anti-ICAM-1	2% BSA in 1x TBS	1:80
Anti-E-Selectin	2% BSA in 1x TBS	1:80
Secondary Antibody:	Antibody Diluent:	Dilution Concentration:
Anti-Mouse HRP	As for primary	1:1000

Table 2.3: Primary Fluorescent and secondary HRP-linked antibody dilutions for the detection of ICAM-1, VCAM-1 and E-Selectin expressed on the endothelial cell surface.

2.19: Preparation and Processing of Human Plasma Samples and Study Ethics

Approval:

For the collection of human serum samples from patients with SIRS / sepsis, ethical approval was first applied for from the Leicestershire, Northamptonshire and Rutland Research Ethics Committee. This application was approved (with amendments) on the 10th of August 2007, and the study was also approved and indemnified by the University Hospitals of Leicester NHS Trust Research and Development Department at the same time. Following appropriate counselling and consent, included trial patients had 2.4 mls of either arterial or venous blood removed from an indwelling vascular catheter, which was transferred into a

purpose-made blood bottle containing EDTA (Monovette[®], Starnstedt, Germany). Collected samples were immediately spun for 10 minutes at 4 °C and 9000 rpm to separate the plasma from the cellular elements of the whole blood. The suspended plasma fraction was then aspirated in 200µl aliquots into sterile containers and snap-frozen in liquid nitrogen before being stored at -80 °C for later use. No comparative analysis on the alteration of plasma contents upon freezing was made. It was therefore assumed that snap freezing did not alter the properties of the plasma, but this would need definitive comparison with fresh plasma to confirm this.

2.20: Statistical analyses:

All graphical data was subjected to statistical analysis when the combined data was collated from *at least three individual experiments*. Furthermore, the vast majority of individual experiments were conducted with duplicate or triplicate conditions. Where data is presented from less than three separate experiments, this is clearly documented and no statistical analysis is performed in these cases. Graphical data is presented as mean values flanked by SEM error bars unless otherwise stated.

Statistical analysis consisted of the un-paired Students t-test throughout, with a confidence interval level set at 95% for all presented data and two-tailed P values recorded within each figure legend.

3.1.1: Creation of Tie Deficient HUVEC:

To investigate the role played by Tie receptors in endothelial responses to inflammation, gene silencing techniques were used to generate Tie1 or Tie2 deficient HUVEC. Gene silencing is a relatively new technique that has developed from the innate property of eukaryotic cells to eliminate unwanted mRNA sequences (such as those associated with replicating viruses) prior to translation. Although this phenomenon was well recognised to occur in plants (termed Post Transcriptional Gene Silencing), only relatively recently has a similar process been understood in animal cells (135). Known as RNA interference, the central feature of the process is the specific destruction of genomic mRNA transcripts that have sequence homology with double stranded RNA (dsRNA) present within the cytoplasm. If necessary, long dsRNA sequences are firstly shortened to lengths of 20 – 25 nucleotides by the enzyme dicer to create so-called Short, interfering RNA sequences (SiRNAs) containing a 2-3 nucleotide overhang at each end. SiRNAs then become incorporated into the RISC complex (RNA-Induced Silencing Complex) where the sense strand is discarded. The anti-sense strand within RISC then hybridises with homologous sequences within target mRNA present in the cytoplasm, leading to their destruction (Figure 3.1).

Since the discovery of RNA interference, it has become a powerful research tool, allowing the function of specific genes to be studied through their selective removal (136). To inhibit gene expression, the gene's nucleotide sequence is first used to design synthetic SiRNA. The SiRNA are then delivered into target cells by the process of transfection, effecting gene silencing by incorporation into RISC as described. Although potentially invaluable as a research tool, successful gene silencing requires a high degree of transfection efficiency, a well chosen target within the gene of interest, and an experimental protocol of sufficient delicacy not to kill the cells being transfected in the process. Furthermore, RNAi is subject to off-target effects, a situation where the target gene contains a sequence common to other genes, leading to their suppression also. To reduce the chances of off-target complications, SiRNA sequences need to be designed with a high specificity for the target gene with minimal cross-reactivity to other known sequences.

3.1.2. SiRNA Generation of Tie1 and Tie2 Deficient HUVEC

To create siRNA sequences targeting Tie1 and Tie2, the siRNA design tool operated by MWI Biotech was used. To begin, the RefSeq mRNA sequences for Tie1 and Tie2 were downloaded from the Center for Bioinformatics Research and Analysis (CBIRA).

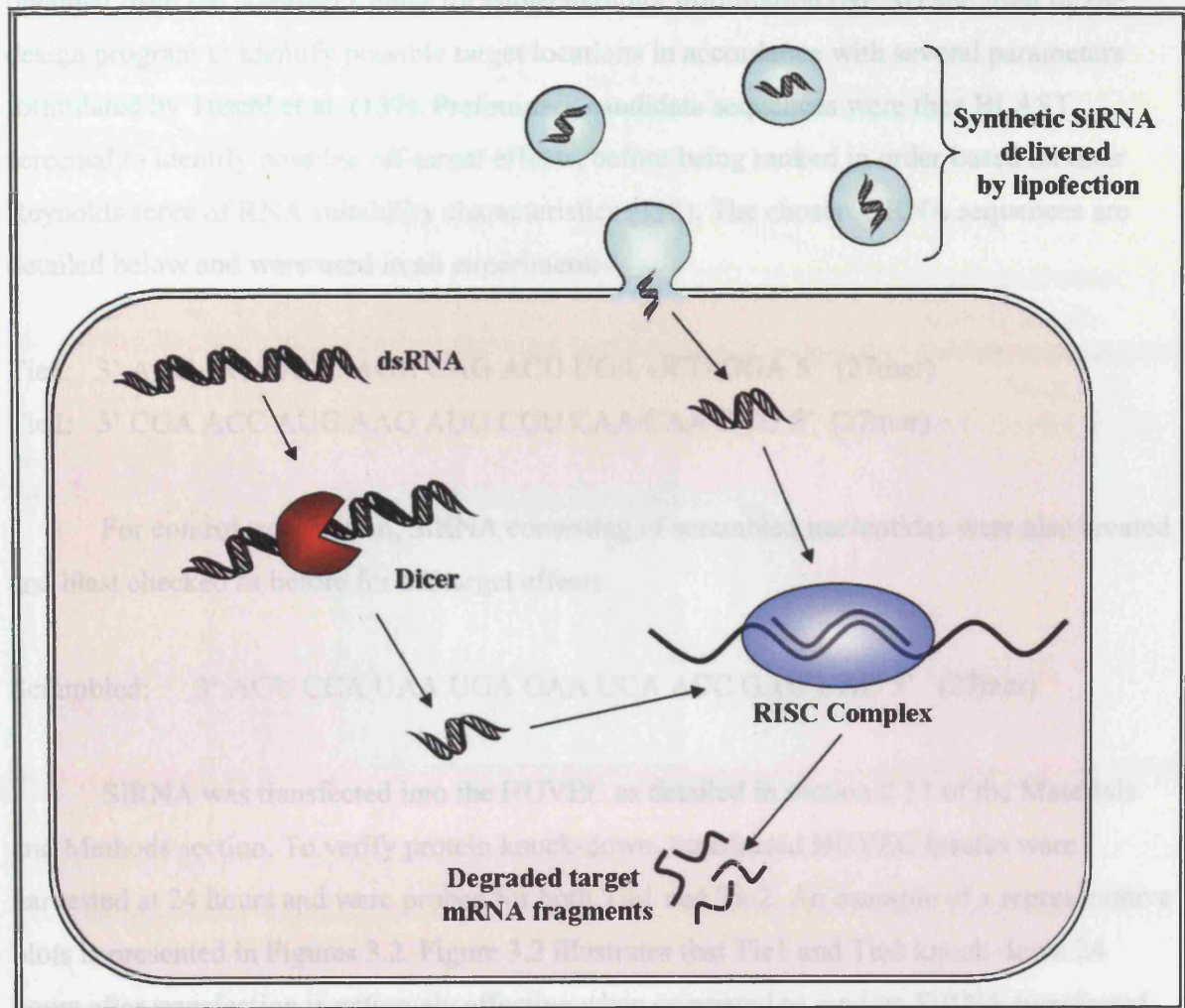


Figure 3.1: Schematic illustration of events involved in RNA interference. dsRNA is degraded into 20 – 25 nucleotide length siRNA by the enzyme dicer. This (or commercial synthetic siRNA introduced by transfection) then undergoes strand separation and the anti-sense copy is incorporated into the RNA-induced silencing complex. This complex then associates with complementary mRNA sequences within the cytoplasm leading to their degradation.

3.1.2: SiRNA Generation of Tie1 and Tie2 Deficient HUVEC:

To create SiRNA sequences targeting Tie1 and Tie2, the SiRNA design tool operated by MWG Biotech was used. To begin, the RefSeq mRNA sequences for Tie1 and Tie2 were obtained from the National Center for Biotechnology Information (NCBI) and used by the design program to identify possible target locations in accordance with several parameters formulated by Tuschl et al. (137). Preliminary candidate sequences were then BLAST screened to identify possible off-target effects, before being ranked in order based on their Reynolds score of RNA suitability characteristics (138). The chosen SiRNA sequences are detailed below and were used in all experiments:

Tie1: 3' AGG AGA AGC AGA CAG ACG UGA UCU GGA 5' (27mer)

Tie2: 3' CGA ACC AUG AAG AUG CGU CAA CAA GCU 5' (27mer)

For control transfection, SiRNA consisting of scrambled nucleotides were also created and blast checked as before for off target effects.

Scrambled: 3' AGU CCA UAA UGA GAA UCA ACC GAU UAU 5' (27mer)

SiRNA was transfected into the HUVEC as detailed in section 2.11 of the Materials and Methods section. To verify protein knock-down, transfected HUVEC lysates were harvested at 24 hours and were probed for both Tie1 and Tie2. An example of a representative blots is presented in Figures 3.2. Figure 3.2 illustrates that Tie1 and Tie2 knock-down 24 hours after transfection is extremely effective when compared to random SiRNA transfected control HUVEC. Both the immature (Lower band) and fully glycosylated (upper band) forms of Tie1 are reduced to an equal degree. Moreover, Tie1 silencing did not appear to alter the expression of Tie2. Similar findings were made for Tie2 silencing, with strong knock-down in comparison to random treated controls. However, in some experiments, the magnitude of receptor knock-down was more variable at 24 hours than for Tie1.

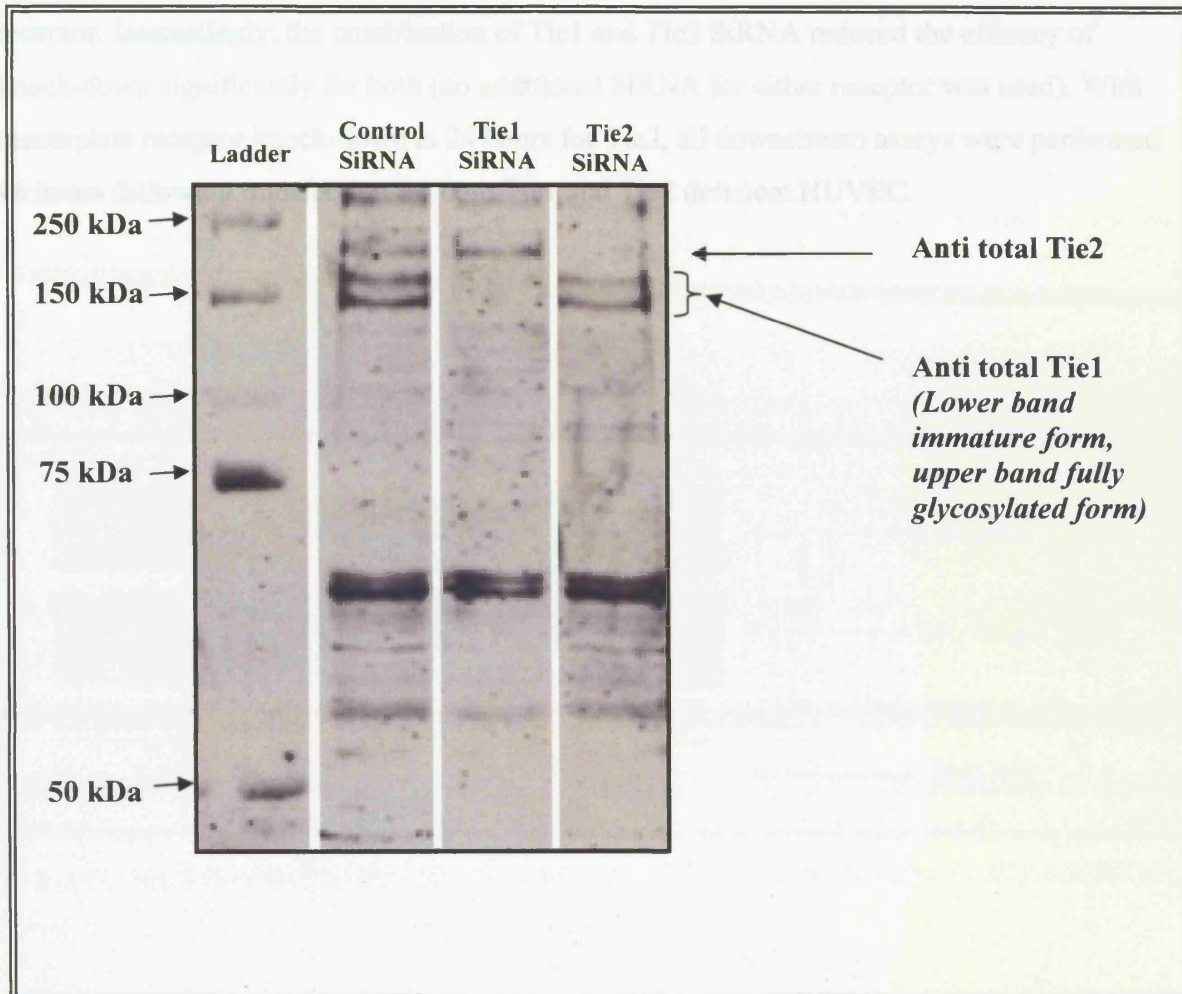
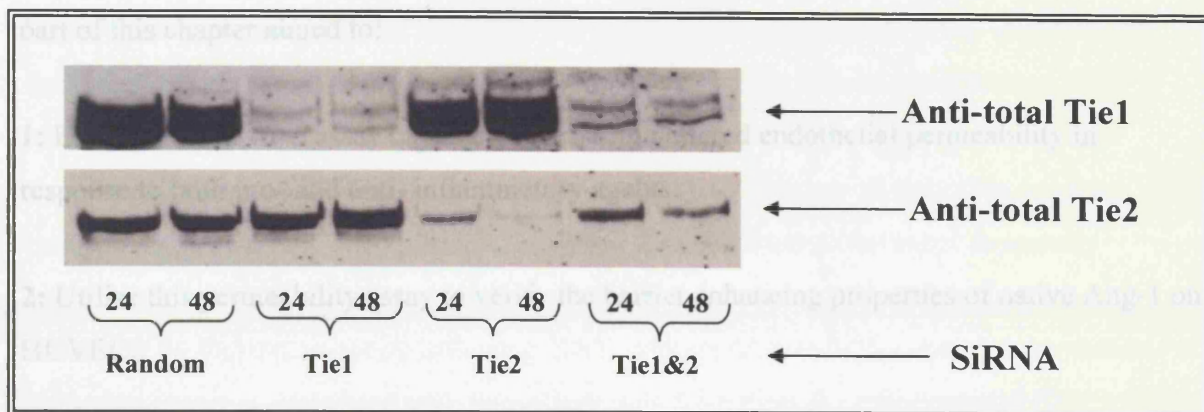


Figure 3.2: SiRNA silencing of Tie1 and Tie2 expression. HUVEC were transfected with control SiRNA plus SiRNA directed against Tie1 or Tie2. Cell lysates were then harvested after 24 hours and subjected to protein separation by SDS-PAGE electrophoresis. Proteins were transferred to a nitrocellulose membrane and probed for Tie1 and Tie2 together. Lane contents as indicated with molecular markers in the left hand column. Antibody probes as indicated. Tie2 SiRNA has a major impact on receptor expression, without affecting band intensity for Tie1 expression; likewise, Tie1 SiRNA greatly reduced Tie1 expression without altering Tie2. Tie1 bands appear as a lower immature form and an upper fully glycosylated form. Representative experiment as performed in association with every subsequent assay performed.

Figure 3.3 repeats the analysis of both receptors expression at 24 hours but also records expression levels at 48 hours following transfection. In this blot, the 24 hour Tie2 knock-down is incomplete, but after a further 24 hours, there is near-total absence of the Tie2 receptor. Interestingly, the combination of Tie1 and Tie2 SiRNA reduced the efficacy of knock-down significantly for both (no additional SiRNA for either receptor was used). With incomplete receptor knock-down at 24 hours for Tie2, all downstream assays were performed 48 hours following transfection for both Tie1 and Tie2 deficient HUVEC.

3.2.1: Regulation of Endothelial Permeability: The Role of Tie Receptor Signalling

From both *in vivo* and *in vitro* studies, Ang-1 has been shown to have a powerful anti-permeability effect on the endothelium (48, 62, 89). As with other areas of research involving the effects of Ang-1, this endothelial barrier function has been ascribed to Tie2 receptor signalling, at least on the basis of *in vitro* experiments conducted in the presence of exogenous soluble Tie2 extracellular domain (used to pharmacologically suppress Ang-1 action in a dose dependent manner). The validity of this was challenged when Weber *et al.* published the findings that a modified protein variant of Ang-1 could enhance monolayer barrier function, possibly through heterodimerisation, even in the absence of Tie2 activation (90). Therefore, given the multiple possible means of permeability control by Ang-1, the second part of this chapter aimed to:



3. Establish a role for Tie1 and Tie2 in regulating Ang-1 enhanced monolayer barrier function through gene silencing techniques.

3.2.2: Establishment of an Endothelial Permeability Assay

Figure 3.3: Time-course experiment for Tie receptor knock-down following SiRNA treatment in HUVEC. HUVEC were transfected with either random, Tie1, Tie2, Tie1 and Tie2 SiRNA. Lysates were harvested after either 24 or 48 hours as indicated and subjected to SDS-PAGE and Western Blotting. Top panel shows membrane probe for Tie1, followed by membrane stripping and re-probing for Tie2 (bottom panel). Tie1 and 2 levels in random cell lysates presented in the left two lanes, corresponding to 24 and 48 hours post transfection respectively. Sequential paired lanes moving to the right represent Tie1, Tie2 and Tie1 and 2 together at 24 and 48 hours post transfection. Single experiment shown from a series of three.

inserts. Initial experiments using the immortalised endothelial cell line HMVEC-96 were used to establish suitable conditions for subsequent experiments and measured fluxes are labelled (FITC) Dextran cleavage across cultured endothelial monolayers. Cells were seeded to insert chambers as described and allowed to form a monolayer over the next 48 hours. Permeability was then recorded by the addition of high-concentration FITC labelled Dextran to the insert

3.2.1: Regulation of Endothelial Permeability: The Role of Tie Receptor Signalling:

From both *in vivo* and *in vitro* studies, Ang-1 has been shown to have a powerful anti-permeability effect on the endothelium (48, 62, 89). As with other areas of research involving the effects of Ang-1, this enhanced barrier function has been ascribed to Tie2 receptor signalling, at least on the basis of *in vitro* experiments conducted in the presence of excess soluble Tie2 extracellular domain (used to stoichiometrically suppress Ang-1 action in a dose dependent manner). The simplicity of this was challenged when Weber et al. published the findings that a modified monomeric form of Ang-1 could enhance monolayer barrier functions, possibly through integrin signalling, even in the absence of Tie2 activation (102). Therefore, given the multiple possible routes of permeability control by Ang-1, the second part of this chapter aimed to:

- 1: Establish an *in vitro* assay capable of measuring altered endothelial permeability in response to both pro- and anti- inflammatory agents.
- 2: Utilise this permeability assay to verify the barrier enhancing properties of native Ang-1 on HUVEC.
- 3: Establish a role for Tie1 and Tie2 in mediating Ang-1 enhanced monolayer barrier function through gene silencing techniques.

3.2.2: Establishment of an Endothelial Permeability Assay:

To measure endothelial monolayer permeability a two chamber diffusion model was used with a protocol based on the method published by Godfrey (134). The details of this model are described in section 2.16.1 of the Materials and Methods chapter, in conjunction with the associated Figure 2.2. Essentially, endothelial cells were allowed to establish a monolayer across the semi-permeable membrane of purpose built 3 μm Falcon[®] culture inserts. Initial experiments using the immortalised endothelial cell line HMEC-98 were used to establish suitable conditions for subsequent experiments and measured fluorescent labelled (FITC) Dextran clearance across cultured endothelial monolayers. Cells were seeded to insert chambers as described and allowed to form a monolayer over the next 48 hours. Permeability was then recorded by the addition of high-concentration FITC labelled Dextran to the insert

chamber followed by measurement of its appearance in the lower chamber every 10 minutes thereafter. Pro-permeability agents or Ang-1 were then added at times indicated in each figure. Using the Falcon system, lower chamber sampling necessitated the temporary removal of the insert in order to allow pipette-tip access and mixing of the well contents. Accordingly, in order to mix, record and return individual samples every 10 minutes, it was only possible to collect individual data points from single wells for each condition under investigation. The first 40 minutes of each assay represented baseline permeability; which was then compared to permeability alteration induced by the addition of inflammatory agents or Ang-1 over the next 60 minutes. An example of HMEC-98 permeability in response to different concentrations of thrombin is presented in Figure 3.4. Figure 3.4 demonstrates the permeability of HMEC-98 monolayers collated from 4 individual experiments using concentrations of thrombin between 2 and 0.066 U/ml added to the insert chamber only. In this figure, individual experimental data has been normalised to the baseline rate of permeability prior to combination, with permeability calculated from the rate of FITC-Dextran clearance per unit time. In this experiment, there was a clear increase in permeability in response to thrombin exposure, most marked when used at 2 U/ml. Indeed, using this concentration of thrombin frequently produced tears in the monolayer itself, as seen when these inserts were subsequently examined by light microscopy following H&E staining (Figure 3.5). Lower concentrations of thrombin were not associated with monolayer hole formation and demonstrated little variation in permeability over the dose range used, remaining approximately fourfold more permeable than the same monolayers under baseline conditions. Consistent with the enhanced permeability associated with thrombin at all concentrations, HMEC-98 cultured on glass coverslips demonstrated profuse stress fiber formation within the cytoplasm following exposure to 2U/ml Thrombin (Figure 3.6).

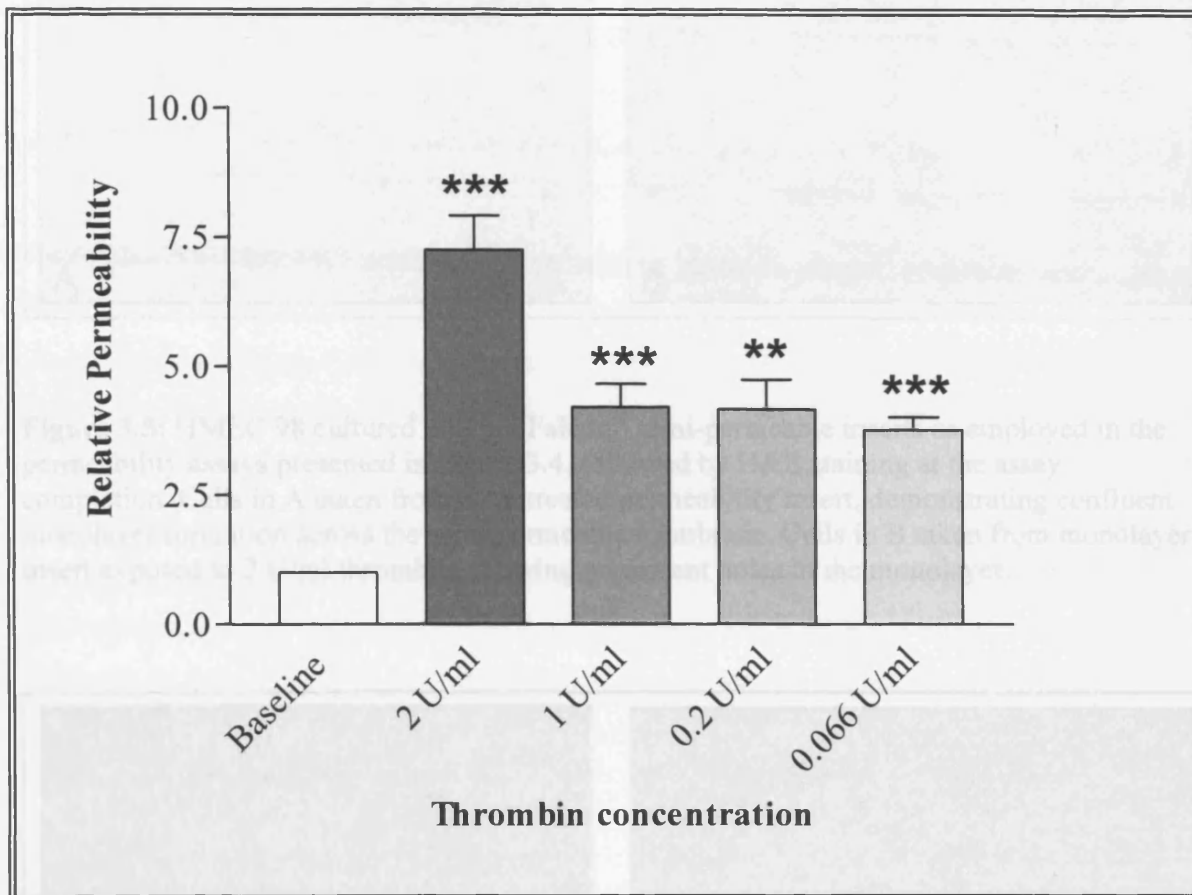


Figure 3.4: HMEC-98 endothelial cell permeability following treatment with thrombin. 1.5×10^5 HMEC-98 cells were seeded to gelatine coated $3\mu\text{m}$ -pore inserts, followed by a 48 hour incubation period to allow monolayer formation. Permeability measured as described in the text and in the materials and methods (section 2.16.1). Rate of permeability calculated from the passage of FITC-dextran per unit time, prior to normalisation to the untreated baseline. Baseline permeability was recorded for the first 40 minutes, followed by thrombin addition to the insert chamber, with further sampling over the next 60 minutes. Data compiled from four separate experiments, each with single data point values (single insert per parameter). Thrombin exerts a statistically significant increase in the rate of permeability in HMEC monolayers at all concentrations used when compared to baseline (*** $P < 0.0001$, ** $P < 0.005$)

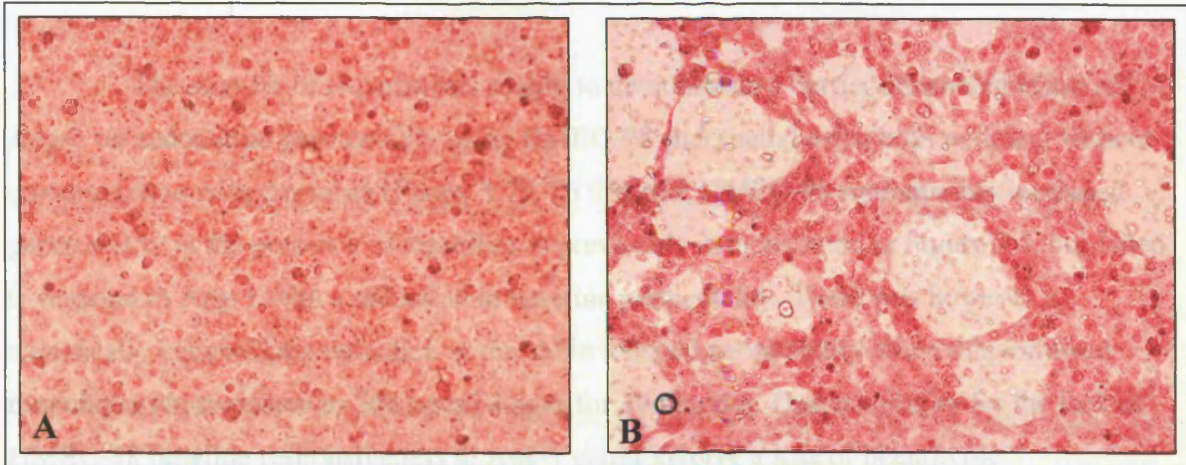


Figure 3.5: HMEC 98 cultured on 3µm Falcon® semi-permeable inserts as employed in the permeability assays presented in Figure 3.4, followed by H&E staining at the assay completion. Cells in A taken from an untreated permeability insert, demonstrating confluent monolayer formation across the semi-permeable membrane. Cells in B taken from monolayer insert exposed to 2 U/ml thrombin, showing prominent holes in the monolayer.

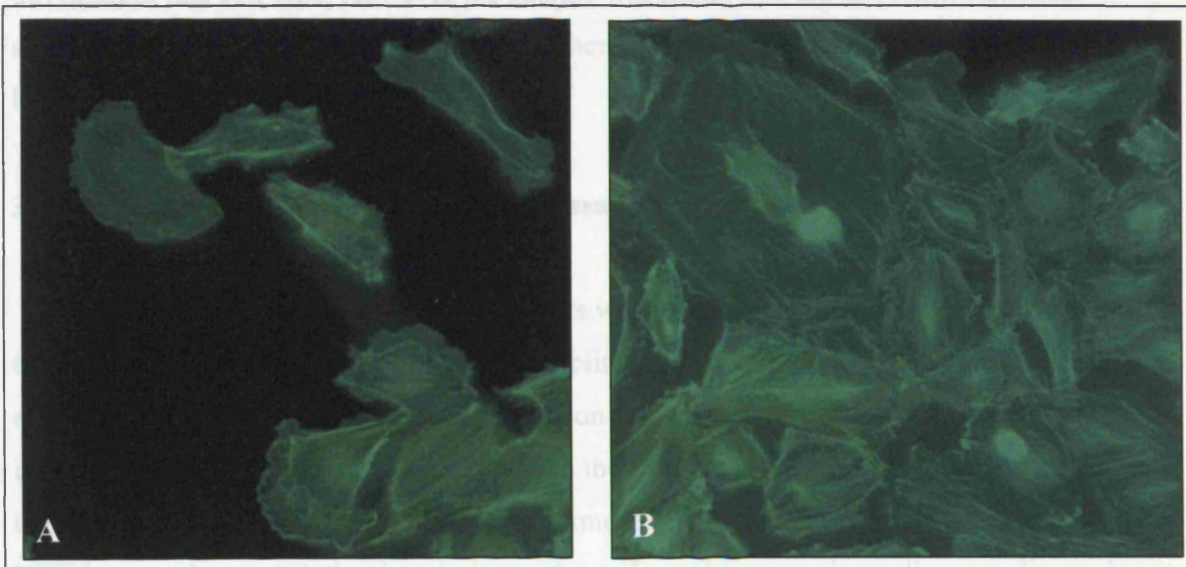


Figure 3.6: HMEC 98 cultured in complete media on gelatine coated glass coverslips and stained with FITC-Phalloidin to demonstrate the actin cytoskeleton as described in the Materials and Methods section. Un-treated cells in photomicrograph A reveal a cortically distributed actin cytoskeleton and exhibit motile behaviour with ruffled cell processes. Endothelial cells in photomicrograph B have been stimulated with 2 U/ml Thrombin for 30 minutes and demonstrate actin rearrangement typical of stress-fibre production and centripetal contraction of the cytoplasm.

3.2.3: Endothelial Permeability and Angiopoietin-1:

The next set of experiments sought to demonstrate a barrier enhancing effect of Ang-1 on endothelial permeability using HMEC-98 endothelial cells, both with and without co-stimulation with thrombin (Figure 3.7). To this end, HMEC-98 reproducibly increased permeability in the presence of thrombin as previously demonstrated in Figure 3.4, but failed to respond to Ang-1 with a reduction in baseline permeability. There was however a statistically insignificant reduction in thrombin induced permeability when this followed monolayer pre-exposure to 200 ng/ml Ang-1 for 30 minutes. One possibility for the lack of HMEC-98 baseline responsiveness to Ang-1 could involve a loss of phenotypic responsiveness to Ang-1 as a consequence of either the immortalisation process used in their creation, or their increasing age after multiple passages. Alternatively there may have been a heterogeneous response between one cell and the next with the monolayer, resulting in an undetectable alteration in overall barrier enhancement following Ang-1 stimulation. It was interesting to see however, that there was a slight reduction in thrombin associated leakage following Ang-1 pre-treatment, suggesting that Ang-1 does have some inhibitory influence on thrombin in this cell type. However the change was minor and did not reach statistical significance as described by Gamble et al. when using Ang-1 to inhibit thrombin stimulated leakage in HUVEC (48).

3.2.4: Modifications to the Permeability Assay:

Although encouraging initial results were obtained using the Falcon[®] insert system; the need for insert removal prior to well sampling allowed only one insert to be used for each experimental condition. Therefore, the decision was taken to move to the Costar Corning insert system that offered both easy access to the well chamber for sampling without the need to disturb the insert itself in doing so. Furthermore, the permeability tracer was changed to HRP in accordance with the description of Li et al., enabling much smaller sampling volumes that produced considerably less hydrostatic disturbance across the monolayer (93). Finally, with no Ang-1 mediated reduction in baseline permeability using HMEC-98 endothelial cells, all subsequent experiments were conducted with primary HUVEC in order to aim for the greatest phenotypic endothelial cell behaviour in response to Ang-1 stimulation. All permeability experiments used HUVEC between passage 2 and 10, seeded at 0.7×10^5 cells per insert (3 μ m pore size). Inserts were coated with 50 mg/ml fibronectin for 30 minutes prior

to cell seeding. Forty eight hours after seeding, culture media was exchanged in both the insert and lower well chambers, followed 2 hours later by the addition of 200 ng/ml Ang-1 to relevant inserts. After a 30 minute incubation period, HRP tracer was added and permeability recorded every 10 minutes as detailed in the Materials and Methods section. All conditions were completed in either duplicate or triplicate in parallel adjacent later-well compartments of different culture effects within each experiment.

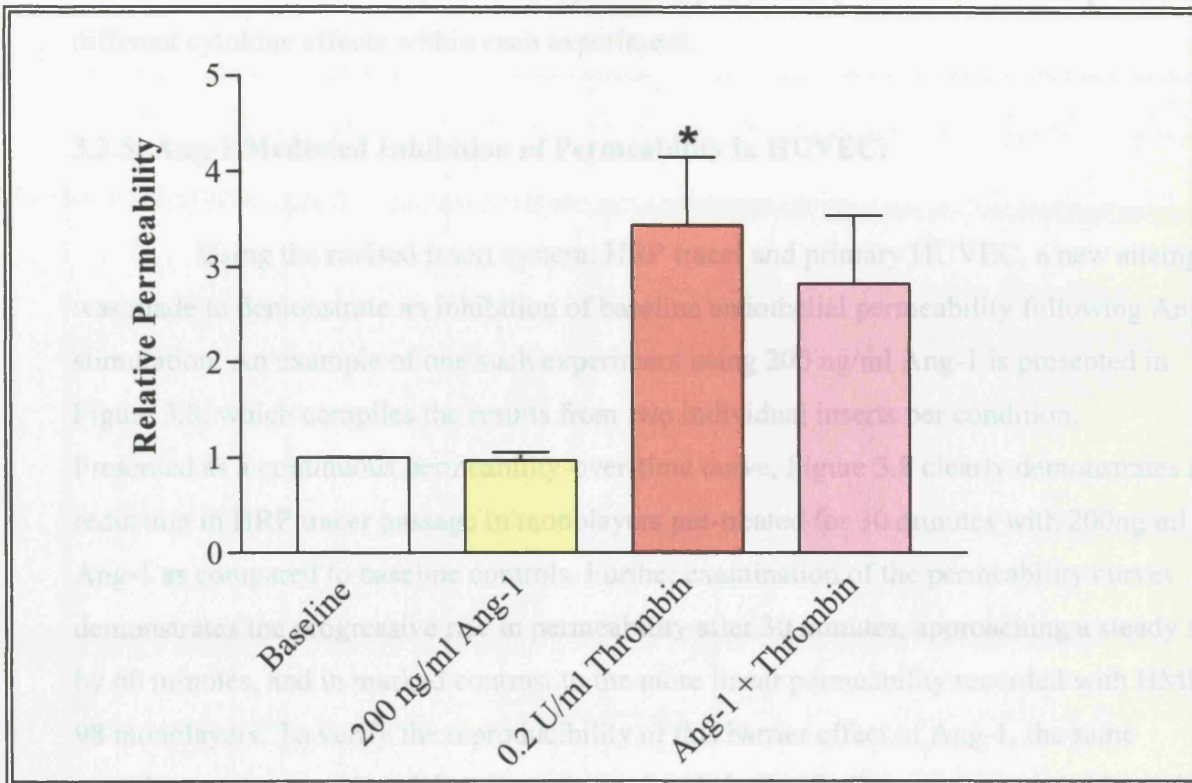


Figure 3.7: HMEC-98 permeability following Ang-1, thrombin and Ang-1 plus thrombin stimulation. HMEC-98 endothelial cells seeded at 1.5×10^5 cells per gelatine-coated insert and left to form a monolayer over the next 48 hours. FITC labelled dextran added to insert chamber with sampling from lower well every 10 minutes thereafter. 200 ng/ml Ang-1 added to relevant insert chambers after 30 minutes with thrombin added after a further 30 minutes. Permeability measurement continued for a further 40 minutes. Individual experiments consist of a single insert per condition, and rate of permeability calculated from FITC-dextran passage per unit time. All permeability rates normalised to baseline within each experiment prior to combination for the summary graph as presented. Data derived from a total of four experiments. 0.2 U/ml thrombin exerted a statistically significant increase in permeability compared to baseline conditions (* $P < 0.05$).

to cell seeding. Forty eight hours after seeding, culture media was exchanged in both the insert and lower well chambers, followed 2 hours later by the addition of 200 ng/ml Ang-1 to relevant inserts. After a 30 minute incubation period, HRP tracer was added and permeability recorded every 10 minutes as detailed in the Materials and Methods section. All conditions were conducted in either duplicate or triplicate to permit adequate inter-well comparison of different cytokine effects within each experiment.

3.2.5: Ang-1 Mediated Inhibition of Permeability in HUVEC:

Using the revised insert system, HRP tracer and primary HUVEC, a new attempt was made to demonstrate an inhibition of baseline endothelial permeability following Ang-1 stimulation. An example of one such experiment using 200 ng/ml Ang-1 is presented in Figure 3.8, which compiles the results from two individual inserts per condition. Presented as a continuous permeability-over-time curve, Figure 3.8 clearly demonstrates a reduction in HRP tracer passage in monolayers pre-treated for 30 minutes with 200ng/ml Ang-1 as compared to baseline controls. Further examination of the permeability curves demonstrates the progressive rise in permeability after 30 minutes, approaching a steady state by 60 minutes, and in marked contrast to the more linear permeability recorded with HMEC-98 monolayers. To verify the reproducibility of this barrier effect of Ang-1, the same experiment was reproduced four times in total and similar findings were recorded in each case. Figure 3.9 presents the compiled data from these four experiments, with individual monolayer permeability calculated as an average over the 80 minute measurement period and combined into a bar graph. This figure also includes the results from two experiments in which 340 ng/ml COMP-Ang1 was used instead of Ang-1. The data presented in figure 3.9 demonstrates that there is nearly a 50% reduction in baseline permeability in monolayers exposed to 200 ng/ml Ang-1, with a similar result using the more potent COMP-Ang1.

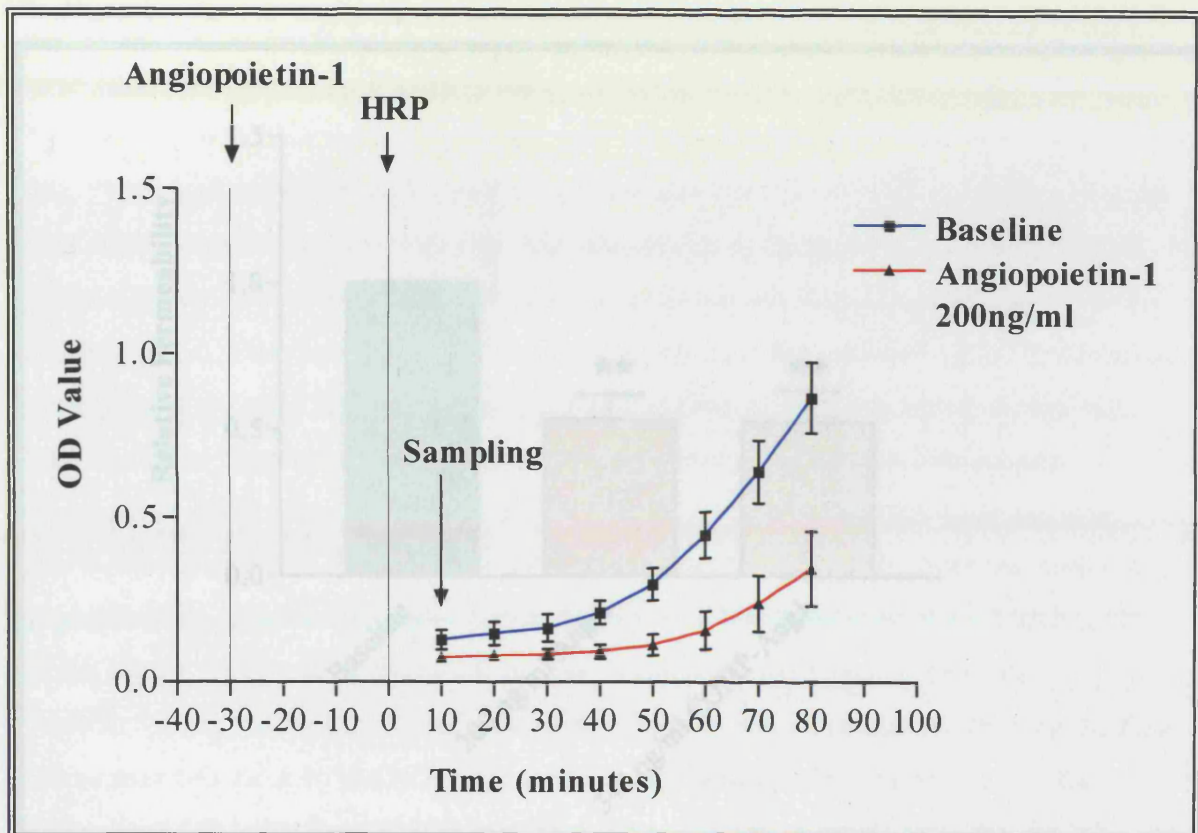


Figure 3.8: HUVEC monolayer permeability under baseline and Ang-1 stimulated conditions. 0.7×10^5 HUVEC seeded to $3 \mu\text{m}$ pore fibronectin-coated Costar inserts followed by a 48 hour monolayer formation period. 200ng/ml Ang-1 added to relevant insert chambers 30 minutes before addition of HRP tracer (arrows), with lower chamber sampling every 10 minutes thereafter. Each data point represents the combined results from three individual monolayers with error bars representing SD about the mean. Representative experiment from a series of four.

3.1.6: Endothelial Permeability in Tiel Deficient HUVEC:

With a clear enhancement of baseline barrier function by the addition of Ang-1 to HUVEC monolayers, the next series of experiments sought to define the role played by Tiel and Tie2 in mediating this effect. To test the impact of Tiel removal on permeability control, Tiel deficient HUVEC were generated by siRNA gene silencing as described in the Materials and Methods chapter section 2.11.2. Initial experiments revealed inhibition of permeability

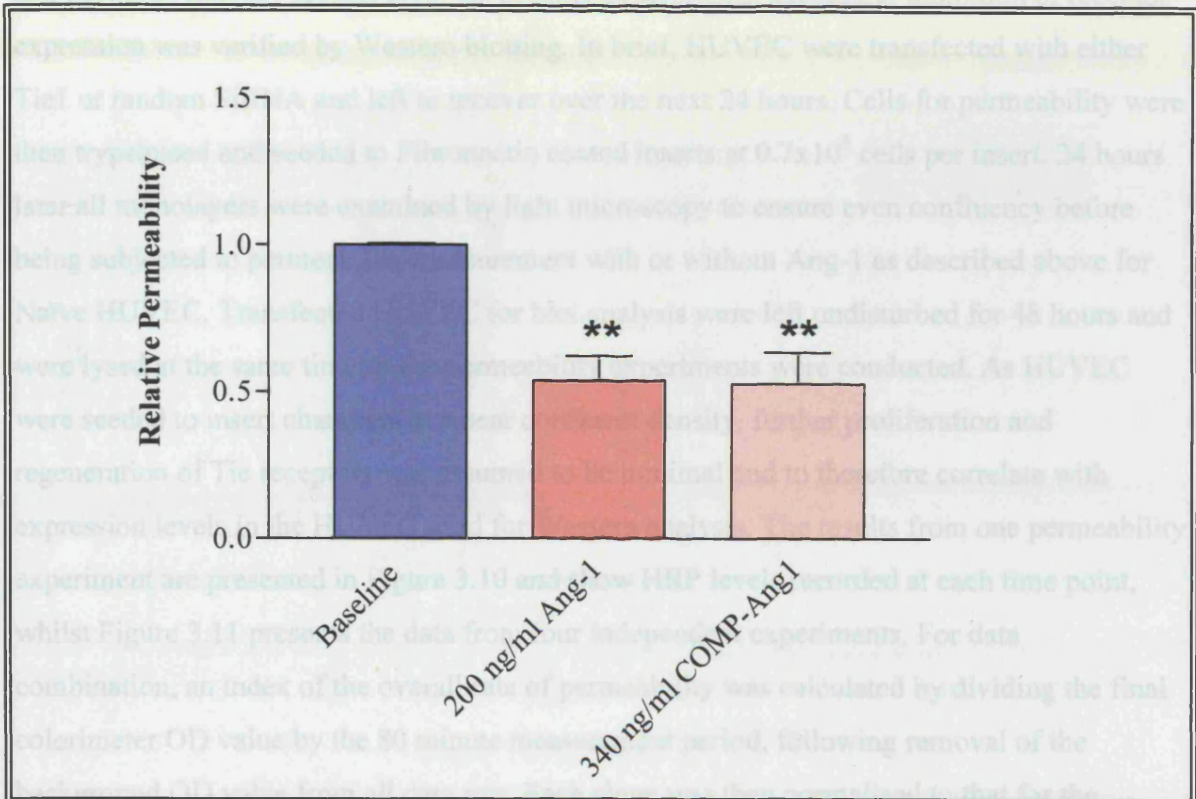
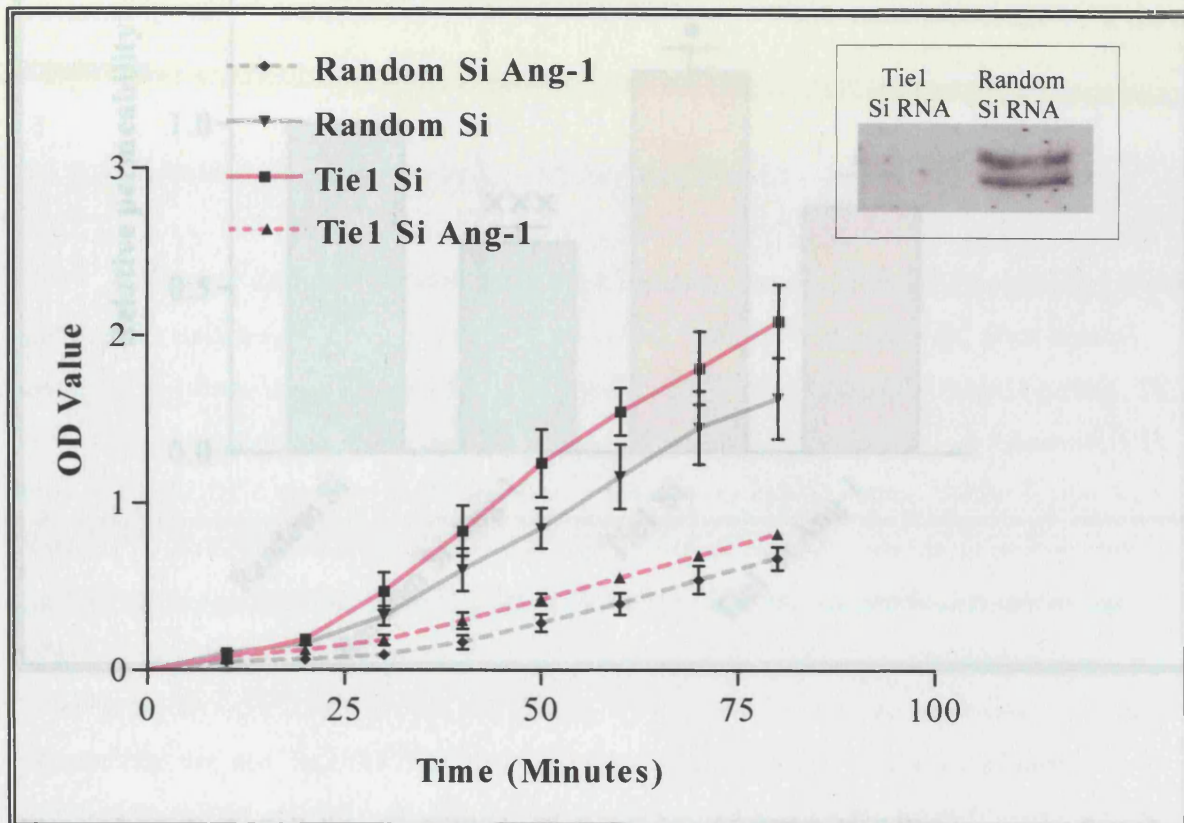


Figure 3.9: Endothelial permeability assay in HUVEC exposed to either Ang-1 or COMP-Ang1. HUVEC were seeded to fibronectin coated 3µm Costar inserts. Permeability was recorded 24 hours later using the HRP technique described in section 2.16.2 of the materials and methods chapter. Individual experiment permeability calculated from HRP passage per unit time over an 80 minute measurement period. Individual experiment data then normalised to the baseline insert values prior to combination into a single graph. Ang-1 and COMP-Ang1 used at the concentrations indicated and added 30 minutes prior to the permeability assay and to the insert chamber only. Values represent the mean of duplicate monolayers, from four individual experiments using Ang-1 and two individual experiments with COMP-Ang1. Both Ang-1 and COMP-Ang1 exert a statistically significant monolayer barrier enhancement (** P=<0.05) compared to baseline monolayer permeability.

3.2.6: Endothelial Permeability in Tie1 Deficient HUVEC:

With a clear enhancement of baseline barrier function by the addition of Ang-1 to HUVEC monolayers, the next series of experiments sought to define the role played by Tie1 and Tie2 in mediating this effect. To test the impact of Tie1 removal on permeability control, Tie1 deficient HUVEC were generated by SiRNA gene silencing as described in the Materials and Methods chapter, section 2.11. As in other experiments, successful inhibition of receptor expression was verified by Western blotting. In brief, HUVEC were transfected with either Tie1 or random SiRNA and left to recover over the next 24 hours. Cells for permeability were then trypsinised and seeded to Fibronectin coated inserts at 0.7×10^5 cells per insert. 24 hours later all monolayers were examined by light microscopy to ensure even confluency before being subjected to permeability measurement with or without Ang-1 as described above for Naïve HUVEC. Transfected HUVEC for blot analysis were left undisturbed for 48 hours and were lysed at the same time as the permeability experiments were conducted. As HUVEC were seeded to insert chambers at a near confluent density, further proliferation and regeneration of Tie receptors was assumed to be minimal and to therefore correlate with expression levels in the HUVEC used for Western analysis. The results from one permeability experiment are presented in Figure 3.10 and show HRP levels recorded at each time point, whilst Figure 3.11 presents the data from four independent experiments. For data combination, an index of the overall rate of permeability was calculated by dividing the final colorimeter OD value by the 80 minute measurement period, following removal of the background OD value from all data sets. Each slope was then normalised to that for the random control baseline before being pooled with the corresponding data from the other experiments in the series. The random control HUVEC data was also combined with control cell data from the subsequent data presenting the permeability in Tie2 deficient HUVEC (Figures 3.13). Therefore the random control data originates from 8 separate experiments and is identically presented in figures 3.11 and 3.13.



With random or Tie1 siRNA and seeded at 8.7×10^4 cells per fibronectin coated 3µm Costar insert after 24 hours. Permeability calculated after a further 24 hours by calculation of overall HRP diffusing gradient over 10 minutes as described in the text. Graph of the combined

Figure 3.10: Endothelial permeability assay comparing Tie1 deficient HUVEC with random SiRNA transfected control HUVEC. HUVEC were transfected with either Tie1 or random SiRNA and allowed to recover for 24 hours before being seeded to fibronectin coated 3µm Costar inserts. Permeability was recorded 24 hours later. Solid lines represent baseline permeability, and dashed lines correspond to permeability following 30 minutes exposure to 200 ng/ml Ang-1 for each cell type. (Ang-1 and HRP addition at the same times as presented in Figure 3.10) Values represent the mean of triplicate monolayers, from a representative experiment of four with error bars corresponding to the SD. Companion blot to the right indicates knockdown efficiency.

From the data presented in Figures 3.10 And 3.11, it is clear that Ang-1 enhancement of barrier function in HUVEC is not solely dependent upon Tie1 receptor signalling, as the ligand exerted a statistically significant effect even in the absence of Tie1 ($P < 0.05$). The baseline level of permeability was also found to be higher in Tie1 deficient HUVEC when compared to random transfected controls ($P < 0.05$). Ang-1 also significantly enhanced

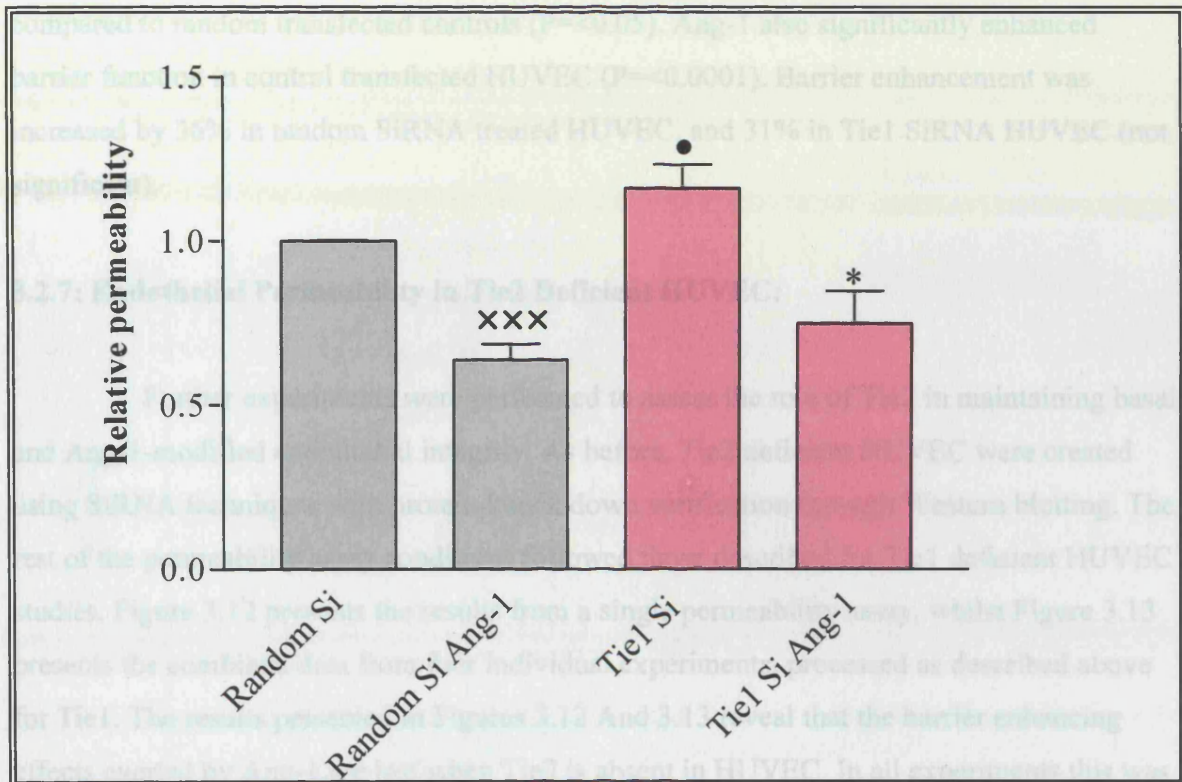


Figure 3.11: Endothelial permeability in Tie1 deficient HUVEC. HUVEC were transfected with random or Tie1 SiRNA and seeded at 0.7×10^5 cells per fibronectin coated $3 \mu\text{m}$ Costar insert after 24 hours. Permeability calculated after a further 24 hours by calculation of overall HRP diffusion gradient over 80 minutes as described in the text. Graph of the combined results from four experiments comparing Tie1 deficient HUVEC permeability with random SiRNA controls, both with and without Ang-1 stimulation. Ang-1 exerts a statistically significant inhibition on baseline permeability in both random control and Tie1 deficient HUVEC (xxx $P < 0.0001$, * $P < 0.05$). Baseline permeability is also increased in Tie1 deficient HUVEC (● $P < 0.05$) Bar values represent the mean of four experiments flanked by SEM error bars.

From the data presented in Figures 3.10 And 3.11, it is clear that Ang-1 enhancement of barrier function in HUVEC is not solely dependent upon Tie1 receptor signalling, as the ligand exerted a statistically significant effect even in the absence of Tie1 ($P < 0.05$). The baseline level of permeability was also found to be higher in Tie1 deficient HUVEC when compared to random transfected controls ($P < 0.05$). Ang-1 also significantly enhanced barrier function in control transfected HUVEC ($P < 0.0001$). Barrier enhancement was increased by 36% in random SiRNA treated HUVEC, and 31% in Tie1 SiRNA HUVEC (not significant).

3.2.7: Endothelial Permeability in Tie2 Deficient HUVEC:

Further experiments were performed to assess the role of Tie2 in maintaining basal and Ang-1-modified endothelial integrity. As before, Tie2 deficient HUVEC were created using SiRNA techniques with protein knock down verification through Western blotting. The rest of the permeability assay conditions followed those described for Tie1 deficient HUVEC studies. Figure 3.12 presents the results from a single permeability assay, whilst Figure 3.13 presents the combined data from four individual experiments, processed as described above for Tie1. The results presented in Figures 3.12 And 3.13 reveal that the barrier enhancing effects exerted by Ang-1 are lost when Tie2 is absent in HUVEC. In all experiments this was found to be the case, demonstrating the critical requirement for Tie2 in mediating Ang-1's effects. The fact that Tie2 deficiency completely abrogates Ang-1's effects indicates that, in this system at least, integrin signalling does not represent a significant route for Ang-1 anti-permeability signalling. The baseline permeability in Tie2 deficient HUVEC was marginally smaller overall in this series of four permeability experiments than in random controls, although the SEM for both Tie2 HUVEC conditions are fairly large.

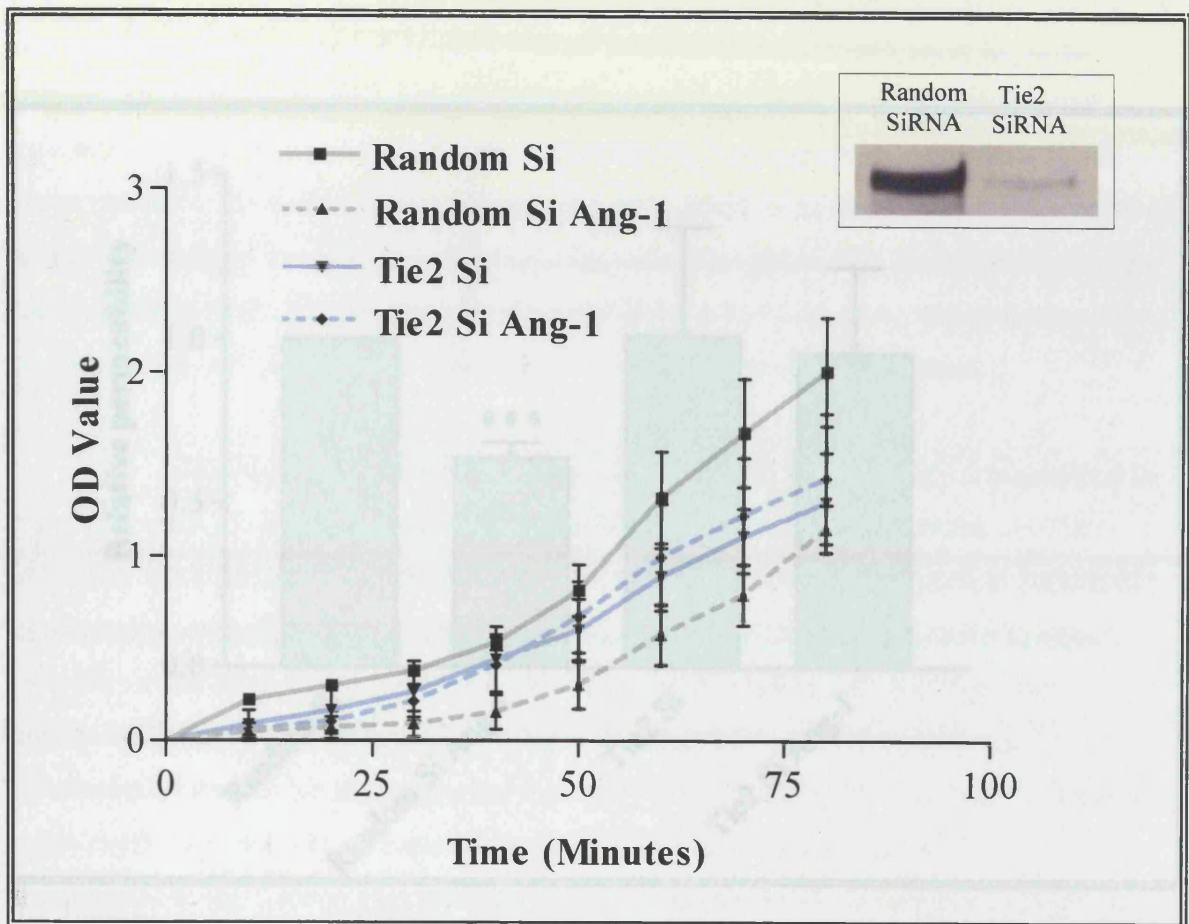


Figure 3.13: Combined results from four permeability experiments with Tie2 deficient and

Figure 3.12: Tie2 deficient HUVEC permeability compared to random transfected control HUVEC with or without 200 ng/ml ang-1. HUVEC were transfected with either Tie2 or random SiRNA and seeded at 0.7×10^5 cells to fibronectin coated $3 \mu\text{m}$ Costar inserts after 24 hours. Following 24 hours incubation to allow monolayer establishment, permeability was recorded 30 minutes after the addition of 200 ng/ml Ang-1 to respective wells. Each data point represents the mean values obtained from three separate monolayers recorded every 10 minutes following addition of HRP tracer. (Error bars represent SD about the mean). Companion blot to the right indicates degree of receptor knockdown. Representative experiment from a series of four.

3.3. Discussion:

To investigate Tie2 receptor function in different aspects of endothelial responses to inflammation, Tie1 and Tie2 deficient HUVEC were created using siRNA techniques. Using a protocol designed for maximum efficiency, removal of individual receptors proved remarkably effective and by preserving cell viability for downstream applications. Removal of both Tie1 and Tie2 simultaneously however was less effective when using the same

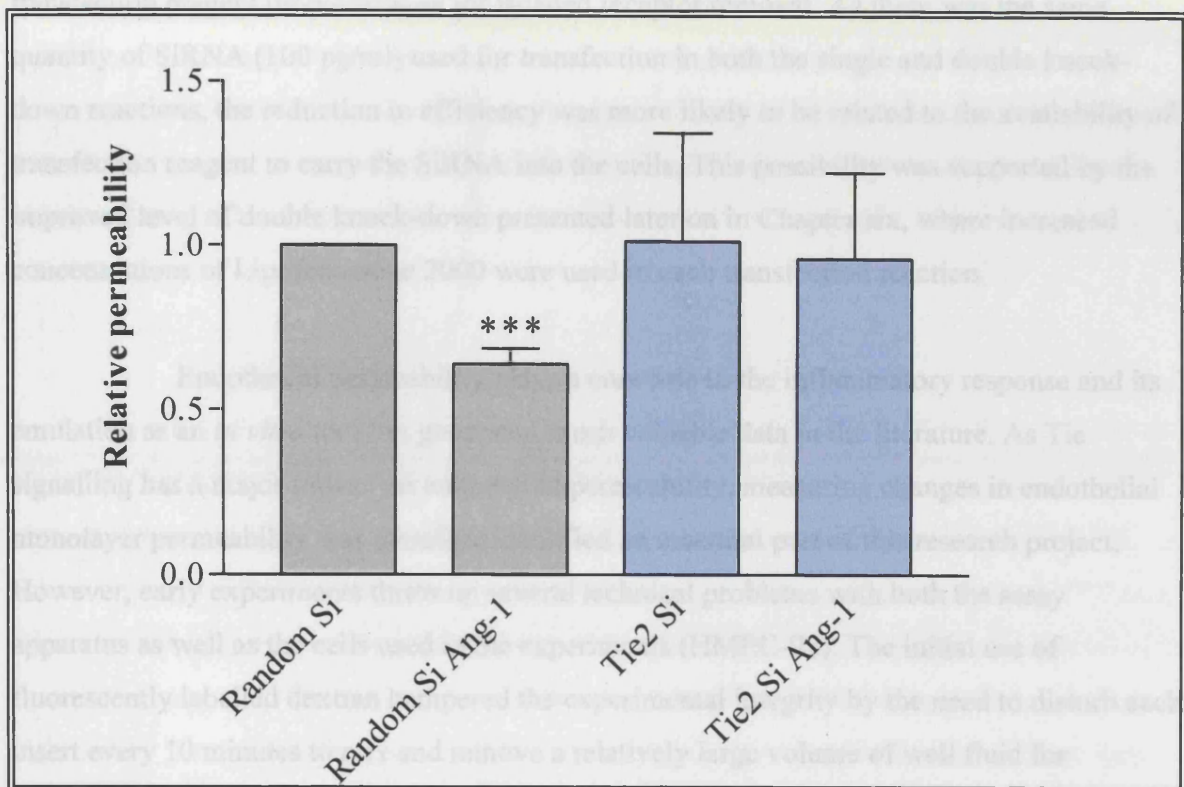


Figure 3.13: Combined results from four permeability experiments with Tie2 deficient and control HUVEC with or without Angiopoitin-1. HUVEC were transfected with random or Tie2 SiRNA and seeded at 0.7×10^5 cells per fibronectin coated $3 \mu\text{m}$ Costar insert 24 hours later. Permeability calculated after a further 24 hours by dividing the final OD value by the 80 minute measurement period as described in the text. Random transfected HUVEC monolayers have a statistically significant barrier enhancement in response to 200ng/ml Ang-1 (***) $P < 0.0005$). There was no difference in permeability between baseline Tie2 deficient HUVEC and those exposed to Ang-1. (Values represent mean permeability flanked by SEM error bars).

3.3: Discussion:

To investigate Tie receptor function in different aspects of endothelial responses to inflammation, Tie1 and Tie2 deficient HUVEC were created using SiRNA techniques. Using a protocol designed for maximal efficiency, removal of individual receptors proved remarkably effective whilst maintaining cell viability for downstream applications. Removal of both Tie1 and Tie2 simultaneously however was less effective when using the same transfection reagent proportions as for isolated receptor removal. As there was the same quantity of SiRNA (100 pg/ml) used for transfection in both the single and double knock-down reactions, the reduction in efficiency was more likely to be related to the availability of transfection reagent to carry the SiRNA into the cells. This possibility was supported by the improved level of double knock-down presented later on in Chapter six, where increased concentrations of Lipofectamine 2000 were used in each transfection reaction.

Endothelial permeability plays a core role in the inflammatory response and its emulation as an *in vitro* tool has generated much valuable data in the literature. As Tie signalling has a major impact on endothelial permeability, measuring changes in endothelial monolayer permeability was therefore identified an essential part of this research project. However, early experiments threw up several technical problems with both the assay apparatus as well as the cells used in the experiments (HMEC-98). The initial use of fluorescently labelled dextran hampered the experimental integrity by the need to disturb each insert every 10 minutes to mix and remove a relatively large volume of well fluid for fluorescence measurement. This led to an assay with relatively low sensitivity to anything other than large concentrations of thrombin, and the inability to demonstrate a barrier enhancing effect of Ang-1 under baseline conditions. This latter point was pursued to no avail for several weeks, and in addition to the aforementioned limitations of the Falcon[®] insert system, the lack of Ang-1 responsiveness also called into question the suitability of HMEC-98 for permeability studies. Although no conclusive reason is offered for the lack of HMEC-98 permeability reduction by Ang-1, it is likely to represent either a failure of universal cell response within an intact monolayer, or a monolayer with sufficient intercellular gaps to overshadow the tightening effects of Ang-1 stimulation by responsive cells. Whilst no overt intercellular gaps were observed by light microscopy, a better impression of HMEC-98 monolayer formation could be achieved by improved resolution imaging together with junctional staining techniques. Either way, the subsequent decision to revise the entire

experimental approach was taken at this point, following several discussions with Professor J Gamble of the University of Adelaide. Professor Gamble provided critical experimental fine tuning advice that led to the first successful endothelial permeability reduction with Ang-1 in HUVEC (Figure 3.8). This and subsequent experiments demonstrated nearly a 50% drop in monolayer leakage using 200 ng/ml Ang-1 over an 80 minute measurement period. Moreover, similar results were obtained with COMP-Ang1; the comparatively high concentration (340 ng/ml) carried over as a continuation of the experiments used to no avail in attempting to stimulate HMEC-98 barrier enhancement (data not shown). Whilst the HMEC-98 experiments investigated the reversibility of thrombin-mediated permeability using Ang-1, this was not included in the HUVEC experiments as the main objective was to define distinct roles for Tie1 and Tie2 in permeability control. With more time, an investigation of the pro-permeability potency of thrombin would have been very interesting in Tie deficient cells both with and without the presence of Ang-1.

In considering the measurement of endothelial permeability, there was a marked contrast between the permeability curves in experiments using HMEC-98 / FITC-dextran, and HUVEC / HRP. HMEC-98 demonstrated a relatively linear tracer passage per unit time (not shown), whereas HUVEC permeability characteristically increased after the first 20 to 50 minutes (Figure 3.8). Considering all of this data, it may be possible that the use of HRP as a tracer actually generated a pro-permeability response in and of itself, and this fits in well with an early *in vivo* study showing a pro-permeability effect for HRP in rat lung microvasculature (139). HRP was never employed with the HMEC-98 experiments, but this would have been an appropriate approach to testing the hypothesis that HRP elicits permeability, through a direct comparison with the permeability curves obtained with FITC-dextran. Whether HRP is an induction agent for endothelial permeability or not, a search of the literature confirms its position as one of the most popular agents for permeability measurement, and its advantages over FITC-dextran were critical in the present experiments. Nevertheless, the non-linearity of permeability seen using HRP in HUVEC was an important consideration when deciding how to calculate the rate of permeability for these experiments, and how to combine individual data sets for cumulative comparison. If the early readings best reflect the effects of Ang-1 prior to any pro-permeability effect of the HRP tracer then this would be a suitable selection for rate calculation (0 – 30 minutes). However, the degree of gradient separation is minimal over this time period, and ignoring subsequent enhanced permeability would have added considerable bias to the method of calculation. Thus it was decided to calculate the overall

permeability from the quantity of HRP tracer present in the lower well chamber at the assays completion at 80 minutes, without specific weighting to variations in individual permeability traces along the way to this time-point.

This work set out to establish the role of each receptor in ang-1 mediated enhanced endothelial barrier functions. HUVEC deficient in Tie1 remain fully capable of responding to Ang-1 stimulated barrier enhancement, whereas Tie2 deficient HUVEC monolayers were completely un-affected. This establishes an essential role for Tie2 in mediating the anti-permeability effects of Ang-1. One previous study using an abrogated monomeric form of Ang-1 found that baseline barrier function could be enhanced in immortalised endothelial cells in a similar manner to that seen in the present work (102). Interestingly, although this abbreviated ligand bound Tie2 but failed to induce its phosphorylation, it did bind the $\alpha 5\beta 1$ integrin with the same avidity as that for Tie2. With existing evidence for $\alpha 5\beta 1$ mediating adhesion and migration on Ang-1 coated surfaces (140), Weber proposed that their monomeric Ang-1 variant might also mediate enhanced monolayer barrier functions in view of the ligands failure to achieve Tie2 activation. However, beyond noting a lack of Tie2 phosphorylation with monomeric Ang-1, this work offered no definitive receptor allocation for Ang-1 mediated barrier enhancement. By systematically removing each Tie receptor in turn this work has defined for the first time the essential requirement for Tie2's importance in the Ang-1 regulation of monolayer permeability. With Tie2 deficiency, the present studies found no alternative integrin mediated pathway that could enhance endothelial barrier function in the context of full-length native Ang-1. This suggests that, *in vivo* at least, the Tie2 receptor is solely responsible for altering permeability in response to oligomeric native Ang-1. In terms of endothelial cell apoptosis, Tie1 deficient HUVEC have a greater survival response to Ang-1 stimulation compared to random SiRNA treated controls. (section 4.4.2). Interestingly, this is not the case for permeability where there is a slightly poorer response to Ang-1 mediated barrier enhancement in Tie1 deficient HUVEC compared to controls. This might suggest an agonist function of Tie1 in permeability control, especially in view of the elevated baseline level of permeability in Tie1 deficient HUVEC monolayers.

This work has demonstrated a critical role for Tie2 in mediating Ang-1 stimulated barrier function in endothelial cells. Further experiments would take this further to look at the impact of individual Tie receptor deletion under inflammatory conditions, especially in response to thrombin.

4.1: Tie Receptors and the Regulation of Endothelial Cell Apoptosis:

Although detailed anti-apoptotic signalling information exists for Tie2 (114), Tie1 has long been described as an orphan receptor due to the apparent lack of phosphorylation by known Angiopoietin ligands. This, combined with the abolition of Angiopoietin-1 mediated cell survival in the presence of soluble Tie2Fc (47, 117, 141), has led to the assumption that Tie2 is primarily responsible for transducing the anti-apoptotic stimuli of Angiopoietin-1 in endothelial cells. However, recent studies using chimaeric Tie1 receptors and other work using COMP-Ang1 has successfully achieved Tie1 phosphorylation with similar characteristics to Tie2 (38, 119). Another study has now postulated that Tie1 is readily capable of being activated by native Ang-1, so long as it is in the presence of functional Tie2 (142). This suggests that care is required when interpreting the results from experiments using Tie receptors in isolation, as their biological function is likely to be contingent upon their interaction with each other and possibly other endothelial specific co-factors. Furthermore, as soluble Tie2Fc but not Tie1Fc abrogates Tie1 activation, these data again suggest that receptor binding and activation require the Tie1 receptor to be present in the cell membrane for it to function properly. With this in mind the focus of the current chapter has been to verify the assumed supremacy of Tie2 in mediating endothelial cell survival and to investigate the anti-apoptotic role, if any, of Tie1. To address this hypothesis, the following objectives and questions have been considered:

- 1:** The creation of an *in vitro* model of endothelial apoptosis with demonstration of an anti-apoptotic property by Angiopoietin-1.
- 2:** The use of this system to ask whether functional Tie1 has any overall effect on Tie2 mediated cell survival through creation of Tie1 deficient endothelial cells.
- 3:** If Tie1 does alter Tie2 mediated cell survival, how do these differences become manifest when Tie1 is absent?
- 4:** Can Tie1 mediate cell survival with angiopoietin-1 in the absence of Tie2?
- 5:** Do Tie receptors play a significant role in mediating cell survival signals from other endothelial growth factors such as VEGF?

To answer these questions, an *in vitro* survival assay was developed to induce and measure endothelial cell apoptosis, using HUVEC. HUVEC were cultured on uncoated plastic ware, where the absence of extracellular matrix cues forced the sole reliance upon factors

present within the culture medium for survival. With removal of the serum component of the culture medium, any remaining pro-survival substances such as VEGF, Ang-1 and bFGF are absent, leading to intrinsic caspase activation via mitochondrial derived cytochrome c and other intermediates. This leads to the production of caspases 3 and 7 which are both readily detectable in apoptosing cells by the use of a commercially available caspase quantitation kit. This was therefore chosen as the principal apoptotic stimulus to be used in all experiments. As described in Section 2.17 of the materials and methods chapter.

4.2: Establishment of Apoptosis in Serum-Starved HUVEC:

To demonstrate the induction of apoptosis under serum-free conditions, HUVEC were cultured in serum free media for 0, 2, 4, 6 and 8 hours prior to lysis and caspase measurement. Figure 4.1 presents these results with each time-point repeated in triplicate. As indicated in graph 4.1, caspase levels progressively rise with increasing duration of exposure to serum-free media in a roughly linear manner over the 8 hour time period measured. Caspase levels increased by nearly threefold over this duration.

4.3: Inhibition of Apoptosis by Angiopoietin-1 in Serum-Starved HUVEC:

With the demonstration of progressive apoptosis under serum free conditions, the next set of experiments aimed to establish the anti-apoptotic effect of Angiopoietin-1 on HUVEC exposed to serum free media. In this experiment, HUVEC were seeded to wells of a 96 well plate as described. Following the addition of serum-free medium, selected wells were then treated with Angiopoietin-1 at 0, 50, 100, 200 and 400 ng/ml. After a 4 hour incubation period, caspase levels were recorded as described and the combined results of three experiments is presented in Figure 4.2. As demonstrated in Figure 4.2, there is a progressive fall in Caspase levels and by inference, apoptosis, in HUVEC treated with increasing doses of Angiopoietin-1 under serum free conditions. In every case this finding reached statistical significance. In contrast to the roughly linear rate of time dependent apoptosis for serum starved HUVEC, Angiopoietin-1 had a greater anti-apoptotic effect over the lower end of the dose range used. As a result of these first two experimental series, standard experimental conditions were established, namely apoptosis induction with serum-free media exposure for 4 hours and, where a fixed dose of Angiopoietin-1 was used, this was set at 200ng/ml.

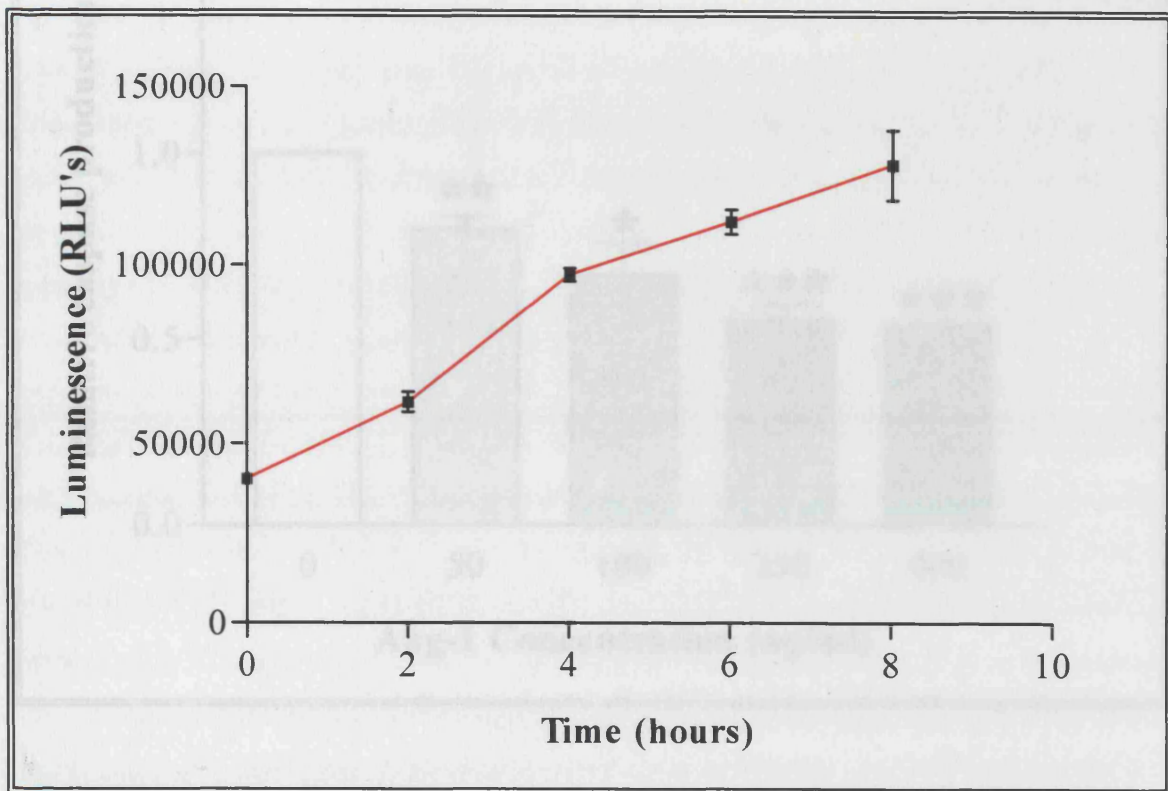


Figure 4.1: HUVEC cells were seeded into individual wells of a 96 well plate and cultured for 24 hours. Cells were then washed into serum free media before culture for 8 hours at the time points indicated (0, 2, 4, 6 and 8 hours). Each time point was repeated in triplicate, with data shown as mean +/- SD. At the end of the assay, Caspase-Glo reagent was added and luminescence recorded (RLU's = Relative Light Units). Data from single experiment.

Figure 4.1: 1×10^4 HUVEC per well were seeded into the wells of a flat-bottomed 96 well plate. Cells were cultured for 24 hours in complete media, before sequential exchange with $50 \mu\text{l}$ per well of serum-free media at 0, 2, 4, 6 and 8 hour time points. Each time point was repeated in triplicate, with data shown as mean +/- SD. At the end of the assay, Caspase-Glo reagent was added and luminescence recorded (RLU's = Relative Light Units). Data from single experiment.

4.4 Establishment of Tie Receptor Involvement in Angiopoietin-1 Protected Serum Starved HUVEC:

With a just demonstration of apoptosis reduction by Angiopoietin-1 in serum starved HUVEC, the next series of experiments sought to verify the relative impact of Tie1 and Tie2 receptors in mediating this process. To address this question, RNA interference techniques

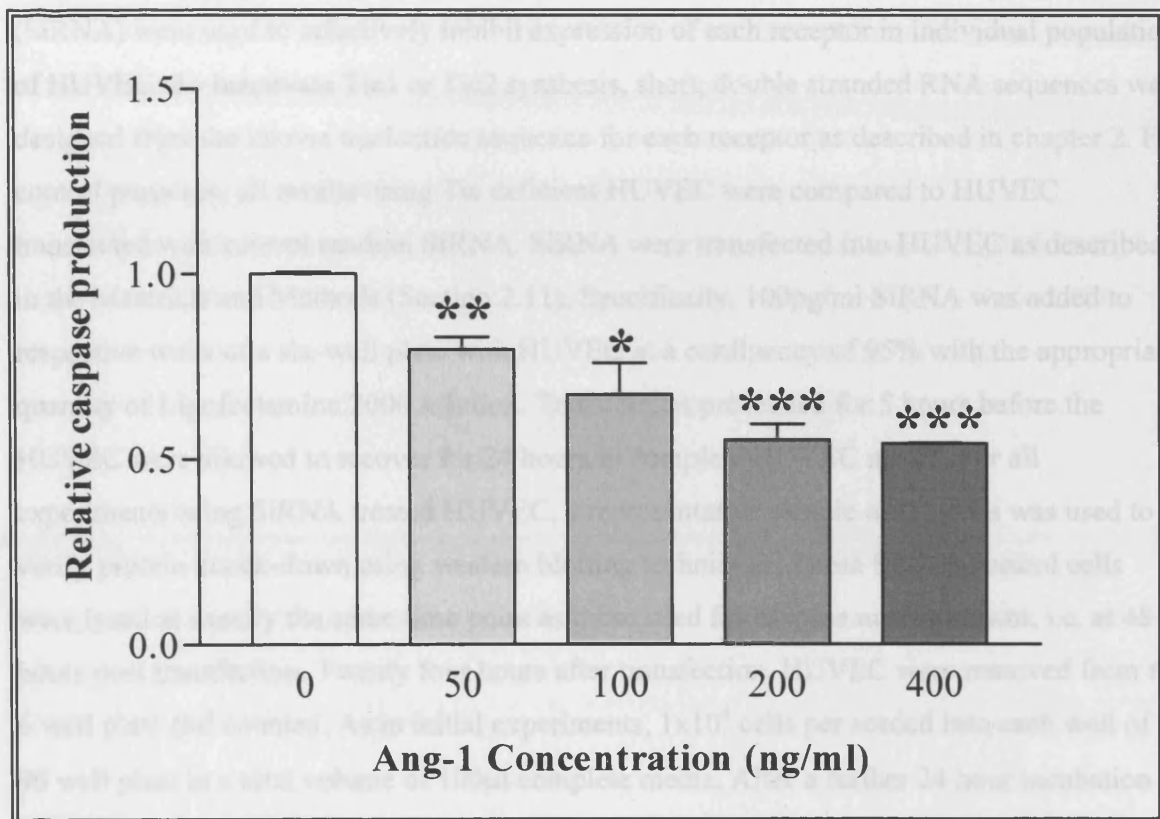


Figure 4.2: HUVEC rescue from apoptosis by Ang-1. 1×10^4 HUVEC were seeded to individual wells of a 96 well plate and cultured for 24 hours. Cells were then washed once in serum free media before culture for 4 hours in the same with or without Ang-1 at the concentrations indicated (0, 50, 100, 200 and 400 ng/ml). Each bar represents the mean of three separate experiments, each conducted with duplicate wells. Data from individual experiments normalised prior to combination for this figure. Data points presented as mean \pm SEM. Ang-1 produces a statistically significant decrease in caspase production in serum starved HUVEC over the four concentrations used (* $P < 0.005$, ** $P < 0.05$, *** $P < 0.001$).

4.4: Establishment of Tie Receptor Involvement in Angiopoietin-1 Protected Serum Starved HUVEC:

With a clear demonstration of apoptosis reduction by Angiopoietin-1 in serum starved HUVEC, the next series of experiments sought to verify the relative impact of Tie1 and Tie2 receptors in mediating this process. To address this question, RNA interference techniques (SiRNA) were used to selectively inhibit expression of each receptor in individual populations of HUVEC. To inactivate Tie1 or Tie2 synthesis, short, double stranded RNA sequences were designed from the known nucleotide sequence for each receptor as described in chapter 2. For control purposes, all results using Tie deficient HUVEC were compared to HUVEC transfected with control random SiRNA. SiRNA were transfected into HUVEC as described in the Materials and Methods (Section 2.11). Specifically, 100pg/ml SiRNA was added to respective wells of a six-well plate with HUVEC at a confluency of 95% with the appropriate quantity of Lipofectamine 2000 solution. Transfection proceeded for 5 hours before the HUVEC were allowed to recover for 24 hours in complete HUVEC media. For all experiments using SiRNA treated HUVEC, a representative sample of the cells was used to verify protein knock-down using western blotting techniques. These SiRNA control cells were lysed at exactly the same time point as those used for caspase measurement, i.e. at 48 hours post transfection. Twenty four hours after transfection, HUVEC were removed from the 6 well plate and counted. As in initial experiments, 1×10^4 cells per seeded into each well of a 96 well plate in a total volume of 100 μ l complete media. After a further 24 hour incubation period, the complete media was changed for 50 μ l of serum free media. Selected wells were then treated with 200 ng/ml Angiopoietin-1 or vehicle for 4 hours prior to determination of caspase levels as described.

4.4.1: Apoptosis in Tie1 Deficient HUVEC:

Tie1 knock-down was highly effective using the described protocol, and Figure 4.3 presents the scanned image of a western blot from a representative sample of Tie1 deficient HUVEC compared to HUVEC transfected with random SiRNA. To verify equal protein loading, the same blot was stripped and re-probed for total Tie2. This approach to semi-quantitative assessment of protein loading assumed that Tie2 had been unaffected by the transfection process as might have occurred through cross-reactivity from Tie1 SiRNA. A

more accurate and reliable technique would have been to strip and re-probe the membrane for a so-called house keeping gene such as α -actin.

Once generated, Tie1 deficient HUVEC were then compared against random transfected HUVEC for caspase production following a 4 hour serum-free media incubation with or without Angiopoietin-1. Figure 4.4 presents the combined results of three such experiments where individual rates of caspase production were calculated and normalised to the baseline rate measured from un-stimulated random transfected controls. In addition, the control SiRNA data consists of the combined results from both this and the subsequent experiments using Tie2 deficient HUVEC. Thus both control SiRNA bars are identical in both figure 4.4 and 4.6, and combine results from six independent experiments overall.

Interpreting the data presented in Figure 4.4, Angiopoietin-1 exerted a statistically significant inhibition of apoptosis in HUVEC treated with random SiRNA ($P < 0.0005$). This finding also holds true for Tie1 deficient HUVEC ($P < 0.05$). Interestingly, the removal of functional Tie1 increased the background level of apoptosis in HUVEC even in the absence of Angiopoietin-1 ($P < 0.0005$).

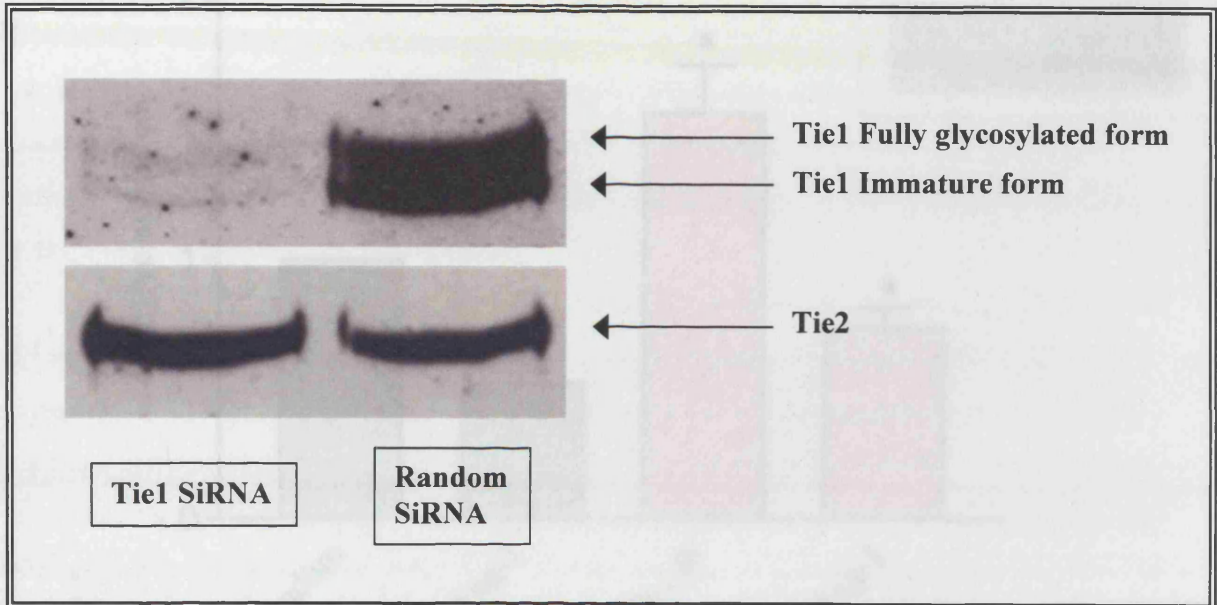


Figure 4.3: HUVEC whole cell lysate western blot 48 hours post transfection with Tie1 SiRNA or random SiRNA. Both immature and fully glycosylated forms of the Tie1 receptor are effectively silenced in this context. Presented beneath is a reprobe of the same membrane with anti-Tie2 antibody in order to verify equal lane loading.

section 4.11 of the materials and methods section. Tie1-deficient HUVECs were treated with Tie1-specific siRNA for 24 hours. Cells were then exposed to serum-free conditions for 4 hours with or without 200 ng/ml Ang-1, followed by determination of caspase-3 activation. Apoptosis in control siRNA treated cells and there is a significant increase in apoptosis in Tie1 siRNA treated cells. Ang-1 treatment did not increase apoptosis in Tie1 siRNA treated cells. Data is presented as mean and SEM of 3 independent experiments. $P < 0.05$ compared with Tie1 siRNA. Control cells were transfected with siRNA of efficiency.

4.4.2: Apoptosis in Tie1 Deficient HUVEC

Having established that Angiopoietin-1 appears able to protect HUVEC against apoptosis induced by serum deprivation in the absence of Tie1, the next set of experiments sought to investigate the role of Tie1 in the same system. As previously described, Tie2

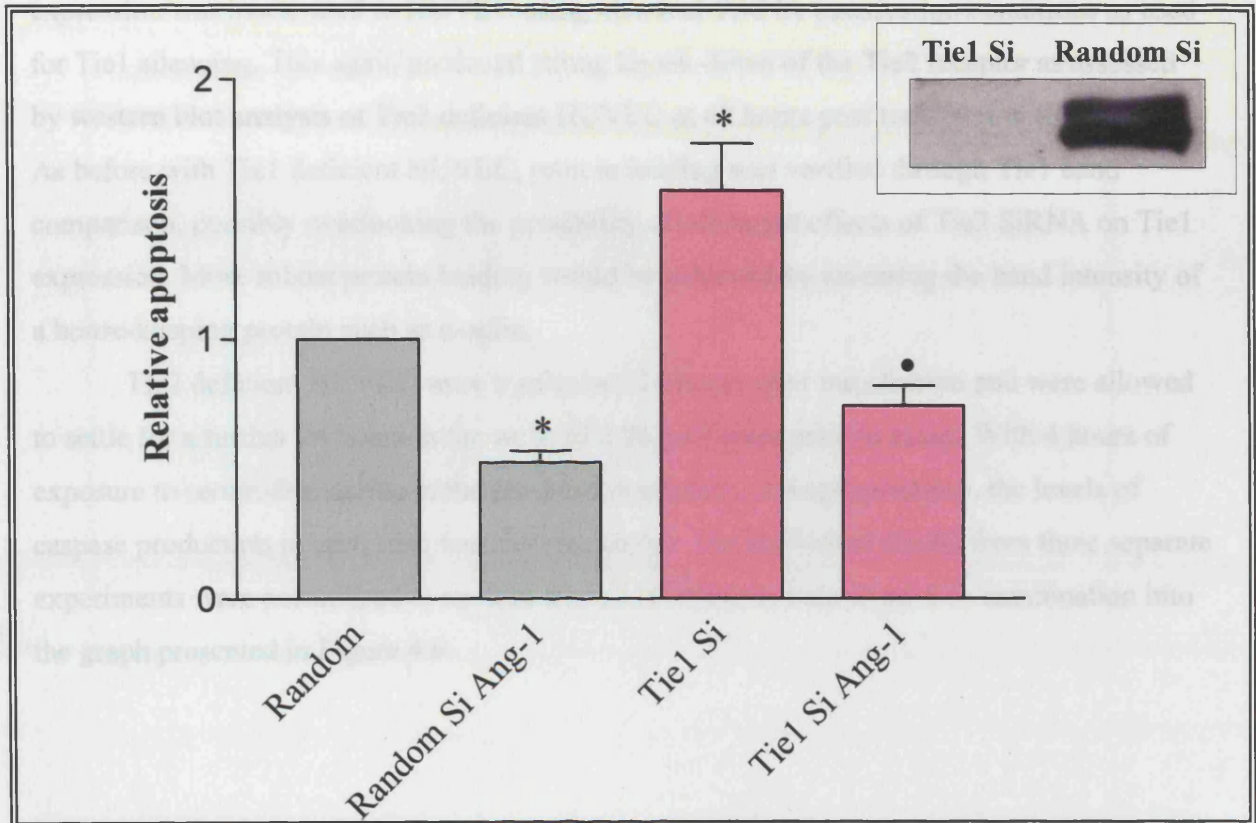


Figure 4.4: Combined normalised results from three individual caspase experiments with Tie1 deficient HUVEC. Tie1 deficient HUVEC were generated according to the protocol in section 2.11 of the materials and methods section. 24 hours after transfection 1×10^4 Tie1 deficient HUVEC were seeded to individual wells of a 96 well plate and cultured for another 24 hours. Cells were then exposed to serum free conditions for 4 hours with or without 200 ng/ml Ang-1, followed by determination of caspase production. Angiopoietin-1 inhibits apoptosis in control SiRNA treated cells and there is a significant increase in baseline apoptosis in Tie1 SiRNA treated cells. Angiopoietin-1 also inhibits apoptosis in Tie1 SiRNA treated cells. Data is presented as mean and SEM (* $P < 0.0005$ compared with random; ● $P < 0.05$ compared with Tie1 SiRNA) Companion blot to the right indicates knockdown efficiency.

4.4.2: Apoptosis in Tie2 Deficient HUVEC:

Having established that Angiopoietin-1 remains able to protect HUVEC against apoptosis induced by serum deprivation in the absence of Tie1, the next set of experiments sought to investigate the role of Tie2 in the same process. As previously described, Tie2 expression was inactivated in HUVEC using identical SiRNA transfection conditions as used for Tie1 silencing. This again produced strong knock-down of the Tie2 receptor as assessed by western blot analysis of Tie2 deficient HUVEC at 48 hours post transfection (Figure 4.5). As before with Tie1 deficient HUVEC, protein loading was verified through Tie1 band comparison, possibly overlooking the possibility of off-target effects of Tie2 SiRNA on Tie1 expression. More robust protein loading would be achieved by assessing the band intensity of a house-keeping protein such as α -actin.

Tie2 deficient HUVEC were trypsinised 24 hours after transfection and were allowed to settle for a further 24 hours in the wells of a 96 well plate prior to assay. With 4 hours of exposure to serum-free media in the presence or absence of Angiopoietin-1, the levels of caspase production in each case was then measured. The individual results from three separate experiments were normalised to random treated HUVEC as before, prior to combination into the graph presented in Figure 4.6.

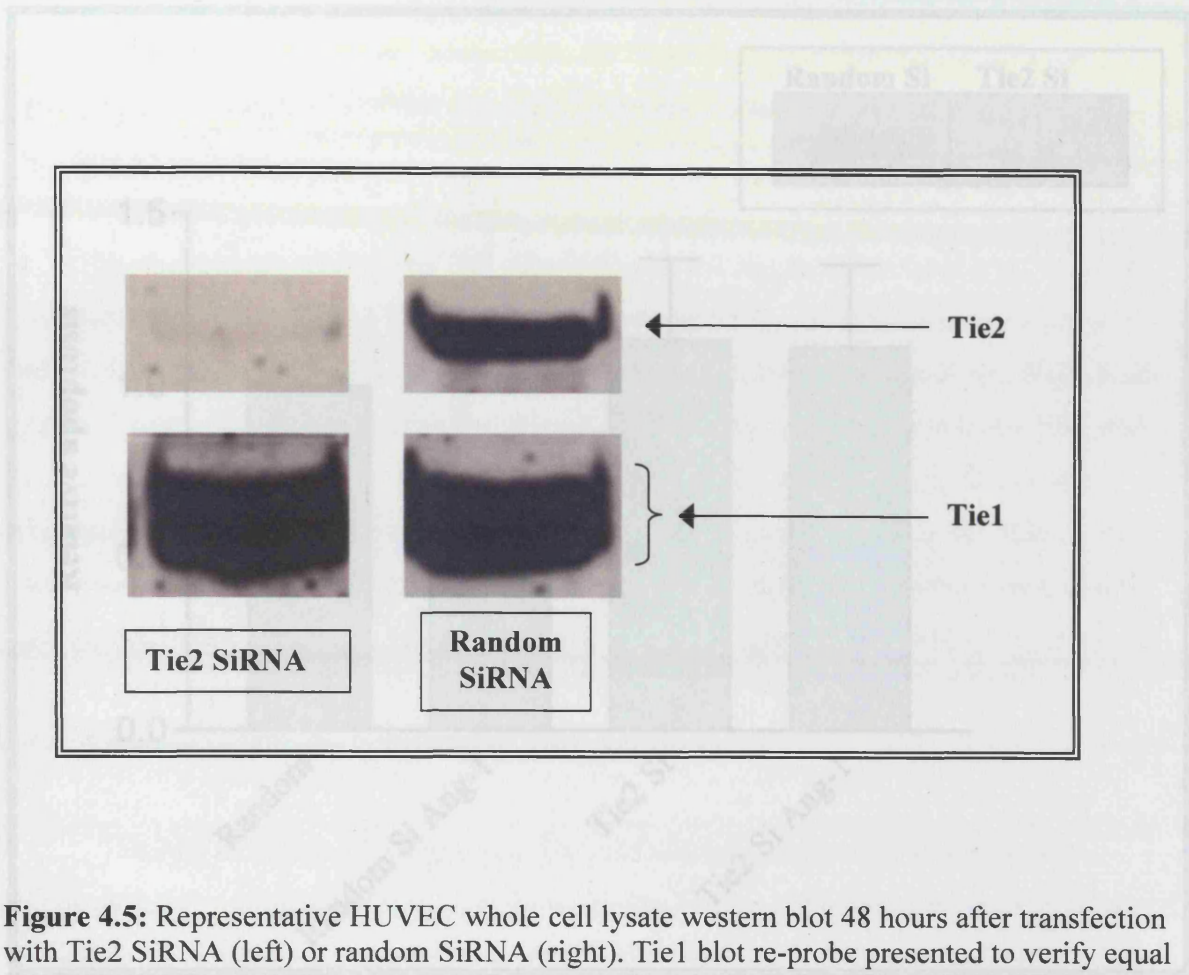


Figure 4.5: Representative HUVEC whole cell lysate western blot 48 hours after transfection with Tie2 SiRNA (left) or random SiRNA (right). Tie1 blot re-probe presented to verify equal loading as in Figure 4.3.

Figure 4.6: Combined normalized results from three individual caspase experiments with Tie2 deficient HUVEC. Tie2 deficient HUVEC were generated according to the protocol in section 2.1 of the materials and methods section. 24 hours after transfection 1×10^5 Tie2 deficient HUVEC were seeded to individual wells of a 96 well plate and cultured for another 24 hours. Cells were then exposed to serum free conditions for 4 hours with or without 200 ng/ml Ang-1, followed by determination of caspase production. The removal of Tie2 abolishes the anti-apoptotic effect of angiopoietin-1 when compared to random treated control HUVEC ($P < 0.005$). Furthermore, the baseline caspase production by Tie2 deficient HUVEC is marginally higher than that seen in random treated HUVEC (not significant). Comparison blot on the right verifies knockdown efficiency.

Examining the data in Figure 4.6, the anti-apoptotic effect of Angiopoietin-1 is lost in the absence of the Tie2 receptor, accepting that the SEM in both baseline and Angiopoietin-1 treated Tie2 deficient HUVEC are larger than those associated with the Tie1 data (Figure 4.4).

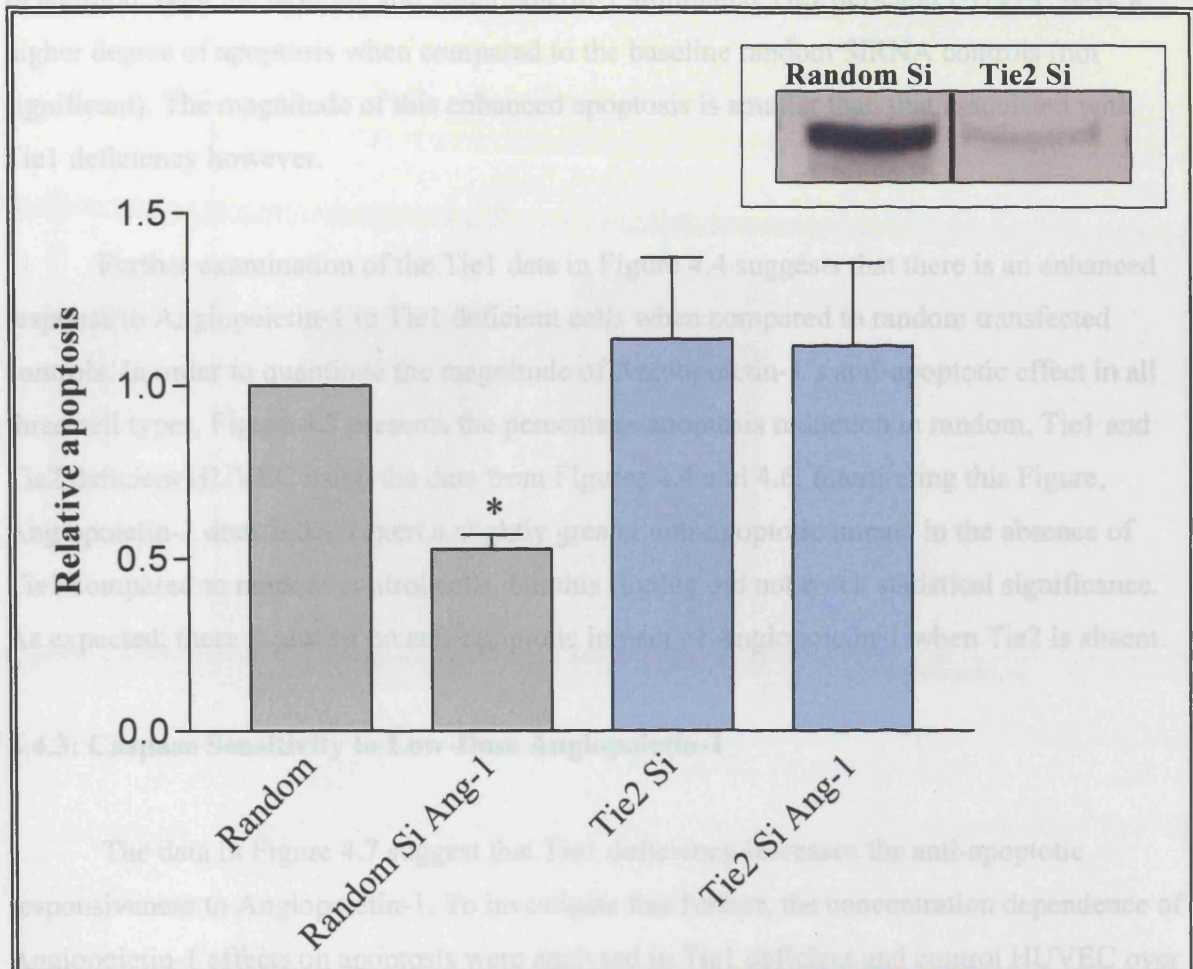


Figure 4.6: Combined normalised results from three individual caspase experiments with Tie2 deficient HUVEC. Tie2 deficient HUVEC were generated according to the protocol in section 2.11 of the materials and methods section. 1×10^4 Tie2 deficient HUVEC were seeded to individual wells of a 96 well plate and cultured for another 24 hours. Cells were then exposed to serum free conditions for 4 hours with or without 200 ng/ml Ang-1, followed by determination of caspase production. The removal of Tie2 abolishes the anti-apoptotic effect of Angiopoietin-1 when compared to random treated control HUVEC (* $P < 0.0005$). Furthermore, the baseline caspase production by Tie2 deficient HUVEC is marginally higher than that seen in random treated HUVEC (not significant) Companion blot to the right indicates knockdown efficiency.

Examining the data in Figure 4.6, the anti-apoptotic effect of Angiopoietin-1 is lost in the absence of the Tie2 receptor; accepting that the SEM in both baseline and Angiopoietin-1 treated Tie2 deficient HUVEC are larger than those associated with the Tie1 data (Figure 4.4). In addition, both the baseline and Angiopoietin-1 stimulated Tie2 deficient HUVEC have a higher degree of apoptosis when compared to the baseline random SiRNA controls (not significant). The magnitude of this enhanced apoptosis is smaller than that associated with Tie1 deficiency however.

Further examination of the Tie1 data in Figure 4.4 suggests that there is an enhanced response to Angiopoietin-1 in Tie1 deficient cells when compared to random transfected controls. In order to quantitate the magnitude of Angiopoietin-1's anti-apoptotic effect in all three cell types, Figure 4.7 presents the percentage apoptosis reduction in random, Tie1 and Tie2 deficient HUVEC using the data from Figures 4.4 and 4.6. Interpreting this Figure, Angiopoietin-1 does indeed exert a slightly greater anti-apoptotic impact in the absence of Tie1 compared to random control cells, but this finding did not reach statistical significance. As expected, there is almost no anti-apoptotic impact of Angiopoietin-1 when Tie2 is absent.

4.4.3: Caspase Sensitivity to Low-Dose Angiopoietin-1

The data in Figure 4.7 suggest that Tie1 deficiency increases the anti-apoptotic responsiveness to Angiopoietin-1. To investigate this further, the concentration dependence of Angiopoietin-1 effects on apoptosis were analysed in Tie1 deficient and control HUVEC over a low dose range. The results from three experiments are presented in Figure 4.8 as a percentage increase in caspase production by Tie1 deficient HUVEC compared to controls at each concentration of Ang-1 used. Figure 4.8 shows that Tie1 deficient HUVEC consistently produce higher caspase levels, under both serum starved baseline and Ang-1 stimulated conditions. The error bars for this experimental series are very large however, indicating large variations between the three experiments undertaken. Accordingly, only the final Ang-1 concentration of 100 ng/ml achieved a statistically significant increase in caspase production by Tie1 deficient HUVEC compared to controls, for any given concentration of Ang-1 or the Ang-1 free baseline. Next, the data from the same three experiments was combined to demonstrate the actual curve of caspase production at each Ang-1 concentration, with all values normalised to the un-stimulated baseline reading in each case (Figure 4.9). By presenting the data in this manner, it is apparent that the dose response to all concentrations of

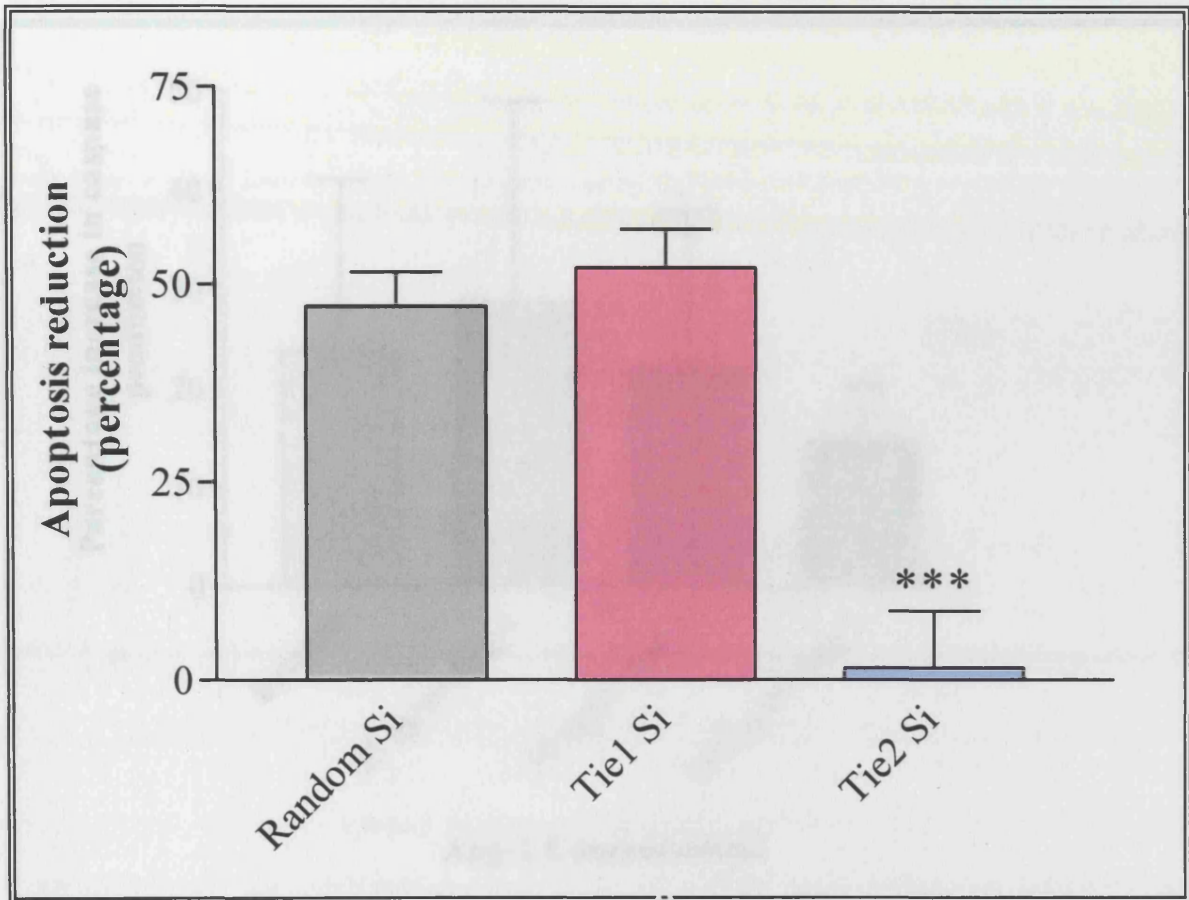


Figure 4.7: Graph to present the magnitude of effect of Angiopoietin-1 on the inhibition of caspase production in control, Tie1 deficient and Tie2 deficient HUVEC. Data compiled from three individual sets of experiments using Tie1 and Tie2 HUVEC respectively. Datamanipulation as described in text, to present the comparative magnitude of Ang-1 anti-apoptotic effect between Tie1 deficient, Tie2 deficient and control HUVEC. Error bars represent SEM about the mean. Although the reduction in caspase levels by Angiopoietin-1 in Tie1 deficient HUVEC is greater than that seen in random treated cells, this effect is not statistically significant. Tie2 deficiency however, nearly completely abolishes the protective properties of Angiopoietin-1 ($P < 0.005$).

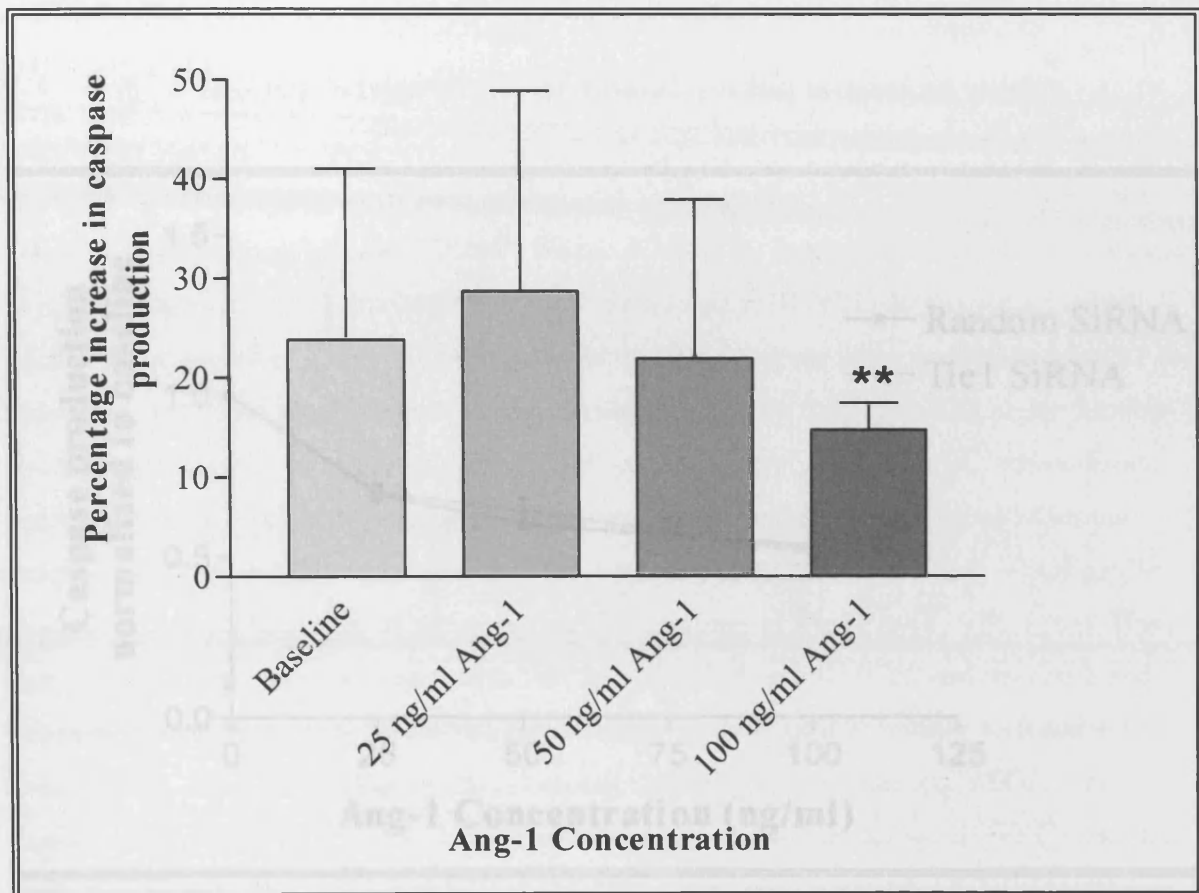


Figure 4.8: Caspase production in Tie1 deficient HUVEC compared to random transfected controls following low-dose Angiopoietin-1 exposure. Data derived from three separate experiments all comprising of at least two repeats per condition. Tie1 values normalised to controls at each Ang-1 concentration, prior to combination and presentation as percentage increase in caspase production flanked by SEM error bars. Both baseline and Ang-1 stimulated Tie1 deficient HUVEC produce greater quantities of caspase compared to comparable random transfected controls, reaching statistical significance at 100 ng/ml Ang-1 (** $P < 0.01$).

Ang-1 is nearly identical, thus ruling out any increase in Ang-1 responsiveness by Tie1 deficient HUVEC over a low dose range, at least in this series of three experiments.

4.9: An Investigation into VEGF Mediated Apoptosis in Tie Receptor Deficient HUVEC

VEGF activates cleavage of Tie1 ectodomain resulting in increased tyrosine phosphorylation of truncated Tie1 intracellular domain and Tie2 (not discussed). It is

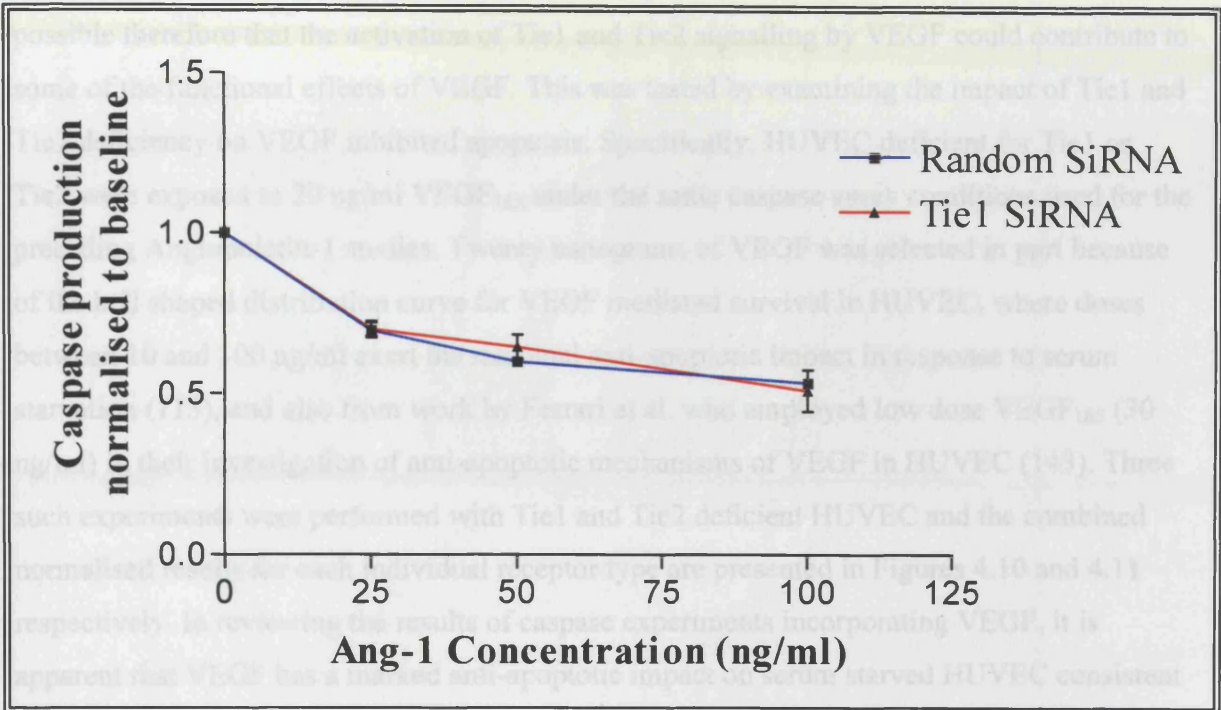


Figure 4.9: Caspase production in Tie1 deficient HUVEC compared to random transfected controls following low-dose Angiopoietin-1 exposure. Data derived from the same three separate experiments presented in Figure 4.8 consisting of at least two repeats per condition. Ang-1 stimulated caspase values normalised to baselines for Tie1 and random transfected HUVEC prior to combination. Each data point flanked by SEM error bars. Both baseline and Ang-1 stimulated Tie1 deficient HUVEC produce very similar dose response curves to increasing concentrations of Ang-1.

Ang-1 is nearly identical, thus ruling out any increase in Ang-1 responsiveness by Tie1 deficient HUVEC over a low dose range, at least in this series of three experiments.

4.5: An Investigation into VEGF Inhibited Apoptosis in Tie Receptor Deficient HUVEC:

VEGF activates cleavage of Tie1 ectodomain resulting in increased tyrosine phosphorylation of truncated Tie1 intracellular domain and Tie2 (see discussion). It is possible therefore that the activation of Tie1 and Tie2 signalling by VEGF could contribute to some of the functional effects of VEGF. This was tested by examining the impact of Tie1 and Tie2 deficiency on VEGF inhibited apoptosis. Specifically, HUVEC deficient for Tie1 or Tie2 were exposed to 20 ng/ml VEGF₁₆₅ under the same caspase assay conditions used for the preceding Angiopoietin-1 studies. Twenty nanograms of VEGF was selected in part because of the bell shaped distribution curve for VEGF mediated survival in HUVEC, where doses between 10 and 100 ng/ml exert the maximal anti-apoptotic impact in response to serum starvation (113), and also from work by Ferrari et al. who employed low dose VEGF₁₆₅ (30 ng/ml) in their investigation of anti-apoptotic mechanisms of VEGF in HUVEC (143). Three such experiments were performed with Tie1 and Tie2 deficient HUVEC and the combined normalised results for each individual receptor type are presented in Figures 4.10 and 4.11 respectively. In reviewing the results of caspase experiments incorporating VEGF, it is apparent that VEGF has a marked anti-apoptotic impact on serum starved HUVEC consistent with findings reported in the literature (141). This observation applies to HUVEC transfected with either random, Tie1 or Tie2 SiRNA, and the magnitude of effect is broadly similar to that seen with Angiopoietin-1 when used at 200ng/ml, with a 58% reduction in caspase production in random controls where both Tie1 and Tie2 are present. However, data in both Figures 4.10 and 4.11 suggest loss of either Tie1 or Tie2 leads to a decrease in the magnitude of VEGF anti-apoptotic effects. To illustrate this more clearly the data was re-plotted to show the percentage drop in anti-apoptotic effect when each receptor is absent, compared to VEGF treated control HUVEC (Figure 4.12). Loss of Tie1 caused an 11 % decrease in anti-apoptotic effect of VEGF compared to control HUVEC. Similarly, a 20.1% reduction of anti-apoptotic effect of VEGF occurred with the loss of Tie2 compared to control HUVEC. Therefore, with the loss of either Tie receptor, the anti-apoptotic efficacy of VEGF is indeed reduced, but to a greater degree with Tie2 deficiency than with Tie1. This suggests a role for both Tie receptors in mediating the anti-apoptotic signals by VEGF in HUVEC, in addition to VEGF's own receptors, VEGFR1 and VEGFR2.

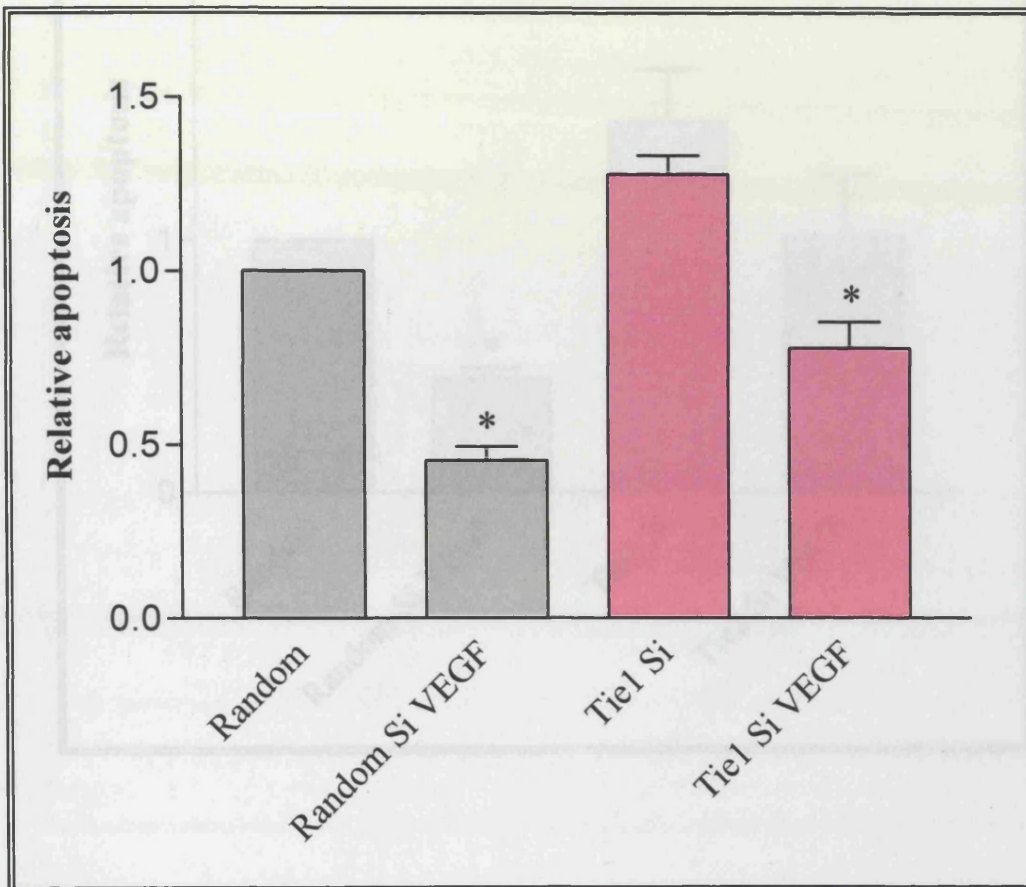


Figure 4.10: Apoptosis in Tie1 deficient HUVEC with or without VEGF₁₆₅. Tie1 deficient HUVEC were generated according to the protocol in section 2.11 of the materials and methods section. 24 hours after transfection 1x10⁴ Tie1 deficient cells were seeded into individual wells of a 96 well plate and cultured for another 24 hours. Cells were then exposed

Figure 4.10: Apoptosis in Tie1 deficient HUVEC with or without VEGF₁₆₅. Tie1 deficient HUVEC were generated according to the protocol in section 2.11 of the materials and methods section. 24 hours after transfection 1x10⁴ Tie1 deficient HUVEC were seeded to individual wells of a 96 well plate and cultured for another 24 hours. Cells were then exposed to serum free conditions for 4 hours with or without 20 ng/ml VEGF₁₆₅, followed by determination of caspase production. Combined results from three experiments (all in triplicate and normalised), with SEM error bars either side of the mean. Both Random and Tie1 deficient HUVEC have a statistically significant anti-apoptotic response to VEGF₁₆₅ (Random P=<0.0001, Tie1 deficient P=<0.01).

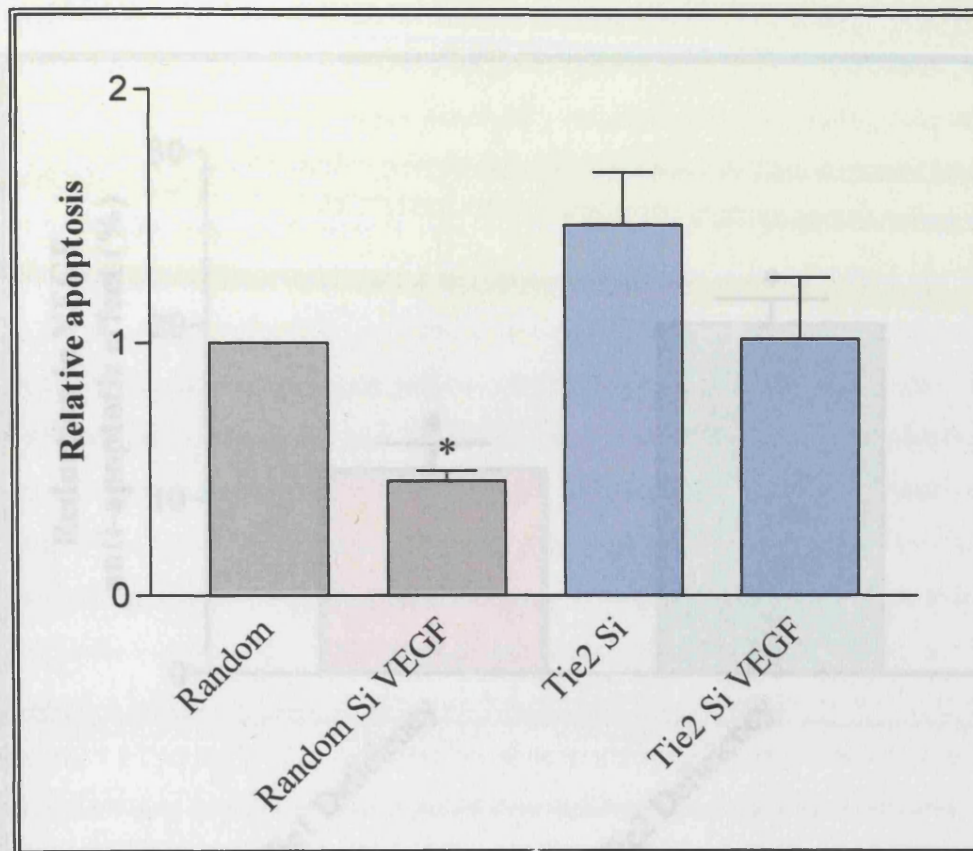


Figure 4.11: Apoptosis in Tie2 deficient HUVEC with or without VEGF₁₆₅. Tie2 deficient HUVEC were generated according to the protocol in section 2.11 of the materials and methods section. 24 hours after transfection 1×10^4 Tie2 deficient cells were seeded to individual wells of a 96 well plate and cultured for another 24 hours. Cells were then exposed to serum free conditions for 4 hours with or without 20 ng/ml VEGF₁₆₅, followed by determination of caspase production. Normalised results from three experiments all performed in triplicate. SEM error bars shown around the mean. Random HUVEC have a statistically significant anti-apoptotic response to VEGF₁₆₅ ($P < 0.0001$), although the reduction in apoptosis in Tie2 deficient cells does not achieve significance.

4.6 Discussion

The focus of this chapter has been to investigate the anti-apoptotic signalling

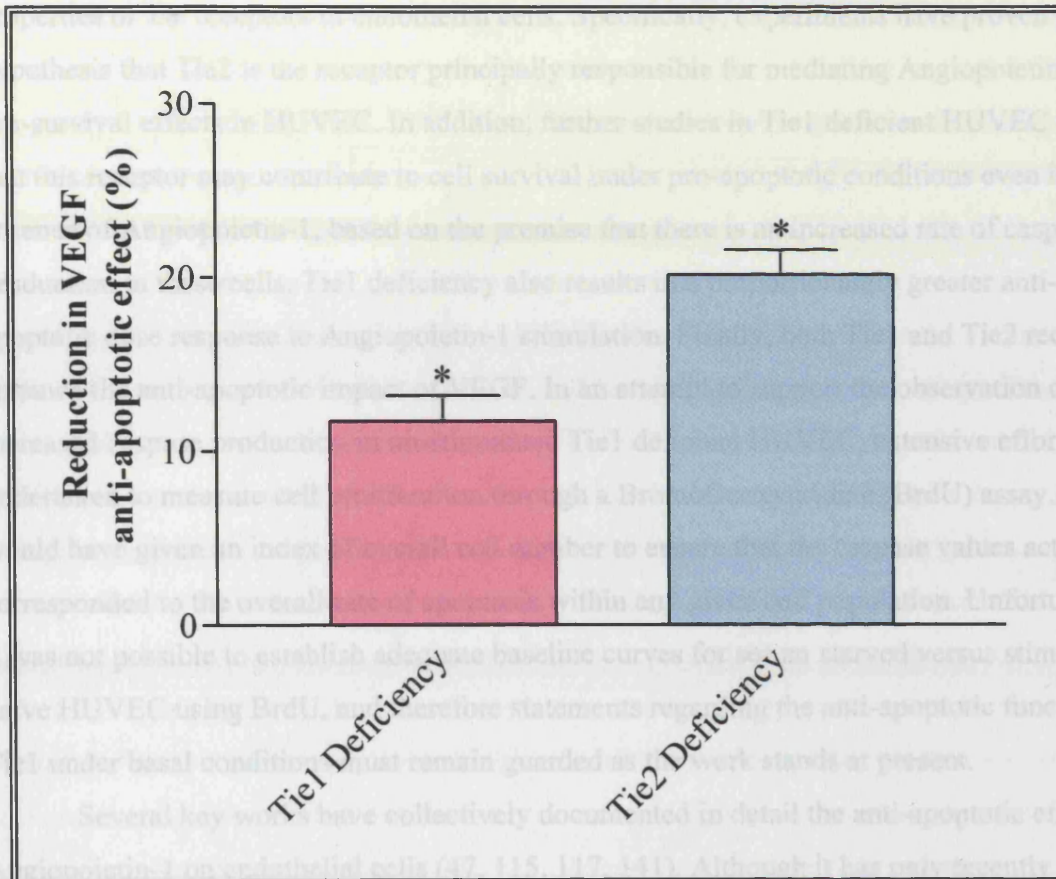


Figure 4.12: Graph demonstrating the reduction in anti-apoptotic efficacy of VEGF₁₆₅ in Tie1 and Tie2 deficient HUVEC in comparison to control HUVEC. Data compiled from the three separate experimental series with Tie1 deficient and Tie2 deficient HUVEC compared to controls presented in Figures 4.9 and 4.10. Data manipulation as described in text, with error bars representing SEM about the mean for three individual experiments. Overall, Tie1 and Tie2 deficient HUVEC have a significantly reduced response to the anti-apoptotic effect of VEGF₁₆₅ compared to random control HUVEC ($P < 0.05$).

4.6: Discussion:

The focus of this chapter has been to investigate the anti-apoptotic signalling properties of Tie receptors in endothelial cells. Specifically, experiments have proven the hypothesis that Tie2 is the receptor principally responsible for mediating Angiopoietin-1's pro-survival effects in HUVEC. In addition, further studies in Tie1 deficient HUVEC suggest that this receptor may contribute to cell survival under pro-apoptotic conditions even in the absence of Angiopoietin-1, based on the premise that there is an increased rate of caspase production in these cells. Tie1 deficiency also results in a proportionately greater anti-apoptotic dose response to Angiopoietin-1 stimulation. Finally, both Tie1 and Tie2 receptors enhance the anti-apoptotic impact of VEGF. In an attempt to support the observation of increased caspase production in un-stimulated Tie1 deficient HUVEC, extensive efforts were undertaken to measure cell proliferation through a BromoDeoxyuridine (BrdU) assay. This would have given an index of overall cell number to ensure that the caspase values actually corresponded to the overall rate of apoptosis within any given cell population. Unfortunately it was not possible to establish adequate baseline curves for serum starved versus stimulated naïve HUVEC using BrdU, and therefore statements regarding the anti-apoptotic function of Tie1 under basal conditions must remain guarded as the work stands at present.

Several key works have collectively documented in detail the anti-apoptotic effects of Angiopoietin-1 on endothelial cells (47, 115, 117, 141). Although it has only recently been possible to effectively activate Tie1, the assertion in these studies that Tie2 is the major receptor mediating pro-survival signalling has proven to be true on the basis of the data presented here. No matter what part is played by Tie1 in this process, the present work demonstrates the essential requirement for Tie2 in Angiopoietin-1 mediated cell survival responses. Indeed, with Tie2 silencing to the degree achieved in these experiments there is a complete loss of the protective effects of Angiopoietin-1.

A number of studies suggest Tie1 may also have an anti-apoptotic role in endothelial cells. Developmentally, Tie1 is an essential receptor, becoming active during late angiogenesis especially in the development of capillaries in tissues such as the brain and kidney (43). In Tie1 knockout mice, vascular development is able to progress normally until E13 but embryos then rapidly die by E14.5 secondary to severe oedema and microvascular rupture (35, 44). To further investigate Tie1 functions *in vivo*, Partanen created chimaeric Tie1 mouse embryos and identified a possible pro-survival role for Tie1 in endothelial cells present in vascular beds such as the lung and kidney. With the suggestion of a putative pro-

survival function for Tie1, Kontos et al. conducted several experiments to further investigate a possible anti-apoptotic role for Tie1 under *in vitro* conditions. By creating a c-fms-Tie1 chimaeric receptor consisting of the membrane and intracellular portion of Tie1 attached to a CSF-1 extracellular domain, they were able to overcome the difficulties of ligand activation associated with wild type Tie1(119). Having stably expressed c-fms-Tie1 in NIH-3T3 cells, this chimaeric receptor was successfully autophosphorylated in response to CFS-1 ligand, even in the absence of Tie2. Moreover, given the more favourable p85 binding sequence surrounding Tyrosine 1113 in Tie1 compared to Tyrosine 1101 of Tie2, c-fms-Tie1 activation led to strong activation of Akt, potently reducing irradiation-induced apoptosis. Indeed, mutation of Y1113 abolished these anti-apoptotic effects establishing it as the preferred binding site for p85 / Akt mediated cell survival signalling. Other studies using a TrkA/Tie1 chimaeric receptor failed to reproduce such ligand induced phosphorylation however, but did identify a close physical interaction between Tie1 and Tie2, although ligand induced Tie2 phosphorylation failed to unidirectionally transphosphorylate Tie1 (144). With the advent of more potent angiopoietin agonists such as COMP-Ang1, Saharinen et al. successfully phosphorylated wild type Tie1, which was further enhanced when Tie1 was co-expressed with Tie2. Taken collectively, these data demonstrate that although Tie1 does not readily phosphorylate in a manner similar to Tie2, it does have the potential to mediate potent downstream anti-apoptotic effects in addition to requiring a close association with Tie2 necessary for its correct function. Therefore although excess Tie2Fc may well abolish Tie2 anti-apoptotic signalling in all studies to date, if Tie1 exerts its functions at least in part through receptor association with Tie2, it would need removal altogether to allow conclusions to be drawn about its relative role in endothelial cell survival. In all the present experiments with Tie1 deficient HUVEC, the baseline level of apoptosis is elevated when compared to HUVEC containing both Tie1 and Tie2. This stands in accord with previous reports identifying a role for Tie1 in cell survival, but suggests that this function is not necessarily dependent upon externally administered angiopoietin-1 stimulation. Once again, this observation needs to be tempered against the lack of proliferation data that could feasibly bias the magnitude of Tie1 deficient HUVEC apoptosis. However, assuming Tie1 does contribute to baseline survival, perhaps the association of Tie1 and Tie2 results in tonic Tie1 phosphorylation that then feeds into the P85 / Akt pathway. Regardless of this, with Angiopoietin-1 stimulation of Tie1 deficient cells, there is an exaggerated anti-apoptotic response compared to controls possessing both functioning receptors. As such an enhanced pro-survival response is less likely to be offset by variation in total cell number, this implies

that Tie2 is somehow more effective in activating P85 / Akt when acting in isolation. This might result from loss of an inhibitory effect of associated Tie1, or from greater availability of downstream signalling intermediaries in Tie1's absence. Studies of the activity of signalling intermediary activation in Tie deficient HUVEC may well provide the answer to this and offer further data on Tie1's anti-apoptotic function.

With the discovery in 1999 that a truncated form of Tie1 appears within endothelial cells following exposure to Phorbol Myristate Acetate (PMA), new light was shed on the dynamic interaction between Tie1 and Tie2 (145). This fragment of Tie1 is 45kD in size and represents the intracellular and transmembrane domains of the full length receptor. Based on the further observation that VEGF causes the release of Tie1 ectodomain (146), Tsiamis et al. used VEGF treatment of HUVEC to demonstrate that the same Tie1 truncation process occurs as seen with PMA, releasing the ectodomain into the culture media to leave the transmembrane and cytoplasmic portions in the cell membrane (147). Further immunoprecipitation work demonstrated that VEGF does not disturb the physical association of Tie1:Tie2 complexes, but rather that the Tie1 portion of the heterodimer takes the truncated form. If Tie1 has a significant role to play in cell survival responses in endothelial cells, then its truncation by VEGF may well have major implications for Angiopoietin-1 / Tie mediated anti-apoptotic processes. To investigate this possibility the present work has demonstrated that Tie1 and Tie2 receptors are indeed both required if the maximal anti-apoptotic impact of VEGF on serum-starved HUVEC is to be achieved. With deficiency in either Tie1 or Tie2 the magnitude of caspase reduction falls markedly but to a greater extent following the loss of Tie2. With the pre-publication data kindly provided by H Singh that Tie1:Tie2 complexes containing truncated Tie1 (via either VEGF or PMA stimulation) display enhanced signalling, it becomes possible to postulate how this might affect the anti-apoptotic role of VEGF. If truncated Tie1:Tie2 heterodimers are blocked from forming through gene silencing of either receptor, then any enhanced Tie activation secondary to heterodimerisation would be lost. This would then leave the anti-apoptotic effect of VEGF to act solely through its own native receptors. One omission in the present data concerns the anti-apoptotic effects of VEGF in the absence of *both* Tie receptors. This would have provided a more complete assessment of Tie receptor function with VEGF and would be of value in planning future experiments.

5.1: Cell Adhesion Molecule Expression in Endothelial Cells and Their Regulation by Angiopoietin / Tie Signalling:

One of the earliest events involved in inflammatory activation of the endothelium involves the expression of cell adhesion molecules (CAMs). These cell surface receptors appear rapidly and interact with complementary receptors on circulating inflammatory cells. By this mechanism, leucocytes marginate from the circulation and diapedese through inter-endothelial junctions into areas of tissue damage or infection. Endothelial CAM expression therefore represents a major component of the inflammatory response both under normal and pathological conditions. ICAM-1, VCAM-1 and E-selectin are three key cell adhesion molecules involved in cell-cell interaction and therefore represent important markers of inflammatory activation.

The purpose of the present project was to:

- 1:** Develop an *in vitro* assay of endothelial activation, offering both qualitative and quantitative assessment of ICAM-1, VCAM-1 and E-selectin expression.
- 2:** Profile the time and dose dependent synthesis of different CAMs in endothelial cells following stimulation with different inflammatory cytokines.
- 3:** Evaluate the impact of Ang-1 on CAM expression during the process of inflammatory activation, focussing specifically on ICAM-1, VCAM-1 and E-selectin.
- 4:** Investigate the impact of selective Tie receptor deficiency on individual CAM expression profiles under inflammatory conditions, and the influence or otherwise of Ang-1 under these conditions.

5.2: Induction of CAM Expression in Endothelial Cells:

To begin studying endothelial CAM expression, endothelial cells were challenged with several different inflammatory cytokines and their CAM profiles visualised using a fluorescent immunocytochemistry technique described fully in section 2.18 of the materials and methods section. In brief, HMEC-98 or HUVEC were seeded into the wells of a 24 well plate containing single, sterile, glass cover slips (coated with 1% gelatine for HMEC-98). Following a 24 hour incubation period, individual cell populations were challenged with Il-1 or TNF α for 6 hours. Coverslip cell sheets were then fixed with 4% paraformaldehyde, and VCAM-1 expression detected with a FITC labelled anti-VCAM-1 antibody as described. Figure 5.1 presents photomicrographs taken of VCAM-1 expression in HMEC-98 stimulated with TNF α (A) and HUVEC stimulated with Il-1 (B). In both cases, there was a heterogeneous response to cytokine stimulation with marked variation in staining from one cell to the next. Those cells reacting strongly to cytokine stimulation had a cell outline that was 'peppered' with green antibody label, clearly revealing the detail of cell membrane processes. From these initial studies, consistently strong VCAM-1 detection always followed Il-1 and TNF α exposure, but little or no response was observed after stimulation with two other inflammatory cytokines, thrombin and VEGF. For this reason, subsequent experiments focussed on CAM expression induced by either TNF α or Il-1 alone.

5.3: CAM Quantitation Assay:

Given the variable cell-to-cell cytokine response within any given endothelial cell population studied, field-counting of stained cells proved insufficiently accurate to offer a quantitative assessment of CAM expression. Moreover, as the fluorophore rapidly bleached during microscopic examination, all data analysis had to be conducted offline, introducing the need for complex camera calibration to set a sensitivity threshold capable of detecting less well stained cells in individual captured frames. For this reason, an alternative technique for CAM quantitation was devised based on a cell-ELISA approach. In brief, endothelial cells were seeded directly into the wells of a 96 well plate, challenged with inflammatory cytokines, fixed in paraformaldehyde and probed with FITC-labelled anti-CAM antibodies as before.

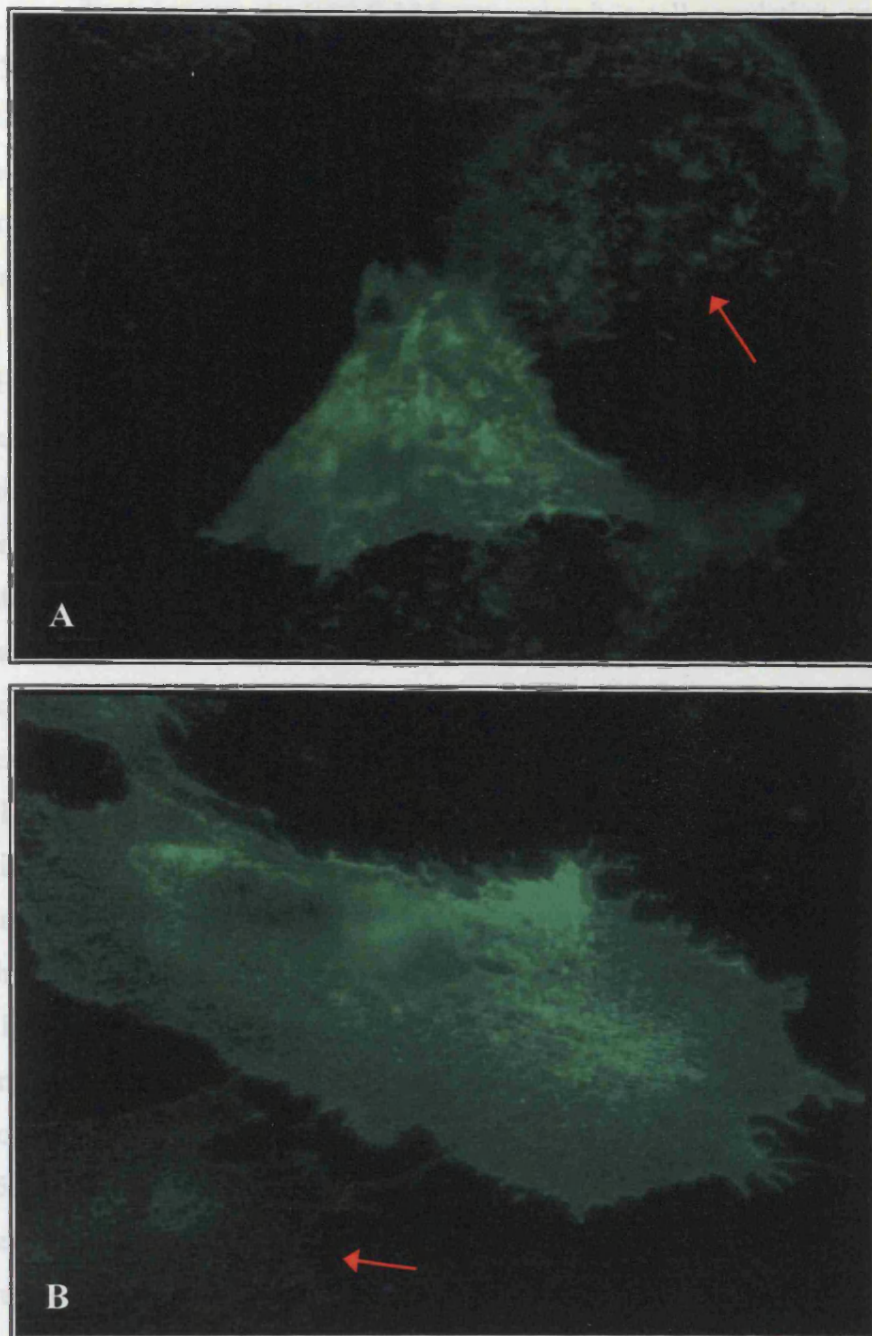


Figure 5.1: VCAM-1 expression in HMEC-98 (A) and HUVEC (B). Endothelial cells were cultured on gelatine coated and uncoated glass coverslips respectively for 24 hours. In photomicrograph A VCAM-1 induction followed exposure to 50 ng/ml TNF α for 4 hours prior to cell fixation and CAM detection as described in section 2.18 of the materials and methods section. VCAM-1 induction in B followed exposure to 10 ng/ml Il-1. Careful inspection of both Figures demonstrates the outline of cells that have not responded to cytokine stimulation (indicated by red arrows), contrasting markedly with the densely stained cell in the centre of each field.

To quantitate the total CAM expression in a cell population, an HRP-linked secondary antibody directed against the FITC-CAM primary antibodies was used. Once all unbound antibody had been washed away, the total CAM present defined the rate of a colourimetric reaction catalysed by the HRP linked secondary antibody. To obtain maximal sensitivity, colourimetric measurement was delayed until the reaction had proceeded towards the upper limit of the plate readers operative range (Around 60 minutes). As all steps were achieved by the addition of reagents directly into individual wells of a 96 well plate, this provided for a high-throughput of different experimental conditions allowing considerable experimental efficiency. Figure 5.2 presents the combined results from three separate CAM quantitation assays, measuring not only VCAM-1 (A) but also ICAM-1 (B) and E-Selectin (C) expression over a six hour time period in HMEC-98 exposed to 10 ng/ml Il-1. All anti-CAM antibodies shared the same animal specificity for the secondary HRP-linked antibody. Individual experiment Il-1 stimulated CAM values were normalised to the baseline CAM expression in un-stimulated cells, prior to data pooling and presentation as relative CAM expression. ICAM-1 and E-Selectin data was then subsequently normalised to baseline VCAM-1 expression, in order to clearly visualise the different baseline CAM expression levels prior to Il-1 exposure. Figure 5.2 (A) demonstrates a progressive, statistically significant increase in VCAM-1 expression with each extra hour of exposure to Il-1, right up to the 6 hour cut off point. Over this time period there is on average a 13.5 fold increase in VCAM-1 expression but with progressively greater inter-well variation towards the end of the measurement period. Surprisingly, ICAM-1 and E-Selectin had a completely unexpected expression profile, demonstrating a non-linear response to the addition of high-dose Il-1 (Figure 5.2 B and C). Firstly, ICAM-1 had a consistently high baseline expression in un-stimulated cells, and this was not further increased by the addition of Il-1 at any concentration. Indeed the ICAM-1 expression mirrored that of the greatly elevated VCAM-1 values following the full 6 hour Il-1 exposure period. In contrast to this, E-Selectin was expressed at very low levels under baseline conditions (similar to un-stimulated VCAM-1 expression), but did show a significant elevation after three hours of Il-1 exposure, before tailing off again towards the 6 hour cut off point. These data indicate that the HMEC-98 cells used for these experiments constitutively express ICAM-1 and to a very high level compared to the other two CAM's, and that with the exception of a small transient rise in E-Selectin, only VCAM-1 responded to increasing durations of exposure to Il-1. Given the absence of a progressive and linear increase on ICAM-1 or E-Selectin expression with high-dose Il-1, all remaining studies on HMEC-98 employed VCAM-1 only.

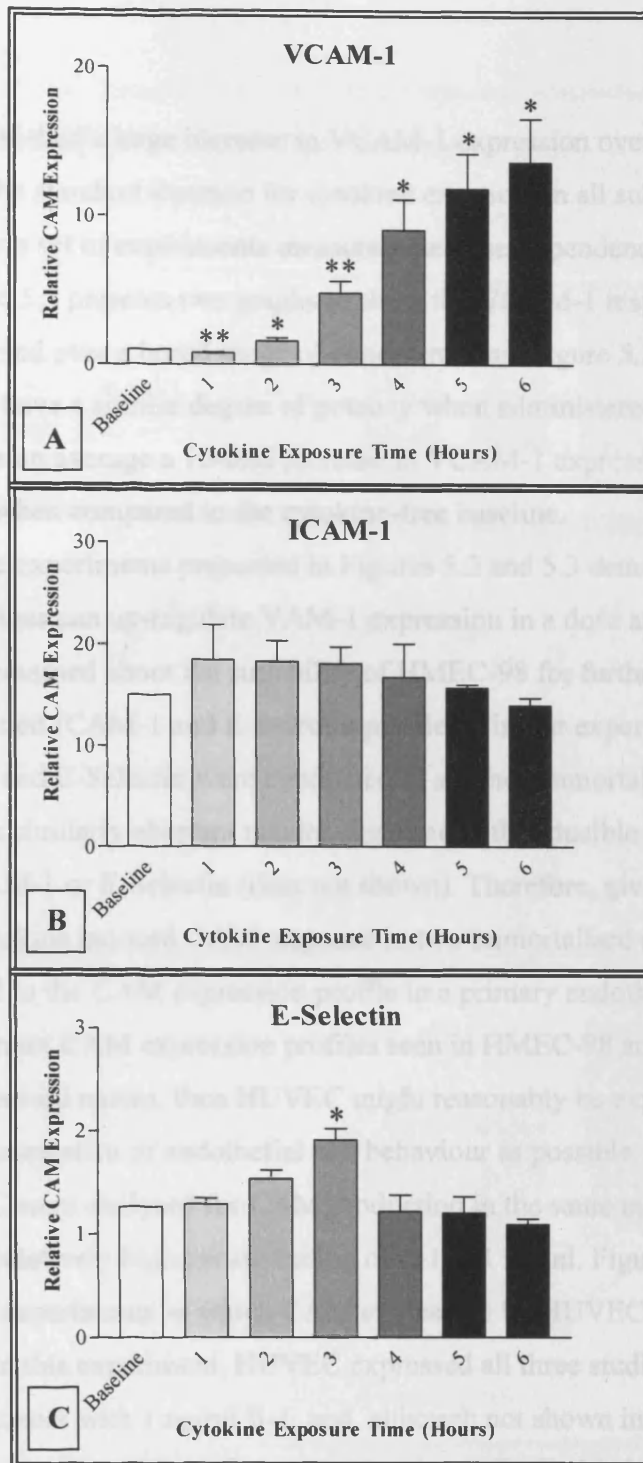


Figure 5.2: VCAM-1 (A), ICAM-1 (B) and E-Selectin (C) expression in HMEC-98. 1.5×10^5 HMEC-98 were seeded into gelatine coated wells of a 96 well plate, followed by a 24 hour incubation period. CAM stimulation with 10 ng/ml Il-1 at time zero with expression levels recorded over the following 6 hours as described in the text and section 2.18 of the materials and methods chapter. Mean values representative of individual wells combined from a total of three separate experiments, presented as relative CAM expression and flanked by SEM error bars. VCAM-1 expression is statistically increased at all time points by 10 ng/ml Il-1 as is E-Selectin at 3 hours time exposure (** $P \leq 0.005$, * $P \leq 0.05$). Note the relative un-stimulated baseline CAM expression; Y axis values set to best demonstrate CAM variation at each timepoint.

Having established a large increase in VCAM-1 expression over a 6 hour time period, this was chosen as the standard duration for cytokine exposure in all subsequent CAM experiments. The next set of experiments measured the dose-dependency of CAM expression in HMEC-98. Figure 5.3 presents two graphs to show the VCAM-1 response to Il-1 (A) and TNF α (B) administered over a broad range of concentrations. Figure 5.3 demonstrates that both Il-1 and TNF α have a similar degree of potency when administered to HMEC-98. In both cases there was on average a 10-fold increase in VCAM-1 expression at the maximal concentration used when compared to the cytokine-free baseline.

Although the experiments presented in Figures 5.2 and 5.3 demonstrate that inflammatory cytokines can up-regulate VCAM-1 expression in a dose and time dependent manner, concerns remained about the suitability of HMEC-98 for further CAM experiments given their un-expected ICAM-1 and E-Selectin profiles. Similar experiments measuring VCAM-1, ICAM-1 and E-Selectin were conducted in another immortalised endothelial cell line, EA.hy926 with similarly aberrant results; this time with inducible ICAM-1 but no response from VCAM-1 or E-Selectin (data not shown). Therefore, given the wide variation in inflammatory cytokine induced CAM response in two immortalised endothelial cell types, attention was turned to the CAM expression profile in a primary endothelial cell line using HUVEC. If the aberrant CAM expression profiles seen in HMEC-98 and EA.hy926 are due in part to their immortalised nature, then HUVEC might reasonably be expected to remain as phenotypically representative of endothelial cell behaviour as possible. To test this hypothesis, HUVEC were analysed for CAM production in the same manner as for HMEC-98 by initially using a relatively high concentration of Il-1 at 1 ng/ml. Figure 5.4 presents data from three separate experiments in which CAM expression by HUVEC exposed to 1 ng/ml Il-1 was determined. In this experiment, HUVEC expressed all three studied CAMs to a high level following treatment with 1 ng/ml Il-1, and, although not shown in the graph, baseline values for every CAM was maintained at a very low level. To further investigate the concentration dependency of CAM up-regulation, HUVEC were treated for 6 hours to a range of Il-1 and TNF α concentrations, with particular emphasis on the effects of low-dose cytokine exposure (Figures 5.5(a) and 5.5(b)). In these combined experiments, both Il-1 and TNF α have a strong dose-dependent relationship with CAM production in HUVEC over a 6 hour time period when used in concentrations between 0.05 and 50 ng/ml. Although there was a variable statistical response in CAM up-regulation in response to Il-1 or TNF α , it is apparent that Il-1 induced a more marked CAM response at the lowest cytokine concentrations used.

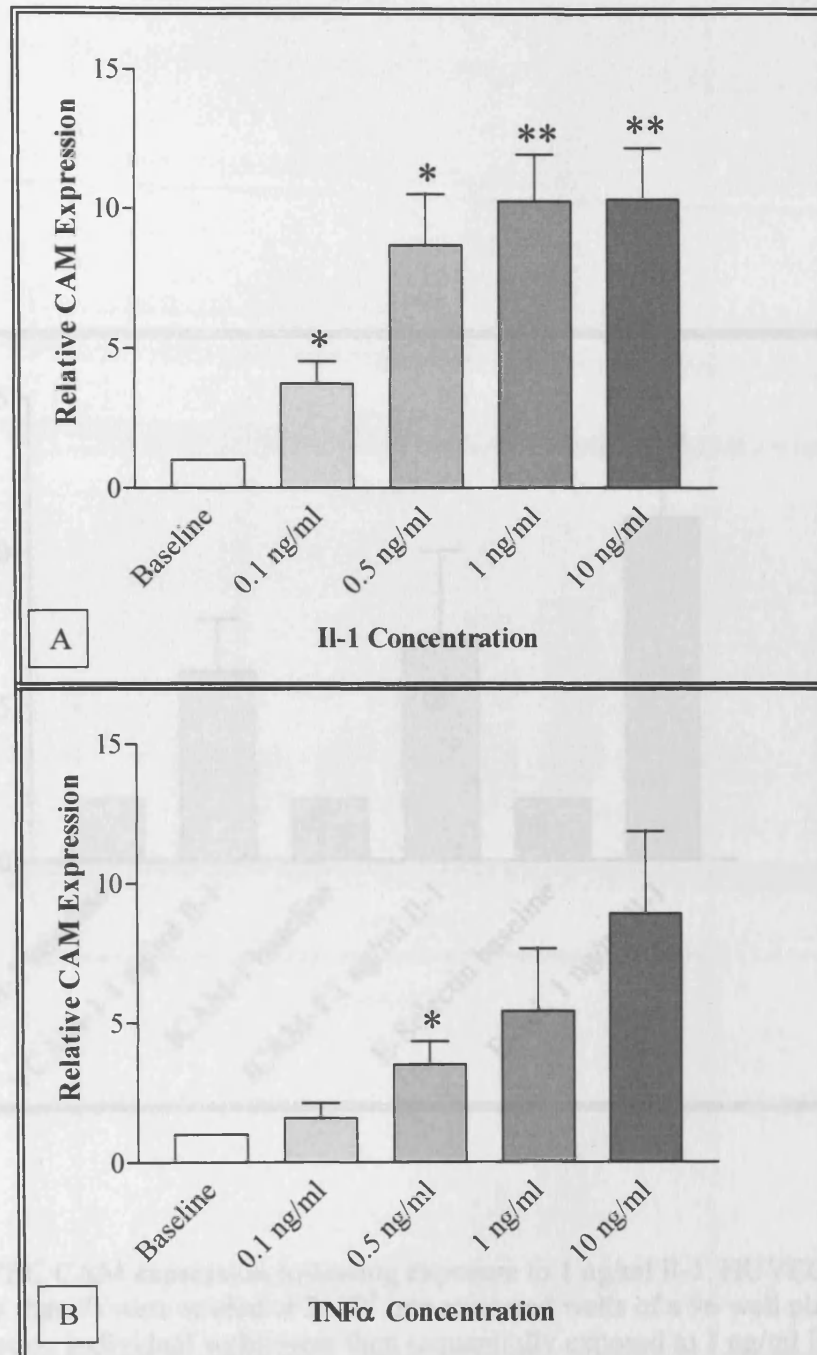


Figure 5.3: VCAM-1 expression in HMEC-98 6 hours after stimulation with Il-1 (A) or TNF α (B). HMEC-98 were seeded at 1.5×10^5 cells per individual gelatine coated well of a 96 well plate. After 24 hours, TNF α or Il-1 was added to respective wells at 0.1, 0.5, 1.0 or 10.0 ng/ml as indicated, followed by VCAM-1 quantitation after a further 6 hours as previously described. Each condition represents the combined data from three individual experiments, with all values normalised to the un-stimulated baseline for each CAM, prior to combination and presentation as relative CAM expression. Error bars represent SEM about the mean. All concentrations of Il-1 and TNF α induce VCAM-1 up-regulation, reaching statistical significance in all cases for Il-1 and at 0.5 ng/ml for TNF α (* P < 0.05, ** P < 0.01).

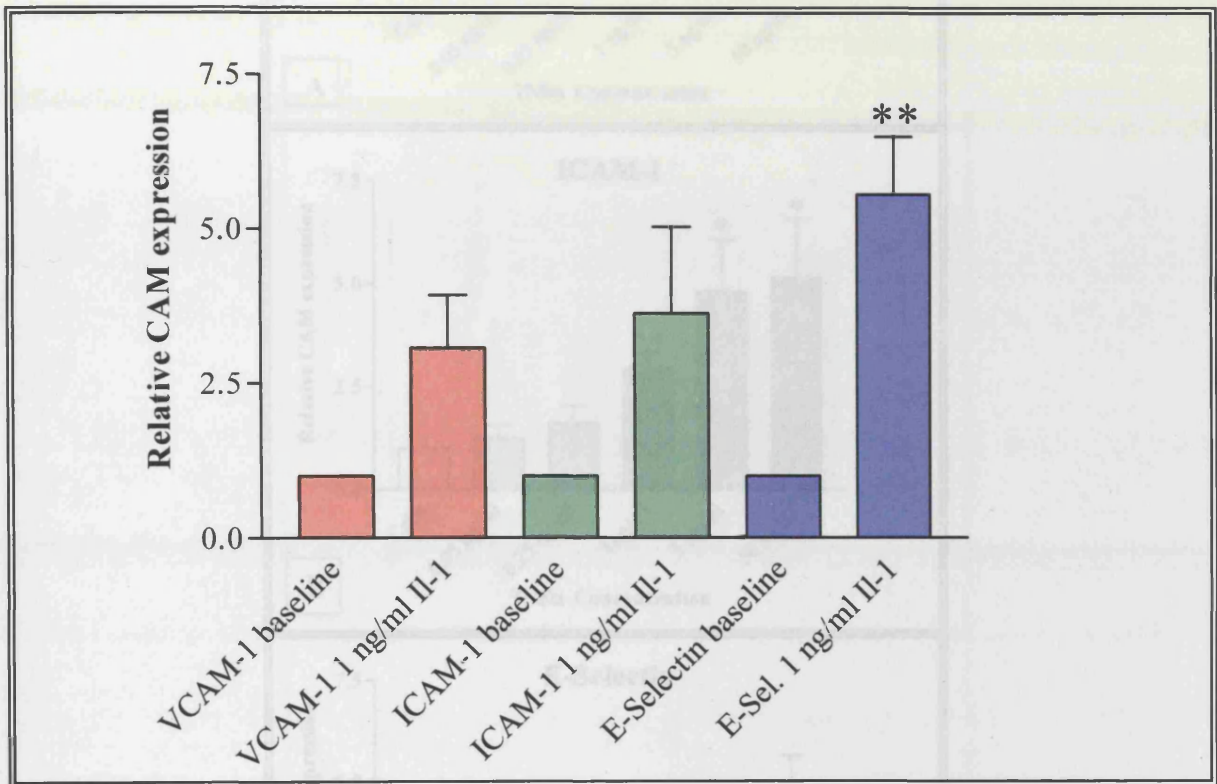


Figure 5.4: HUVEC CAM expression following exposure to 1 ng/ml Il-1. HUVEC (Passage number no higher than 7) were seeded at 2×10^5 into uncoated wells of a 96 well plate and cultured for 24 hours. Individual wells were then sequentially exposed to 1 ng/ml Il-1 for 6 hours, followed by VCAM-1, ICAM-1 and E-Selectin quantitation as previously described. Data compiled from three separate experiments where all CAM data has been normalised to the respective un-stimulated baseline, prior to combination as mean values flanked by SEM error bars. E-Selectin is significantly increased by exposure to 1 ng/ml Il-1 (** $P < 0.01$)

Figure 5.5 (a): HUVEC dose-dependent CAM expression following exposure to TNF α . HUVEC were seeded at 2×10^5 cells per un-coated well in a 96 well plate and cultured for 24 hours. Wells were then exposed to TNF α at the indicated doses, followed by VCAM-1 (Graph A), ICAM-1 (Graph B) and E-Selectin (Graph C) determination after a further 6 hours as described. Representative experiment from three separate experiments, with SEM error bars about the mean (* $P < 0.05$, ** $P < 0.01$).

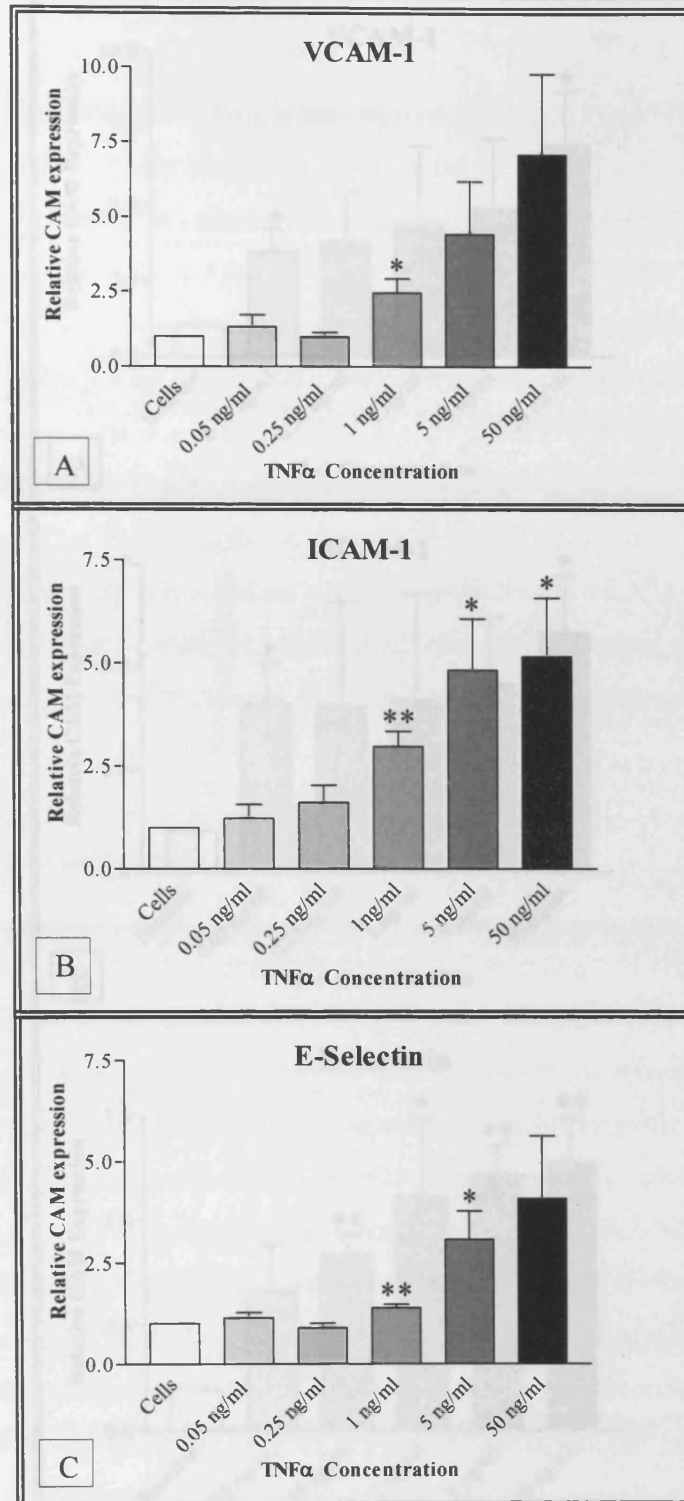


Figure 5.5 (a): HUVEC dose-dependent CAM expression following exposure to TNF α . HUVEC were seeded at 2×10^5 cells per un-coated well in a 96 well plate and cultured for 24 hours. Wells were then exposed to TNF α at the indicated doses, followed by VCAM-1 (Graph A), ICAM-1 (Graph B) and E-Selectin (Graph C) determination after a further 6 hours as described. Representative experiment from three separate experiments, with SEM error bars about the mean (* $P < 0.05$, ** $P < 0.01$).

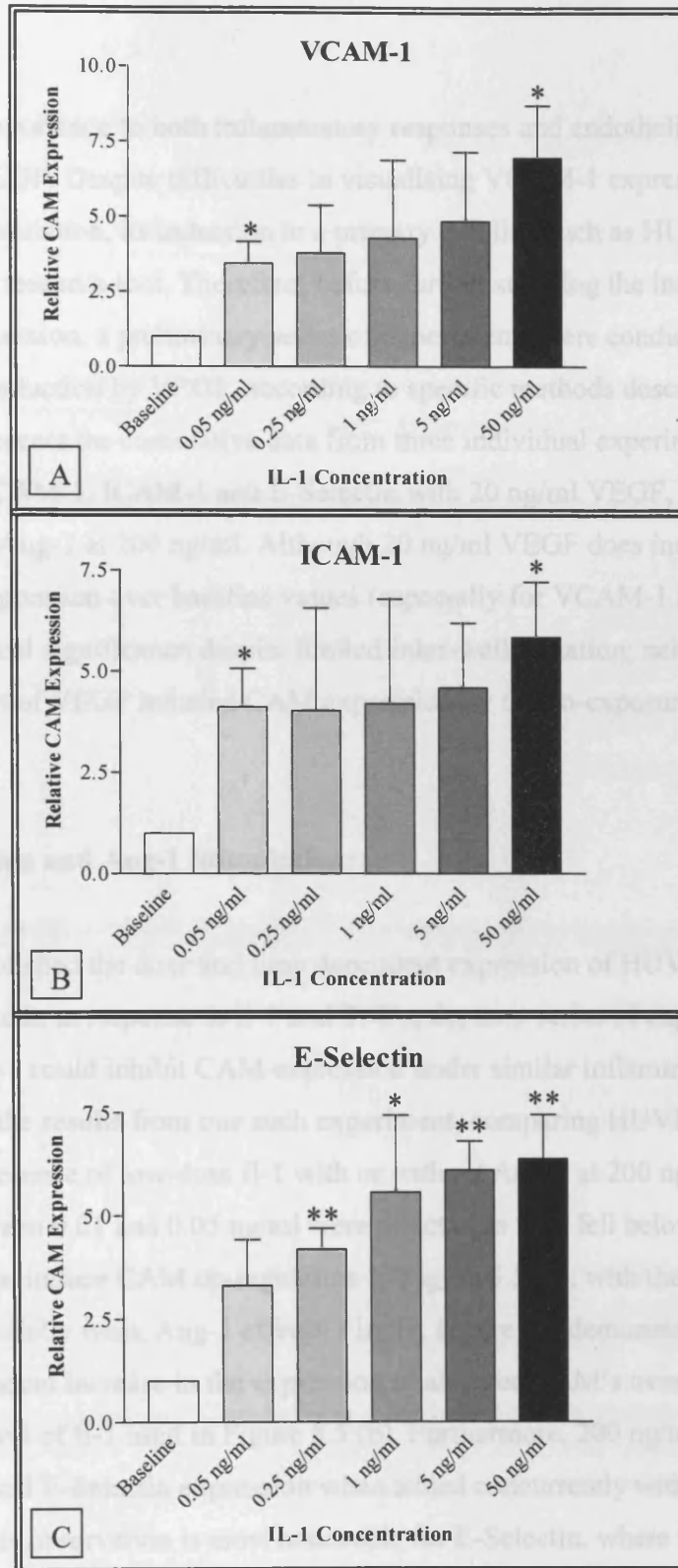


Figure 5.5 (b): HUVEC dose-dependent CAM expression following exposure to IL-1. HUVEC were seeded at 2×10^5 cells per un-coated well in a 96 well plate and cultured for 24 hours. Wells were then exposed to IL-1 at the indicated doses, followed by VCAM-1 (Graph A), ICAM-1 (Graph B) and E-Selectin (Graph C) determination after a further 6 hours as described. Data combined from three separate experiments, with SEM error bars about the mean (* $P < 0.05$, ** $P < 0.01$).

Of central importance to both inflammatory responses and endothelial proliferation is the growth factor VEGF. Despite difficulties in visualising VCAM-1 expression in HMEC-98 following VEGF stimulation, its induction in a primary cell line such as HUVEC would represent a valuable research tool. Therefore, before further studying the impact of Il-1 and TNF α on CAM expression, a preliminary series of experiments were conducted to attempt to demonstrate CAM induction by VEGF, according to specific methods described by Kim et al. (132). Figure 5.6 presents the cumulative data from three individual experiments, comparing the expression of VCAM-1, ICAM-1 and E-Selectin with 20 ng/ml VEGF, both on its own or in conjunction with Ang-1 at 200 ng/ml. Although 20 ng/ml VEGF does induce a very small increase in CAM expression over baseline values (especially for VCAM-1 and ICAM-1), this fails to reach statistical significance despite limited inter-well variation; neither is there any significant inhibition of VEGF induced CAM expression by the co-exposure with 200 ng/ml Ang-1.

5.4: CAM Expression and Ang-1 Stimulation:

Having established the dose and time dependent expression of HUVEC VCAM-1, ICAM-1 and E-Selectin in response to Il-1 and TNF α , the next series of experiments sought to test whether Ang-1 could inhibit CAM expression under similar inflammatory conditions. Figure 5.7 presents the results from one such experiment, comparing HUVEC CAM expression in the presence of low-dose Il-1 with or without Ang-1 at 200 ng/ml. Il-1 concentrations between 0.01 and 0.05 ng/ml were selected as they fell below the lowest concentration used to induce CAM up-regulation in Figure 5.5 (b), with the intention to avoid swamping any potentially weak Ang-1 effects. Firstly, Figure 5.7 demonstrates a clear concentration dependent increase in the expression of all three CAM's over a dosage range below the lowest level of Il-1 used in Figure 5.5 (b). Furthermore, 200 ng/ml Ang-1 appears to inhibit ICAM-1 and E-Selectin expression when added concurrently with either 0.03 or 0.05 ng/ml Il-1. This observation is most noticeable for E-Selectin, where its stimulation by Il-1 is halved in the presence of Ang-1. Also of note is the apparent synergistic effect between Ang-1 and Il-1 on VCAM-1, ICAM-1 and E-Selectin expression at 0.01 ng/ml Il-1. To establish the reproducibility of these findings, the same experiment was performed four times in total, and the results of this series are presented in Figures 5.8 (a) through 5.8 (c).

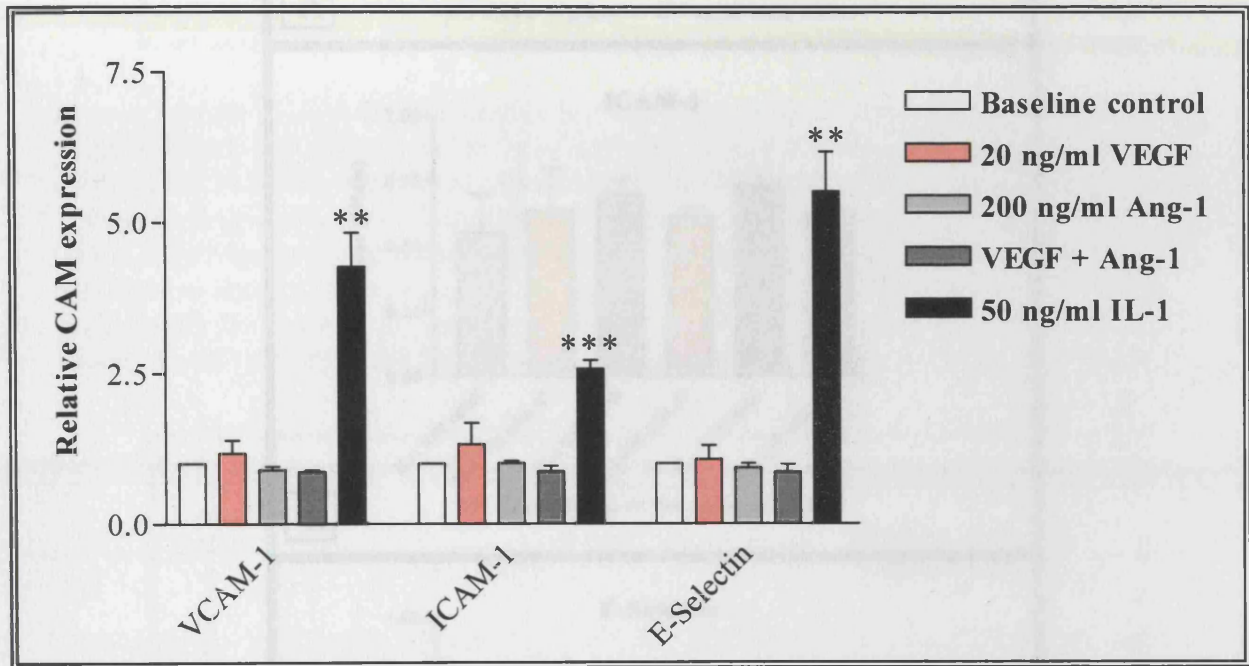


Figure 5.6: HUVEC CAM expression following exposure to VEGF (20 ng/ml) with or without Ang-1 (200 ng/ml). HUVEC were seeded at 2×10^5 cells per un-coated well in a 96 well plate and cultured for 24 hours. Wells were then exposed to either VEGF on its own or VEGF and Ang-1 together, followed by VCAM-1, ICAM-1 and E-Selectin determination after a further 6 hours as described. Composite graph from three independent experiments all conducted in triplicate, where all values have been normalised to that obtained for baseline CAM expression. SEM error bars about the mean. 50 ng/ml IL-1 included as a positive control (** $P < 0.005$, *** $P < 0.0005$).

Figure 5.7: HUVEC CAM expression following exposure to VEGF (20 ng/ml) with or without Ang-1. HUVEC were seeded at 2×10^5 cells per un-coated well in a 96 well plate and cultured for 24 hours. Wells were then exposed to either VEGF on its own or VEGF and Ang-1 together, followed by VCAM-1, ICAM-1 and E-Selectin determination after a further 6 hours as described in the materials and methods section. The relative level of expression of each CAM has been subtracted from all per centiles. Representative data for each marker, with SD error bars about the mean. Representative data are shown as a mean of three.

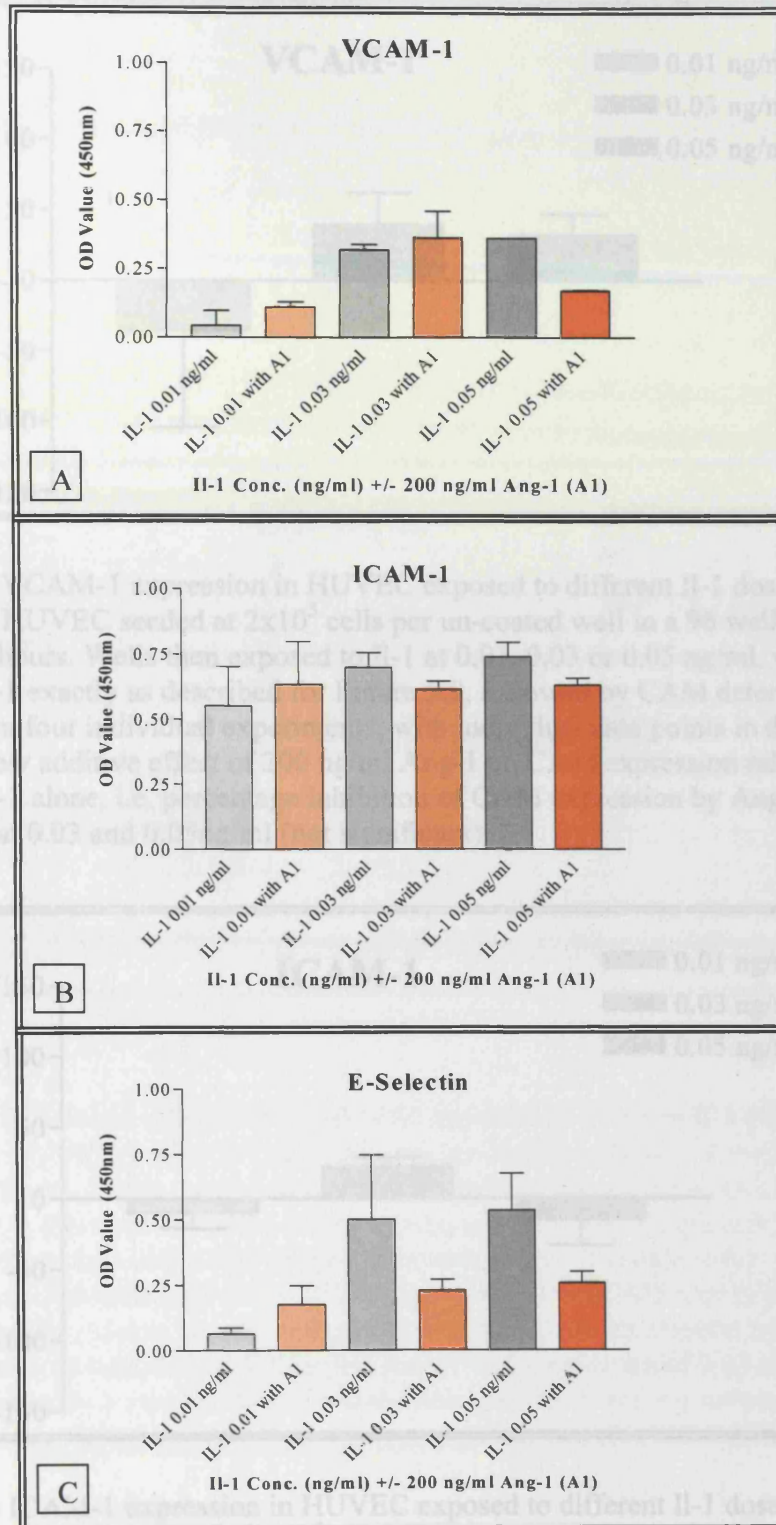


Figure 5.7: HUVEC CAM expression following exposure different IL-1 doses with or without Ang-1. HUVEC were seeded at 2×10^5 cells per un-coated well in a 96 well plate and cultured for 24 hours. Wells were then exposed to IL-1 at 0.01, 0.03 or 0.05 ng/ml, with or without 200 ng/ml Ang-1 (added simultaneously). VCAM-1 (Graph A), ICAM-1 (Graph B) and E-Selectin (Graph C) expression was then determined after a further 6 hours as described in the materials and methods section. The baseline level of expression of each CAM has been subtracted from all presented data. Replicate wells for each condition, with SD error bars about the mean. Representative experiment shown from a series of four.

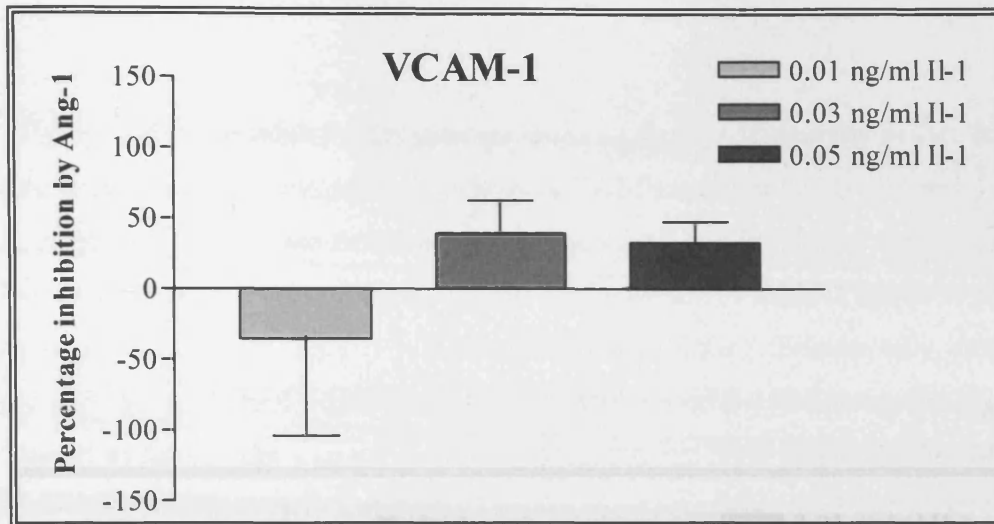


Figure 5.8 (a): VCAM-1 expression in HUVEC exposed to different Il-1 doses, with or without Ang-1. HUVEC seeded at 2×10^5 cells per un-coated well in a 96 well plate and cultured for 24 hours. Wells then exposed to Il-1 at 0.01, 0.03 or 0.05 ng/ml, with or without 200 ng/ml Ang-1 exactly as described for Figure 5.9, followed by CAM determination after 6 hours. Data from four individual experiments, with individual data points in duplicate. Data presented to show additive effect of 200 ng/ml Ang-1 on CAM expression relative to that produced by IL-1 alone, i.e. percentage inhibition of CAM expression by Ang-1. VCAM-1 expression fell at 0.03 and 0.05ng/ml (not significant).

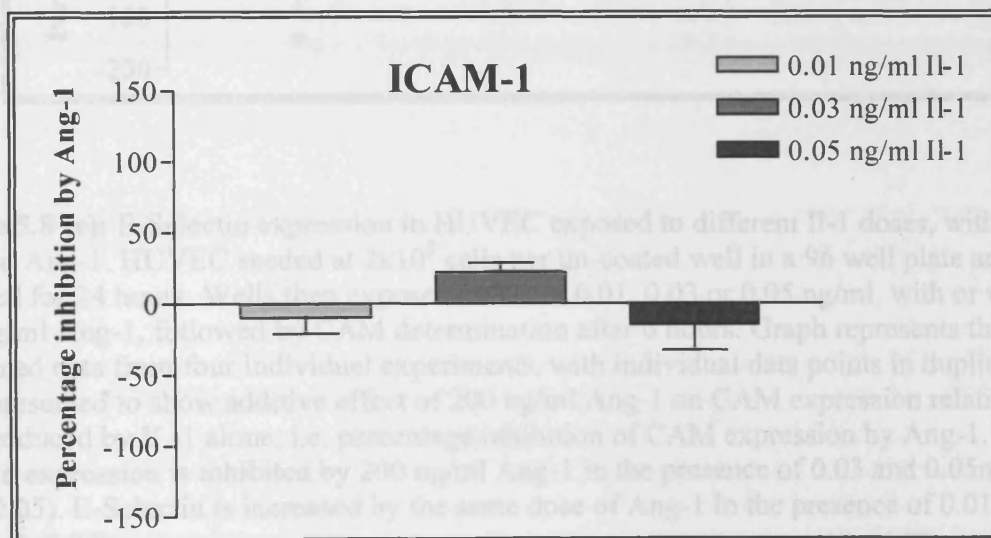


Figure 5.8 (b): ICAM-1 expression in HUVEC exposed to different Il-1 doses, with or without Ang-1. HUVEC seeded at 2×10^5 cells per un-coated well in a 96 well plate and cultured for 24 hours. Wells then exposed to Il-1 at 0.01, 0.03 or 0.05 ng/ml, with or without 200 ng/ml Ang-1, followed by CAM determination after 6 hours. Graph represents the combined data from four individual experiments, with individual data points in duplicate. Data presented to show additive effect of 200 ng/ml Ang-1 on CAM expression relative to that produced by IL-1 alone, i.e. percentage inhibition of CAM expression by Ang-1. ICAM-1 expression is inhibited by 200 ng/ml Ang-1 in the presence of 0.03 ng/ml Il-1 only (not significant).

Figure 5.8 (a) through 5.8(c) presents the compiled CAM expression data from four individual experiments, presenting each individual CAM separately on its own axis, whilst each bar represents the increase or decrease in CAM expression in relation to that produced by IL-1 alone for each concentration tested. Ang-1 inhibits both VCAM-1 and E-Selectin expression at 0.03 and 0.05 ng/ml IL-1, reaching significance for E-Selectin only. Ang-1 also inhibited ICAM-1 expression when combined with 0.03 ng/ml IL-1, but not at the higher dose of 0.05 ng/ml as for VCAM-1.

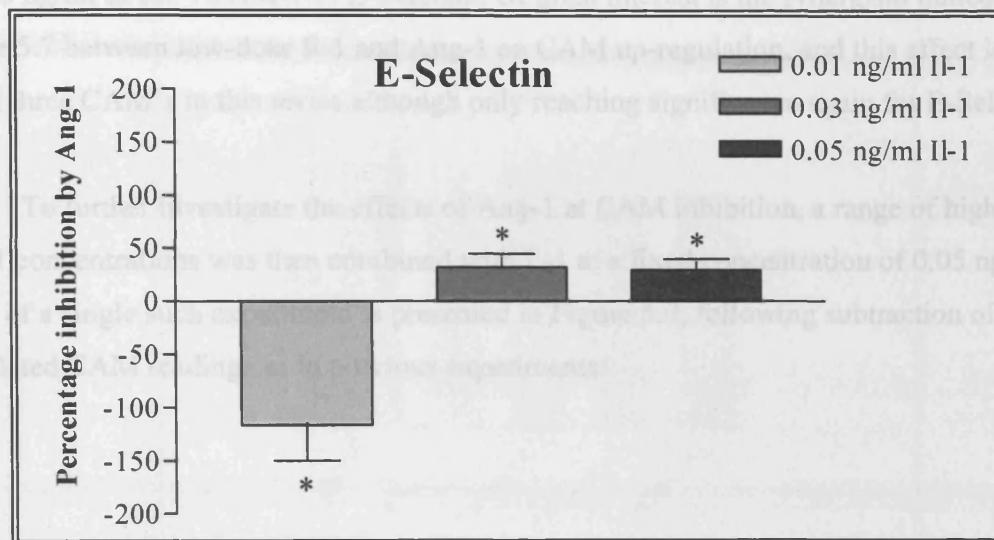


Figure 5.8 (c): E-Selectin expression in HUVEC exposed to different IL-1 doses, with or without Ang-1. HUVEC seeded at 2×10^5 cells per un-coated well in a 96 well plate and cultured for 24 hours. Wells then exposed to IL-1 at 0.01, 0.03 or 0.05 ng/ml, with or without 200 ng/ml Ang-1, followed by CAM determination after 6 hours. Graph represents the combined data from four individual experiments, with individual data points in duplicate. Data presented to show additive effect of 200 ng/ml Ang-1 on CAM expression relative to that produced by IL-1 alone, i.e. percentage inhibition of CAM expression by Ang-1. E-selectin expression is inhibited by 200 ng/ml Ang-1 in the presence of 0.03 and 0.05 ng/ml IL-1 (* P=0.05). E-Selectin is increased by the same dose of Ang-1 in the presence of 0.01 ng/ml IL-1 (* P=0.05).

Figures 5.8 (a) through 5.8 (c) presents the compiled CAM expression data from four individual experiments, presenting each individual CAM separately on its own axis, whilst each bar represents the increase or decrease in CAM expression in relation to that produced by Il-1 alone for each concentration stated. Ang-1 inhibits both VCAM-1 and E-Selectin expression at 0.03 and 0.05 ng/ml Il-1, reaching significance for E-Selectin only. Ang-1 also inhibited ICAM-1 expression when combined with 0.03 ng/ml Il-1, but not at the higher dose of 0.05 ng/ml as for VCAM-1 or E-Selectin. Of great interest is the synergism hinted at in Figure 5.7 between low-dose Il-1 and Ang-1 on CAM up-regulation, and this effect is present for all three CAM's in this series although only reaching significance again for E-Selectin.

To further investigate the effects of Ang-1 at CAM inhibition, a range of high-dose Ang-1 concentrations was then combined with Il-1 at a fixed concentration of 0.05 ng/ml. The result of a single such experiment is presented in Figure 5.9, following subtraction of un-stimulated CAM readings as in previous experiments.

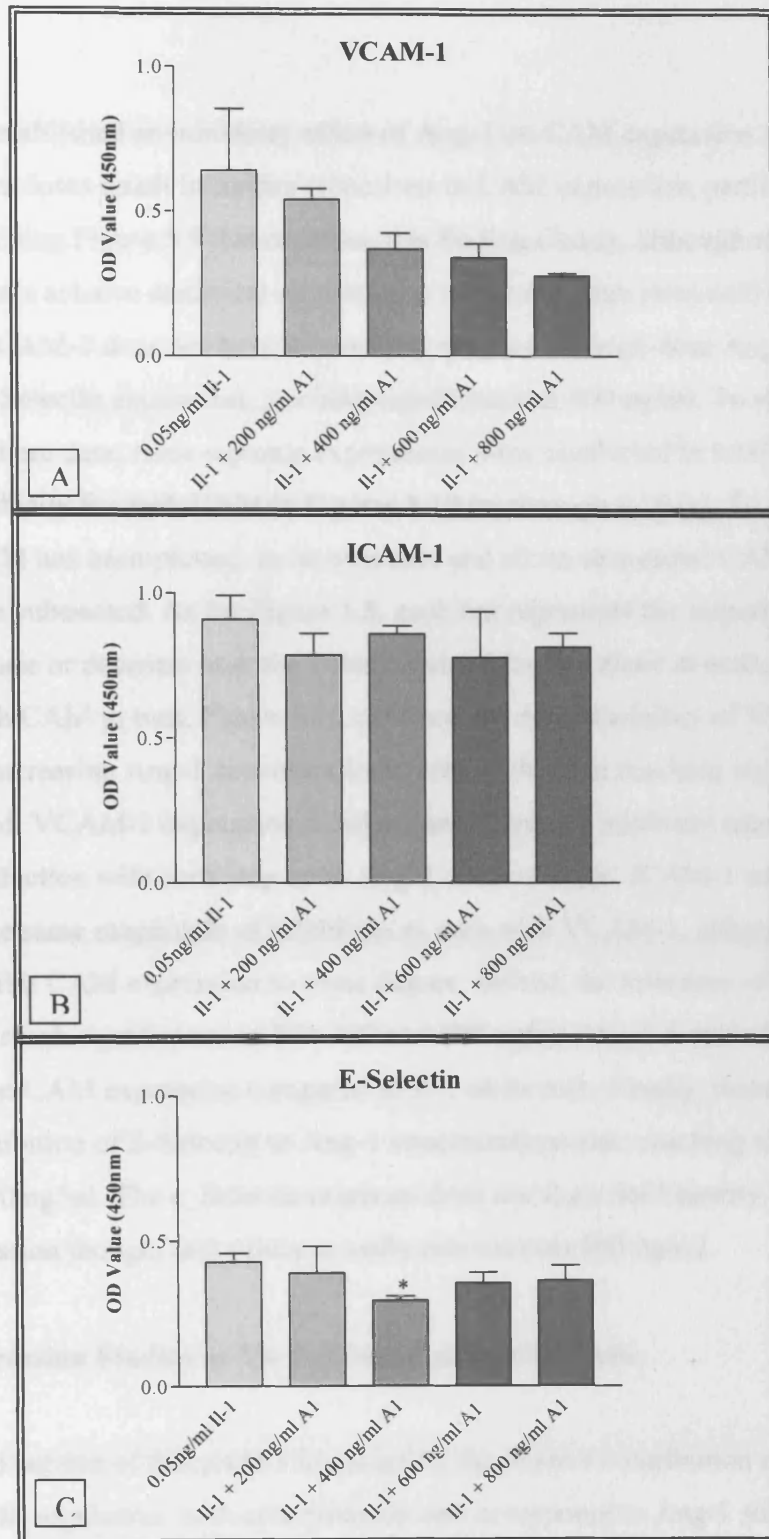


Figure 5.9: VCAM-1 ICAM-1 and E-Selectin expression in HUVEC exposed to 0.05 ng/ml Il-1 and increasing concentrations of Ang-1. HUVEC seeded at 2×10^5 cells per un-coated well in a 96 well plate and cultured for 24 hours. Wells then exposed to 0.05 ng/ml Il-1 plus 0, 200, 400, 600 or 800 ng/ml Ang-1, followed by ICAM-1 (Graph A), VCAM-1 (Graph B) and E-Selectin (Graph C) determination after 6 hours. All graph data presented following subtraction of un-stimulated CAM baseline values. Each data point represents duplicate wells, with SD error bars about the mean. Representative experiment from a series of four shown. (* $P < 0.05$).

Having established an inhibitory effect of Ang-1 on CAM expression when used at 200 ng/ml, higher doses result in further reductions in CAM expression, particularly for VCAM-1. Examining Figure 5.9 demonstrates this finding clearly, although none of the higher Ang-1 doses achieve statistical significance because of high inter-well variability in the Il-1 solo wells. ICAM-1 does not have any striking response to high-dose Ang-1, but there is a small fall in E-Selectin expression, reaching significance at 400 ng/ml. To verify the repeatability of these data, three separate experiments were conducted in total, and they are presented individually for each CAM in Figures 5.10 (a) through 5.10 (c). To create these graphs, each CAM has been plotted on its own axis and all un-stimulated CAM baseline values have been subtracted. As for Figure 5.8, each bar represents the impact of Ang-1 as a percentage increase or decrease over the value obtained for Il-1 alone at each stated dose. Considering each CAM in turn, Figure 5.10 confirms the reproducibility of VCAM-1 inhibition with increasing Ang-1 concentrations, with each value reaching significance. At the highest dose used, VCAM-1 expression is halved and there is a relatively smooth linearity to the VCAM-1 reduction with each step up in Ang-1 concentration. ICAM-1 on the other hand does not have the same magnitude of inhibition as seen with VCAM-1, although Ang-1 at any dosage does inhibit CAM expression to some degree. Indeed, the tolerance of each data set is close enough to reach significance at 200, 400 and 800 ng/ml Ang-1 despite the very small overall impact on CAM expression compared to Il-1 on its own. Finally, there is a considerable inhibition of E-Selectin as Ang-1 concentrations rise, reaching significance at 400, 600 and 800 ng/ml. The e_Selectin response does not share the linearity associated with VCAM-1 expression though, and values actually rise towards 800 ng/ml.

5.5: CAM Expression Studies in Tie deficient Endothelial Cells:

The final section of this project investigated the relative contribution made by Tie receptors to CAM regulation, both constitutively and in response to Ang-1 stimulation. To approach this objective, Tie deficient HUVEC were generated as described in the previous two chapters and in detail in section 2.11 of the Materials and Methods chapter. Tie deficient HUVEC were then assayed for CAM expression in response to Il-1 stimulation both with and without Ang-1. As in previous experiments, Tie receptor removal was highly effective using SiRNA techniques. Furthermore, as Ang-1 exerted a consistent, dose dependent reduction in VCAM-1 expression in naïve HUVEC, this CAM was selected as the sole marker of Ang-1 activity in Tie deficient cells. Figure 5.11 presents the VCAM-1 profile from a single

experiment using Tie1, Tie2 and random transfected HUVEC exposed to increasing concentrations of Ang-1 in conjunction with Il-1 at 0.05 ng/ml. Unfortunately, HUVEC transfection was subsequently plagued with technical problems and no further data was generated with Tie deficient HUVEC. As such, it was not possible to draw conclusions upon either the baseline CAM expression profile in Tie deficient HUVEC, nor their response to stimulation with either inflammatory cytokines or Ang-1.

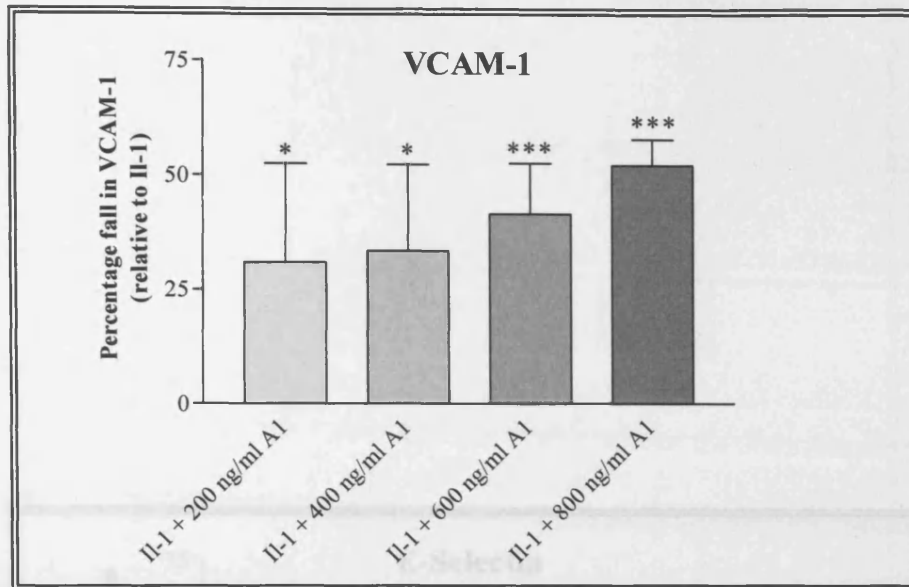


Figure 5.10 (a): VCAM-1 expression in HUVEC exposed to 0.05 ng/ml Il-1 and increasing concentrations of Ang-1. HUVEC seeded at 2×10^5 cells per un-coated well in a 96 well plate and cultured for 24 hours. Wells then exposed to 0.05 ng/ml Il-1 plus 0, 200, 400, 600 or 800ng/ml Ang-1, followed by CAM determination after 6 hours. Graph presents the percentage fall in CAM expression associated with increasing Ang-1 concentrations as compared to the level expressed with Il-1 alone at 0.05 ng/ml. Data combined from three individual experiments each in duplicate. Error bars represent the SEM about the mean for each value. Statistical significance shown by asterisks (* P=0.05 and *** P=0.0001).

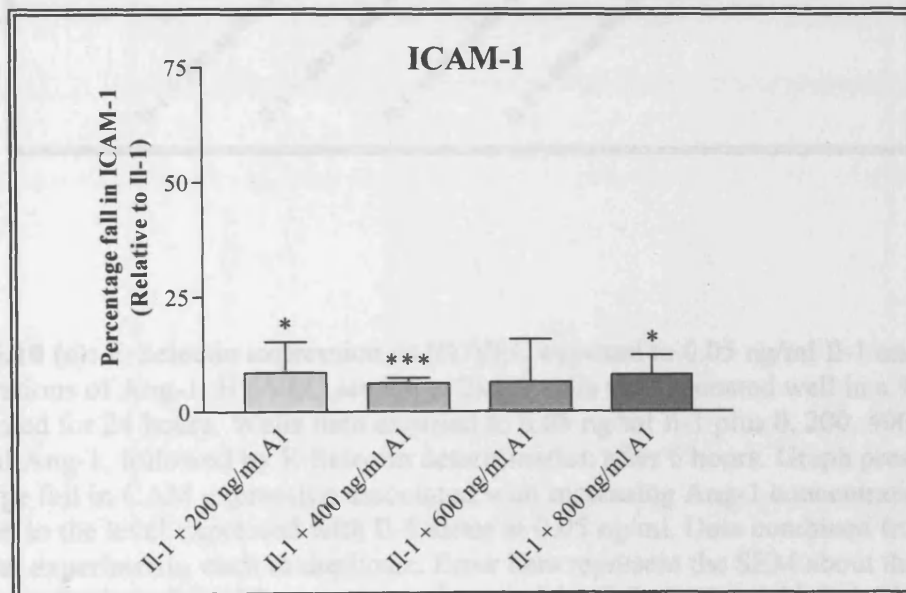


Figure 5.10 (b): ICAM-1 expression in HUVEC exposed to 0.05 ng/ml Il-1 and increasing concentrations of Ang-1. HUVEC seeded at 2×10^5 cells per un-coated well in a 96 well plate and cultured for 24 hours. Wells then exposed to 0.05 ng/ml Il-1 plus 0, 200, 400, 600 or 800ng/ml Ang-1, followed by CAM determination after 6 hours. Graph presents the percentage fall in CAM expression associated with increasing Ang-1 concentrations as compared to the level expressed with Il-1 alone at 0.05 ng/ml. Data from three individual experiments, each in duplicate. Error bars represent the SEM about the mean for each value. Statistical significance shown by asterisks (* P=0.05 and *** P=0.0001).

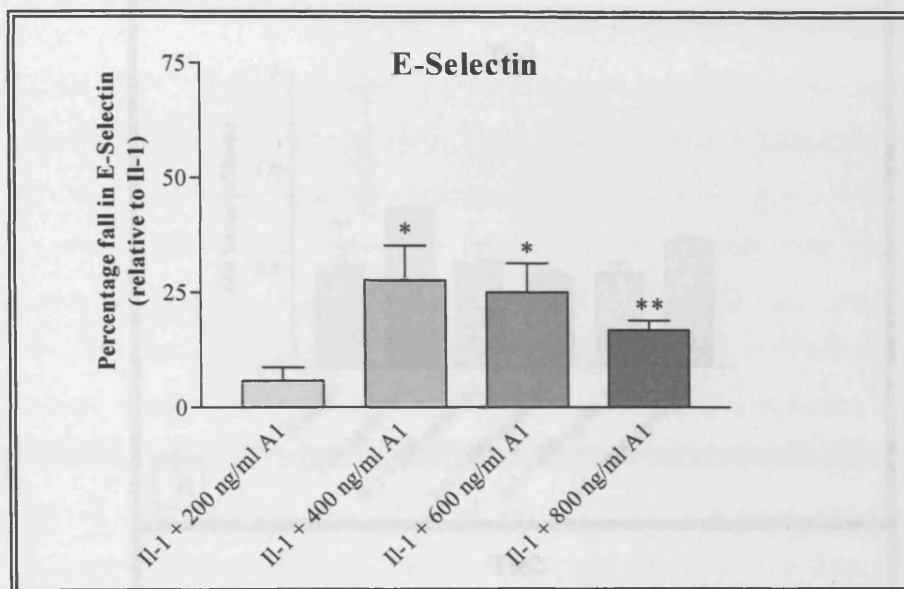


Figure 5.10 (c): E-Selectin expression in HUVEC exposed to 0.05 ng/ml Il-1 and increasing concentrations of Ang-1. HUVEC seeded at 2×10^5 cells per un-coated well in a 96 well plate and cultured for 24 hours. Wells then exposed to 0.05 ng/ml Il-1 plus 0, 200, 400, 600 or 800ng/ml Ang-1, followed by E-Selectin determination after 6 hours. Graph presents the percentage fall in CAM expression associated with increasing Ang-1 concentrations as compared to the level expressed with Il-1 alone at 0.05 ng/ml. Data combined from three individual experiments, each in duplicate. Error bars represent the SEM about the mean for each value. Statistical significance shown by asterisks (* P=0.05 and ** P=0.0005).

Figure 5.11: Relative expression of VCAM-1 in wild-type (W), Tie2 deficient (T2) and Tie2 deficient (C) HUVEC VCAM-1 expression following exposure to 0.05 ng/ml Il-1 and increasing concentrations of Ang-1. Each graph presents the CAM expression associated with increasing Ang-1 concentrations in addition to 0.05 ng/ml Il-1 per well. Wild-type, Tie2 deficient and Tie2 deficient HUVEC seeded at 2×10^5 cells per un-coated well in a 96 well plate and cultured for 24 hours. Wells then exposed to 0.05 ng/ml Il-1 plus 0, 200, 400, 600 or 800 ng/ml Ang-1, followed by VCAM-1 determination after 6 hours. Error bars represent the SD about the mean for each value. Data presented from a single experiment.

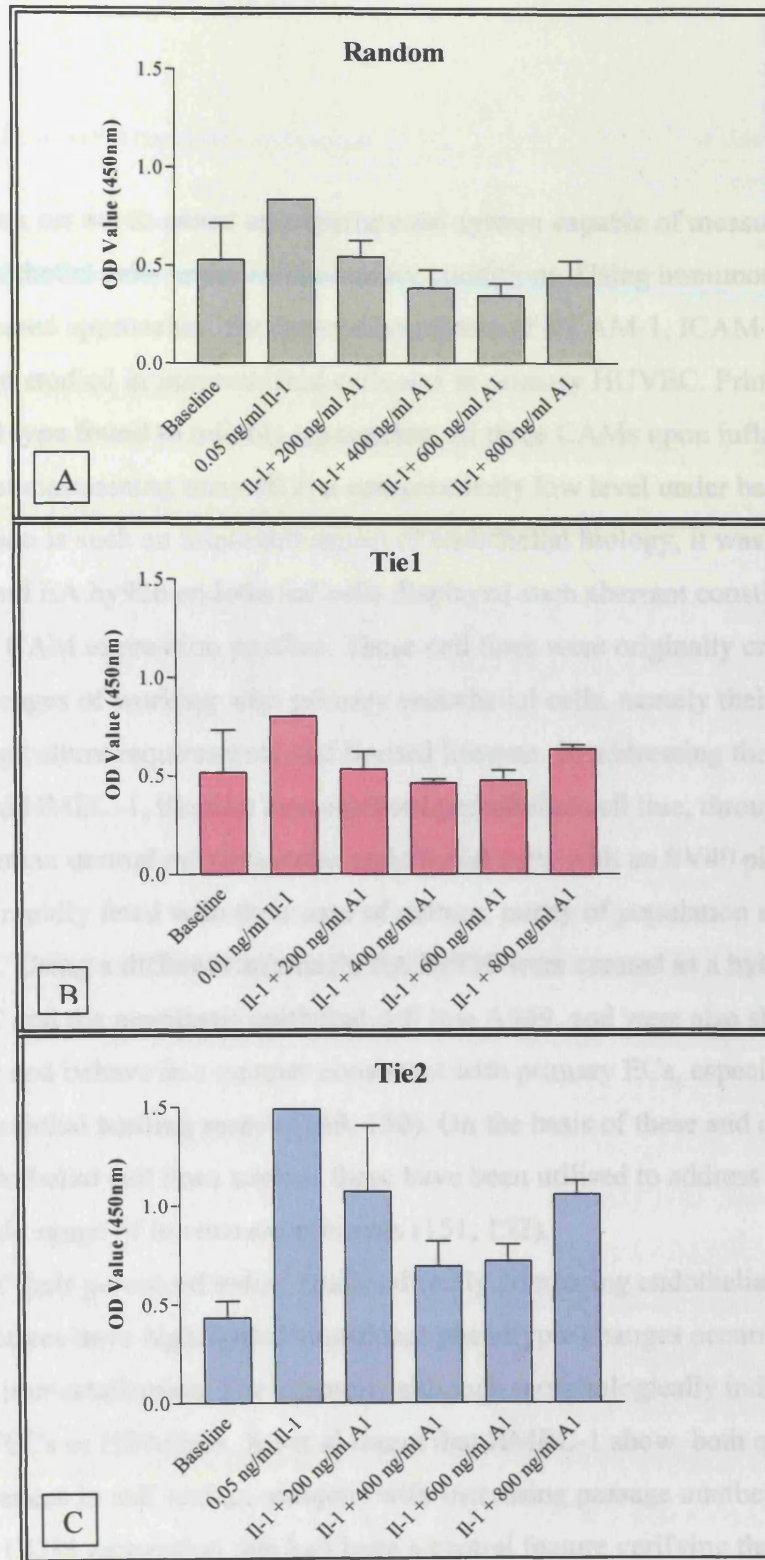


Figure 5.11: Random control (A), Tie1 deficient (B) and Tie2 deficient (C) HUVEC VCAM-1 expression following exposure to 0.05 ng/ml Il-1 and increasing concentrations of Ang-1. Each graph presents the CAM expression associated with increasing Ang-1 concentrations in addition to 0.05 ng/ml Il-1 per well. Random, Tie1 deficient and Tie2 deficient HUVEC seeded at 2×10^5 cells per un-coated well in a 96 well plate and cultured for 24 hours. Wells then exposed to 0.05 ng/ml Il-1 plus 0, 200, 400, 600 or 800 ng/ml Ang-1, followed by VCAM-1 determination after 6 hours. Error bars represent the SD about the mean for each value. Data presented from a single experiment.

5.6: Discussion:

This chapter set out to create an experimental system capable of measuring CAM expression in endothelial cells under inflammatory conditions. Using immunocytochemistry and cell-ELISA based approaches, the expression pattern of VCAM-1, ICAM-1 and E-Selectin have been studied in immortalized cells and in primary HUVEC. Primary HUVEC were the only cell type found to reliably up-regulate all three CAMs upon inflammatory stimulation, whilst maintaining them all at a comparatively low level under basal conditions. As CAM expression is such an important aspect of endothelial biology, it was surprising that both HMEC-98 and EA.hy926 endothelial cells displayed such aberrant constitutive and cytokine induced CAM expression profiles. These cell lines were originally created to address some of the challenges of working with primary endothelial cells, namely their difficulty of isolation, exacting culture requirements and limited lifespan. In addressing these problems, Ades et al. created HMEC-1, the first immortalised endothelial cell line, through the transfection of human dermal microvascular endothelial cells with an SV40 plasmid (148). These cells were rapidly feted with their ease of culture, purity of population and indefinite passage potential. Using a different approach, EA.hy926 were created as a hybridoma between HUVEC and the neoplastic epithelial cell line A549, and were also shown to grow with great vigour and behave in a manner consistent with primary ECs, especially when used in leucocyte-endothelial binding assays (149, 150). On the basis of these and other reports, immortalised endothelial cell lines such as these have been utilised to address numerous questions in a wide range of *in vitro* experiments (151, 152).

In spite of their perceived value, studies directly comparing endothelial cell lines with their primary relatives have highlighted significant phenotypic changes occurring subsequent to the process of immortalization. For example, although morphologically indistinguishable from either HUVECs or HDMECs, Xu et al found that HMEC-1 show both quantitative and qualitative differences in cell surface antigens with increasing passage number, especially the loss of vWF and CD36 expression that had been a central feature verifying the cells endothelial lineage in the first place (152, 153). Similar studies have described difficulties with immortalised endothelial cells used in blood brain barrier permeability experiments, where the immortalisation of isolated brain endothelial cells generally fail to achieve a monolayer barrier comparable to that achievable with low passage primary endothelial cells, despite a comparable overall morphology and the presence of key junctional complexes such as Occludin, Claudins 1 to 5 and JAM (154). With greatest relevance to the present work,

Lidington et al conducted a thorough assessment of CAM expression in several endothelial cell lines including HMEC-1, EA.hy926, ECV304 and primary HUVEC (155). This work described the expression of VCAM-1, ICAM-1 and E-Selectin in EA.hy926 with similar findings to those presented here, namely an ability to induce ICAM-1 expression with TNF α but with no response from the other two despite inflammatory stimulation. Interestingly, Lidington found that HMEC-1 expressed lower levels of ICAM-1 compared to the HMEC-98 used in this work, suggesting that this is either a specific difference between these two HMEC variants or that individual variations can appear within a given population with increasing passage number. This latter possibility was explored by van Waarde-Verhagen et al. who looked at the long term effects of repeated passage in immortalized VH25 human fibroblasts (156). After 150 population doublings, half of the clones studied showed genetic alteration, such as changes in ploidy or abnormal expression of the regulatory cell cycle and tumour suppressor genes p21 and p53. With such progressive dysfunctional cell cycle regulation, sub-clones of affected cells might come to dominate within a mixed population with the subsequent loss of the original genotypic and phenotypic properties characteristic of the cells of origin.

In order to replicate the *in vivo* state as closely as possible, HUVEC CAM expression formed the mainstay of the experiments presented in this chapter. Initial experiments conducted to evaluate the ability of VEGF to up-regulate inflammatory CAM expression were disappointing, with no statistically detectable response to a challenge from 20 ng/ml VEGF₁₆₅. This particular concentration was selected so as to closely replicate the experiments conducted by Kim et al. who successfully demonstrated increased CAM mRNA *and* protein expression in VEGF₁₆₅ treated HUVEC (132). However, whilst Stannard et al. also recorded small rises in CAM mRNA in response to VEGF stimulation, this failed to elicit detectable protein expression levels when using flow cytometry., suggesting that the CAM upregulation by VEGF is below the threshold for detection by this or cell-ELISA approaches (Stannard). Despite this, Stannard *did* demonstrate an additive and synergistic effect on CAM expression when VEGF and TNF α were administered together. Whilst further experiments in this work could have investigated the impact of higher concentrations of VEGF on CAM up-regulation, the focus of this investigation was maintained towards the potent pro-inflammatory effects of Il-1 and TNF α . Indeed, there was a broad-spectrum response and high sensitivity to different concentrations of both TNF α and Il-1 which went on to provide an excellent basis for the subsequent analysis of Ang-1 on CAM expression. Interestingly, there was an additive effect on the up-regulation of all three CAM's when Ang-1 was combined with Il-1 at 0.01 ng/ml,

compared to Il-1 administered on its own. Given Ang-1s inhibition of CAM expression with Il-1 at 0.03 and 0.05 ng/ml, this synergistic effect at the lowest Il-1 dose was unexpected. These results imply that Ang-1 acts to prime the endothelium towards a transient increase CAM expression in the presence of low concentrations of inflammatory cytokines, and can therefore be considered to be acting in a pro-inflammatory manner under such conditions. If this is the case then a pro-inflammatory role clearly does not persist with higher doses of Ang-1, where there is a progressive and significant inhibition of VCAM-1 when combined with a constant concentration of Il-1 at 0.05 ng/ml. The effect of higher Ang-1 doses had a far less obvious impact on either ICAM-1 or E-Selectin expression, although they were all reduced to some degree and significantly so in many cases.

To complete the studies on endothelial CAM expression within the context of this thesis, the last experiments concerned CAM expression in Tie deficient cells. Tie receptor removal proved highly effective using an SiRNA approach as in other experimental chapters, and initial cell preparations remained fully capable of raising an adhesion molecule responses to stimulation with pro-inflammatory cytokines. Unfortunately limited data is presented for the VCAM-1 expression pattern in Tie deficient HUVEC, following intractable technical difficulties with transfection, experienced towards the end of the research project. Therefore, there is only one CAM dataset available for analysis (Figure 5.11), that correlated with efficient Tie receptor knock down when batch tested by Western Blotting. Despite this, the available data does provide a provisional demonstration of a dose-dependent Ang-1 inhibition of VCAM-1 expression in random treated, Tie1 and Tie2 deficient HUVEC. Whilst the profile of VCAM-1 expression was similar in Tie1 and random treated HUVEC, its expression was markedly more intense in Tie2 deficient HUVEC. Interestingly, in each case any progressive inhibition of CAM expression was lost when 800 ng/ml Ang-1 was used, suggesting that VCAM-1 inhibition is only linearly responsive to Ang-1 stimulation within a defined dose range. The lack of multiple repeat datasets and associated statistical analyses preclude further analyses or conclusions.

6.1: Intracellular Signalling in Tie deficient HUVEC:

As discussed in chapter 1, Akt is a key signalling intermediary involved in Ang-1 mediated inhibition of apoptosis. Another important anti-apoptotic mediator is p42/44 MAPK, and this too is activated through phosphorylation in Ang-1 stimulation of endothelial cells. In this chapter an SiRNA approach was used to determine the impact of suppressing Tie1, Tie2 or both receptors on Ang-1 activation of Akt and MAPK.

Figure 6.1 demonstrates the quantitative efficacy of individual Tie receptor knock-down derived from the same cell populations used in the subsequent experiments on Akt and MAPK activation with Ang-1. The graph in part A demonstrates that both Tie1 and Tie2 receptor expression is strongly inhibited using the SiRNA protocol described in chapter 2. One of the two separate immunoblots used to compile this graph is presented underneath in part B. HUVEC deficient in Tie1 or Tie2 were next compared to random transfected controls for their Akt activation in response to Ang-1 at doses between 25 and 200 ng/ml. Figure 6.2 presents the cumulative data for Akt activation at Serine 473 from three separate experiments. All cell lysates were analysed on the same immunoblot, allowing a direct quantitative comparison between Tie1 deficient, Tie2 deficient and control HUVEC Akt activation.

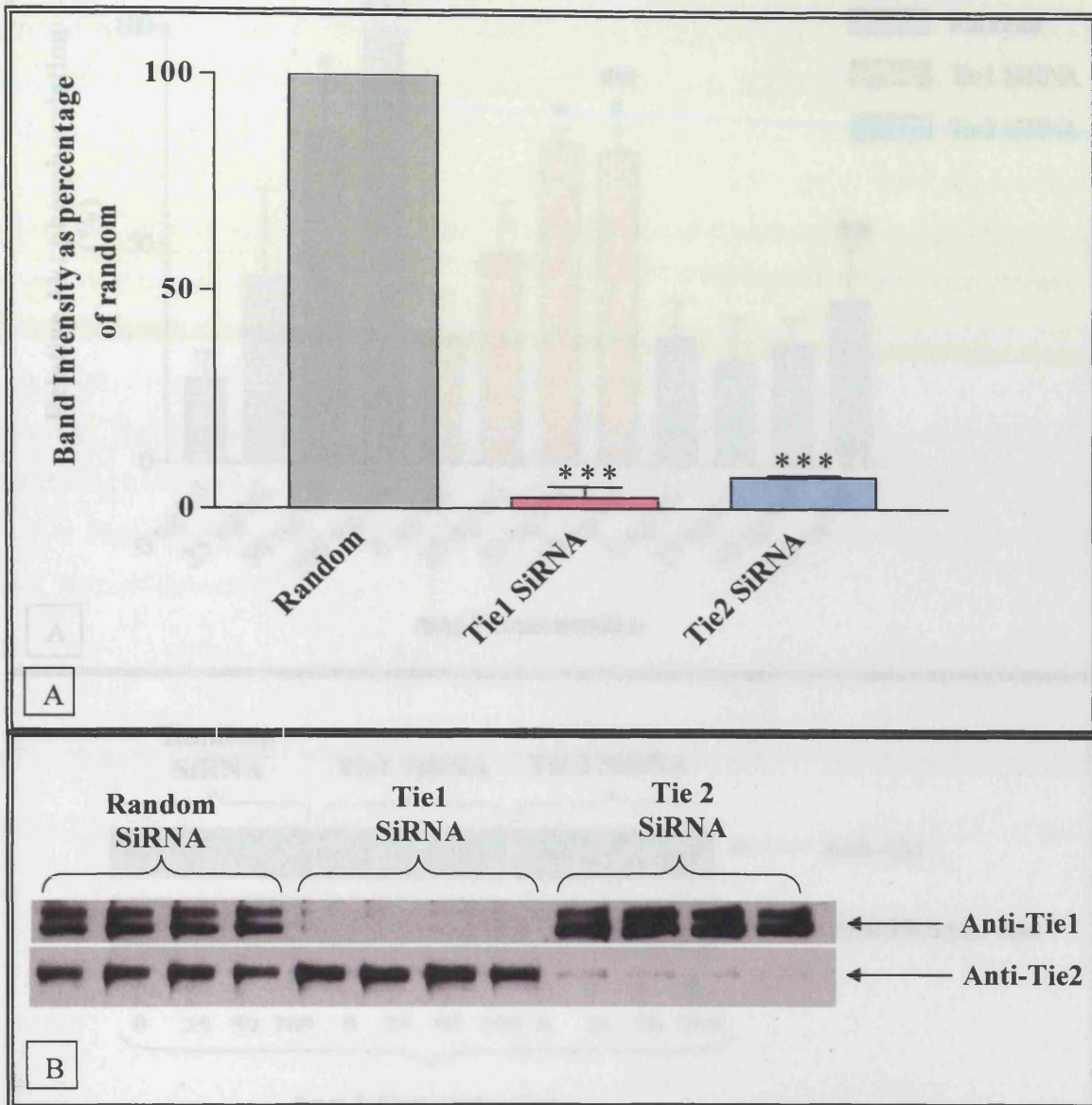


Figure 6.1: Efficiency of Tie receptor silencing in HUVEC. HUVEC between passage 4-7 were seeded to the wells of a six well plate and cultured for up to 72 hours or until a confluency of 95% was attained. Cells were given fresh complete media for 1 hour prior to transfection, which was then done according to the protocol described in the materials and methods section. Transfection with either Tie1 or Tie2 SiRNA progressed for 5 hours followed by recovery in complete media for the next 36 hours. Receptor expression was quantitated from Western Blot band intensity analysis following cell harvest and lysate formation. Representative blot from two experiments shown in B, with SEM error bars around the mean in the graph above (A, $P < 0.0001$). Graph compiled from three separate Experiments.

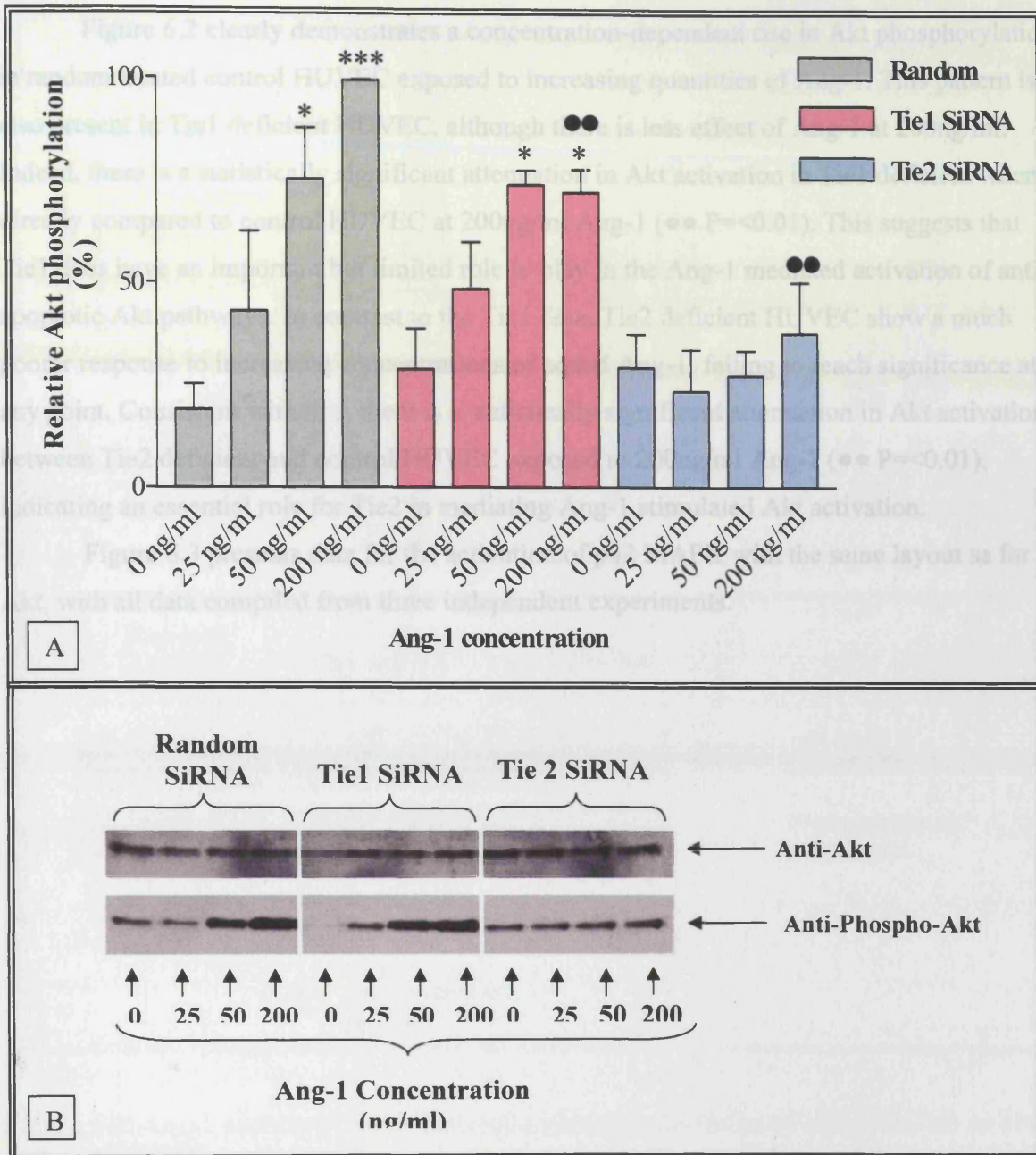


Figure 6.2: Ang-1 stimulated Akt phosphorylation in Tie deficient HUVEC. Tie1 or Tie2 deficient HUVEC were generated as described in the materials and methods section. Thirty six hours after transfection, cells were washed once in serum free HUVEC media and cultured in 1ml of the same for 45 minutes further. Ang-1 was then added to respective wells at concentrations of 0, 25, 50 and 200 ng/ml before cell lysis and harvest after a further 15 minutes. Whole cell lysates were subjected to Western blotting with estimation of both total and phosphorylated forms of Akt at serine 473 (B). Band densitometry presented as percentage phosphorylation in the graph in A (all normalised to highest intensity phosphorylated band). Representative blot from a series of 3 experiments, with SEM error bars about the mean in (A). Akt activation was statistically significant in random and Tie1 deficient HUVEC at 50 and 200ng/ml Ang-1 ($^* = <0.05$, $^{***} = <0.0001$). Akt activation was statistically smaller at 200ng/ml Ang-1 in Tie1 and Tie2 deficient HUVEC compared to random controls ($^{\bullet\bullet} P = <0.01$)

Figure 6.2 clearly demonstrates a concentration-dependent rise in Akt phosphorylation in random treated control HUVEC exposed to increasing quantities of Ang-1. This pattern is also present in Tie1 deficient HUVEC, although there is less effect of Ang-1 at 200ng/ml. Indeed, there is a statistically significant attenuation in Akt activation in Tie1 deficient when directly compared to control HUVEC at 200ng/ml Ang-1 (●● $P < 0.01$). This suggests that Tie1 does have an important but limited role to play in the Ang-1 mediated activation of anti-apoptotic Akt pathways. In contrast to the Tie1 data, Tie2 deficient HUVEC show a much poorer response to increasing concentrations of added Ang-1, failing to reach significance at any point. Consistent with this, there is a statistically significant attenuation in Akt activation between Tie2 deficient and control HUVEC exposed to 200ng/ml Ang-1 (●● $P < 0.01$), indicating an essential role for Tie2 in mediating Ang-1 stimulated Akt activation.

Figure 6.3 presents data for the activation of p42 MAPK with the same layout as for Akt, with all data compiled from three independent experiments.

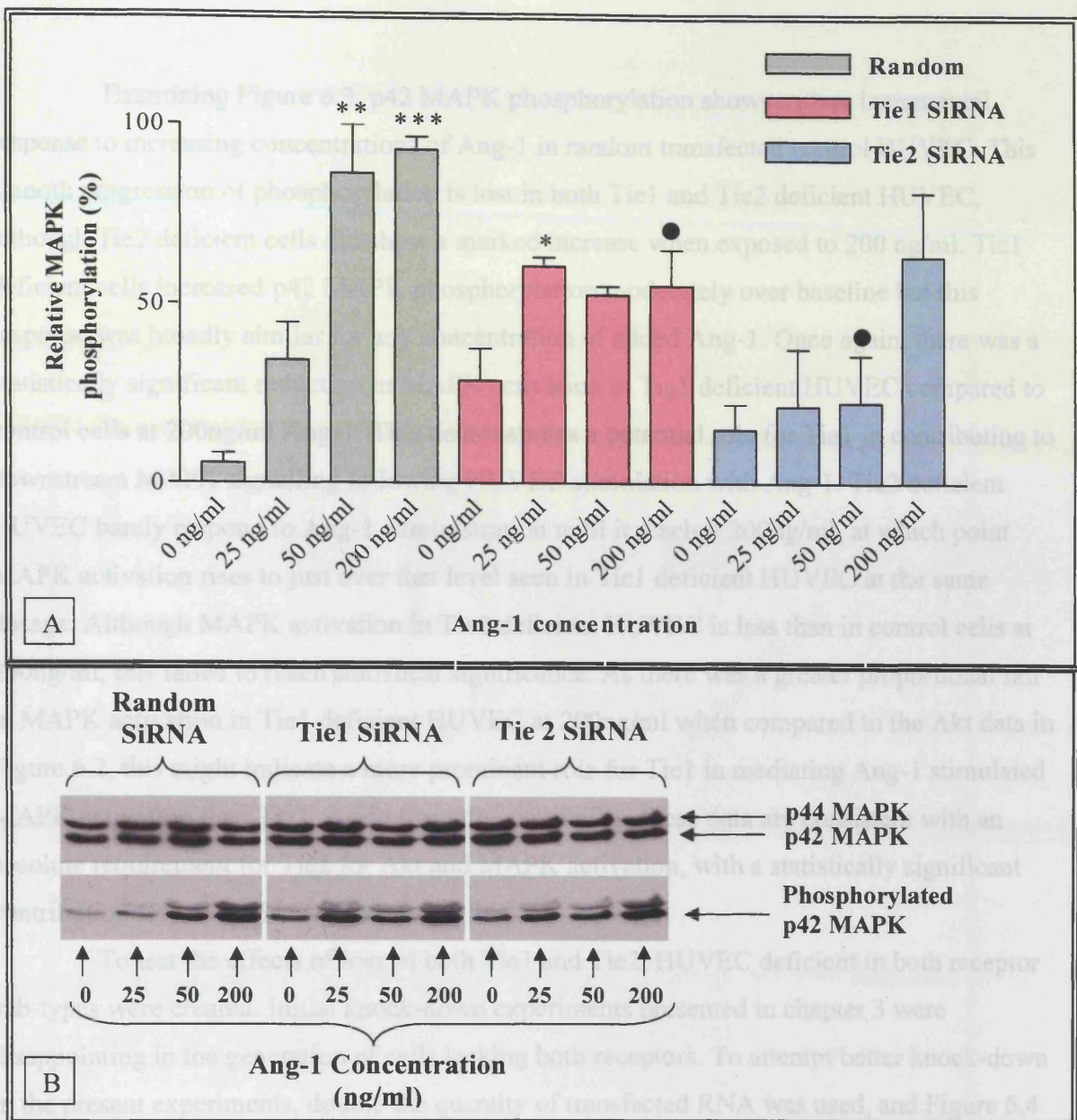


Figure 6.3: Ang-1 stimulated MAPK phosphorylation in Tie deficient HUVEC. Tie1 or Tie2 deficient HUVEC were generated, with receptor inactivation confirmed by Western Blotting (see Figure 6.1). Thirty six hours after transfection, cells were washed once in serum free HUVEC media and cultured in 1ml of the same for a further 45 minutes. Ang-1 was then added to respective wells at concentrations of 0, 25, 50 and 200 ng/ml before cell lysis and harvest after a further 15 minutes. Whole cell lysates were subjected to Western blotting with estimation of both total and phosphorylated forms of p42/44 MAPK (B). Band densitometry was calculated and presented as percentage phosphorylation of the p42 fragment only in the graph in (A) (data normalised to highest intensity phosphorylated band). Representative blot from a series of 3 experiments, with SEM error bars about the mean. p42 MAPK activation in response to Ang-1 is statistically significant at 50 and 200ng/ml for control cells and at 25ng/ml in Tie1 deficient HUVEC (* $P < 0.05$, ** $P < 0.01$, *** $P < 0.0001$). MAPK activation was statistically smaller at 200ng/ml Ang-1 between Tie1 deficient HUVEC and random controls (● $P < 0.05$), and at 50ng/ml between Tie2 deficient and control HUVEC (● $P < 0.05$).

Examining Figure 6.3, p42 MAPK phosphorylation shows a clear incremental response to increasing concentrations of Ang-1 in random transfected control HUVEC. This smooth progression of phosphorylation is lost in both Tie1 and Tie2 deficient HUVEC, although Tie2 deficient cells did show a marked increase when exposed to 200 ng/ml. Tie1 deficient cells increased p42 MAPK phosphorylation moderately over baseline but this response was broadly similar for any concentration of added Ang-1. Once again, there was a statistically significant reduction in MAPK activation in Tie1 deficient HUVEC compared to control cells at 200ng/ml Ang-1. This demonstrates a potential role for Tie1 in contributing to downstream MAPK signalling following HUVEC stimulation with Ang-1. Tie2 deficient HUVEC barely respond to Ang-1 administration until it reaches 200ng/ml, at which point MAPK activation rises to just over that level seen in Tie1 deficient HUVEC at the same dosage. Although MAPK activation in Tie2 deficient HUVEC is less than in control cells at 200ng/ml, this failed to reach statistical significance. As there was a greater proportional fall in MAPK activation in Tie1 deficient HUVEC at 200ng/ml when compared to the Akt data in Figure 6.2, this might indicate a more prominent role for Tie1 in mediating Ang-1 stimulated MAPK activation than Tie2. Aside from this possibility, these data are consistent with an absolute requirement for Tie2 for Akt and MAPK activation, with a statistically significant contribution from Tie1 in each case.

To test the effects of loss of both Tie1 and Tie2, HUVEC deficient in both receptor sub-types were created. Initial knock-down experiments presented in chapter 3 were disappointing in the generation of cells lacking both receptors. To attempt better knock-down in the present experiments, double the quantity of transfected RNA was used, and Figure 6.4 presents the level of Tie receptor removal achieved using this modification. Figure 6.4 demonstrates once again that Tie1 and Tie2 can be successfully knocked down in isolation, although in this combined series of two experiments, the magnitude of silencing was less than that presented in Figure 6.1. When attempting to silence both receptor sub-types simultaneously, equally good results were obtained, but between 15 and 20% of receptor expression did still persist in each case.

To evaluate the impact of Ang-1 on these Tie1 and Tie2 deficient HUVEC, Figure 6.5 presents the level of Akt phosphorylation following exposure to 200 ng/ml of the ligand.

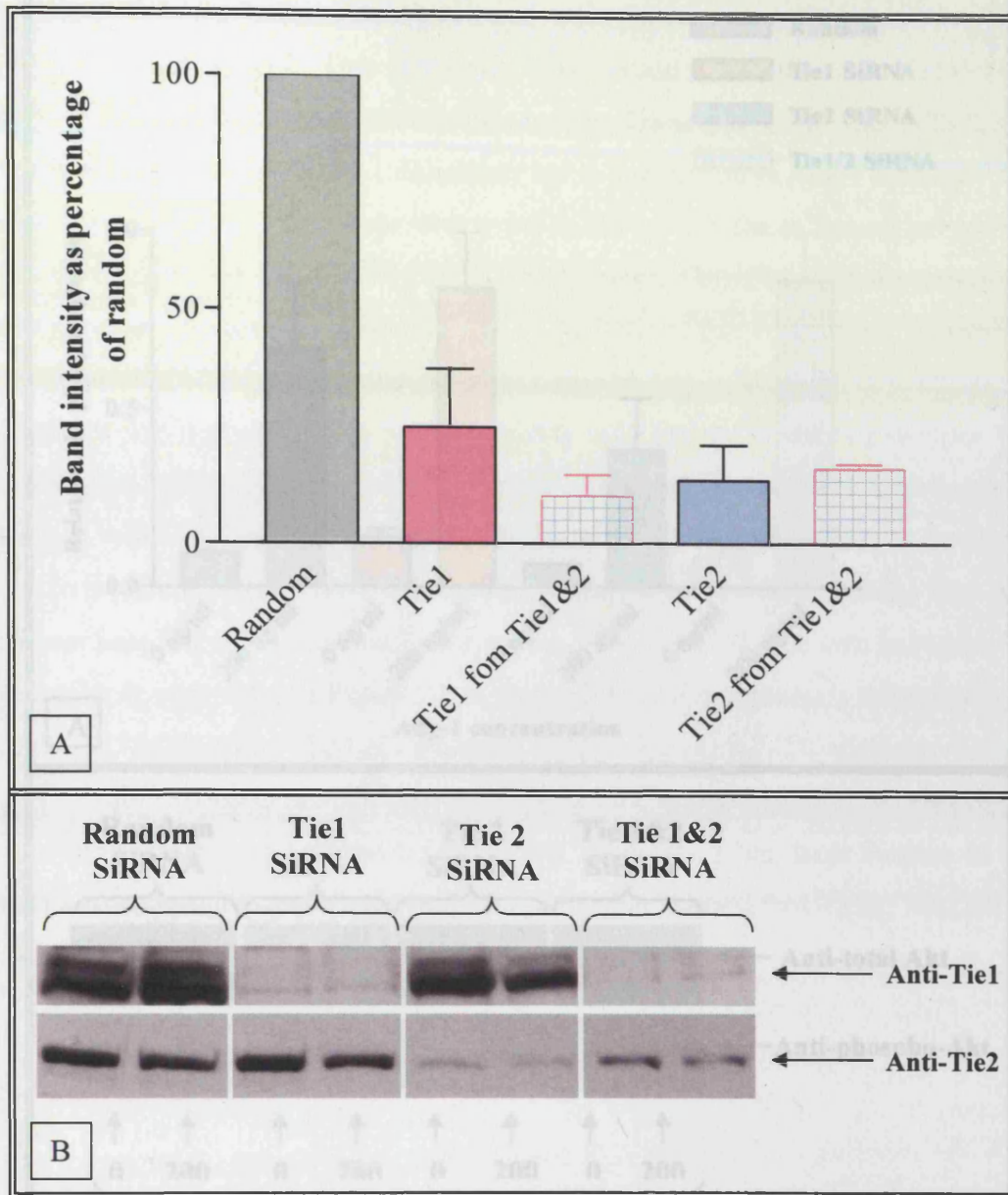


Figure 6.4: Efficiency of Tie receptor silencing in HUVEC. HUVEC between passage 4-7 were seeded to the wells of a six well plate and cultured for up to 72 hours or until a confluency of 95% was attained. Cells were given fresh complete media for 1 hour prior to transfection, which was then done according to the protocol described in the materials and methods section. Transfection with either Tie1, Tie2 or Tie1 and Tie2 SiRNA progressed for 5 hours followed by recovery in complete media for the next 18 hours. Receptor expression was quantitated from Western Blot band intensity analysis following cell lysis. Representative blot shown in B, with SEM error bars around the mean in graph A. All data derived from two separate experiments.

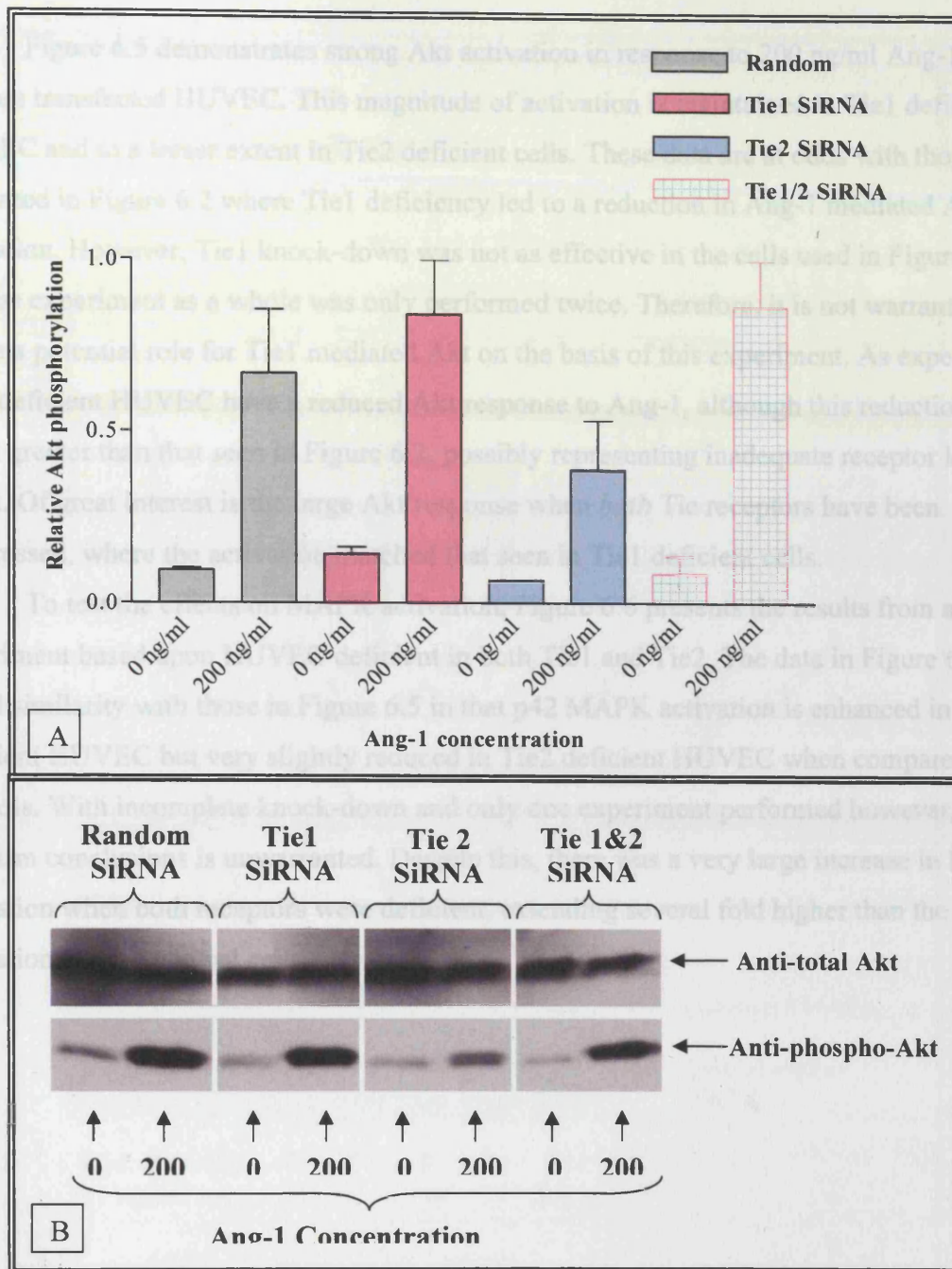


Figure 6.5: Ang-1 stimulated Akt phosphorylation in Tie deficient HUVEC. Tie1, Tie2 or Tie1 and Tie2 deficient HUVEC were generated as described with sample knock-down analysis presented in Figure 6.4. 18 hours post transfection, wells were washed once in serum free HUVEC media and then cultured in 1ml of the same for 45 minutes. Ang-1 was then added to respective wells at 200 ng/ml before cell lysis and harvest after a further 15 minutes. Whole cell lysates were subjected to Western blotting with estimation of both total and phosphorylated forms of Akt at Serine 473 (B). Band densitometry was calculated as described in the text and presented as percentage phosphorylation in the graph in (A) all data normalised to the highest intensity phosphorylated band. Representative blot from a series of 2 experiments, with SEM error bars about the mean in the graph of percentage phosphorylation.

Figure 6.5 demonstrates strong Akt activation in response to 200 ng/ml Ang-1 in random transfected HUVEC. This magnitude of activation is maintained in Tie1 deficient HUVEC and to a lesser extent in Tie2 deficient cells. These data are at odds with those presented in Figure 6.2 where Tie1 deficiency led to a reduction in Ang-1 mediated Akt activation. However, Tie1 knock-down was not as effective in the cells used in Figure 6.5, and the experiment as a whole was only performed twice. Therefore, it is not warranted to refute a potential role for Tie1 mediated Akt on the basis of this experiment. As expected, Tie2 deficient HUVEC have a reduced Akt response to Ang-1, although this reduction was again greater than that seen in Figure 6.2, possibly representing inadequate receptor knock-down. Of great interest is the large Akt response when *both* Tie receptors have been suppressed, where the activation matched that seen in Tie1 deficient cells.

To test the effects on MAPK activation, Figure 6.6 presents the results from a single experiment based upon HUVEC deficient in both Tie1 and Tie2. The data in Figure 6.6 share broad similarity with those in Figure 6.5 in that p42 MAPK activation is enhanced in Tie1 deficient HUVEC but very slightly reduced in Tie2 deficient HUVEC when compared to controls. With incomplete knock-down and only one experiment performed however, drawing any firm conclusions is unwarranted. Despite this, there was a very large increase in MAPK activation when both receptors were deficient, extending several fold higher than the level of activation seen in control cells.

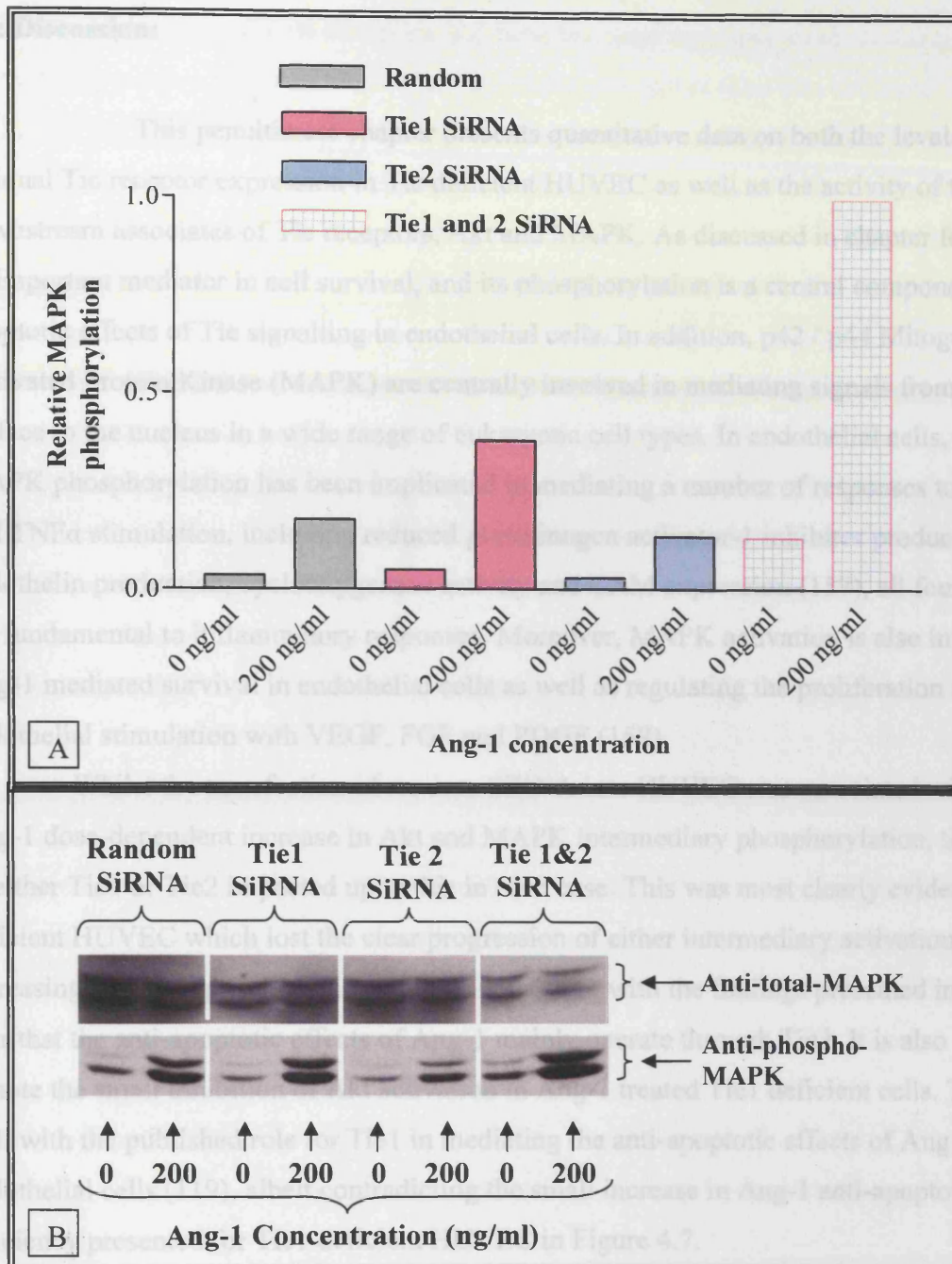


Figure 6.6: Ang-1 stimulated p42 MAPK phosphorylation in Tie deficient HUVEC. Tie1, Tie2 or Tie1 and Tie2 deficient HUVEC were generated as described in the materials and methods section, with sample knock-down analysis confirmed and presented in Figure 6.4. 18 hours after transfection, wells were washed once in serum free HUVEC media and cultured in 1ml of the same for 45 minutes. Ang-1 was then added to respective wells at 200 ng/ml before cell lysis and harvest after a further 15 minutes. Whole cell lysates were subjected to Western blotting with estimation of both total and phosphorylated forms of p42 MAPK (B). Band densitometry was calculated as described in the text and presented as percentage phosphorylation in the graph in (A), all data normalised to the highest intensity phosphorylated band. Single experiment performed.

6.2: Discussion:

This penultimate chapter presents quantitative data on both the levels of residual Tie receptor expression in Tie deficient HUVEC as well as the activity of two downstream associates of Tie receptors, Akt and MAPK. As discussed in chapter four, Akt is an important mediator in cell survival, and its phosphorylation is a central component of anti-apoptotic effects of Tie signalling in endothelial cells. In addition, p42 / p44 Mitogen Activated Protein Kinase (MAPK) are centrally involved in mediating signals from the cell surface to the nucleus in a wide range of eukaryotic cell types. In endothelial cells, p42 MAPK phosphorylation has been implicated in mediating a number of responses to both Il-1 and TNF α stimulation, including reduced plasminogen activator-1 inhibitor production, endothelin production, cyclooxygenase activity and CAM expression (157), all four of which are fundamental to inflammatory responses. Moreover, MAPK activation is also involved in Ang-1 mediated survival in endothelial cells as well as regulating the proliferation following endothelial stimulation with VEGF, FGF and PDGF (158).

Whilst the transfection of random SiRNA into HUVEC was associated with a clear Ang-1 dose-dependent increase in Akt and MAPK intermediary phosphorylation, the removal of either Tie1 or Tie2 impacted upon this in each case. This was most clearly evident in Tie2 deficient HUVEC which lost the clear progression of either intermediary activation with increasing Ang-1 exposure. This would be consistent with the findings presented in chapter four that the anti-apoptotic effects of Ang-1 mainly operate through Tie2. It is also interesting to note the small inhibition of Akt activation in Ang-1 treated Tie1 deficient cells. This fits well with the published role for Tie1 in mediating the anti-apoptotic effects of Ang-1 in endothelial cells (119), albeit contradicting the small increase in Ang-1 anti-apoptotic efficiency presented for Tie1 deficient HUVEC in Figure 4.7.

The final experiments looking at the effect of dual Tie1 and Tie2 deficiency did not match the high degree of receptor knock-down found in the previous experiments, and were not completed in triplicate due to persistent technical problems with the transfection process towards the end of the study. It was not established what caused the poor results of the transfection process, but it is likely to have related to the health of the HUVEC. In order to address the possibility of infection, fresh batches of media and cells were utilised, but problems persisted to the close of the data collection period. This was also the case affecting data collection with Tie deficient HUVEC in chapter five. Nevertheless, it was surprising to see such strong Akt and MAPK activation in response to Ang-1 stimulation in those knock-

down experiments when both receptors had been successfully suppressed. Although the average Tie receptor expression level in these cells was higher than that observed for each individual receptors removal (Figure 6.1), the degree of intermediary activation was unexpectedly high. Is it possible that Ang-1 can activate endothelial cell Akt and MAPK phosphorylation through non-Tie receptors such as integrins, and is this enhanced by the loss of a major proportion of the Tie receptor population. If this were to be the case, then perhaps the presence of either Tie receptor alone acts to inhibit alternative Ang-1 signalling pathways that are well recognised to mediate cell survival through integrin receptors in non-endothelial cell types such as cardiac myocytes (159). Answering this possibility will first require a consistent series of experiments demonstrating elevated Akt and MAPK following Ang-1 stimulation in the absence of Tie1 and Tie2. As the data stands, it is hard to draw further conclusions without establishing greater statistical significance through repeated experiments, due to the variation in the data as currently presented.

7.1: Effects of Plasma From SIRS Patients on Endothelial Inflammatory Responses:

In this final chapter, preliminary experiments undertaken to establish a human model for the effects of SIRS plasma on endothelial responses, including the impact of Ang-1, are described. Thus far, Ang-1 has been studied for its effects on HUVEC in isolation or in conjunction with individual research grade cytokine preparations. Whilst this data is extremely important for identifying and quantitating the potential benefits of Ang-1 administration in models of SIRS, it remains somewhat far removed from the inflammatory environment seen *in vivo*. Patients with SIRS have numerous pro and anti-inflammatory mediators in circulation, and the proportions of these are likely to alter continuously dependent on the status of the overall inflammatory process. Therefore, drawing conclusions from the effects of Ang-1 in conjunction with isolated cytokines fails to address how this might alter *in vivo*, which is where future drug preparations would have to work. To address this problem, plasma from patients actively undergoing treatment for SIRS related organ dysfunction was incorporated in the endothelial assays described in the previous three chapters. Whilst this approach is less sophisticated than the administration of Ang-1 in full-scale animal models of SIRS, it represents a significant step closer to future therapies based on Ang-1, as well as offering a rapid means of data collection. Full approval from regional Ethics Committee and Trust R&D approval boards was successfully secured for this final project, albeit with very limited time to run before the conclusion of laboratory work.

7.2: SIRS plasma and CAM expression:

The first series of experiments explored the ability of SIRS plasma to initiate CAM up-regulation in HUVEC. Specifically, CAM expression was measured in HUVEC exposed to increasing concentrations of plasma from either a healthy control subject or a patient suffering SIRS related pathology. CAM expression was stimulated during a 6 hour period during which HUVEC were cultured in serum free media supplemented with plasma at between 1 and 20% overall. Figure 7.1 presents the individual CAM expression profiles for HUVEC exposed to increasing plasma concentrations from a healthy control subject, in order to establish a baseline for the assay.

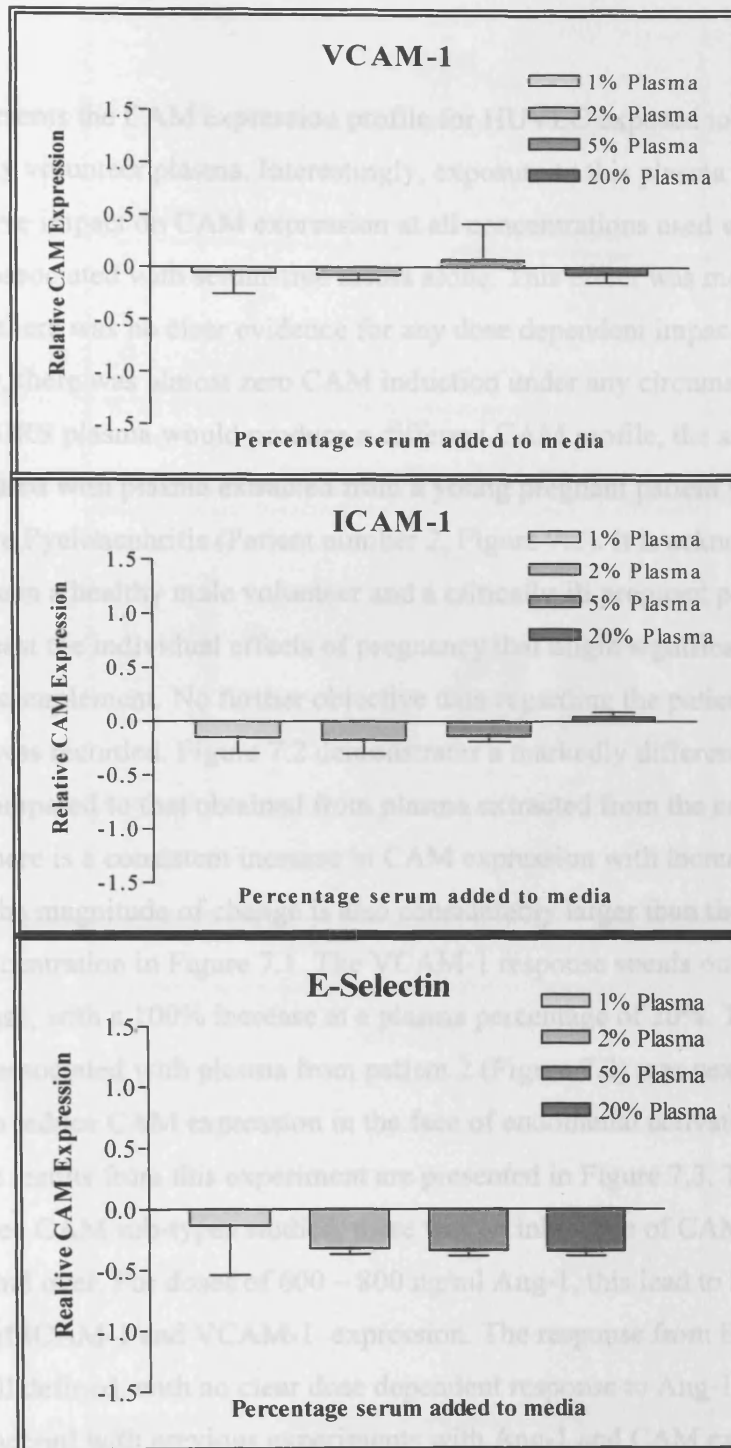


Figure 7.1: HUVEC CAM profile following plasma exposure from a healthy 32 year old volunteer. 2×10^5 HUVEC were cultured in individual wells of a 96 well plate for 24 hours. Cells were then washed once in serum free media before further culture for 6 hours in serum free media supplemented with control plasma at the indicated percentages. After 6 hours, CAM quantitation was undertaken as described in the materials and methods section. Data presented as CAM response to progressive increments in plasma percentage, with all values normalised to the CAM level associated with un-supplemented serum-free media, which was then subtracted from all values (\Rightarrow Baseline = 0; not presented in graphs). Single experiment shown with all data points in duplicate.

Figure 7.1 presents the CAM expression profile for HUVEC exposed to increasing percentages of healthy volunteer plasma. Interestingly, exposure to this plasma had a predominantly negative impact on CAM expression at all concentrations used when compared to expression levels associated with serum-free media alone. This effect was most marked with E-Selectin, and there was no clear evidence for any dose dependent impact on CAM expression. Certainly, there was almost zero CAM induction under any circumstance. To investigate whether SIRS plasma would produce a different CAM profile, the same experiment was repeated with plasma extracted from a young pregnant patient with SIRS associated with severe Pyelonephritis (Patient number 2, Figure 7.2). It is acknowledged that the comparison between a healthy male volunteer and a critically-ill pregnant patient is beset with problems, not least the individual effects of pregnancy that might significantly alter the serum growth factor complement. No further objective data regarding the patients physiological status was recorded. Figure 7.2 demonstrates a markedly different CAM expression pattern compared to that obtained from plasma extracted from the control subject. For all CAM types there is a consistent increase in CAM expression with increasing plasma concentrations, and the magnitude of change is also considerably larger than the changes observed at each concentration in Figure 7.1. The VCAM-1 response stands out as the most marked CAM response, with a 100% increase at a plasma percentage of 20%. The strong CAM up-regulation associated with plasma from patient 2 (Figure 7.2) was next used as a test for Ang-1's ability to reduce CAM expression in the face of endothelial activation from SIRS blood cytokines. The results from this experiment are presented in Figure 7.3. This Figure shows that for all three CAM sub-types studied, there was an inhibition of CAM expression at doses of 400 ng/ml and over. For doses of 600 – 800 ng/ml Ang-1, this lead to between a 20 and 30% inhibition of ICAM-1 and VCAM-1 expression. The response from E-Selectin analysis was less well defined, with no clear dose dependent response to Ang-1 concentration. Interestingly and in accord with previous experiments with Ang-1 and CAM expression, there was a small increase in CAM up-regulation at the lowest Ang-1 dosage used, 200 ng/ml.

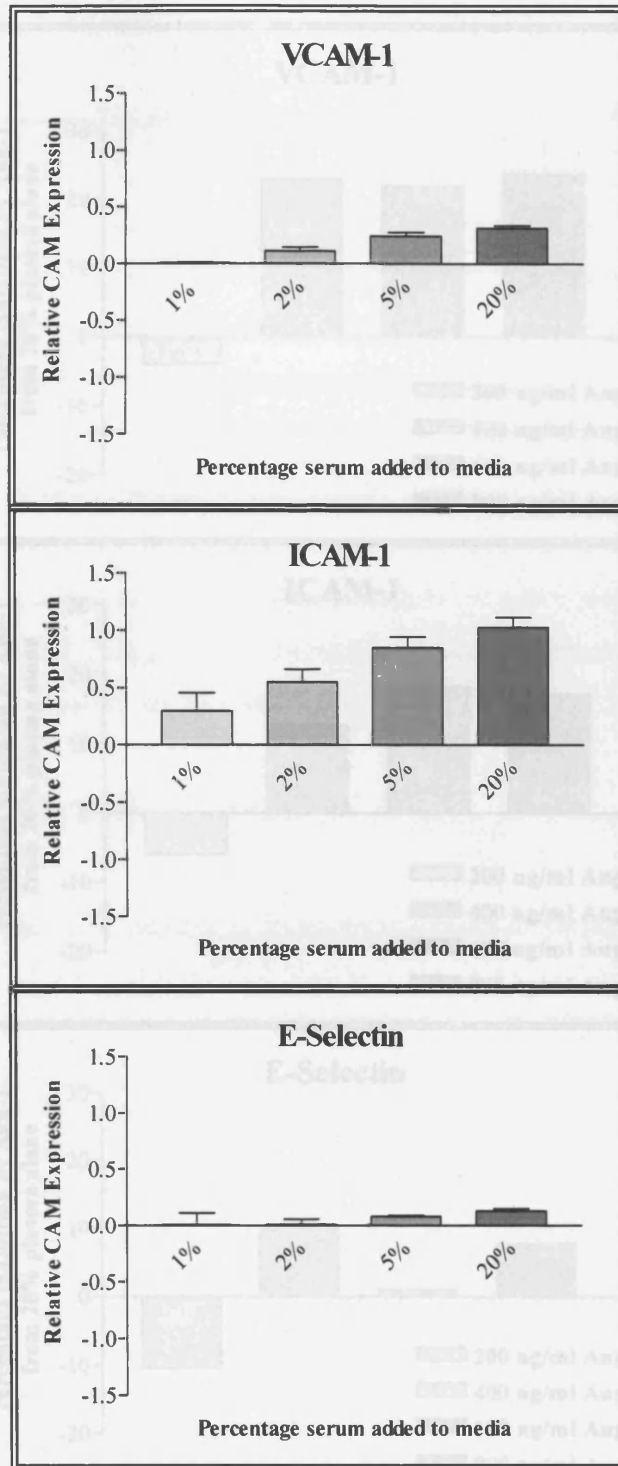


Figure 7.2: CAM profile from patient number 2. This young female patient was receiving treatment for acute pyelonephritis and was pregnant at the time of blood sample collection. 2×10^5 HUVEC were cultured in individual wells of a 96 well plate for 24 hours. Cells were then washed once in serum free media before being cultured for a further 6 hours in serum free media supplemented with patient plasma at the indicated percentages. After 6 hours, CAM quantitation was undertaken as described in the materials and methods section. Data presented as CAM response to progressive increments in plasma percentage, with all values normalised to the CAM level associated with un-supplemented serum-free media, which was then subtracted from all values (\Rightarrow Baseline = 0; not presented in graphs). Single experiment shown with all data points in duplicate.

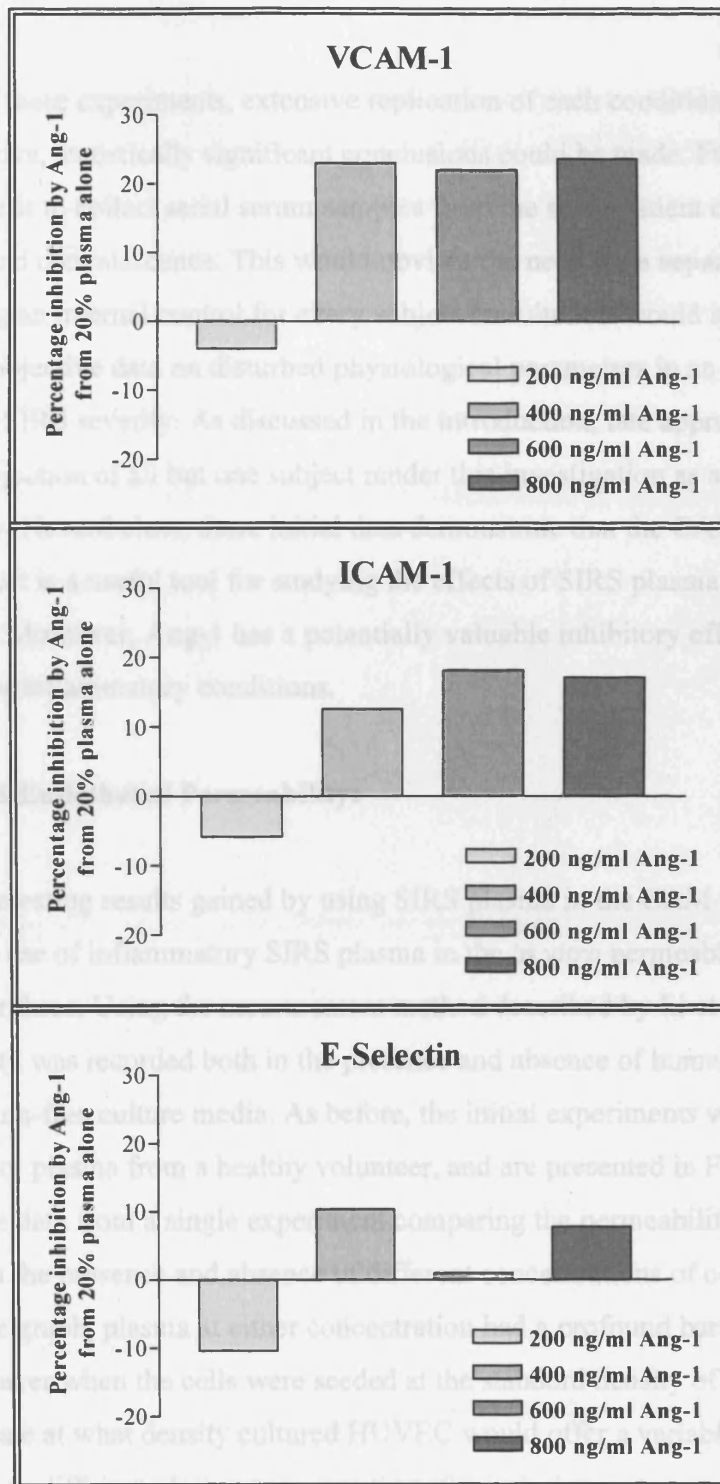


Figure 7.3: CAM expression profile in HUVEC exposed to 20% plasma from patient number 2 plus increasing concentrations of Ang-1. 2×10^5 HUVEC were cultured in individual wells of a 96 well plate for 24 hours. Cells were then washed once in serum free media before further culture for 6 hours in serum free media supplemented with patient number 2's plasma at 20% in all cases together with Ang-1 at the indicated concentrations. After 6 hours, CAM quantitation was undertaken as described in the materials and methods section. Data presented as percentage CAM inhibition, assigning maximum expression to that associated with 20% plasma alone. Single experiment with single value data.

In all of these experiments, extensive replication of each condition would be required before definitive, statistically significant conclusions could be made. Furthermore, it would be of great benefit to collect serial serum samples from the same patient during periods of maximal sickness and convalescence. This would obviate the need for a separate control population, by offering an internal control for every subject recruited. It would also be of great value to collect objective data on disturbed physiological parameters in an attempt to quantify each patient's SIRS severity. As discussed in the introduction, late approval for this study, together with rejection of all but one subject render this investigation as a proof-of-principal exercise only. Nevertheless, these initial data demonstrate that the CAM assay developed in this project is a useful tool for studying the effects of SIRS plasma on endothelial activation. Moreover, Ang-1 has a potentially valuable inhibitory effect upon CAM expression under inflammatory conditions.

7.3: SIRS plasma and Endothelial Permeability:

With interesting results gained by using SIRS plasma in the CAM assay, the next step involved the use of inflammatory SIRS plasma in the *in vitro* permeability assay documented in chapter three. Using the measurement method described by Li et al, HUVEC monolayer permeability was recorded both in the presence and absence of human plasma added to the basal serum-free culture media. As before, the initial experiments were conducted using control plasma from a healthy volunteer, and are presented in Figure 7.4. Figure 7.4 presents the data from a single experiment comparing the permeability of a HUVEC monolayer in the presence and absence of different concentrations of control plasma. As is obvious from the graph, plasma at either concentration had a profound barrier enhancing effect upon the monolayer when the cells were seeded at the standard density of 0.7×10^5 cells per insert. To investigate at what density cultured HUVEC would offer a variable permeability response to different plasma concentrations (if any), the next experiment repeated the method used in Figure 7.4 but with the HUVEC seeded at 0.2×10^5 HUVEC per insert. The data in Figure 7.5 demonstrates that even at a much reduced cell density, it is still not possible to effectively compare HUVEC monolayer permeability between conditions using plasma at 20%, whether from control subjects or patients with SIRS. Despite the differences in CAM expression induced by control versus patient number 2's plasma, there did not appear to be any effect of SIRS plasma that was different from control plasma. It is important to bear in mind that these data derive from only two experiments however, and with

further preliminary work it might be possible to alter the method protocol sufficiently to enable discrimination in permeability changes induced by SIRS and normal plasma. The reduced permeability baseline with control or patient plasma suggests that there are sufficient growth factors present to offset any potential pro-permeability factors and that the overall conditions are far more favourable for an enhanced barrier than those associated with serum-free media alone.

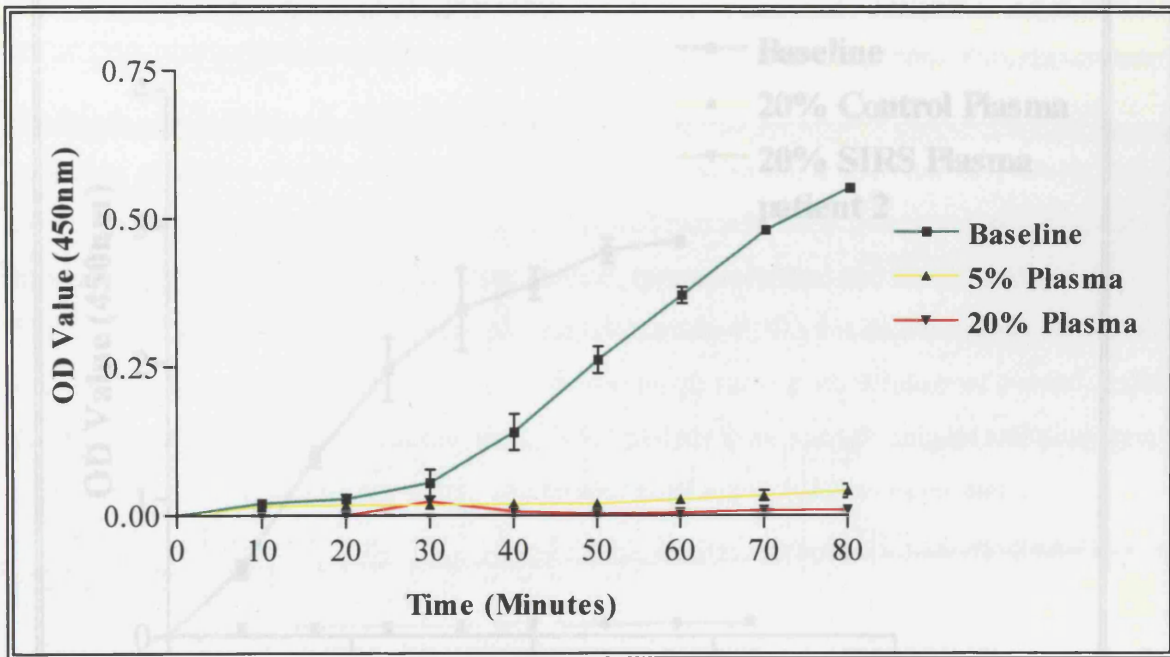


Figure 7.4: Permeability assay incorporating plasma from patient number 2. 0.7×10^5 HUVEC were seeded to individual culture inserts and allowed to form a monolayer over a 24 hour period. Media was then refreshed in both well and insert chambers as described in the materials and methods chapter, reserving the necessary insert volume for the quantity of added plasma to achieve either a 0, 5 or 20% insert concentration which was then immediately added. Permeability recorded using the HRP method of Li et al. as described in the materials and methods chapter, with sampling every 10 minutes (single experiment with duplicate values; error bars representing standard deviation about the mean).

7.4 SIRS plasma and Endothelial Survival

The first experiment of this chapter investigated the effects of SIRS plasma on endothelial survival. Previous work [121] has demonstrated an increase in HUVEC cell number in response to human-derived HUVEC, and Figure 7.5 presents

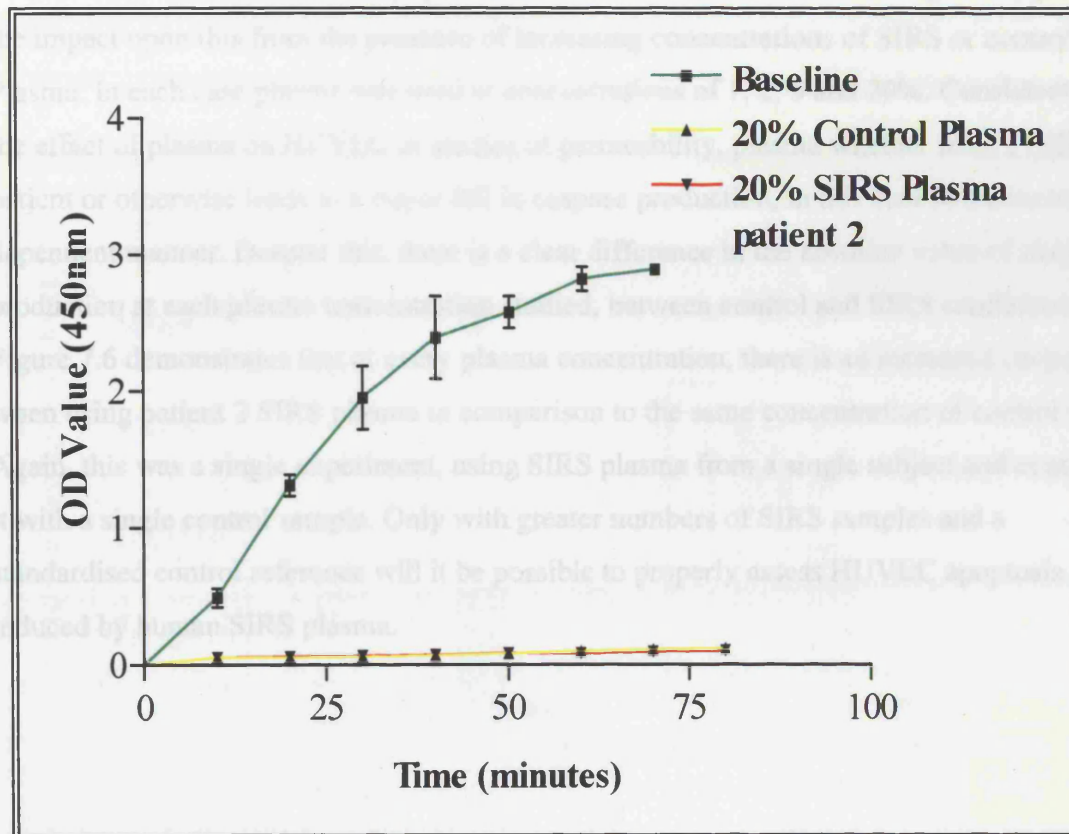


Figure 7.5: Permeability assay incorporating plasma from patient number 2 and control plasma. 0.2×10^5 HUVEC were seeded to individual culture inserts and allowed to form a low-density monolayer over the next 24 hours. Media was then exchanged in both well and insert chambers as described in the materials and methods chapter, reserving the necessary insert volume for the quantity of added plasma to achieve either a 0 or 20% insert concentration. Permeability recorded using the HRP method described in the materials and methods chapter, with sampling every 10 minutes. (single experiment with duplicate values; error bars representing standard deviation about the mean).

7.4: SIRS plasma and Endothelial Survival:

The last experiment of this final chapter investigated the effects of SIRS plasma on endothelial survival. Previous experiments have demonstrated an increase in caspase activity as a marker of apoptosis in serum-starved HUVEC, and Figure 7.6 presents the impact upon this from the presence of increasing concentrations of SIRS or control Plasma. In each case plasma was used at concentrations of 1, 2, 5 and 20%. Consistent with the effect of plasma on HUVEC in studies of permeability, plasma whether from a SIRS patient or otherwise leads to a major fall in caspase production, in this case in a concentration dependent manner. Despite this, there is a clear difference in the absolute value of caspase production at each plasma concentration studied, between control and SIRS conditions. Figure 7.6 demonstrates that at every plasma concentration, there is an increased caspase level when using patient 2 SIRS plasma in comparison to the same concentration of control plasma. Again, this was a single experiment, using SIRS plasma from a single subject and comparing it with a single control sample. Only with greater numbers of SIRS samples and a standardised control reference will it be possible to properly assess HUVEC apoptosis induced by human SIRS plasma.

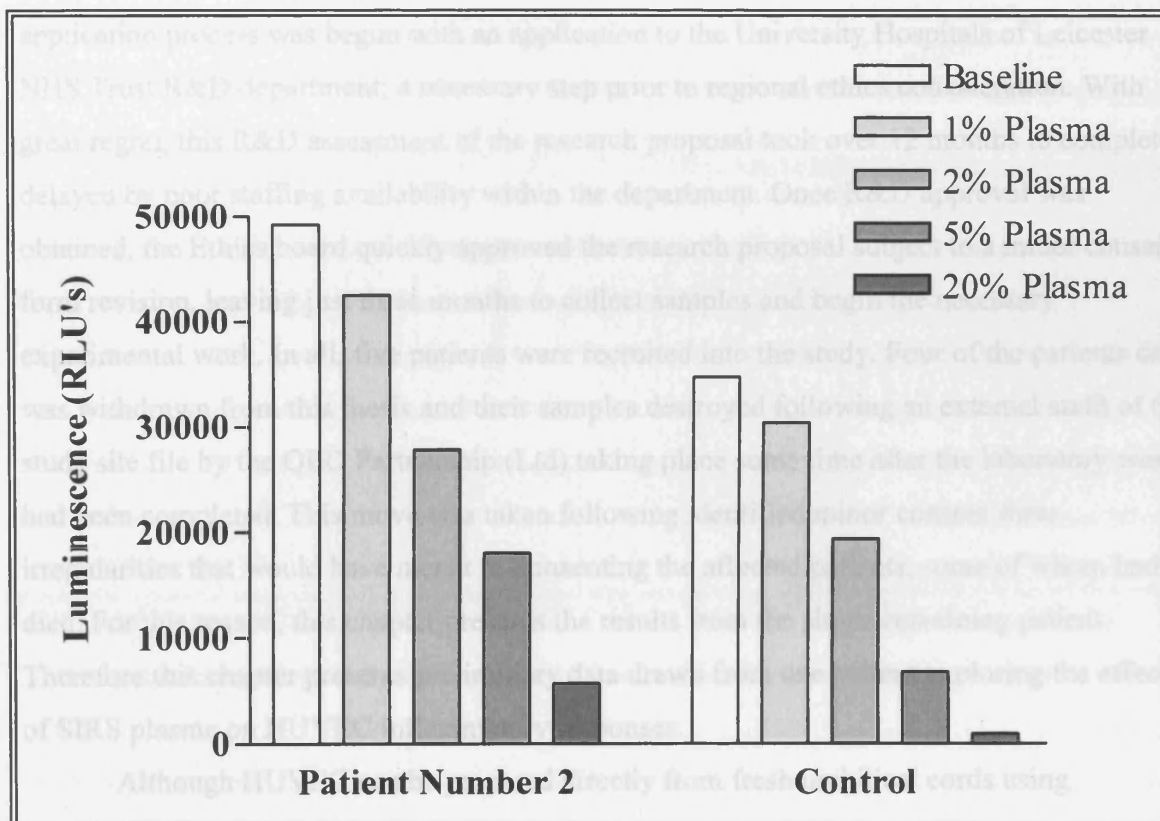


Figure 7.6: Caspase assay with SIRS or control plasma. 1×10^5 HUVEC were seeded into individual wells of a 96 well plate and allowed to settle over the following 24 hours. Media was then changed to serum free, supplemented with either control or SIRS plasma at the concentrations indicated, followed by incubation for 4 hours. Caspase activity was then measured according to the protocol detailed in the materials and methods chapter. Plasma from patient 2 and healthy volunteer. (Single experiment with single data points).

7.5: Discussion:

This final chapter set out to develop the experimental assays used in previous sections to include serum from patients with SIRS / sepsis. Before this could be undertaken, it was necessary to obtain permission for blood sample collection from the local Ethics Board. This application process was begun with an application to the University Hospitals of Leicester NHS Trust R&D department; a necessary step prior to regional ethics consideration. With great regret, this R&D assessment of the research proposal took over 12 months to complete, delayed by poor staffing availability within the department. Once R&D approval was obtained, the Ethics board quickly approved the research proposal subject to a minor consent form revision, leaving just three months to collect samples and begin the necessary experimental work. In all, five patients were recruited into the study. Four of the patients data was withdrawn from this thesis and their samples destroyed following an external audit of the study site file by the QED Partnership (Ltd) taking place some time after the laboratory work had been completed. This move was taken following identified minor consent form irregularities that would have meant re-consenting the affected patients, some of whom had died. For this reason, this chapter presents the results from the single remaining patient. Therefore this chapter presents preliminary data drawn from one patient exploring the effects of SIRS plasma on HUVEC inflammatory responses.

Although HUVEC can be prepared directly from fresh umbilical cords using standardised methodology, the HUVEC used throughout this research project were sourced commercially from PromoCell. This particular supplier has specifically developed their accompanying complete culture media as a low-serum formulation (2%), in an effort to limit any effects upon the HUVEC from unknown elements contained within the serum component (personal communication from the Manufacturers representative). By taking this approach, PromoCell have developed a HUVEC culture system robust enough to withstand stressful manipulation such as transfection, whilst retaining responsiveness to exogenously administered growth factors and cytokines such as Ang-1. This is an important consideration when interpreting the results of experiments involving PromoCell HUVEC exposed to human plasma, whether that be from healthy control subjects or patients with SIRS. In two of the three assays studied (permeability and caspase production), the addition of control or SIRS human plasma dramatically promoted quiescent responses through enhanced monolayer barrier properties and rescue from serum-starved apoptosis respectively. This suggests that the added plasma contained levels of nutrients, growth factors and cytokines capable of

promoting HUVEC health and survival way in excess of what is available from the basal media formulations alone. Although it was not possible to test effects of plasma upon permeability using the system designed in chapter three for Tie deficient HUVEC, there may be future value in using plasma in the HUVEC caspase assay, as despite the progressive fall in apoptosis with increasing plasma, Figure 7.6 suggests a differential anti-apoptotic response between control and SIRS plasma samples. This experimental design could also be improved by maintaining the added concentration of plasma constant, whilst establishing a more credible control through combined data from multiple control subjects. By measuring the average anti-apoptotic impact of multiple control subject plasma samples, it would be possible to create a normal population distribution with which to compare the plasma from any single patient with SIRS. Such a control cohort would need to be matched in key parameters such as age, sex and general health, but would then represent a credible benchmark for caspase experiments and also potentially for CAM assay studies as well.

In contrast, the application of plasma samples to the CAM model of endothelial activation did alter CAM expression. The data presented in Figures 7.1 and 7.2 demonstrate that HUVEC CAM expression is sensitive enough to reveal variations between SIRS plasma and control plasma from a healthy volunteer. Indeed, although control plasma reduced the CAM expression below that associated with baseline serum-free culture media, this was only a minor difference in contrast to the major CAM up-regulation from using isolated cytokines such as Il-1 for example (positive control data, as presented in chapter five). With the baseline CAM expression calibrated to zero in these Figures, the predomination of either pro or anti-inflammatory factors within individual plasma samples determined whether HUVEC increased or decreased their CAM production relative to the plasma-free baseline. Although this work has not analysed the quantities of key inflammatory cytokines in the SIRS plasma used, this would potentially give an indication of which cytokine combinations are most potent at CAM generation in conjunction with the CAM expression profiles for each plasma sample.

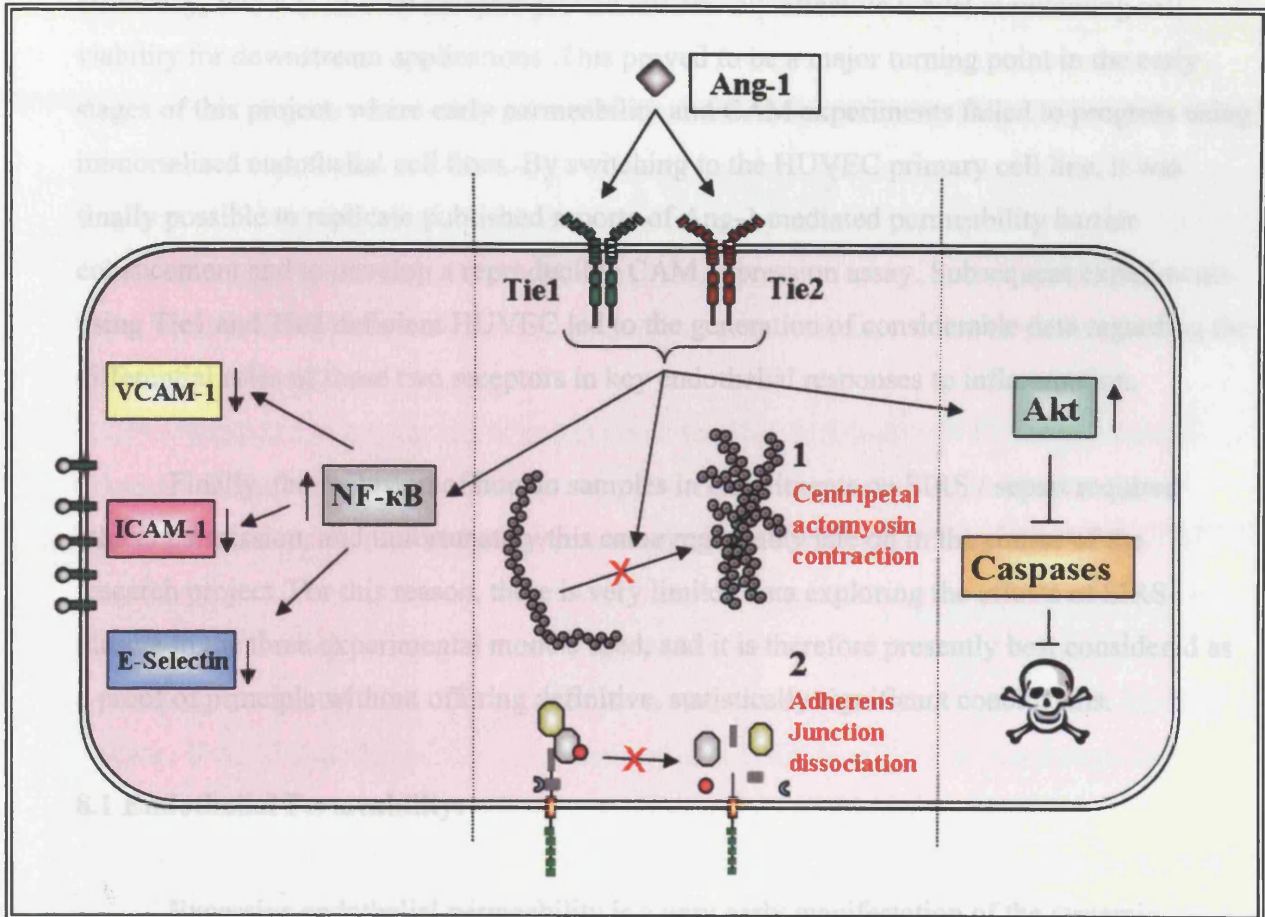
Despite the limited data available at this stage of the SIRS trial, it is of great interest to find Ang-1 acting to inhibit CAM expression elicited following exposure to SIRS plasma. Although the effect was limited, potential Ang-1 based therapy may contribute to reduced pro-inflammatory events in part through its inhibition of CAM expression as well as its known anti-permeability and anti-apoptotic properties. It should be emphasised that these data are preliminary and require duplication with larger patient groups before any conclusions can be made.

8. General Discussion and Future Work:

Despite tireless research, dysregulated inflammatory responses remain at the core of the morbidity and mortality associated with critical illness. Present best medical practice is principally limited to the provision of organ support through mechanical and pharmacological measures, whilst a targeted reduction of the underlying inflammatory response remains elusive. Until this situation is addressed, patients challenged by severe tissue injury such as major burns will continue to spend long periods in critical care, at further risk from secondary lethal complications, particularly overwhelming sepsis. Acknowledging the disappointing results with therapeutic approaches towards isolated components of the inflammatory system (65), modulating vascular endothelial responses is emerging as a promising alternative treatment target. There now exists a large body of data from *in vitro* experiments, animal models and clinical observations, that the endothelium can be manipulated to counteract key parts of the inflammatory phenotype. The facet of endothelial involvement investigated in this work has concerned the anti-inflammatory responses of the endothelial growth factor Angiopoietin-1 (Figure 8.1). To this end this research project has been devoted to establishing a better understanding of the differential roles played by Ang-1's two dedicated receptor tyrosine kinases, Tie1 and Tie2 in key anti-inflammatory responses. Specifically, endothelial permeability, survival and cell adhesion molecule expression have all been used as the biological end point variables in experiments designed to test the hypothesis that Tie2 is the receptor subtype principally responsible for mediating the anti-inflammatory effects of Ang-1. In terms of permeability and cell survival, this work has supported the hypothesis that Tie2 is essential for mediating Ang-1's actions, but in addition has identified a possible constitutive role for Tie1 in these processes, even in the absence of Ang-1. It was not possible, due to transfection problems, to test the hypothesis that Tie2 is the dominant Ang-1 binding partner in the ligands' CAM reduction properties in endothelial cells. The second hypothesis argued for distinct intracellular signalling roles for Tie1 and Tie2 following Ang-1 stimulation, and this was demonstrated to be the case for Akt and MAPK activation, where Tie1 deficient cells have a statistically poorer level of phosphorylation of these intermediaries when compared to control cells. Therefore Tie1 does contribute to downstream signalling events, either directly or through modulation of Tie2 signalling following heterodimeric association. Finally, these experiments were given greater clinical applicability through preliminary work with human SIRS plasma samples. The SIRS plasma studies in chapter seven provide initial support for

the hypothesis that Ang-1 can reduce endothelial permeability by endothelial manifestations, at least from the point of view of CAM up-regulation.

To address the remaining questions raised in the introduction, Tie deficient endothelial cells were created by gene silencing methods and, using a protocol designed for maximal



inflammatory response, playing a central role in the subsequent development of SIRS related organ dysfunction (59). Despite this, therapies targeting excessive permeability remain at the

Figure 8.1: Schematic illustration depicting some of the known actions of Ang-1. Acting through the Tie receptor tyrosine kinases Tie1 and Tie2, Ang-1 enhances endothelial barrier properties through inhibition of actomyosin contraction and IEJ disruption (central panel), enhances endothelial survival (right panel) and reduces inflammatory-stimulated CAM expression (left panel). This represents only those properties of Ang-1 of relevance to this work; Ang-1 has numerous other roles in endothelial biology.

lead to enhanced endothelial barrier generation (48, 61, 91, 96, 162). Most recently, it appears that Ang-1 mediated barrier control is mediated in part through *direct* Tie2-Tie2 homotypic association between contacting endothelial cells, a novel observation for Tie receptor function where inter-endothelial cell contacts have largely been studied in terms of IEJ components such as VE-Cadherin (163).

the hypothesis that Ang-1 can reduce inflammatory endothelial manifestations, at least from the point of view of CAM up-regulation.

To address the research questions set out in the introduction, Tie deficient endothelial cells were created by gene silencing techniques and, using a protocol designed for maximal efficiency, removal of each receptor proved remarkably effective whilst maintaining cell viability for downstream applications. This proved to be a major turning point in the early stages of this project, where early permeability and CAM experiments failed to progress using immortalised endothelial cell lines. By switching to the HUVEC primary cell line, it was finally possible to replicate published reports of Ang-1 mediated permeability barrier enhancement and to develop a reproducible CAM expression assay. Subsequent experiments using Tie1 and Tie2 deficient HUVEC led to the generation of considerable data regarding the differential roles of these two receptors in key endothelial responses to inflammation.

Finally, the inclusion of human samples in experiments on SIRS / sepsis required ethical permission, and unfortunately this came regrettably late on in the course of the research project. For this reason, there is very limited data exploring the effects of SIRS plasma in the three experimental models used, and it is therefore presently best considered as a proof of principle without offering definitive, statistically significant conclusions.

8.1 Endothelial Permeability:

Excessive endothelial permeability is a very early manifestation of the systemic inflammatory response, playing a central role in the subsequent development of SIRS related organ dysfunction (59). Despite this, therapies targeting excessive permeability remain at the pre-clinical stage, most recently including interest in the potential anti-permeability effects of Activated Protein C, already well regarded for its significant anti-apoptotic benefits in severe sepsis (160, 161). Promisingly, there now exists much information regarding the anti-leakage properties of Ang-1, including the intracellular signalling events and structural changes that lead to enhanced endothelial barrier generation (48, 62, 91, 96, 162). Most recently, it appears that Ang-1 mediated barrier control is mediated in part through *direct* Tie2-Tie2 homotypic association between contacting endothelial cells, a novel observation for Tie receptor function where inter-endothelial cell contacts have largely been studied in terms of IEJ components such as VE-Cadherin (163).

The generally held belief holds that Ang-1 operates through Tie2 for the majority of its biological effects on endothelial cells, based on the competitive inhibition observed when excess soluble Tie2 is present in conjunction with Ang-1 (48, 132). For endothelial permeability control however, this dogma was challenged by Weber's experiments with a synthetic Ang-1 ligand that achieved permeability reduction *without* activating Tie2, possibly signalling through an integrin mediated pathway instead (102). Whilst integrins do indeed interact with Ang-1 (particularly in non-endothelial tissues), the data presented in this study have confirmed an absolute requirement for the Tie2 receptor in mediating enhanced permeability barrier control in HUVEC, at least when using the native form of Ang-1 as found *in vivo* (Figure 8.2) (140, 159). Attempting to reconcile Weber's data with the present work, this suggests that endothelial cell integrins are not able to respond to native Ang-1 with altered permeability, which suggests they may require a truncated form of the ligand for this to occur, as was used in that study.

Work in this project has hinted at a role for Tie1 deficient HUVEC in permeability control, where even in the absence of Ang-1, there is a statistically higher baseline rate of permeability in Tie1 deficient monolayers as compared to controls. This suggests that Tie1 may function to establish a small constitutive degree of barrier function even though it is not necessary for the much stronger Ang-1 mediated barrier enhancement that mandates the presence of functional Tie2. If this were the case, then this data would complement well the findings from Tie1 deficient mouse embryos, shown to die *in utero* from microvascular

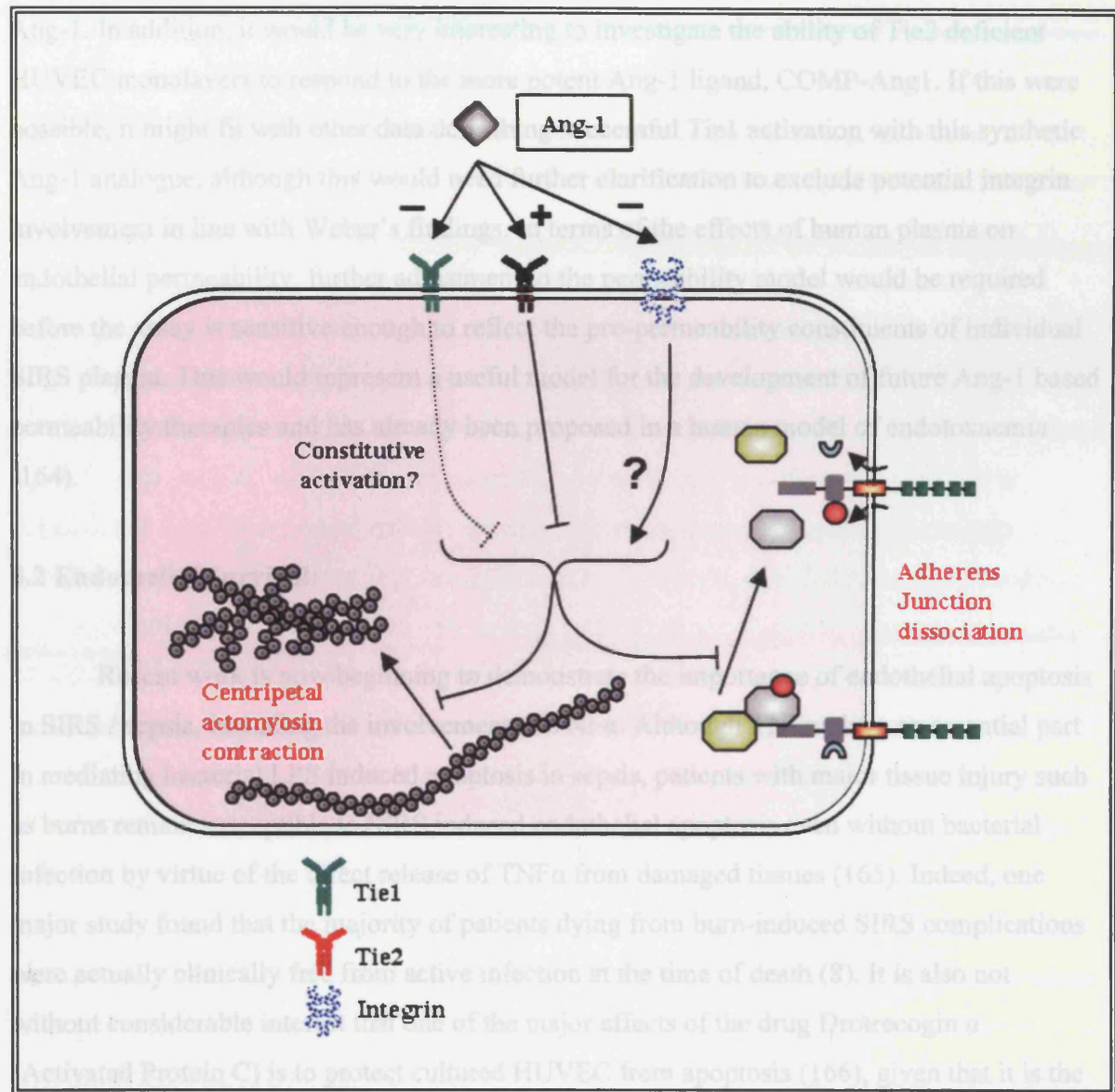


Figure 8.2: Schematic illustration depicting the mechanism of Ang-1 in mediating barrier control in endothelial permeability. Tie2 is essential for endothelial barrier enhancement in response to Ang-1 stimulation. Tie1 offers no contribution in this regard, although it may produce a low-level constitutive contribution to endothelial barrier functions even without Ang-1 being present. Integrins are unable to mediate the barrier enhancing effects of Ang-1 in the absence of Tie2.

haemorrhage and tissue oedema (35). In taking the present permeability studies further, future experiments would examine the permeability response of Tie deficient HUVEC monolayers to permeability inducing cytokines such as thrombin, both with and without protection from Ang-1. In addition, it would be very interesting to investigate the ability of Tie2 deficient HUVEC monolayers to respond to the more potent Ang-1 ligand, COMP-Ang1. If this were possible, it might fit with other data describing successful Tie1 activation with this synthetic Ang-1 analogue, although this would need further clarification to exclude potential integrin involvement in line with Weber's findings. In terms of the effects of human plasma on endothelial permeability, further adjustment to the permeability model would be required before the assay is sensitive enough to reflect the pro-permeability constituents of individual SIRS plasma. This would represent a useful model for the development of future Ang-1 based permeability therapies and has already been proposed in a human model of endotoxaemia (164).

8.2 Endothelial Survival:

Recent work is now beginning to demonstrate the importance of endothelial apoptosis in SIRS / sepsis, including the involvement of TNF α . Although TNF α plays an essential part in mediating bacterial LPS induced apoptosis in sepsis, patients with major tissue injury such as burns remain susceptible to SIRS induced endothelial apoptosis even without bacterial infection by virtue of the direct release of TNF α from damaged tissues (165). Indeed, one major study found that the majority of patients dying from burn-induced SIRS complications were actually clinically free from active infection at the time of death (8). It is also not without considerable interest that one of the major effects of the drug Drotrecogin α (Activated Protein C) is to protect cultured HUVEC from apoptosis (166), given that it is the only pharmacological agent that has been proven to have a significant impact on sepsis mortality in an ITU setting (17). Although there is little evidence to directly link Ang-1 mediated cell survival to the beneficial effects in animal studies of systemic inflammation, Witzenbichler et al found that mice over-expressing Ang-1 fared far better in response to LPS exposure than controls, and that this was associated with an increase in endothelial eNOS activity; a known anti-apoptotic downstream event stimulated by Angiopoietin-1 (46). In another study, Nag et.al. found that elevated levels of the Tie2 antagonist ligand Ang-2 was strongly associated with blood brain barrier breakdown in an *in vivo* rat model, and that this occurred through endothelial cell apoptosis (100). Moreover, there is now a battery of recent

human and animal studies identifying a positive correlation between the severity of illness in sepsis and serum Angiopoietin-2 levels, whilst some series have also noted an inverse relationship between serum Angiopoietin-1 and septic shock (167-169).

If endothelial apoptosis plays a major role in perpetuating the SIRS / sepsis state, then it again becomes imperative to define the nature of the anti-apoptotic signalling mechanism induced following Ang-1 stimulation of endothelial cells if Ang-1 is to be used as a therapeutic agent in the future. Work in chapter four of this project has established the absolute requirement for Tie2 in mediating the anti-apoptotic effects of Ang-1 (Figure 8.3), whilst Tie2 deficient HUVEC were found to have a marginally higher baseline level of apoptosis under serum free conditions. This proves the assertion in existing studies that Tie2 is the major receptor mediating pro-survival signalling in endothelial cells, and that Tie2 may also be important for endothelial survival under baseline conditions (47, 115, 117, 141). Once again though, without definitive data on cell proliferation in Tie deficient HUVEC it is important to treat such assertions with caution until caspase production can be directly correlated to cell number, possibly through the use of matrigel or TUNEL assays. In contrast, Tie1 deficient HUVEC responded well to Ang-1 administration, with an even greater degree of anti-apoptotic effect than that seen when Tie1 is present. However, Tie1 deficient HUVEC were found to have a markedly elevated basal apoptotic rate compared to controls, again possibly implicating Tie1 in cell survival under pro-apoptotic conditions even in the absence of Ang-1. Therefore, in a similar manner to the findings for Tie1 in permeability regulation, Tie1 may possibly have an important constitutive role in endothelial survival, despite its apparent redundancy under conditions of Ang-1 stimulated survival, which ultimately necessitates Tie2. There already exists published data demonstrating anti-apoptotic activation of a chimaeric Tie1 receptor and Tie1 activation with COMP-Ang-1, but both of these studies merely affirm the well recognised difficulty of Tie1 activation with native Ang-1 (38, 119). It is interesting then to find a statistically significant drop in Akt activation in Tie1 deficient HUVEC compared to controls following exposure to 200 ng/ml Ang-1 (Figure 6.2), which suggests that even though Tie1 in isolation is unable to mediate detectable caspase reduction under pro-apoptotic conditions, there may be a degree of Tie1 activation present nevertheless. This possibility is supported by the reduced rise in Akt activation seen in stressed Tie2 deficient HUVEC exposed to 200 ng/ml Ang-1, when compared to controls (Figure 6.2). Alternatively, from a signalling point of view, it may be that there only needs to be a very small proportion of functional Tie2 to mediate the downstream anti-apoptotic effects of

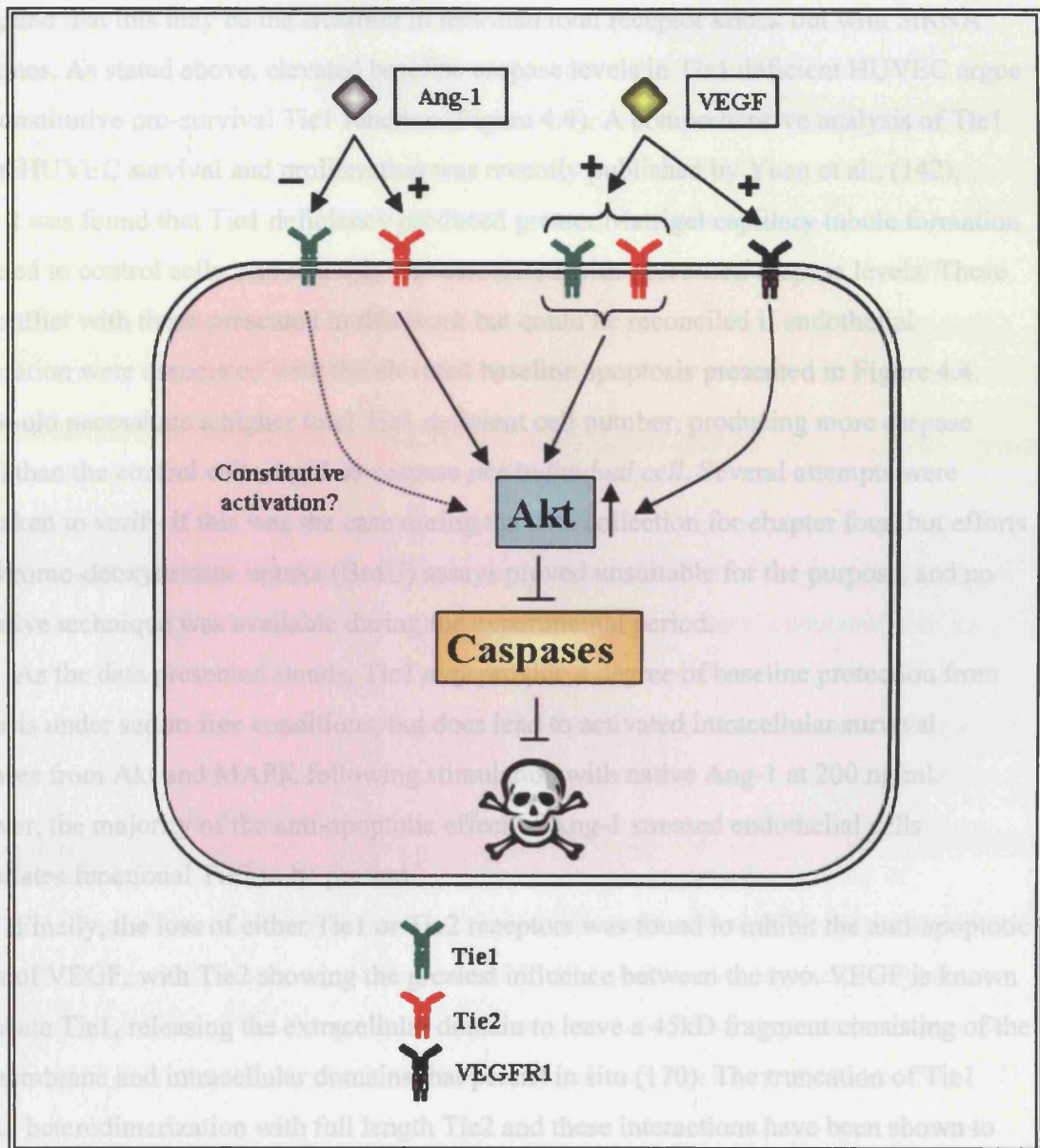


Figure 8.3: Schematic illustration depicting the mechanism of Ang-1 in mediating endothelial cell survival. Tie2 is essential for endothelial survival enhancement in response to Ang-1 stimulation. Tie1 offers no contribution in this regard, although it does appear to generate a low-level pro-survival signal in endothelial cells even when Ang-1 is absent. N.B., this conclusion requires further qualification with experiments verifying an absence of endothelial cell proliferation observed by others in the absence of Tie1. VEGF owes part of its pro-survival response to signalling through both Tie1 and Tie2, in addition to its native VEGFR1 endothelial receptor.

Ang-1, and that this may be the situation in less than total receptor knock out with SiRNA techniques. As stated above, elevated baseline caspase levels in Tie1 deficient HUVEC argue for a constitutive pro-survival Tie1 function (Figure 4.4). A comprehensive analysis of Tie1 roles in HUVEC survival and proliferation was recently published by Yuan et al., (142), where it was found that Tie1 deficiency produced greater Matrigel capillary tubule formation compared to control cells, and that this was associated with *decreased* caspase levels. These data conflict with those presented in this work but could be reconciled if endothelial proliferation were associated with the elevated baseline apoptosis presented in Figure 4.4. This would necessitate a higher total Tie1 deficient cell number, producing more caspase overall than the control cells, but *less caspase per individual cell*. Several attempts were undertaken to verify if this was the case during the data collection for chapter four, but efforts using bromo-deoxyuridine uptake (BrdU) assays proved unsuitable for the purpose, and no alternative technique was available during the experimental period.

As the data presented stands, Tie1 *may* provide a degree of baseline protection from apoptosis under serum free conditions, but does lead to activated intracellular survival responses from Akt and MAPK following stimulation with native Ang-1 at 200 ng/ml. However, the majority of the anti-apoptotic effect of Ang-1 stressed endothelial cells necessitates functional Tie2 to be present.

Finally, the loss of either Tie1 or Tie2 receptors was found to inhibit the anti-apoptotic impact of VEGF, with Tie2 showing the greatest influence between the two. VEGF is known to truncate Tie1, releasing the extracellular domain to leave a 45kD fragment consisting of the transmembrane and intracellular domains that persist in situ (170). The truncation of Tie1 leads to heterodimerization with full length Tie2 and these interactions have been shown to enhance Tie2 activation following Ang-1 stimulation (144, 171). Data implicating Tie receptor involvement in VEGF mediated endothelial survival in the present work complements other work in the same laboratory, investigating the consequences of Tie receptor signalling following VEGF induced Tie1 truncation. It has now been established that Tie1 truncation leads to a novel form of RTK transactivation, leading to the phosphorylation of both full-length Tie2 and truncated Tie1 (Singh et al, submitted to Oncogene February 2008). This serves as a possible explanation for how reduced VEGF mediated survival occurs following the loss of either Tie receptor, as both are likely to be required for the summative downstream effects of Tie1 truncated heterodimeric transactivation.

8.3 Endothelial CAM Expression and Current Sepsis Strategies:

The expression of complementary cell adhesion molecules on endothelial cells and circulating leucocytes is an essential step in leucocyte migration into damaged tissue. Where this occurs as a result of inappropriate endothelial activation in SIRS, the destructive results of activated leucocyte degranulation can lead to significant organ damage (4). Therefore inhibition of CAM expression as a part of endothelial activation is an attractive therapeutic target. Several reports now exist for a role for angiopoietin/ Tie signalling in a variety of activated endothelial responses, both *in vivo* and *in vitro*. Focussed molecular studies demonstrating reduced CAM mRNA synthesis following Ang-1 treatment of activated HUVEC (132, 133), are echoed in Witzembichler's *in vivo* sepsis model demonstrating a reduction in inflammatory CAM expression in the presence of adenovirally expressed Ang-1 in pulmonary endothelial tissue (46). Furthermore, Fiedler et al. recently demonstrated an essential role for the Tie receptor antagonist Ang-2 in firm endothelial-leucocyte adhesion in another *in vivo* sepsis model, through Ang-2 mediated endothelial sensitization to circulating TNF α (41). Moreover, there are now numerous reports emerging that reinforce the broader role of Angiopoietins in SIRS / sepsis. Clinical observational work by Ganter and Guiliano has shown that serum Ang-2 concentration positively correlates with the severity of inflammatory processes in humans, whereas Ang-1 levels have an inversely proportional relationship to this outcome measure (167, 168, 172) (Karmaliotitis). This has prompted several studies using tools such as gene therapy to successfully effect improvements in acute lung injury (ALI) through the systemic administration of Ang-1 or its synthetic relatives (173-177).

Working towards angiopoietin therapy in humans, data in chapter five documents the production of a simple assay for endothelial CAM expression such that the anti-inflammatory effects of Ang-1 can be further investigated under defined inflammatory stimuli. Chapter seven took this work a step further, providing provisional data for the usage of such an assay in experiments on the anti-inflammatory properties of Ang-1 in the presence of human SIRS plasma.

To begin, inducible CAM expression was initially detected in cultured endothelial cells by immunohistochemistry, followed by CAM quantitation using a simple, reliable and high-throughput cell-ELISA system developed specifically for this project. Using the cell-ELISA assay, initial results using the immortalised endothelial cell lines HMEC-98 and EA.hy926 demonstrated the loss of phenotypic characteristics that immortalised cell lines can

develop, with both excessive constitutive ICAM-1 expression in the former cell type and a lack of any Il-1 induced VCAM-1 and E-Selectin expression in the latter. Therefore all further work was undertaken on HUVEC, which consistently proved to be a reliable and sensitive system for studying inflammatory CAM responses. Whilst Ang-1 was unable to reduce CAM expression in the presence of VEGF, it was found to be effective in suppressing the up-regulation of both VCAM-1 and E-Selectin in the presence of 0.03 and 0.05 ng/ml Il-1. Moreover, using increasing quantities of Ang-1 led to progressive inhibition of IL-1 induced VCAM-1, reaching a 50% reduction at 800 ng/ml. E-selectin was also inhibited by increasing concentrations of Ang-1, but without the clear dose-dependent relationship seen with VCAM-1. Taking this a step closer to the *in vivo* setting, data in chapter 7 showed that plasma from a patient suffering SIRS related pathology was able to induce CAM up-regulation using the cell-ELISA method in HUVEC. Moreover, the inhibitory impact of increasing Ang-1 on VCAM-1 expression in HUVEC exposed to SIRS plasma remained, and was associated with similar suppression of ICAM-1. It must be stressed however, that these data derive from a single experiment using a single patient suffering SIRS. Therefore, whilst a potential positive benefit of Ang-1 in a human model of CAM expression is extremely attractive, it would need corroboration through a much larger series of patients with comparisons drawn with an appropriate control population.

Finally, attempts to define a specific role for Tie1 and Tie2 in Ang-1-reduced CAM responses were hampered by intractable transfection difficulties towards the end of the experimental series. Therefore several repeat observations on CAM inhibition by Ang-1 in properly Tie1 and Tie2 deficient HUVEC will need to be made before it will be possible to prove or refute the assumed role of Tie2 in mediating these responses in endothelial cells (132).

Putting the results of the present study's findings in context with published data on Angiopoietin signalling in sepsis, Ang-1 CAM reduction in the face of Il-1 and TNF α has been reproduced, and a potentially valuable model for evaluating the clinical efficacy of Ang-1 using human SIRS plasma has been described. To continue these experiments further, the impact of Ang-2 on CAM expression and relative roles of each Tie receptor would be of great interest.

Appendix 1:

Meeting Presentations - Scientific

The vascular endothelium – A prime target
for treating burn induced inflammatory dysfunction.

C S Milner and N P J Brindle

ANZBA 2007

Perth, Australia

September 2007

Role of Tie2 in suppression of endothelial
permeability by Angiopoietin-1

C S Milner, H Singh, T A Tahir and N P J Brindle

8th World Microcirculation Congress

Milwaukee, USA

August 2007

Treating the burn induced systemic inflammatory
Response syndrome, Angiopoietin-1 and the
Vascular endothelium.

C S Milner and N P J Brindle

Summer BAPRAS, Deauville, France

July 2007

Cell Culture in Burns Research:

Counting the Cost of Immortalisation

C S Milner N P J Brindle

BAPRAS Winter Meeting

The Royal College of Surgeons of England

December 2006

Tie Receptors and the Vascular Endothelium:

New Solutions to Old Problems

C S Milner

Douglas Murray Prize National Meeting, Birmingham

October 2006

Meeting Presentations – Academic and Fundraising

Round table presentation to Healing Foundation November 2005

Private donor

Healing Foundation, RCS, London

Research presentation to Board of Trustees January 2006

Healing Foundation, RCS, London

Presentation to Freemasons on RCS regional visit March 2006

Freemasons Lodge, Hereford

Presentation of research findings to Sir John Dellow June 2006

Attended by Professor G McGrouther

£5000 awarded towards my research

Healing Foundation, RCS, London

Organisation of NEXT Plc / Healing Foundation August 2006

site visit and presentation of current research

Department of Plastic Surgery,

Leicester Royal Infirmary

Papers:

Roles of the receptor tyrosine kinases Tie1 and Tie2 in mediating the effects of Angiopoietin-1 on endothelial permeability and apoptosis. C S Milner, T M Hansen, H Singh, N P J Brindle. Accepted for publication by Microvascular Research, September 2008.

VEGF activates the Tie family of receptor tyrosine kinases. H Singh, C S Milner, N Patel, N P J Brindle. Submitted to FEBS letters 2008.

Participant Information Sheet	01 Aug
Participant Consent Form	01 Aug
Participant Consent Form Assent	01 Aug
Response to Request for Further Information	10 Aug

Leicestershire, Northamptonshire & Rutland Research Ethics Committee 1

1 Standard Court
Park Row
Nottingham
NG1 6GN

Telephone: 01159123344 Ext: 68575
Facsimile: 01159123300

10 August 2007

Mr Chris Stephen Milner
Healing Foundation Clinical Research Fellow, Cardiovascular Sciences
University of Leicester
Department of Cardiovascular Sciences, Vascular Surgery Group
Robert Kilpatrick Clinical Sciences Building
Leicester Royal Infirmary
LE2 7LX

Dear Mr Milner,

Full title of study: Endothelial inflammation in Systemic Inflammatory Response Syndrome; the role of the Tie / Angiopoietin system

REC reference number: 07/H0406/150

Thank you for your letter of 09 August 2007, responding to the Committee's request for further information on the above research and submitting revised documentation.

The further information has been considered on behalf of the Committee by the Chair.

Confirmation of ethical opinion

On behalf of the Committee, I am pleased to confirm a favourable ethical opinion for the above research on the basis described in the application form, protocol and supporting documentation as revised.

Ethical review of research sites

The favourable opinion applies to the research sites listed on the attached form.

Conditions of approval

The favourable opinion is given provided that you comply with the conditions set out in the attached document. You are advised to study the conditions carefully.

Approved documents

The final list of documents reviewed and approved by the Committee is as follows:

Document	Version	Date
Application		04 July 2007
Investigator CV		01 August 2006
Protocol	1	07 May 2007
Peer Review		12 May 2007

Participant Information Sheet	2	09 August 2007
Participant Information Sheet: Relatives	2	09 August 2007
Participant Consent Form	2	09 August 2007
Participant Consent Form: Assent	2	09 August 2007
Response to Request for Further Information		09 August 2007

R&D approval

All researchers and research collaborators who will be participating in the research at NHS sites should apply for R&D approval from the relevant care organisation, if they have not yet done so. R&D approval is required, whether or not the study is exempt from SSA. You should advise researchers and local collaborators accordingly.

Guidance on applying for R&D approval is available from <http://www.riform.nhs.uk/riform.htm>.

Statement of compliance

The Committee is constituted in accordance with the Governance Arrangements for Research Ethics Committees (July 2001) and complies fully with the Standard Operating Procedures for Research Ethics Committees in the UK.

Feedback on the application process

Now that you have completed the application process you are invited to give your view of the service you received from the National Research Ethics Service. If you wish to make your views known please use the feedback form available on the NRES website at:

<https://www.nresform.org.uk/AppForm/Modules/Feedback/EthicalReview.aspx>

We value your views and comments and will use them to inform the operational process and further improve our service.

07/H0406/150

Please quote this number on all correspondence

With the Committee's best wishes for the success of this project

Yours sincerely

Dr C Edwards/Ms L Ellis
Chair/Co-ordinator

Email: Linda.ellis@nottinghamshirecounty-tpct.nhs.uk

Enclosures: Standard approval conditions
Site approval form

Copy to: R&D office for NHS care organisation at lead site - University Hospitals Leicester NHS Trust

Leicestershire, Northamptonshire & Rutland Research Ethics Committee 1

LIST OF SITES WITH A FAVOURABLE ETHICAL OPINION

For all studies requiring site-specific assessment, this form is issued by the main REC to the Chief Investigator and sponsor with the favourable opinion letter and following subsequent notifications from site assessors. For issue 2 onwards, all sites with a favourable opinion are listed, adding the new sites approved.

REC reference number:	07/H0406/150	Issue number:	0	Date of issue:	10 August 2007
Chief Investigator:	Mr Chris Stephen Milner				
Full title of study:	Endothelial inflammation in Systemic Inflammatory Response Syndrome; the role of the Tie / Angiotensin system				
<p><i>This study was given a favourable ethical opinion by Leicestershire, Northamptonshire & Rutland Research Ethics Committee 1 on 08 August 2007. The favourable opinion is extended to each of the sites listed below. The research may commence at each NHS site when management approval from the relevant NHS care organisation has been confirmed.</i></p>					
<i>Principal Investigator</i>	<i>Post</i>	<i>Research site</i>	<i>Site assessor</i>	<i>Date of favourable opinion for this site</i>	<i>Notes ⁽¹⁾</i>
Mr Chris Stephen Milner	Healing Foundation Clinical Research Fellow, Cardiovascular Sciences	Leicester Royal Infirmary	Leicestershire, Northamptonshire & Rutland Research Ethics Committee 1	10/08/2007	
<p>Approved by the Chair on behalf of the REC:</p> <p>..... (Signature of Chair/Co-ordinator) (Delete as applicable)</p> <p>..... (Name)</p>					

(1) *The notes column may be used by the main REC to record the early closure or withdrawal of a site (where notified by the Chief Investigator or sponsor), the suspension or termination of the favourable opinion for an individual site, or any other relevant development. The date should be recorded.*

References:

1. Rankin, J.A., *Biological mediators of acute inflammation*. AACN Clinical Issues, 2004. **15**(1): p. 3-17.
2. Bone, R.C., *Sir Isaac Newton, sepsis, SIRS, and CARS*. Critical Care Medicine, 1996. **24**(7): p. 1125-8.
3. Munford, R.S. and J. Pugin, *Normal responses to injury prevent systemic inflammation and can be immunosuppressive*. American Journal of Respiratory & Critical Care Medicine, 2001. **163**(2): p. 316-21.
4. Matsuda, N. and Y. Hattori, *Systemic inflammatory response syndrome (SIRS): molecular pathophysiology and gene therapy*. Journal of Pharmacological Sciences, 2006. **101**(3): p. 189-98.
5. Rangel-Frausto, M.S., et al., *The natural history of the systemic inflammatory response syndrome (SIRS). A prospective study. [see comment]*. JAMA, 1995. **273**(2): p. 117-23.
6. Riedemann, N.C., R.-F. Guo, and P.A. Ward, *Novel strategies for the treatment of sepsis*. Nature Medicine, 2003. **9**(5): p. 517-24.
7. Brun-Buisson, C., et al., *Incidence, risk factors, and outcome of severe sepsis and septic shock in adults. A multicenter prospective study in intensive care units. French ICU Group for Severe Sepsis*. JAMA, 1995. **274**(12): p. 968-74.
8. Sheridan, R.L., et al., *Death in the burn unit: sterile multiple organ failure*. Burns, 1998. **24**(4): p. 307-11.
9. McCloskey, R.V., et al., *Treatment of septic shock with human monoclonal antibody HA-1A. A randomized, double-blind, placebo-controlled trial. CHESS Trial Study Group. [see comment]*. Annals of Internal Medicine, 1994. **121**(1): p. 1-5.
10. Smail, N., et al., *Role of systemic inflammatory response syndrome and infection in the occurrence of early multiple organ dysfunction syndrome following severe trauma*. Intensive Care Medicine, 1995. **21**(10): p. 813-6.
11. Baker, P.J. and S.G. Osofsky, *Activation of human complement by heat-killed, human kidney cells grown in cell culture*. Journal of Immunology, 1980. **124**(1): p. 81-6.
12. Gelfand, J.A., M. Donelan, and J.F. Burke, *Preferential activation and depletion of the alternative complement pathway by burn injury*. Annals of Surgery, 1983. **198**(1): p. 58-62.

13. Zilow, G., et al., *Complement activation and the prognostic value of C3a in patients at risk of adult respiratory distress syndrome*. *Clinical & Experimental Immunology*, 1990. **79**(2): p. 151-7.
14. Marshall, J.C., *Inflammation, coagulopathy, and the pathogenesis of multiple organ dysfunction syndrome*. *Critical Care Medicine*, 2001. **29**(7 Suppl): p. S99-106.
15. De Maio, A., M.B. Torres, and R.H. Reeves, *Genetic determinants influencing the response to injury, inflammation, and sepsis*. *Shock*, 2005. **23**(1): p. 11-7.
16. Aird, W.C., *The role of the endothelium in severe sepsis and multiple organ dysfunction syndrome*. *Blood*, 2003. **101**(10): p. 3765-77.
17. Bernard, G.R., et al., *Efficacy and safety of recombinant human activated protein C for severe sepsis.[see comment]*. *New England Journal of Medicine*, 2001. **344**(10): p. 699-709.
18. Fisher, C.J., Jr., et al., *Recombinant human interleukin 1 receptor antagonist in the treatment of patients with sepsis syndrome. Results from a randomized, double-blind, placebo-controlled trial. Phase III rhIL-1ra Sepsis Syndrome Study Group.[see comment]*. *JAMA*, 1994. **271**(23): p. 1836-43.
19. Reinhart, K. and W. Karzai, *Anti-tumor necrosis factor therapy in sepsis: update on clinical trials and lessons learned*. *Critical Care Medicine*, 2001. **29**(7 Suppl): p. S121-5.
20. Mantovani, A., S. Sozzani, and M. Introna, *Endothelial activation by cytokines*. *Annals of the New York Academy of Sciences*, 1997. **832**: p. 93-116.
21. Stevens, T., et al., *NHLBI workshop report: endothelial cell phenotypes in heart, lung, and blood diseases*. *American Journal of Physiology - Cell Physiology*, 2001. **281**(5): p. C1422-33.
22. Badger, A.M., et al., *Pharmacological profile of SB 203580, a selective inhibitor of cytokine suppressive binding protein/p38 kinase, in animal models of arthritis, bone resorption, endotoxin shock and immune function*. *Journal of Pharmacology & Experimental Therapeutics*, 1996. **279**(3): p. 1453-61.
23. Branger, J., et al., *Anti-inflammatory effects of a p38 mitogen-activated protein kinase inhibitor during human endotoxemia*. *Journal of Immunology*, 2002. **168**(8): p. 4070-7.
24. Liu, S.F., X. Ye, and A.B. Malik, *Inhibition of NF-kappaB activation by pyrrolidine dithiocarbamate prevents In vivo expression of proinflammatory genes*. *Circulation*, 1999. **100**(12): p. 1330-7.

25. Rahman, A., K.N. Anwar, and A.B. Malik, *Protein kinase C-zeta mediates TNF-alpha-induced ICAM-1 gene transcription in endothelial cells*. *American Journal of Physiology - Cell Physiology*, 2000. **279**(4): p. C906-14.
26. Rahman, A., et al., *Protein kinase C-delta regulates thrombin-induced ICAM-1 gene expression in endothelial cells via activation of p38 mitogen-activated protein kinase*. *Molecular & Cellular Biology*, 2001. **21**(16): p. 5554-65.
27. Szabo, C., G.J. Southan, and C. Thiemermann, *Beneficial effects and improved survival in rodent models of septic shock with S-methylisothiourrea sulfate, a potent and selective inhibitor of inducible nitric oxide synthase*. *Proceedings of the National Academy of Sciences of the United States of America*, 1994. **91**(26): p. 12472-6.
28. Dumont, D.J., et al., *tek, a novel tyrosine kinase gene located on mouse chromosome 4, is expressed in endothelial cells and their presumptive precursors*. *Oncogene*, 1992. **7**(8): p. 1471-80.
29. Maisonpierre, P.C., et al., *Distinct rat genes with related profiles of expression define a TIE receptor tyrosine kinase family*. *Oncogene*, 1993. **8**(6): p. 1631-7.
30. Partanen, J., et al., *A novel endothelial cell surface receptor tyrosine kinase with extracellular epidermal growth factor homology domains*. *Molecular & Cellular Biology*, 1992. **12**(4): p. 1698-707.
31. Davis, S., et al., *Isolation of angiopoietin-1, a ligand for the TIE2 receptor, by secretion-trap expression cloning.[see comment]*. *Cell*, 1996. **87**(7): p. 1161-9.
32. Maisonpierre, P.C., et al., *Angiopoietin-2, a natural antagonist for Tie2 that disrupts in vivo angiogenesis.[see comment]*. *Science*, 1997. **277**(5322): p. 55-60.
33. Suri, C., et al., *Requisite role of angiopoietin-1, a ligand for the TIE2 receptor, during embryonic angiogenesis.[see comment]*. *Cell*, 1996. **87**(7): p. 1171-80.
34. Barton, W.A., et al., *Crystal structures of the Tie2 receptor ectodomain and the angiopoietin-2-Tie2 complex*. *Nature Structural & Molecular Biology*, 2006. **13**(6): p. 524-32.
35. Sato, T.N., et al., *Distinct roles of the receptor tyrosine kinases Tie-1 and Tie-2 in blood vessel formation*. *Nature*, 1995. **376**(6535): p. 70-4.
36. Korhonen, J., et al., *The mouse tie receptor tyrosine kinase gene: expression during embryonic angiogenesis.[erratum appears in Oncogene 1996 Feb 15;12(4):943]*. *Oncogene*, 1994. **9**(2): p. 395-403.

37. Cho, C.-H., et al., *COMP-Ang1: a designed angiopoietin-1 variant with nonleaky angiogenic activity*. Proceedings of the National Academy of Sciences of the United States of America, 2004. **101**(15): p. 5547-52.
38. Saharinen, P., et al., *Multiple angiopoietin recombinant proteins activate the Tie1 receptor tyrosine kinase and promote its interaction with Tie2*. Journal of Cell Biology, 2005. **169**(2): p. 239-43.
39. Jones, N., et al., *Tie receptors: new modulators of angiogenic and lymphangiogenic responses*. Nature Reviews Molecular Cell Biology, 2001. **2**(4): p. 257-67.
40. Oshima, Y., et al., *Different effects of angiopoietin-2 in different vascular beds: new vessels are most sensitive*. FASEB Journal, 2005. **19**(8): p. 963-5.
41. Fiedler, U., et al., *Angiopoietin-2 sensitizes endothelial cells to TNF-alpha and has a crucial role in the induction of inflammation. [see comment]*. Nature Medicine, 2006. **12**(2): p. 235-9.
42. Gale, N.W., et al., *Angiopoietin-2 is required for postnatal angiogenesis and lymphatic patterning, and only the latter role is rescued by Angiopoietin-1. [see comment]*. Developmental Cell, 2002. **3**(3): p. 411-23.
43. Partanen, J., et al., *Cell autonomous functions of the receptor tyrosine kinase TIE in a late phase of angiogenic capillary growth and endothelial cell survival during murine development*. Development, 1996. **122**(10): p. 3013-21.
44. Puri, M.C., et al., *The receptor tyrosine kinase TIE is required for integrity and survival of vascular endothelial cells*. EMBO Journal, 1995. **14**(23): p. 5884-91.
45. Hanahan, D., *Signaling vascular morphogenesis and maintenance. [comment]*. Science, 1997. **277**(5322): p. 48-50.
46. Witzenbichler, B., et al., *Protective role of angiopoietin-1 in endotoxic shock. [see comment]*. Circulation, 2005. **111**(1): p. 97-105.
47. Kim, I., et al., *Angiopoietin-1 regulates endothelial cell survival through the phosphatidylinositol 3'-Kinase/Akt signal transduction pathway. [see comment]*. Circulation Research, 2000. **86**(1): p. 24-9.
48. Gamble, J.R., et al., *Angiopoietin-1 is an antipermeability and anti-inflammatory agent in vitro and targets cell junctions*. Circulation Research, 2000. **87**(7): p. 603-7.
49. Risau, W., *Mechanisms of angiogenesis*. Nature, 1997. **386**(6626): p. 671-4.
50. Betsholtz, C. and A. Armulik, *Homeostatic functions of vascular endothelial growth factor in adult microvasculature. [comment]*. American Journal of Physiology - Heart & Circulatory Physiology, 2006. **290**(2): p. H509-11.

51. Kim, W., et al., *Adrenomedullin reduces VEGF-induced endothelial adhesion molecules and adhesiveness through a phosphatidylinositol 3'-kinase pathway*. *Arteriosclerosis, Thrombosis & Vascular Biology*, 2003. **23**(8): p. 1377-83.
52. Esser, S., et al., *Vascular endothelial growth factor induces VE-cadherin tyrosine phosphorylation in endothelial cells*. *Journal of Cell Science*, 1998. **111**(Pt 13): p. 1853-65.
53. Gavard, J. and J.S. Gutkind, *VEGF controls endothelial-cell permeability by promoting the beta-arrestin-dependent endocytosis of VE-cadherin*. *Nature Cell Biology*, 2006. **8**(11): p. 1223-34.
54. Wang, Y., et al., *Opposing effect of angiopoietin-1 on VEGF-mediated disruption of endothelial cell-cell interactions requires activation of PKC beta*. *Journal of Cellular Physiology*, 2004. **198**(1): p. 53-61.
55. Hayes, A.J., et al., *Angiopoietin-1 and its receptor Tie-2 participate in the regulation of capillary-like tubule formation and survival of endothelial cells*. *Microvascular Research*, 1999. **58**(3): p. 224-37.
56. Koblizek, T.I., et al., *Angiopoietin-1 induces sprouting angiogenesis in vitro*. *Current Biology*, 1998. **8**(9): p. 529-32.
57. Kanda, S., et al., *Angiopoietin 1 is mitogenic for cultured endothelial cells*. *Cancer Research*, 2005. **65**(15): p. 6820-7.
58. Cho, C.-H., et al., *COMP-angiopoietin-1 promotes wound healing through enhanced angiogenesis, lymphangiogenesis, and blood flow in a diabetic mouse model. [erratum appears in Proc Natl Acad Sci U S A. 2006 Jun 27;103(26):10146]*. *Proceedings of the National Academy of Sciences of the United States of America*, 2006. **103**(13): p. 4946-51.
59. Mehta, D. and A.B. Malik, *Signaling mechanisms regulating endothelial permeability*. *Physiological Reviews*, 2006. **86**(1): p. 279-367.
60. Majno, G. and G.E. Palade, *Studies on inflammation. 1. The effect of histamine and serotonin on vascular permeability: an electron microscopic study*. *Journal of Biophysical & Biochemical Cytology*, 1961. **11**: p. 571-605.
61. McDonald, D.M., G. Thurston, and P. Baluk, *Endothelial gaps as sites for plasma leakage in inflammation*. *Microcirculation*, 1999. **6**(1): p. 7-22.
62. Thurston, G., et al., *Angiopoietin-1 protects the adult vasculature against plasma leakage*. *Nature Medicine*, 2000. **6**(4): p. 460-3.

63. Wu, N.Z. and A.L. Baldwin, *Transient venular permeability increase and endothelial gap formation induced by histamine*. American Journal of Physiology, 1992. **262**(4 Pt 2): p. H1238-47.
64. Leach, R.M. and D.F. Treacher, *The pulmonary physician in critical care * 2: oxygen delivery and consumption in the critically ill*. Thorax, 2002. **57**(2): p. 170-7.
65. van Nieuw Amerongen, G.P. and V.W.M. van Hinsbergh, *Targets for pharmacological intervention of endothelial hyperpermeability and barrier function*. Vascular Pharmacology, 2002. **39**(4-5): p. 257-72.
66. Bazzoni, G. and E. Dejana, *Endothelial cell-to-cell junctions: molecular organization and role in vascular homeostasis*. Physiological Reviews, 2004. **84**(3): p. 869-901.
67. Simionescu, M., N. Simionescu, and G.E. Palade, *Segmental differentiations of cell junctions in the vascular endothelium. The microvasculature*. Journal of Cell Biology, 1975. **67**(3): p. 863-85.
68. Vincent, P.A., et al., *VE-cadherin: adhesion at arm's length*. American Journal of Physiology - Cell Physiology, 2004. **286**(5): p. C987-97.
69. Moy, A.B., et al., *Histamine and thrombin modulate endothelial focal adhesion through centripetal and centrifugal forces*. Journal of Clinical Investigation, 1996. **97**(4): p. 1020-7.
70. Navarro, P., et al., *Catenin-dependent and -independent functions of vascular endothelial cadherin*. Journal of Biological Chemistry, 1995. **270**(52): p. 30965-72.
71. Sheldon, R., et al., *Role of myosin light-chain phosphorylation in endothelial cell retraction*. American Journal of Physiology, 1993. **265**(6 Pt 1): p. L606-12.
72. Lampugnani, M.G., et al., *Cell confluence regulates tyrosine phosphorylation of adherens junction components in endothelial cells*. Journal of Cell Science, 1997. **110**(Pt 17): p. 2065-77.
73. Nawroth, R., et al., *VE-PTP and VE-cadherin ectodomains interact to facilitate regulation of phosphorylation and cell contacts. [erratum appears in EMBO J. 2005 Sep 7;24(17):3158]*. EMBO Journal, 2002. **21**(18): p. 4885-95.
74. Iyer, S., et al., *VE-cadherin-p120 interaction is required for maintenance of endothelial barrier function*. American Journal of Physiology - Lung Cellular & Molecular Physiology, 2004. **286**(6): p. L1143-53.
75. Adamson, R.H., et al., *PAF- and bradykinin-induced hyperpermeability of rat venules is independent of actin-myosin contraction*. American Journal of Physiology - Heart & Circulatory Physiology, 2003. **285**(1): p. H406-17.

76. Winter, M.C., et al., *Histamine selectively interrupts VE-cadherin adhesion independently of capacitive calcium entry*. American Journal of Physiology - Lung Cellular & Molecular Physiology, 2004. **287**(4): p. L816-23.
77. Aramoto, H., et al., *Vascular endothelial growth factor stimulates differential signaling pathways in in vivo microcirculation*. American Journal of Physiology - Heart & Circulatory Physiology, 2004. **287**(4): p. H1590-8.
78. Garcia, J.G., H.W. Davis, and C.E. Patterson, *Regulation of endothelial cell gap formation and barrier dysfunction: role of myosin light chain phosphorylation*. Journal of Cellular Physiology, 1995. **163**(3): p. 510-22.
79. Ferro, T., et al., *Protein kinase C- α mediates endothelial barrier dysfunction induced by TNF- α* . American Journal of Physiology - Lung Cellular & Molecular Physiology, 2000. **278**(6): p. L1107-17.
80. Konstantoulaki, M., P. Kouklis, and A.B. Malik, *Protein kinase C modifications of VE-cadherin, p120, and beta-catenin contribute to endothelial barrier dysregulation induced by thrombin*. American Journal of Physiology - Lung Cellular & Molecular Physiology, 2003. **285**(2): p. L434-42.
81. Sandoval, R., et al., *Ca²⁺ signalling and PKC α activate increased endothelial permeability by disassembly of VE-cadherin junctions*. Journal of Physiology, 2001. **533**(Pt 2): p. 433-45.
82. Weis, S., et al., *Src blockade stabilizes a Flk/cadherin complex, reducing edema and tissue injury following myocardial infarction*. Journal of Clinical Investigation, 2004. **113**(6): p. 885-94.
83. Sandoval, R., et al., *Requirement for Ca²⁺ signaling in the mechanism of thrombin-induced increase in endothelial permeability*. American Journal of Physiology - Lung Cellular & Molecular Physiology, 2001. **280**(2): p. L239-47.
84. Kimura, K., et al., *Regulation of myosin phosphatase by Rho and Rho-associated kinase (Rho-kinase)[see comment]*. Science, 1996. **273**(5272): p. 245-8.
85. Amano, M., et al., *Formation of actin stress fibers and focal adhesions enhanced by Rho-kinase*. Science, 1997. **275**(5304): p. 1308-11.
86. Narumiya, S., T. Ishizaki, and N. Watanabe, *Rho effectors and reorganization of actin cytoskeleton*. FEBS Letters, 1997. **410**(1): p. 68-72.
87. Tinsley, J.H., et al., *Src-dependent, neutrophil-mediated vascular hyperpermeability and beta-catenin modification*. American Journal of Physiology - Cell Physiology, 2002. **283**(6): p. C1745-51.

88. Tinsley, J.H., et al., *Activated neutrophils induce hyperpermeability and phosphorylation of adherens junction proteins in coronary venular endothelial cells.* Journal of Biological Chemistry, 1999. **274**(35): p. 24930-4.
89. Thurston, G., et al., *Leakage-resistant blood vessels in mice transgenically overexpressing angiopoietin-1.* Science, 1999. **286**(5449): p. 2511-4.
90. Pizurki, L., et al., *Angiopoietin-1 inhibits endothelial permeability, neutrophil adherence and IL-8 production.* British Journal of Pharmacology, 2003. **139**(2): p. 329-36.
91. Baffert, F., et al., *Angiopoietin-1 decreases plasma leakage by reducing number and size of endothelial gaps in venules.[see comment].* American Journal of Physiology - Heart & Circulatory Physiology, 2006. **290**(1): p. H107-18.
92. Jho, D., et al., *Angiopoietin-1 opposes VEGF-induced increase in endothelial permeability by inhibiting TRPC1-dependent Ca² influx.* Circulation Research, 2005. **96**(12): p. 1282-90.
93. Li, X., et al., *Role of protein kinase C ζ in thrombin-induced endothelial permeability changes: inhibition by angiopoietin-1.* Blood, 2004. **104**(6): p. 1716-24.
94. Baumer, S., et al., *Vascular endothelial cell-specific phosphotyrosine phosphatase (VE-PTP) activity is required for blood vessel development.* Blood, 2006. **107**(12): p. 4754-62.
95. Fachinger, G., U. Deutsch, and W. Risau, *Functional interaction of vascular endothelial-protein-tyrosine phosphatase with the angiopoietin receptor Tie-2.* Oncogene, 1999. **18**(43): p. 5948-53.
96. Mammoto, T., et al., *Angiopoietin-1 requires p190 RhoGAP to protect against vascular leakage in vivo.* Journal of Biological Chemistry, 2007. **282**(33): p. 23910-8.
97. Orfanos, S.E., et al., *Angiopoietin-2 is increased in severe sepsis: correlation with inflammatory mediators.* Critical Care Medicine, 2007. **35**(1): p. 199-206.
98. Parikh, S.M., et al., *Excess circulating angiopoietin-2 may contribute to pulmonary vascular leak in sepsis in humans.* PLoS Medicine / Public Library of Science, 2006. **3**(3): p. e46.
99. Bhandari, V., et al., *Hyperoxia causes angiopoietin 2-mediated acute lung injury and necrotic cell death.* Nature Medicine, 2006. **12**(11): p. 1286-93.
100. Nag, S., et al., *Increased angiopoietin2 expression is associated with endothelial apoptosis and blood-brain barrier breakdown.* Laboratory Investigation, 2005. **85**(10): p. 1189-98.

101. Roviezzo, F., et al., *Angiopoietin-2 causes inflammation in vivo by promoting vascular leakage*. *Journal of Pharmacology & Experimental Therapeutics*, 2005. **314**(2): p. 738-44.
102. Weber, C.C., et al., *Effects of protein and gene transfer of the angiopoietin-1 fibrinogen-like receptor-binding domain on endothelial and vessel organization*. *Journal of Biological Chemistry*, 2005. **280**(23): p. 22445-53.
103. von Tell, D., A. Armulik, and C. Betsholtz, *Pericytes and vascular stability*. *Experimental Cell Research*, 2006. **312**(5): p. 623-9.
104. Baffert, F., et al., *Cellular changes in normal blood capillaries undergoing regression after inhibition of VEGF signaling. [see comment]*. *American Journal of Physiology - Heart & Circulatory Physiology*, 2006. **290**(2): p. H547-59.
105. Dimmeler, S. and A.M. Zeiher, *Endothelial cell apoptosis in angiogenesis and vessel regression*. *Circulation Research*, 2000. **87**(6): p. 434-9.
106. Michel, J.B., *Anoikis in the cardiovascular system: known and unknown extracellular mediators*. *Arteriosclerosis, Thrombosis & Vascular Biology*, 2003. **23**(12): p. 2146-54.
107. Haunstetter, A. and S. Izumo, *Apoptosis: basic mechanisms and implications for cardiovascular disease*. *Circulation Research*, 1998. **82**(11): p. 1111-29.
108. Durand, E., et al., *In vivo induction of endothelial apoptosis leads to vessel thrombosis and endothelial denudation: a clue to the understanding of the mechanisms of thrombotic plaque erosion*. *Circulation*, 2004. **109**(21): p. 2503-6.
109. Bannerman, D.D. and S.E. Goldblum, *Mechanisms of bacterial lipopolysaccharide-induced endothelial apoptosis*. *American Journal of Physiology - Lung Cellular & Molecular Physiology*, 2003. **284**(6): p. L899-914.
110. Riedl, S.J. and Y. Shi, *Molecular mechanisms of caspase regulation during apoptosis*. *Nature Reviews Molecular Cell Biology*, 2004. **5**(11): p. 897-907.
111. Boatright, K.M. and G.S. Salvesen, *Mechanisms of caspase activation*. *Current Opinion in Cell Biology*, 2003. **15**(6): p. 725-31.
112. Wang, Z.B., Y.Q. Liu, and Y.F. Cui, *Pathways to caspase activation*. *Cell Biology International*, 2005. **29**(7): p. 489-96.
113. Gerber, H.P., et al., *Vascular endothelial growth factor regulates endothelial cell survival through the phosphatidylinositol 3'-kinase/Akt signal transduction pathway. Requirement for Flk-1/KDR activation*. *Journal of Biological Chemistry*, 1998. **273**(46): p. 30336-43.

114. Kontos, C.D., et al., *Tyrosine 1101 of Tie2 is the major site of association of p85 and is required for activation of phosphatidylinositol 3-kinase and Akt*. *Molecular & Cellular Biology*, 1998. **18**(7): p. 4131-40.
115. Daly, C., et al., *Angiopoietin-1 modulates endothelial cell function and gene expression via the transcription factor FKHR (FOXO1)*. *Genes & Development*, 2004. **18**(9): p. 1060-71.
116. Dimmeler, S., et al., *Suppression of apoptosis by nitric oxide via inhibition of interleukin-1beta-converting enzyme (ICE)-like and cysteine protease protein (CPP)-32-like proteases*. *Journal of Experimental Medicine*, 1997. **185**(4): p. 601-7.
117. Papapetropoulos, A., et al., *Angiopoietin-1 inhibits endothelial cell apoptosis via the Akt/survivin pathway*. *Journal of Biological Chemistry*, 2000. **275**(13): p. 9102-5.
118. O'Connor, D.S., et al., *Control of apoptosis during angiogenesis by survivin expression in endothelial cells*. *American Journal of Pathology*, 2000. **156**(2): p. 393-8.
119. Kontos, C.D., et al., *The endothelial receptor tyrosine kinase Tie1 activates phosphatidylinositol 3-kinase and Akt to inhibit apoptosis*. *Molecular & Cellular Biology*, 2002. **22**(6): p. 1704-13.
120. Etzioni, A., C.M. Doerschuk, and J.M. Harlan, *Of man and mouse: leukocyte and endothelial adhesion molecule deficiencies*. *Blood*, 1999. **94**(10): p. 3281-8.
121. Kakkar, A.K. and D.J. Lefer, *Leukocyte and endothelial adhesion molecule studies in knockout mice*. *Current Opinion in Pharmacology*, 2004. **4**(2): p. 154-8.
122. Schall, T.J. and K.B. Bacon, *Chemokines, leukocyte trafficking, and inflammation*. *Current Opinion in Immunology*, 1994. **6**(6): p. 865-73.
123. Vaporciyan, A.A., et al., *Involvement of platelet-endothelial cell adhesion molecule-1 in neutrophil recruitment in vivo*. *Science*, 1993. **262**(5139): p. 1580-2.
124. Cernuda-Morollon, E. and A.J. Ridley, *Rho GTPases and leukocyte adhesion receptor expression and function in endothelial cells*. *Circulation Research*, 2006. **98**(6): p. 757-67.
125. Millan, J. and A.J. Ridley, *Rho GTPases and leucocyte-induced endothelial remodelling*. *Biochemical Journal*, 2005. **385**(Pt 2): p. 329-37.
126. Hordijk, P.L., *Endothelial signalling events during leukocyte transmigration*. *FEBS Journal*, 2006. **273**(19): p. 4408-15.
127. Varani, J., et al., *Human umbilical vein endothelial cell killing by activated neutrophils. Loss of sensitivity to injury is accompanied by decreased iron content*

- during *in vitro* culture and is restored with exogenous iron. *Laboratory Investigation*, 1992. **66**(6): p. 708-14.
128. Collins, T., et al., *Transcriptional regulation of endothelial cell adhesion molecules: NF-kappa B and cytokine-inducible enhancers*. *FASEB Journal*, 1995. **9**(10): p. 899-909.
 129. Faure, E., et al., *Bacterial lipopolysaccharide and IFN-gamma induce Toll-like receptor 2 and Toll-like receptor 4 expression in human endothelial cells: role of NF-kappa B activation*. *Journal of Immunology*, 2001. **166**(3): p. 2018-24.
 130. Spiecker, M., H.B. Peng, and J.K. Liao, *Inhibition of endothelial vascular cell adhesion molecule-1 expression by nitric oxide involves the induction and nuclear translocation of IkappaBalpha*. *Journal of Biological Chemistry*, 1997. **272**(49): p. 30969-74.
 131. Lemieux, C., et al., *Angiopoietins can directly activate endothelial cells and neutrophils to promote proinflammatory responses*. *Blood*, 2005. **105**(4): p. 1523-30.
 132. Kim, I., et al., *Angiopoietin-1 reduces VEGF-stimulated leukocyte adhesion to endothelial cells by reducing ICAM-1, VCAM-1, and E-selectin expression*. *Circulation Research*, 2001. **89**(6): p. 477-9.
 133. Kim, I., et al., *Angiopoietin-1 negatively regulates expression and activity of tissue factor in endothelial cells*. *FASEB Journal*, 2002. **16**(1): p. 126-8.
 134. Godfrey, H.P. and X. Quan, *In vitro Study of Cytokine-Mediated Activation of Endothelial Cell Permeability Using Falcon Cell Culture Inserts*. *Falcon Technical Bulletin*, 1998. **413**: p. 1 - 3.
 135. Fire, A., et al., *Potent and specific genetic interference by double-stranded RNA in *Caenorhabditis elegans*. [see comment]*. *Nature*, 1998. **391**(6669): p. 806-11.
 136. Hannon, G.J. and J.J. Rossi, *Unlocking the potential of the human genome with RNA interference*. *Nature*, 2004. **431**(7006): p. 371-8.
 137. Yuan, B., et al., *siRNA Selection Server: an automated siRNA oligonucleotide prediction server*. *Nucleic Acids Research*, 2004. **32**(Web Server issue): p. W130-4.
 138. Reynolds, A., *Rational siRNA Design for RNA interference*. *Nature Biotechnology*, 2004. **22**: p. 326 - 330.
 139. Clementi, F., *Effect of horseradish peroxidase on mice lung capillaries' permeability*. *Journal of Histochemistry & Cytochemistry*, 1970. **18**(12): p. 887-92.
 140. Carlson, T.R., et al., *Direct cell adhesion to the angiopoietins mediated by integrins*. *Journal of Biological Chemistry*, 2001. **276**(28): p. 26516-25.

141. Kwak, H.J., et al., *Angiopoietin-1 inhibits irradiation- and mannitol-induced apoptosis in endothelial cells*. *Circulation*, 2000. **101**(19): p. 2317-24.
142. Yuan, H.T., et al., *Activation of the orphan endothelial receptor Tie1 modifies Tie2-mediated intracellular signaling and cell survival*. *FASEB Journal*, 2007. **21**(12): p. 3171-83.
143. Ferrari, G., et al., *VEGF, a prosurvival factor, acts in concert with TGF-beta1 to induce endothelial cell apoptosis*. *Proceedings of the National Academy of Sciences of the United States of America*, 2006. **103**(46): p. 17260-5.
144. Marron, M.B., et al., *Evidence for heterotypic interaction between the receptor tyrosine kinases TIE-1 and TIE-2*. *Journal of Biological Chemistry*, 2000. **275**(50): p. 39741-6.
145. McCarthy, M.J., et al., *Potential roles of metalloprotease mediated ectodomain cleavage in signaling by the endothelial receptor tyrosine kinase Tie-1*. *Laboratory Investigation*, 1999. **79**(7): p. 889-95.
146. Yabkowitz, R., et al., *Regulation of tie receptor expression on human endothelial cells by protein kinase C-mediated release of soluble tie*. *Blood*, 1997. **90**(2): p. 706-15.
147. Tsiamis, A.C., et al., *Vascular endothelial growth factor modulates the Tie-2:Tie-1 receptor complex*. *Microvascular Research*, 2002. **63**(2): p. 149-58.
148. Ades, E.W., et al., *HMEC-1: establishment of an immortalized human microvascular endothelial cell line*. *Journal of Investigative Dermatology*, 1992. **99**(6): p. 683-90.
149. Brown, K.A., et al., *Application of an immortalized human endothelial cell line to the leucocyte:endothelial adherence assay*. *Journal of Immunological Methods*, 1993. **163**(1): p. 13-22.
150. Edgell, C.J., C.C. McDonald, and J.B. Graham, *Permanent cell line expressing human factor VIII-related antigen established by hybridization*. *Proceedings of the National Academy of Sciences of the United States of America*, 1983. **80**(12): p. 3734-7.
151. Ribeiro, M.J., et al., *Hemostatic properties of the SV-40 transfected human microvascular endothelial cell line (HMEC-1). A representative in vitro model for microvascular endothelium*. *Thrombosis Research*, 1995. **79**(2): p. 153-61.
152. Xu, Y., et al., *Characterization of expression and modulation of cell adhesion molecules on an immortalized human dermal microvascular endothelial cell line (HMEC-1)*. *Journal of Investigative Dermatology*, 1994. **102**(6): p. 833-7.

153. Bosse, D., et al., *Antigen presentation by a continuous human microvascular endothelial cell line, HMEC-1, to human T cells*. Pathobiology, 1993. 61(3-4): p. 236-8.
154. Omidi, Y., et al., *Evaluation of the immortalised mouse brain capillary endothelial cell line, b.End3, as an in vitro blood-brain barrier model for drug uptake and transport studies*. Brain Research, 2003. 990: p. 95 - 112.
155. Lidington, E.A., et al., *A comparison of primary endothelial cells and endothelial cell lines for studies of immune interactions*. Transplant Immunology, 1999. 7(4): p. 239-46.
156. van Waarde-Verhagen, M.A.W.H., H.H. Kampinga, and M.H.K. Linskens, *Continuous growth of telomerase-immortalised fibroblasts: how long do cells remain normal?* Mechanisms of Ageing & Development, 2006. 127(1): p. 85-7.
157. May, M.J., et al., *Activation of p42mapk in human umbilical vein endothelial cells by interleukin-1 alpha and tumor necrosis factor-alpha*. American Journal of Physiology, 1998. 274(3 Pt 1): p. C789-98.
158. Harfouche, R., et al., *Angiopoietin-1 activates both anti- and proapoptotic mitogen-activated protein kinases*. FASEB Journal, 2003. 17(11): p. 1523-5.
159. Dallabrida, S.M., et al., *Angiopoietin-1 promotes cardiac and skeletal myocyte survival through integrins*. Circulation Research, 2005. 96(4): p. e8-24.
160. Jacobson, J.R. and J.G.N. Garcia, *Novel therapies for microvascular permeability in sepsis*. Current Drug Targets, 2007. 8(4): p. 509-14.
161. Regnault, V. and B. Levy, *Recombinant activated protein C in sepsis: endothelium protection or endothelium therapy?* Critical Care (London, England), 2007. 11(1): p. 103.
162. Gavard, J., V. Patel, and J.S. Gutkind, *Angiopoietin-1 prevents VEGF-induced endothelial permeability by sequestering Src through mDia*. Developmental Cell, 2008. 14(1): p. 25-36.
163. Saharinen, P., et al., *Angiopoietins assemble distinct Tie2 signalling complexes in endothelial cell-cell and cell-matrix contacts*. Nature Cell Biology, 2008. 10(5): p. 527-37.
164. van Eijk, L.T., et al., *Plasma obtained during human endotoxemia increases endothelial albumin permeability in vitro*. Shock, 2006. 25(4): p. 358-62.
165. Chen, J., Y.P. Zhou, and X.Z. Rong, *An experimental study on systemic inflammatory response syndrome induced by subeschar tissue fluid*. Burns, 2000. 26(2): p. 149-55.

166. Joyce, D.E., et al., *Gene expression profile of antithrombotic protein c defines new mechanisms modulating inflammation and apoptosis*. Journal of Biological Chemistry, 2001. **276**(14): p. 11199-203.
167. Ganter, M.T., et al., *Angiopoietin-2, marker and mediator of endothelial activation with prognostic significance early after trauma?* Annals of Surgery, 2008. **247**(2): p. 320-6.
168. Giuliano, J.S., Jr., et al., *Admission angiopoietin levels in children with septic shock*. Shock, 2007. **28**(6): p. 650-654.
169. Karpaliotis, D., et al., *Angiogenic growth factors in the pathophysiology of a murine model of acute lung injury*. American Journal of Physiology - Lung Cellular & Molecular Physiology, 2002. **283**(3): p. L585-95.
170. Yabkowitz, R., et al., *Inflammatory cytokines and vascular endothelial growth factor stimulate the release of soluble tie receptor from human endothelial cells via metalloprotease activation*. Blood, 1999. **93**(6): p. 1969-79.
171. Marron, M.B., et al., *Regulated proteolytic processing of Tie1 modulates ligand responsiveness of the receptor-tyrosine kinase Tie2*. Journal of Biological Chemistry, 2007. **282**(42): p. 30509-17.
172. Simoes, D.C.M., et al., *Angiopoietin-1 protects against airway inflammation and hyperreactivity in asthma*. American Journal of Respiratory & Critical Care Medicine, 2008. **177**(12): p. 1314-21.
173. Huang, Y.Q., et al., *Angiopoietin-1 increases survival and reduces the development of lung edema induced by endotoxin administration in a murine model of acute lung injury*. Critical Care Medicine, 2008. **36**(1): p. 262-7.
174. Lee, K.S., et al., *Blockade of airway inflammation and hyper-responsiveness by an angiopoietin-1 variant, COMP-Ang1*. Experimental & Molecular Medicine, 2007. **39**(6): p. 733-45.
175. McCarter, S.D., et al., *Cell-based angiopoietin-1 gene therapy for acute lung injury*. American Journal of Respiratory & Critical Care Medicine, 2007. **175**(10): p. 1014-26.
176. Mei, S.H.J., et al., *Prevention of LPS-induced acute lung injury in mice by mesenchymal stem cells overexpressing angiopoietin 1*. PLoS Medicine / Public Library of Science, 2007. **4**(9): p. e269.

177. Xu, J., et al., *Mesenchymal stem cell-based angiopoietin-1 gene therapy for acute lung injury induced by lipopolysaccharide in mice*. *Journal of Pathology*, 2008. **214**(4): p. 472-81.